

Carbon Monoxide and Carbon Monoxide -  
Releasing Molecules as Novel Antibacterial Agents:  
Mechanisms of Toxicity and Resistance



A Thesis submitted by

**Helen Elizabeth Jesse**

In part fulfilment of the requirement for the degree of  
Doctor of Philosophy

August 2013

Department of Molecular Biology and Biotechnology,  
The University of Sheffield,  
Firth court,  
Western Bank,  
Sheffield,  
S10 2TN,  
United Kingdom

All substances are poisons,  
there are none which is not a poison,  
only the dose permits something not to be poisonous.

Paracelsus

\*\*\*

True happiness is not made in getting something.  
True happiness is becoming something.  
This can be done by being committed to lofty goals.  
We cannot become something without commitment.

Marvin J. Ashton

## Abstract

Carbon monoxide (CO) is commonly considered to be toxic due to the propensity of this gaseous molecule to bind to ferrous iron in haemoglobin and cytochromes, thereby inhibiting respiration and the transport of oxygen around the body. However, CO is produced endogenously by haem oxygenases and has various cytoprotective functions including being vasodilatory, anti-inflammatory and anti-apoptotic. The development of CO-RMs (Carbon Monoxide-Releasing Molecules), which are generally transition metal carbonyls that release CO under certain conditions, has facilitated research into the physiological effects of CO and the potential use of CO as a therapeutic agent. Furthermore, CO-RMs have been found to reduce significantly the viability of various Gram-positive and Gram-negative bacteria, which is thought to be caused in part by the binding of CO from CO-RMs to the terminal oxidases of aerobic respiratory chains. Interestingly, CO-RMs are known to elicit many effects distinct from those of CO gas, including acting as more potent bactericidal agents.

This thesis aims to increase the current knowledge of the antibacterial effects of CO-RMs, with a particular focus on the interactions with respiration, oxidases and thiol compounds. In contrast to CO gas, CORM-3 was not preferentially inhibitory to respiration at low oxygen tensions; however, in accordance with the relative resistance of cytochrome *bd-I* to CO gas, this oxidase was found to be the most resistant of *E. coli* to respiratory inhibition by CORM-3, and possession of this oxidase conferred some protection against growth inhibition in the presence of this CO-RM.

Inhibition of *E. coli* respiration by CORM-3 was photosensitive and light reduced significantly the toxic effects of this compound, suggesting that CO from CORM-3 binds to ferrous haems in a classical, light-sensitive manner. This supports the hypothesis that the binding of CO from CORM-3 to haemoproteins is largely responsible for killing by these compounds. However, in opposition to this hypothesis, the non-haem oxidase AOX from *Vibrio fischeri* was found to be hypersensitive to inhibition by CORM-3, but not to CO, emphasising the complex effects of these compounds.

Data are presented to show that thiol-containing compounds, which have been widely reported to abolish the biological effects of CO-RMs, substantially reduce the uptake of ruthenium-containing CO-RMs. The generation of reactive oxygen species by CO-RMs is also demonstrated and investigated.

Finally, the generation and preliminary characterisation of CO-RM-resistant *E. coli* mutants is described. This work was done with the aim of revealing previously unappreciated bacterial targets for CO-RMs. Sugar-transporting phosphotransferase systems were identified as a possible means of CO-RM entry into the bacterial cell.

## **Acknowledgements**

I am so grateful that I have had this opportunity to work towards a PhD, and so my initial thanks must go to my supervisor Professor Robert Poole. It means so much to me that you believed that I could do this. It has been an honour to work for you, and one that I have thoroughly enjoyed. Thank you for your time, support and friendship. My thanks also go to Professor Brian Mann for advice on the chemical aspects of CO-RMs and to Dr. Dimitri Svistunenko for enabling me to perform EPR spectroscopy.

I am lucky to have worked with a lovely group of people in my time in the Poole lab, and so am thankful to all the Pooligans for their support and friendship and in particular to Dr. Kelly Davidge and Dr. Jayne Louise Wilson, who were incredibly kind and patient in teaching me about CO-RMs and countless laboratory techniques in my first few years in the lab.

To (soon to be Dr.) Mariana Tinajero Trejo, you have taught me more than you know, both inside and outside the lab. Your friendship means so much to me, I cannot thank you enough. You are a truly amazing scientist and a wonderful person.

Thank you to Mark for always being there and making me smile and of course to Molly, for greeting me each day with a wagging tail and reminding me of all that is important in life.

My final thanks go to my wonderful parents and to my sister, Rachel. I am so grateful for all you have done for me and could not have done this without your life-long support and encouragement; thank you.

## Publications

The work presented in this thesis has been, or will be published in the following papers:

Wilson, J.L., **Jesse, H.E.**, Poole, R.K., & Davidge, K.S. (2012). Antibacterial effects of carbon monoxide. *Curr Pharm Biotechnol* **13**: 760 – 768.

Wilson, J.L., **Jesse, H.E.**, Hughes, B., Lund, V., Naylor, K., Davidge, K.S., Mann, B. E. & Poole, R.K. (2013) Ru(CO)<sub>3</sub>Cl(glycinate) (CORM-3): A CO-releasing molecule with broad-spectrum antimicrobial and photosensitive activities against respiration and cation transport in *Escherichia coli* *Antiox. Redox Signal*. (In Press, doi:10.1089/ars.2012.4784.)

McLean, S., Begg, R., **Jesse, H.E.**, Mann, B.E., Sanguinetti, G. and Poole, R.K. (2013) Analysis of the bacterial response to Ru(CO)<sub>3</sub>Cl(glycinate) (CORM-3) and the inactivated compound identifies the role played by the ruthenium compound and reveals sulfur-containing species as a major target of CORM-3 action. *Antiox. Redox. Signal*. (In press, doi:10.1089/ars.2012.5103).

**Jesse, H.E.**, Nye, T.L, McLean, S., Mann, B. E., Green, J., Poole, R.K. (2013) The terminal oxidase cytochrome *bd-I* in *Escherichia coli* has lower susceptibility than cytochromes *bd-II* or *bo'* to inhibition by the carbon monoxide-releasing molecule, CORM-3: N-acetylcysteine reduces CO-RM uptake and inhibition of respiration. *Biochim Biophys Acta, Proteins and Proteomics*. 1834 (9): 1693–1703.

Tinajero-Trejo, M., **Jesse, H.E.** and Poole, R.K. (2013) Gasotransmitters, Poisons and Antimicrobials: It's a gas, gas, gas. **F1000Prime Reports**. 5 (28).

**Jesse, H.E.**, Collinson, E., Mann, B.E. and Poole, R.K.: Differential sensitivities of the di-iron oxidase AOX and haem oxidases of *Vibrio fischeri* to CO and CO-releasing molecules (in preparation).

## Presentations at scientific meetings

- 2012: Poster presented at the 7<sup>th</sup> International Congress on Heme Oxygenases in Biology and Medicine. Edinburgh. Title: The Effects of Carbon Monoxide-Releasing Molecules (CO-RMs) on the Terminal Oxidases of the Aerobic Respiratory Chains of *E. coli* and *V. fischeri*.
- 2011: Poster presented at The 7<sup>th</sup> European Conference on Bacterial Respiratory Chains. Sweden. Title: The Effects of Carbon Monoxide-Releasing Molecules (CO-RMs) on the three Terminal Oxidases of the Aerobic Respiratory Chains of *E. coli*.
- 2010: Poster presented at the XVIth International Conference on Oxygen Binding and Sensing Proteins (O<sub>2</sub>BiP), Antwerp, Belgium. Title: Effects of Carbon Monoxide-Releasing Molecule-3 (CORM-3) on *Escherichia coli* O<sub>2</sub> Metabolism

## Abbreviations

AOX	Alternative oxidase
BMPO	5-tert-butoxycarbonyl 5-methyl-1-pyrroline N-oxide
BSA	Bovine Serum albumin
CCCP	Carbonylcyanide m-chlorophenylhydrazone
CD	Circular dichroism
cGMP	Cyclic guanosine monophosphate
CIO	Cyanide-insensitive oxidase
CLP	Cecal ligation and puncture
CNS	Central nervous system
CODH	CO dehydrogenase
COHb	Carbonmonoxy-haemoglobin
COMb	Carbonmonoxy-myoglobin
CO-RM	Carbon monoxide-releasing molecule
DMSO	Dimethyl sulfoxide
DTNB	5,5'-dithiobis-[2-nitrobenzoic acid]
EDTA	Ethylene diamine tetraacetic acid
EGTA	Ethylene glycol tetraacetic acid
EPR	Electron paramagnetic resonance
ERK1/2	Extracellular signal-related kinases
ET-CORM	Enzyme triggered-CORM
GCS	Globin-coupled sensors
GM-CSF	Granulocyte macrophage colony-stimulating factor
GSH	Reduced glutathione
Hb	Haemoglobin
HO	Haem oxygenase
HPA	Hypothalamic pituitary adrenal
ICAM-1	Intercellular adhesion molecule-1
iCO-RM	Inactive carbon monoxide-releasing molecule
ICP-MS	Inductively-coupled plasma-mass spectrometry
IL-X	Interleukin - X
iNOS	Inducible nitric oxide synthase
IR	Infrared
Kca	Calcium-activated potassium channel
$K_d$	Dissociation constant



$K_{La}$	Gas transfer coefficient (gas to liquid)
$K_m$	Michaelis constant; the concentration of substrate that gives half-maximal velocity
$K_{off}$	Off rate
KPi	Inorganic potassium phosphate buffer
LB	Luria Bertani broth
LBS	Luria Bertani Salt
LED	Light emitting diode
LPS	Lipopolysaccharide
MAPK	Mitogen-activated protein kinase
Mb	Myoglobin
miCORM-3	Myoglobin-inactivated carbon monoxide releasing molecule
NA	Nutrient agar
NAC	<i>N</i> -acetyl cysteine
NCBI	National Center for Biotechnology Information
NF- $\kappa$ B	Nuclear factor kappa-light-chain-enhancer of activated B cell
NMR	Nuclear magnetic resonance
NOS	Nitric oxide synthase
NPAS-2	Neuronal PAS domain protein
$^1O_2$	Singlet oxygen
PBS	Phosphate buffered saline
pfu	Plaque forming units
photoCO-RM	Photoactivated carbon monoxide-releasing moiety
ppm	Parts per million
psi	Pounds per square inch
ROS	Reactive oxygen species
rpm	Revolutions per minute
sGC	Soluble guanylate cyclase
Slo BK	Large conductance $Ca^{2+}$ and voltage gates $K^+$ channels
SOD	Superoxide dismutase
TB	Terrific broth
TLR-4	Toll-like receptor-4
TNF- $\alpha$	Tumour necrosis factor-alpha
TY	Tryptone-yeast extract
$V_{max}$	Maximal rate

v/v	Volume for volume
w/v	Weight for volume

# Contents

	Abstract	III
	Acknowledgements	V
	Publications	VI
	Presentations at scientific meetings	VII
	Abbreviations	VIII
	Contents	XI
	List of Figures	XIX
	List of Tables	XXII
<b>Chapter 1</b>	<b>Introduction</b>	<b>1</b>
1.1	Carbon Monoxide (CO)	1
1.1.1	Gasotransmitters	1
1.1.2	Historical use of CO as an experimental tool	2
1.1.3	CO in mammalian systems	3
1.1.3.1	Toxicity of CO	3
1.2.3.2	CO as an inhibitor of respiration	4
1.2.3.3	A comparison with other respiratory inhibitors	7
1.1.3.4	Endogenous production of CO	8
1.1.3.5	The physiological functions of endogenous CO	11
1.1.4	CO in bacteria	13
1.1.4.1	Bacterial haem oxygenases	13
1.1.4.2	Bacterial metabolism of CO	14
1.1.4.3	Bacterial sensing of CO	16
1.2	Carbon Monoxide-Releasing Molecules (CO-RMs)	17
1.2.1	An introduction to CO-RMs	17
1.2.2	Early CO-RMs	19
1.2.2.1	CORM-1	19
1.2.2.2	CORM-2	19
1.2.3	Water soluble CO-RMs	19
1.2.3.1	CORM-3	19
1.2.3.2	CORM-A1	21
1.2.3.3	CORM-401	22

1.2.3.4	Iron indenyl carbonyls	22
1.2.4	PhotoCO-RMs	22
1.2.5	Recently designed CO-RMs with modified CO release or delivery mechanisms	24
1.2.5.1	Enzyme-Triggered CO releasers	24
1.2.5.2	Carbon monoxide-releasing micelles	24
1.2.5.3	Other modifications of interest	25
1.2.6	The future of CO-RM development	25
1.2.7	Methods of detecting CO	26
1.2.8	The therapeutic effects of CO and CO-RMs	27
1.2.8.1	CO inhalation therapy	27
1.2.8.2	The therapeutic effects of CO-RMs	28
1.2.8.2.1	Vasoactive properties	28
1.2.8.2.2	Anti-Inflammatory properties	32
1.2.8.2.3	The effects of CO and CO-RMs on organ transplantation	33
1.2.8.2.4	The effects of CO and CO-RMs on cell proliferation and apoptosis involves MAPK signalling and ROS production	34
1.2.8.2.5	Limitations to the therapeutic use of CO-RMs	35
1.3	Antimicrobial activity of CO and CO-RMs	35
1.3.1	The effects of CO and CO-RMs on the clearance of bacteria by the innate immune response	35
1.3.2	The effects of CO-RMs on bacterial growth and viability	37
1.3.3	The effects of CO-RMs on bacterial respiration	39
1.3.4	The effects of CO-RMs on gene expression	41
1.4	The aerobic respiratory chain of <i>Escherichia coli</i>	43
1.4.1	The terminal oxidases of the aerobic respiratory chain	46
1.4.1.1	Cytochrome <i>bo'</i>	46
1.4.1.2	Cytochrome <i>bd-I</i>	46
1.4.1.3	Cytochrome <i>bd-II</i>	48
1.4.1.4	Kinetics of CO binding to and dissociation from the terminal oxidases of <i>E. coli</i>	49
1.4.2	An exception to the rule: the alternative oxidase (AOX)	50
1.5	Conclusions and scope of thesis	50

<b>Chapter 2</b>	<b>Materials and methods</b>	<b>54</b>
2.1	Bacteriological Methods	54
2.1.1	Strains	54
2.1.2	Media	54
2.1.2.1	Luria Bertani broth (LB)	54
2.1.2.2	Defined minimal medium	54
2.1.2.3	Trace elements solution for defined minimal medium	54
2.1.2.4	Evans medium	56
2.1.2.5	Trace elements solution for Evans medium	56
2.1.2.6	LBS medium	56
2.1.2.7	Artificial sea water (ASW)	56
2.1.1.8	SOC medium	56
2.1.2.9	TY medium	57
2.1.2.10	TB medium	57
2.1.2.11	TB soft agar	57
2.1.2.12	Nutrient agar (NA)	57
2.1.2.13	Phage lysate plates	57
2.1.2.14	LBS Plates	57
2.1.3	Buffers and solutions	57
2.1.3.1	Phosphate buffered saline (PBS)	57
2.1.3.2	KPi buffer	58
2.1.3.3	Sonication buffer	58
2.1.3.4	<i>Vibrio</i> phosphate buffer	58
2.1.3.5	TAE buffer (50X)	58
2.1.3.6	Phage lysate buffer	58
2.1.3.7	Sodium dithionite solution	58
2.1.3.8	CO-saturated solution	59
2.1.3.9	N <sub>2</sub> -saturated solution	59
2.1.4	Strain storage	59
2.1.4.1	<i>E. coli</i>	59
2.1.4.2	<i>V. fischeri</i>	59
2.1.4.3	Bacteriophage	59
2.1.4.4	Antibiotics	60
2.1.5	Culture conditions	60
2.1.5.1	Cultures for <i>E. coli</i> growth and viability studies	60
2.1.5.2	Cultures for <i>V. fischeri</i> growth studies	60
2.1.5.3	Cultures for the preparation of <i>E. coli</i> membrane particles	61
2.1.5.4	Cultures for the preparation of <i>V. fischeri</i> membrane particles	61

2.1.5.5	Growing and sampling bacterial cells for ruthenium analysis (ICP-MS)	61
2.1.6	Culture turbidity measurements	62
2.1.7	Screening a library of <i>E. coli</i> transposon mutants	62
2.1.7.1	The initial CORM-2 screen	62
2.1.7.2	The second stage of the screen	62
2.1.7.3	CORM-2 susceptibility assay	62
2.1.7.4	The growth of transposon mutants of interest on plates containing CORM-2	63
2.1.7.5	Gradient plates	63
2.1.8	Viability Studies	63
2.1.8.1	Viability Studies with <i>E. coli</i>	63
2.1.8.1.1	Measuring the effect of photolysis on the viability of <i>E. coli</i>	64
2.1.9	Isolation of bacterial membrane particles	64
2.2	Biochemical Methods	65
2.2.1	Carbon monoxide-releasing molecules (CO-RMs)	65
2.2.1.1	Synthesis of CORM-3	65
2.2.1.2	Preparation of CO-RM stock solutions and control compounds	65
2.2.1.2.1	CORM-2	65
2.2.1.2.2	CORM-3	65
2.2.1.2.3	CORM-401	65
2.2.1.2.4	Preparation of RuCl <sub>2</sub> (DMSO) <sub>4</sub>	66
2.2.1.2.5	Preparation of iCORM-3 (inactive CORM-3)	66
2.2.1.2.6	Preparation of miCORM-3	66
2.2.2	Determination of protein concentration	66
2.2.3	DTNB thiol assay	67
2.2.3.1	The DTNB assay with variation of thiol concentration	67
2.2.3.2	The DTNB assay with variation of CO-RM concentration	67
2.2.3.3	The DTNB assay to determine intracellular thiol concentration	67
2.2.4	Superoxide Assay	68
2.2.5	Amplex red assay for hydrogen peroxide	68
2.2.6	Oxygen electrode for measurement of respiration rates	69
2.2.6.1	Closed electrode experiments	69
2.2.6.2	Photolysis of the haem-CO bond	71
2.2.6.3	Open electrode experiments	71
2.2.6.3.1	Respiratory studies utilising membranes subjected to various oxygen tensions	71
2.2.6.3.2	Measuring the time taken for the electrode chamber to reoxygenate	73

2.3	Spectroscopic methods	74
2.3.1	Measurement of CO release from CO-RMs	74
2.3.1.1	Myoglobin assay for the measurement of CO loss from CORM-3	74
2.3.1.2	Haemoglobin assay	75
2.3.1.3	Measurement of CO binding to cytochromes	75
2.3.1.4	ICP-MS	76
2.3.1.5	Electron paramagnetic resonance (EPR) spectroscopy	76
2.4	Genetic and molecular techniques	76
2.4.1	Generalised transduction with bacteriophage P1 <i>vir</i>	76
2.4.1.1	Preparation of lysates	77
2.4.1.2	P1 <i>vir</i> transduction of the recipient strain	77
2.4.2	Transposon mutagenesis	77
2.4.3	High Efficiency Transformation Protocol	78
2.4.4	Primer design and cloning	78
2.4.5	Genomic DNA extraction	78
2.4.6	Restriction enzyme digestion	78
2.4.7	Ligation of Fragmented DNA	79
2.4.8	PCR	79
2.4.9	Agarose gel electrophoresis	81
2.4.10	Purification of DNA samples	81
2.4.11	DNA sequencing	81
2.4.12	Sequence and database analysis for identification of genes inactivated by transposon mutagenesis	81
<b>Chapter 3</b>	<b>CO-RMs as inhibitors of the terminal oxidases of <i>E. coli</i></b>	<b>82</b>
3.1	Introduction	82
3.2	Results	83
3.2.1	CORM-2, CORM-3 and CO gas inhibit respiration in <i>E. coli</i> membrane particles	83
3.2.2	The oxygen tension at which CORM-3 is added does not affect the degree of respiratory inhibition.	86
3.2.3	Cytochrome <i>bd-I</i> is the most resistant oxidase of <i>E. coli</i> to respiratory inhibition by CORM-3 and a strain containing only this oxidase is partially protected from growth inhibition by this compound.	88
3.2.4	A spectroscopic study of the binding of CO from CORM-3 to each of the terminal oxidases of <i>E. coli</i>	92

3.2.5	Photolysis alleviates the inhibition of respiration by CO from CORM-3 and reduces killing by CORM-3	98
3.3	Discussion	102
3.3.1	CORM-2, CORM-3 and CO gas inhibit respiration in <i>E. coli</i> membrane particles	102
3.3.2	The oxygen tension at which CORM-3 is added does not affect the degree of respiratory inhibition.	105
3.3.3	Cytochrome <i>bd-I</i> is the most resistant oxidase of <i>E. coli</i> to CORM-3	106
3.3.4	Time-resolved spectra of CO from CORM-3 binding to each of the terminal oxidases of <i>E. coli</i>	108
3.3.5	Photolysis alleviates the inhibition of respiration by CO from CORM-3 and reduces killing by CORM-3.	109
<b>Chapter 4</b>	<b>The non-haem oxidase AOX from <i>Vibrio fischeri</i> is sensitive to inhibition by CORM-3</b>	112
4.1	Introduction	112
4.1.1	Respiration in <i>V. fischeri</i>	112
4.1.2	Alternative oxidase	112
4.1.2.1	Structure of AOX	114
4.1.2.2	Regulation of AOX activity and expression	114
4.1.2.3	The role of AOX	115
4.1.2.4	Interaction of AOX with gaseous ligands	117
4.1.3	The aim of this work	118
4.2	Results	118
4.2.1	The growth of <i>V. fischeri</i> in rich medium	118
4.4.2	The effects of CO gas and CO-RMs on the terminal oxidases of <i>V. fischeri</i>	120
4.2.3	The effects of CORM-2 and CORM-3 on the growth of <i>V. fischeri</i>	124
4.2.4	Spectroscopic studies of <i>V. fischeri</i> cell suspensions and membrane preparations treated with CORM-3	126
4.3	Discussion	132



<b>Chapter 5</b>	<b>The effects of thiol-containing compounds and antioxidants on the activities of CO-RMs</b>	<b>138</b>
5.1	Introduction	138
5.2	Results	140
5.2.1	Thiol-containing compounds completely prevent the inhibitory effects of CORM-2 and CORM-3 on respiration	140
5.2.2	Investigating the hypothesis that thiol-containing compounds affect the rate or amount of CO released from CORM-3.	145
5.2.3	NAC does not prevent the interaction between CO from CORM-3 and the terminal oxidases of the aerobic respiratory chain of <i>E. coli</i>	149
5.2.4	A glutathione-deficient <i>E. coli</i> mutant is more resistant to killing than a wild type strain.	149
5.2.5	CORM-2 and CORM-3 react with thiol groups	151
5.2.6	Superoxide is generated by CORM-2 and CORM-3 in solution	153
5.2.7	Antioxidants do not consistently prevent the inhibitory effects of CORM-3 on respiration	156
5.2.8	The use of EPR spectroscopy and the spin trap BMPO to assess whether reactive oxygen species are generated from solutions of CORM-2 and CORM-3	159
5.2.9	Assay of H <sub>2</sub> O <sub>2</sub> production <i>in vitro</i> by CORM-3 treated <i>E. coli</i>	167
5.2.10	NAC significantly reduces CORM-2 and CORM-3 uptake of <i>E. coli</i> cells	167
5.3	Discussion	170
5.3.1	The effect of thiol compounds on the release of CO from CORM-3	170
5.3.2	The influence of endogenous thiol compounds on the bactericidal effects of CORM-3	172
5.3.3	Could ROS account for the bactericidal effects of CO-RMs?	173
5.3.4	The effects of NAC on the uptake of CORM-2 and CORM-3 by bacterial cells	177
5.3.5	Conclusions	178
<b>Chapter 6</b>	<b>The generation and characterisation of CORM-2 resistant mutants</b>	<b>180</b>
6.1	Introduction	180

6.2	Results	181
6.2.1	The use of random transposon mutagenesis to generate <i>E. coli</i> mutants followed by screening for CORM -2 resistance.	181
6.2.2	Characterisation of mutants of interest.	184
6.2.3	Sequencing the CORM-2 resistant mutants	191
6.2.4	The characterisation of independent mutants	195
6.2.5	The effects of sub-inhibitory concentrations of CO-RM on bacterial growth	200
6.2.6	Uptake of CORM-2 by <i>sgaU</i> and <i>frvB</i> mutants	200
6.3	Discussion	202
<b>Chapter 7</b>	<b>General Discussion</b>	<b>211</b>
7.1	Summary	211
7.1.1	The effects of CO-RMs on bacterial respiration	212
7.1.2	The redox properties of CO-RMs	214
7.1.3	Other potential mechanisms of killing by CO-RMs	215
7.1.4	The entry of CO-RMs into bacterial cells	217
7.2	Future directions and outstanding questions	218
7.3	Conclusions	221
	<b>References</b>	<b>223</b>

## List of Figures

Figure 1.1	The structure of eukaryotic cytochrome <i>c</i> oxidase and the sites of interaction of the inhibitors NO and CO.	6
Figure 1.2	The breakdown products of haem and their effects	9
Figure 1.3	The interaction of CO with biological targets and the subsequent effects	30
Figure 1.4	The branched aerobic respiratory chain of <i>E. coli</i>	45
Figure 1.5	The terminal oxidases of <i>E. coli</i>	47
Figure 1.6	The effects of CO-RMs on the bacterial cell	53
Figure 2.1	Oxygen electrode for measurement of respiration rates	70
Figure 2.2	Apparatus to measure oxygen consumption following photolysis	72
Figure 3.1	CO gas, CORM-3 and CORM-2 inhibit respiration in wild type <i>E. coli</i> membrane particles.	85
Figure 3.2	The oxygen tension at which CORM-3 is added does not affect the degree of respiratory inhibition.	87
Figure 3.3	The degree of respiratory inhibition experienced by wild type <i>E. coli</i> membrane particles treated with CORM-3 is not exacerbated at very low oxygen tensions.	89
Figure 3.4	A strain containing only cytochrome <i>bd-I</i> is resistant to growth inhibition by CORM-3.	90
Figure 3.5	Cytochrome <i>bd-I</i> is resistant to respiratory inhibition by CORM-3.	93
Figure 3.6	Difference spectra of single oxidase membrane particles.	94
Figure 3.7	Binding of CO from CORM-3 to haem <i>d</i> and haem <i>b<sub>595</sub></i> of the terminal oxidases of <i>E. coli</i> .	96
Figure 3.8	Binding of CO from a saturated solution to haem <i>d</i> and haem <i>b<sub>595</sub></i> of the terminal oxidases of <i>E. coli</i> .	97
Figure 3.9	Photolysis of CORM-3 treated membrane particles confirms that the heme-CO bond is photolabile in each terminal oxidase of <i>E. coli</i> .	99
Figure 3.10	Light can reduce the toxic effect of CORM-3 by photolysing the haem – CO bond.	103
Figure 4.1	AOX and the respiratory chain of <i>V. fischeri</i> .	113
Figure 4.2	Factors that affect the activity of plant AOX	116
Figure 4.3	The growth of three strains of <i>V. fischeri</i> in LBS medium.	119
Figure 4.4	AOX from <i>V. fischeri</i> is resistant to respiratory inhibition by CO-saturated solution, but hypersensitive to CORM-3 and CORM-401	121
Figure 4.5	Respiration rates of <i>V. fischeri</i> membrane particles treated with CO, CORM-3, iCORM-3 or CORM-401 as a percentage of the control rate.	122
Figure 4.6	AOX is the most sensitive oxidase of <i>V. fischeri</i> to respiratory	125

	inhibition by CORM-3.	
Figure 4.7	The effect of various concentrations of CORM-2 and CORM-3 on the growth of <i>V. fischeri</i> .	127
Figure 4.8	Reduced minus oxidised spectra of <i>V. fischeri</i> membrane particles.	128
Figure 4.8	CORM-3 difference spectra of <i>V. fischeri</i> whole cells.	130
Figure 4.10	CORM-3 difference spectra <i>V. fischeri</i> membrane particles	131
Figure 5.1	NAC prevents CORM-2 and CORM-3 - dependent inhibition of respiration in <i>E. coli</i> membrane particles.	141
Figure 5.2	Reduced glutathione and cysteine prevent CORM-3 dependent inhibition of respiration in <i>E. coli</i> membrane particles.	143
Figure 5.3	NAC prevents CORM-3-dependent inhibition of respiration in <i>E. coli</i> membrane particles.	144
Figure 5.4	Increasing the ratio of NAC to CORM-3 to some extent reduces the amount of CO lost to myoglobin up to a 50-fold NAC excess.	146
Figure 5.5	The haemoglobin assay: NAC does not promote CO loss from CORM-3.	148
Figure 5.6	Reaction of the terminal oxidases in wild type <i>E. coli</i> membrane particles with CORM-3.	150
Figure 5.7	A glutathione deficient <i>E. coli</i> mutant is more resistant to killing than a wild type strain.	152
Figure 5.8	CORM-2 and CORM-3, but not CORM-A1 or control compounds react with NAC.	154
Figure 5.9	CORM-3 reacts with glutathione, cysteine and sulfide.	155
Figure 5.10	Both CORM-2 and CORM-3 generate superoxide.	157
Figure 5.11	Antioxidants and superoxide dismutase (SOD) do not prevent CORM-3-dependent inhibition of respiration to the same extent as thiol compounds.	158
Figure 5.12	EPR spectra	161
Figure 5.13	Reference spectra of superoxide	164
Figure 5.14	CORM-2 EPR spectra.	165
Figure 5.15	CORM-3 EPR spectra.	166
Figure 5.16	NAC significantly reduces the uptake of CORM-2 and CORM-3 into bacterial cells.	168
Figure 6.1	The survival of <i>I<sup>q</sup></i> Express <i>E. coli</i> in the presence of various concentrations of CORM-2.	182
Figure 6.2	The growth of selected transposon mutants in the presence and absence of CORM-2.	186
Figure 6.3	CORM-2 susceptibility assay.	187
Figure 6.4	CORM-2 gradient plates	190

Figure 6.5	The sequence of the EZ Tn5 transposon.	192
Figure 6.6	Identifying the transposon insertion site.	193
Figure 6.7	Confirmation of the absence of the mutated gene in the MG1655 transductants.	197
Figure 6.8	CORM-2 growth assays with the putative CORM-2 resistant mutants in an MG1655 background.	198
Figure 6.9	CORM-2 susceptibility assay with the putative CORM-2 resistant mutants in an MG1655 background.	199
Figure 6.10	CORM-3 and CORM-401 susceptibility assay with the putative CORM-2 resistant mutants in an MG1655 background.	201
Figure 6.11	The uptake of CORM-2 by wild type MG1655 <i>E. coli</i> and the <i>sgaU</i> and <i>frvB</i> mutants.	203

## List of Tables

Table 1.1	The physiological effects of CO	12
Table 1.2	The structures of several commonly used CO-RMs and their properties	18
Table 1.3	The pharmacological effects of CO-RMs	29
Table 2.1	Bacterial strains used in this work	55
Table 2.2	List of primers	80
Table 3.1	The respiration rates calculated from the gradients of the traces at four different time points.	100
Table 6.1	OD <sub>600</sub> of the mutants of interest obtained from the second stage of the CORM-2 screen.	185
Table 6.2	The growth of transposon mutants of interest on plates containing CORM-2.	189
Table 6.3	The genes disrupted in the transposon mutant strains that have been identified as CORM-2 resistant.	194
Table 6.4	The chemical structures and molecular weights of CORM-2 and CORM-3 and the sugars ascorbate, mannose and fructose	205

# Chapter 1

## Introduction

### 1.1 Carbon Monoxide (CO)

Carbon Monoxide (CO), a small, diatomic, gaseous molecule, is commonly considered to be a poison and an atmospheric pollutant. Natural sources of CO include photosynthesis and natural combustion such as forest fires and volcanoes, while a major source of anthropogenic CO is the partial oxidation of carbon containing compounds during energy generation from fossil fuels and the exhausts of internal combustion engines. CO inhalation causes approximately 170 deaths each year in the USA when gas appliances such as household boilers are used without adequate ventilation (U.S Consumer Product Safety Commission). CO also contributes to damaging ozone production by reacting with other pollutants, thereby reducing levels of atmospheric NO, which is then less effective at eliminating ozone (Assembly of Life Sciences (U.S.). Committee on Medical and Biologic Effects of Environmental Pollutants, 1977).

CO has a molecular weight of 28 and is relatively unreactive due to a stable triple bond between the two atoms and, consequently, has a high activation energy of  $213 \text{ kJ mol}^{-1}$ . It is however, able to form complexes with some transition metals that have low oxidation states (Davidge *et al.*, 2009a). Despite these complexes being stable due to the triple M-C $\equiv$ O bond, this process renders the CO susceptible to hydroxide attack, and therefore more reactive than in the diatomic form. CO has a low boiling point ( $-191.5 \text{ }^{\circ}\text{C}$ ) and therefore exists as a gas at room temperature.

#### 1.1.1 Gasotransmitters

Together with NO and H<sub>2</sub>S, CO is classified as a gasotransmitter (for more information see the following comprehensive reviews; (Kajimura *et al.*, 2010; Kajimura *et al.*, 2012; Li *et al.*, 2009; Tinajero Trejo *et al.*, 2013). These three molecules share many properties; they are all small, uncharged, membrane-permeable gases, and are highly toxic, primarily due to their interactions with metalloproteins and propensity to inhibit

respiration (Wikstrom *et al.*, 1981), yet all are produced endogenously in small amounts by mammalian systems and play vital roles within the body. All three gases are regulators of the cardiovascular and nervous systems (Furchgott, 1999; Liu *et al.*, 2011; Marks *et al.*, 1991; Murad, 1999; Wang, 2003), and NO and CO also have important effects on the immune system. Indeed, the realisation that CO was more than just a toxic molecule (Marks *et al.*, 1991) followed on from the initial appreciation of the vital beneficial activities of NO (Ryter *et al.*, 2004), for which Murad (1999), Furchgott (1999) and Ignarro (1999) were awarded the Nobel Prize for Physiology or Medicine in 1998. Each gasotransmitter is considered to have potential in a variety of therapeutic applications (Szabo, 2010). NO is an effective pulmonary vasodilator in patients with pulmonary hypertension (reviewed by Griffiths and Evans, 2005) and decreases the risk of brain injury in premature infants with respiratory failure (Kinsella *et al.*, 2006). H<sub>2</sub>S induces relaxation of blood vessels, inhibits inflammation, and modulates neuronal activity (Gadalla and Snyder, 2010). CO is an anti-inflammatory (Boczkowski *et al.*, 2006) and protective agent following organ transplants (Akamatsu *et al.*, 2004) and of the cardiovascular system (Furchgott and Jothianandan, 1991) (see sections 1.1.2.5 and 1.2.8.2).

### **1.1.2 Historical use of CO as an experimental tool**

The history of the experimental use of CO to elucidate the cellular components responsible for respiration has been comprehensively reviewed by Keilin (1966). Early work investigating the interaction of CO with biological systems was conducted by Haldane and Smith (Keilin, 1966), who in 1896, showed that the binding of CO to haemoglobin was reversible by light. Critical work was also performed by Louis Soret, who obtained UV absorption spectra of dilute blood samples and found that treatment of these samples with CO caused a red shift in the spectra of these samples (Keilin, 1966). Soret's pioneering work led to the designation of the  $\gamma$ -band of visible absorption spectra as the 'Soret' region.

Inhibition of respiration in yeast was first noted by Warburg (reviewed by Keilin, 1966). Warburg concluded that the CO/O<sub>2</sub> ratio was critical in determining the extent of respiratory inhibition caused by CO, thereby confirming that CO and O<sub>2</sub> compete for the same respiratory protein. He further investigated the finding of Haldane and Smith



that inhibition of respiration by CO was photosensitive, a property shared by haemoglobin (Hb), which led to his realisation that the unidentified respiratory components and haemoglobin were related (reviewed by Keilin, 1966). Warburg proceeded to develop photochemical action spectra, which involved examining the effects of light on respiration by yeast in the presence of CO, in order to further investigate the nature of the respiratory component (Keilin, 1966).

Britton Chance (Chance *et al.*, 1953) developed the work of Warburg and obtained photochemical action spectra of a variety of eukaryotic tissues and of prokaryotes, leading to a demonstration of the photodissociation of the CO-bound adduct of cytochrome *a<sub>3</sub>*, which in turn led to him identifying the oxidase of the mitochondrial respiratory chain. The use of action spectra to study the photorelief of inhibition of respiration by CO became an established assay to confirm the presence of terminal oxidases (Castor and Chance, 1959; Lemberg and Barrett, 1973). The relationship between cytochromes and aerobic respiration was further appreciated by Keilin (1966), who studied microorganisms spectroscopically and found cytochromes to be present in aerobic yeast and the bacterium *Bacillus subtilis*, but not in the obligate anaerobe *Clostridium sporogenes*.

### **1.1.3 CO in mammalian systems**

#### **1.1.3.1 Toxicity of CO**

In mammalian systems, prolonged inhalation of CO leads to tissue hypoxia, as the preferential binding of CO to haemoglobin prevents the transport of O<sub>2</sub> around the body (Goldbaum *et al.*, 1975; Stewart, 1974). The toxic effects of CO inhalation depend on the relative CO and O<sub>2</sub> tensions (Wu and Wang, 2005). The affinity of haemoglobin for CO is 200 – 250-fold higher than that of O<sub>2</sub> (Rodkey *et al.*, 1974); therefore upon inhalation, the majority of CO is sequestered by haemoglobin. Currently, the United States Occupational Health and Safety Administration (OSHA) has advocated a safe carbonmonoxyhaemoglobin (COHb) level of 8–10%, which is equivalent to exposure to 50 parts per million (ppm) for 8 h.

Hypoxia is most evident and detrimental in the brain and heart as these organs have a high requirement for oxygen. Symptoms of exposure to CO include headaches (which

typically begin when blood COHb levels reach 20%), dizziness and vomiting (typically experienced with COHb levels of 30%). Higher levels of COHb in the blood lead to collapse, convulsions (COHb of 40 – 50%), coma and death (COHb of 60 – 80%) (Roughton and Darling, 1944). However death has been reported at COHb levels of 30 – 40%, while other individuals with more than 40% CO-bound Hb have shown no symptoms (Goldbaum *et al.*, 1975). These discrepancies suggest that it is not the oxygen-carrying capacity of the blood, but rather, the dissolved CO level, that is critical in determining toxicity, as it is this free CO that is able to bind to other cellular targets such as respiratory cytochromes, a view shared by Chance *et al.* (1970). Indeed, when dogs inhaled 13% CO, they died within 15 min – 1 h and were found to have COHb levels of 54 – 90%, yet when dogs were bled to anaemia and then the blood replaced with blood from a donor dog with 80% COHb, the dogs were able to survive with COHb levels of 60% (Goldbaum *et al.*, 1975).

More recently, Alonso *et al.* (2003) presented further evidence that COHb levels are not sufficient to explain the toxicity of CO, and proposed that this involves both tissue hypoxia and direct cellular damage. In this work, mitochondria from muscle tissue were treated with 50, 100 and 500 ppm CO, which reduced cytochrome *c* oxidase activity by 20, 42 and 55% respectively. However, the conclusion that CO is toxic due to binding to respiratory cytochromes was to some extent disputed by Coburn (1979), who reviewed data that suggests that CO tensions of more than 1000-times those that occur when HbCO is at 5 to 10% saturation only cause a slight reduction in oxygen uptake. Instead, he suggests that CO binding to myoglobin (Mb) in heart and skeletal muscle, is a major cause of toxicity, even at less than 5% HbCO saturation (Coburn, 1979). This is supported by recent evidence, which shows that exposure to chronic levels of CO can cause arteriosclerotic heart disease and cardiac hypertrophy (Wang, 2004). Other toxic effects of CO are caused by the interaction of CO with haem proteins including cytochrome P450, cytochrome *c* oxidase, catalase and myoglobin (Piantadosi, 2002).

### **1.1.3.2 CO as an inhibitor of respiration**

The final step in aerobic respiration in mammalian systems, in which oxygen is reduced to water, is catalysed by cytochrome *c* oxidase. This enzyme contains haem and is

therefore susceptible to inhibition by CO, a compound that binds avidly to Fe<sup>II</sup> in the ferrous form of haem (Cotton and Wilkinson, 1980).

Haem consists of a porphyrin ring and a central iron ion. There are several different types of haem, each with variation in the functional groups attached to the main porphyrin ring. For example, *c*-type haems are very similar to *b*-type haems, but have cysteine SH-groups attached to the vinyl side chains, thus covalently binding haem to the apoprotein. This has no effect on the redox or catalytic properties of the haem, but in bacteria, *c*-type haems are only present in the periplasm, (Wood, 1983). Depending on the redox state of the iron, several small molecules, such as O<sub>2</sub>, NO, H<sub>2</sub>S, HCN<sup>-</sup>, can bind to this moiety.

In general, high spin haem proteins are able to bind ligands, while low spin haems are involved in electron transfer (Collman *et al.*, 1980). Cytochrome *c* oxidase has 4 redox centers that partake in the reduction of O<sub>2</sub>; Cu<sub>A</sub> and Cu<sub>B</sub> and haems *a* and *a*<sub>3</sub>. Electrons are transferred from ferrocytochrome to Cu<sub>A</sub>, and then passed to haem *a*, and subsequently to the haem *a*<sub>3</sub>/Cu<sub>B</sub> binuclear center, before finally being transferred to O<sub>2</sub> (Babcock and Wikstrom, 1992). Both O<sub>2</sub> and CO are able to bind to this site only when both the iron and copper are in the reduced state. The site at which O<sub>2</sub> is reduced to water, haem *a*<sub>3</sub>/Cu<sub>B</sub>, is hydrophobic and therefore preferentially binds neutral species (or anions associated with a proton) (Rich *et al.*, 1996). Figure 1.1 shows a diagrammatic representation of the redox centers of cytochrome *c* oxidase, and indicates the sites of binding of CO.

A recent study on the effects of endogenous CO on mammalian respiration showed that treatment of HEK293 cells with 20 μM CO inhibits respiration by 40% in the presence of 20 μM O<sub>2</sub>, and that the degree of respiratory inhibition is greater at lower oxygen concentrations, consistent with competitive inhibition by this compound (D'Amico *et al.*, 2006). Furthermore, mitochondrial oxygen uptake has been shown to be significantly reduced in kidneys after the endogenous production of CO was increased (Sandouka *et al.*, 2005).

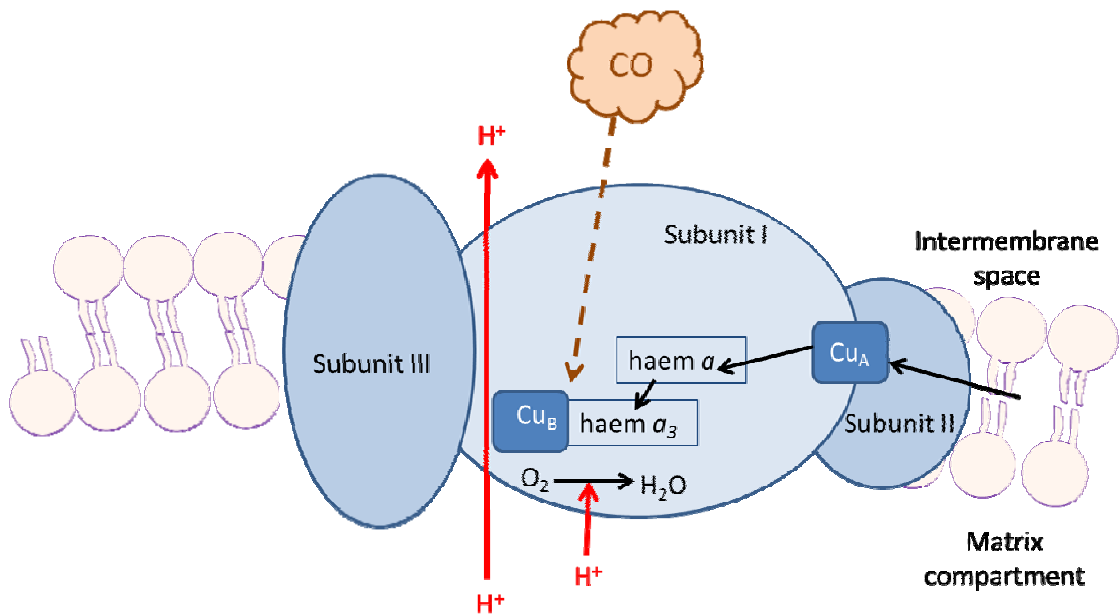


**Figure 1.1** The structure of eukaryotic cytochrome *c* oxidase and the sites of interaction of CO. Like oxygen, CO binds to cytochrome *c* oxidase only when copper B/haem *a*<sub>3</sub> binuclear center is fully reduced (ferrous/cuprous). CO is therefore a competitive inhibitor of cytochrome *c* oxidase with respect to oxygen. The black arrows represent the flow of electrons through the complex, the red arrows the movement of H<sup>+</sup>. This figure is adapted from a figure published in Boczkowski *et al.*, (2006), and information from Cooper and Brown, (2008).

### 1.1.3.3 A comparison with other respiratory inhibitors

CO is not unique as an inhibitor of respiratory oxidases. These enzymes are also inhibited by other small gaseous molecules, including NO, H<sub>2</sub>S and hydrogen cyanide. The roles of the first two as gasotransmitters are discussed above, here the mechanisms by which they inhibit cytochrome *c* oxidase will be compared, a subject that has recently been comprehensively reviewed by Cooper and Brown (2008).

NO has more complex effects on cytochrome *c* oxidase than CO, as it is able to inhibit this enzyme by both competitive and non-competitive mechanisms (Cooper and Brown, 2008) and is able to bind to both the reduced and oxidised enzyme. Non-competitive inhibition is mediated by the binding of NO to Cu<sub>B</sub> in oxidised cytochrome *c* oxidase (Cooper *et al.*, 1997) and results in the oxidation of NO to nitrite and the reduction of the enzyme (Torres *et al.*, 2000). The inhibition of respiration by NO causes reduction of the components of the electron transport chain, which leads to formation of superoxide and hydrogen peroxide (H<sub>2</sub>O<sub>2</sub>), which can act as important signalling molecules, as described below (section 1.2.8.2.4).

H<sub>2</sub>S also binds to and inhibits cytochrome *c* oxidase in a non-competitive manner and at more than one site, at reduced Cu<sub>B</sub> and at oxidised haem *a*<sub>3</sub> (Hill *et al.*, 1984). As with NO, H<sub>2</sub>S can be oxidised by this enzyme (Petersen, 1977).

Like CO, cyanide inhibits respiration by binding to the binuclear center of cytochrome *c* oxidase, but unlike CO, it binds to these components in their oxidised or reduced forms and in a non-competitive manner (Antonini and Brunori, 1971). It is thought that HCN inhibits a turnover intermediate (Mitchell *et al.*, 1992). Cyanide-insensitive, terminal oxidases exist, such as alternative oxidase (AOX) present in plants and some bacteria, which is resistant to CN<sup>-</sup> due to an absence of haem (see Chapter 5) and the CIO (cyanide insensitive oxidase) subfamily of oxidases present in some species of bacteria (Matsushita, 1983). *P. aeruginosa* contains a CIO, which is homologous to cytochrome *bd* quinol oxidases, but does not contain haem *d* (Cunningham *et al.*, 1997). This oxidase is induced upon entry into stationary phase (Cooper, 2003), during which HCN (at approximately 300 μM) is produced as one of many virulence factors (Blumer and Haas, 2000) and is therefore proposed to be involved in growth under cyanogenic

conditions (Cunningham *et al.*, 1997; Cunningham and Williams, 1995) and in the pathogenicity of this bacterium (Gallagher and Manoil, 2001) as demonstrated in *Caenorhabditis elegans* (Zlosnik *et al.*, 2006).

#### **1.1.3.4 Endogenous production of CO**

Despite the established perception of CO as a toxic gas, CO has more recently been recognised as an important biological molecule that is produced endogenously in both prokaryotes (Engel *et al.*, 1972) and eukaryotes (Sjostrand, 1949) and which has many beneficial roles (see section 1.1.7 below). Sjostrand (1949), found that the decomposition of Hb led to the production of CO. Coburn *et al.* (1963) then showed that when a person breathes into a closed system, the amount of CO detected over time increases, which confirmed that CO is produced endogenously in humans, and that CO production by the body is substantially increased during conditions such as haemolysis, when the levels of free haem are raised.

The enzyme required for the breakdown of haem, haem oxygenase (HO), was identified by Tenhunen *et al.* (1969). The breakdown of haem by HO requires molecular oxygen and NADPH. NADPH activates O<sub>2</sub> and reduces Fe<sup>III</sup> in haem to Fe<sup>II</sup>, which is necessary for the cleavage of haem. The breakdown of haem produces CO, Fe<sup>II</sup> and biliverdin (a green pigment) (Tenhunen *et al.*, 1969), which is later converted to bilirubin (a yellow pigment) by biliverdin reductase; this process and the biological effects of the breakdown products are summarised in Figure 1.2. Haem breakdown can be visualised during bruising. Such an injury will initially appear purple / red as oxygenated haem is released under the skin. Haem oxygenase uses oxygen to break down haem, generating anaerobic conditions and therefore deoxy-haem, causing the bruise to appear blue. The formation of bilirubin will then lead to the bruise becoming yellow (Mann, 2012).

Haem oxygenase exists in most mammalian species in both an inducible (HO-1) and a constitutive (HO-2) form (Tenhunen *et al.*, 1969), although a third isoform, HO-3, has been found in rats. HO-3 is a less powerful enzyme than HO-1 or HO-2 and is thought to be involved in haem-sensing (McCoubrey *et al.*, 1997). The degradation of haem is necessary in mammalian systems, as excess free haem is cytotoxic due to its oxidative

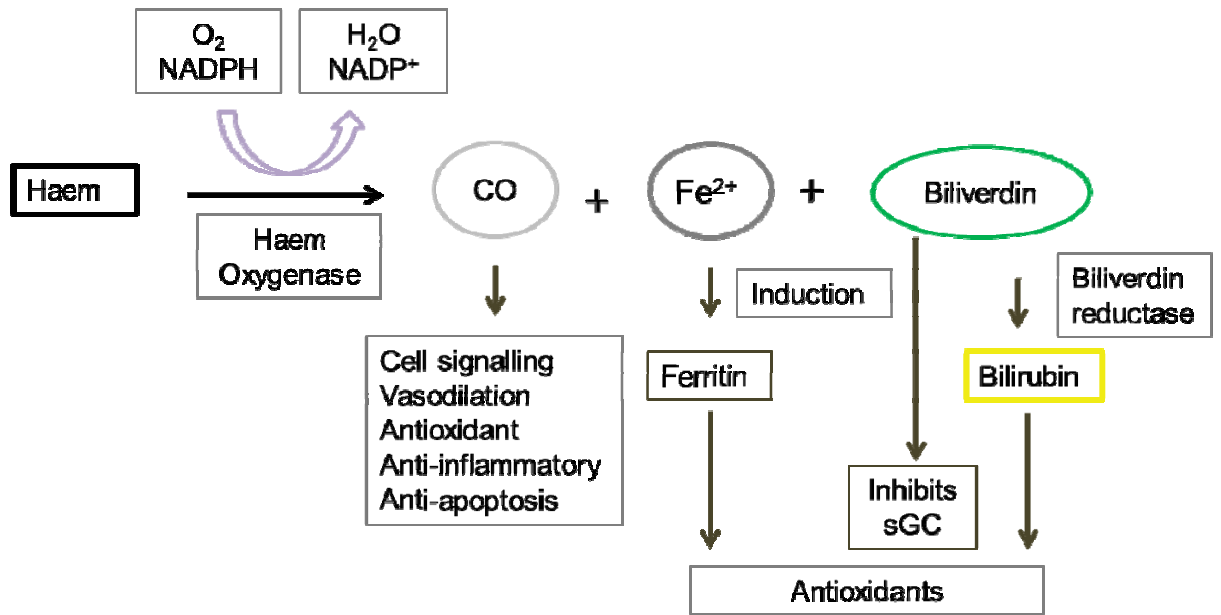


**Figure 1.2 The breakdown products of haem and their effects.** This figure was constructed using information obtained from Wu and Wang (2005).

effect. Additionally, the products of haem breakdown, CO and bilirubin, have beneficial effects; bilirubin has antioxidant (Stocker *et al.*, 1987) and anti-inflammatory properties (Sarady-Andrews *et al.*, 2005), while CO is also anti-inflammatory and is involved in regulating the generation of cGMP, which has many important roles in the cell.

The different isoforms of HO share some cellular defence functions, but also have distinct roles within the body. HO-2 is most abundant in the brain and testes, but is also constitutively expressed in other tissues, such as in endothelial tissues and the liver (Ewing and Maines, 1992). In the neuronal system, CO is an important signalling molecule that regulates neurotransmitters and neuropeptide release. HO-2 is also responsible for maintaining homeostatic haem levels within the cell, and has an important role in inactivating radicals derived from NO (Maines and Panahian, 2001).

Induction of HO-1 protects ischemic kidneys against tissue damage by degrading oxidant-generating haem from denatured hemoproteins and converting it to bilirubin and CO. The production of cytoprotective compounds by HO-1 necessitates that its expression is up-regulated by various stimuli that cause cellular stress, such as hyperoxia, heat shock and bacterial endotoxins, as well as haem and haem derivatives (Sardana *et al.*, 1981), including CO itself (Carraway *et al.*, 2002). Induction of HO-1 can comprise several different pathways including those involving cAMP (Durante *et al.*, 1997), protein kinase C, Ca<sup>2+</sup>-calmodulin-dependent protein kinase and the phosphoinositol pathway (Terry *et al.*, 1999). In some tissues, mitogen-activated protein kinases and the phosphorylation of tyrosine also play a role in the activation of HO-1 (Elbirt *et al.*, 1998). In contrast, there are conditions under which it is important to preserve haem by the down-regulation of HO-1 expression. This can occur in response to hypoxia (Nakayama *et al.*, 2000) or interferon- $\gamma$  (Takahashi *et al.*, 1999) and can involve Bach1, a haem-regulated repressor (Sun *et al.*, 2002).

Although the majority of the CO produced endogenously is derived from the degradation of haem by haem oxygenase enzymes, some CO is also produced by the breakage of methylene bridges in haem by hydrogen peroxide or ascorbic acid (Bonnett and McDonagh, 1973), or by the inactivation of cytochrome P450, which also leads to haem breakdown (Karuzina *et al.*, 1999).



### **1.1.3.5 The physiological functions of endogenous CO**

Contrary to the traditional view of CO as a toxic molecule, it is now known to have various cytoprotective functions such as acting as a neural messenger (Verma *et al.*, 1993) and having vasodilatory (Furchgott and Jothianandan, 1991), anti-inflammatory and anti-apoptotic properties (Boczkowski *et al.*, 2006). Examples of studies that have furthered our understanding of the effects of CO in these systems are listed in Table 1.1. CO is also involved in the regulation of many other physiological systems including the reproductive system (Ewing and Maines, 1995; Middendorff *et al.*, 2000), the renal system (Hill-Kapturczak *et al.*, 2002) and the control of circadian rhythms in a process involving sGC (soluble guanylate cyclase), and cGMP (cyclic guanosine monophosphate) (Artinian *et al.*, 2001), and through interaction with the NPAS2 (neuronal PAS domain protein) transcription factor (Dioum *et al.*, 2002). HO-1 knockout mice have been important in increasing our understanding of the important roles that CO plays within the body and in particular the understanding that HO-1 is required for mammalian iron reutilization. Such mice have an embryonic survival rate of only 5%, and individuals that survive are extremely vulnerable to stress and do not have a normal life span (Poss and Tonegawa, 1997).

The most abundant and obvious target for CO is ferrous iron in haem and cytochromes. However, CO exerts some of its biological effects via a variety of signalling pathways within the cell, although the precise mechanisms by which CO mediates its effects on targets that do not contain a transition metal are not well understood (Boczkowski *et al.*, 2006). Section 1.2.8.2 provides a more detailed explanation of the mechanisms by which CO interacts with biological targets in order to evoke these effects.

Abnormalities in CO metabolism and function are associated with a range of pathological conditions such as hypertension, heart failure, inflammation and neurodegenerative disease (Wu and Wang, 2005). Elevated production of CO has been noted in inflammatory pulmonary diseases, including cystic fibrosis, asthma and infectious lung disease (Kharitonov and Barnes, 2002). The important role of HO-1 in human health was highlighted by a case of an individual who lacked the ability to produce HO-1. This person experienced growth retardation, anaemia, thrombocytosis, hyperlipidaemia and leukocytosis, as well as high levels of ferritin and haem in their

<b>Biological effect</b>	<b>Evidence</b>	<b>Reference</b>
Vasorelaxation	<p>The relaxation of pulmonary blood vessels in response to exogenous CO (involving binding of CO to cytochrome P450).</p> <p>The relaxation of rat coronary arteries in response to CO.</p> <p>Inhibition of HO activity by zinc protoporphyrin-IX increased vascular resistance by decreasing the production of CO.</p> <p>CO causes vasorelaxation of vascular smooth muscle cells via the cGMP signalling pathway and by affecting the activity of calcium-activated K (KCa) channels.</p> <p>CO caused vasorelaxation of rabbit aorta by stimulation of sGC, but was 1000-fold less potent than NO at eliciting these effects.</p> <p>CO relaxes vascular tone in the heart, thereby improving cardiac blood supply.</p>	<p>(Sylvester and McGowan, 1978)</p> <p>(McGrath and Smith, 1984)</p> <p>(Suematsu <i>et al.</i>, 1994)</p> <p>(Wang <i>et al.</i>, 1997)</p> <p>(Furchgott and Jothianandan, 1991)</p> <p>(Grilli <i>et al.</i>, 2003)</p>
Neuronal effects	<p>HO co-localises with NOS in the CNS leading to the suggestion that CO is an endogenous neuronal messenger.</p> <p>CO modulates the HPA response.</p> <p>CO inhibits the secretion of oxytocin by the hypothalamus.</p>	<p>(Verma <i>et al.</i>, 1993)</p> <p>(Snyder <i>et al.</i>, 1998)</p> <p>(Kostoglou-Athanassiou <i>et al.</i>, 1996)</p>
Anti-inflammatory effects	<p>Low concentrations of CO inhibit the expression of LPS-induced pro-inflammatory cytokines: TNF-<math>\alpha</math>, IL-1<math>\beta</math>, and macrophage inflammatory protein-1<math>\beta</math>, and increase the LPS-induced expression of the anti-inflammatory cytokine IL-10 via activation of MAPK.</p> <p>CO inhibits LPS-induced GM-CSF production in macrophages (GM-CSF is a cytokine generated in response to LPS, which promotes proliferation, maturation, and effector functions of leukocytes). It does this by preventing the activation of the transcription factor NF-<math>\kappa</math>B, which regulates GM-CSF transcription, by preventing the phosphorylation and degradation of the regulatory subunit I<math>\kappa</math>B-<math>\alpha</math>.</p>	<p>(Otterbein <i>et al.</i>, 2000)</p> <p>(Sarady <i>et al.</i>, 2002)</p>
Anti-apoptotic effects	<p>Heme oxygenase-1 inhibits TNF-<math>\alpha</math>-induced apoptosis in cultured fibroblasts and these effects are mimicked by the exogenous administration of low concentrations of CO.</p> <p>CO produced by HO-1 protects endothelial cells from TNF-alpha-mediated apoptosis by activating p38 MAPK.</p> <p>CO protects pancreatic beta-cells from apoptosis in a process involving sGC activation.</p>	<p>(Petrache <i>et al.</i>, 2000)</p> <p>(Brouard <i>et al.</i>, 2002)</p> <p>(Gunther <i>et al.</i>, 2002)</p>

**Table 1.1 The physiological effects of CO.** This table summarises some of the key studies that have led to our appreciation of some of the main roles CO plays within the body.

serum and low levels of bilirubin, and sadly died aged 6 years (Ohta *et al.*, 2000; Yachie *et al.*, 1999).

CO-based therapies are currently in the early stage of development, and include CO inhalation therapy, development of CO-RMs and induction of HO-1 to increase the production of endogenous CO (see section 1.2.8 below).

#### **1.1.4 CO in bacteria**

##### **1.1.4.1 Bacterial haem oxygenases**

The production of CO by bacteria was first noted by Engel *et al.* (1972) who detected the generation of this gas by species of *Bacillus* and *Staphylococcus* using gas chromatography. The first bacterial HO, HmuO from *Corynebacterium diphtheriae* (Schmitt, 1997), was discovered because of its homology to human HO-1. Interestingly, there is relatively little sequence identity between bacterial HOs; however, important regions within the protein are conserved and these proteins often have the same overall fold with key ligands located with the same spatial relationship to the haem (Schuller *et al.*, 2001; Zhu *et al.*, 2000a). Bacterial HO genes are often confirmed by the inability of mutants in the gene to grow when haem or haemoglobin is the sole source of iron (for examples, see (Ratliff *et al.*, 2001; Ridley *et al.*, 2006; Schmitt, 1997). The ability to produce bilirubin is also indicative of HO-1 activity (Wegele *et al.*, 2004; Zhu *et al.*, 2000b).

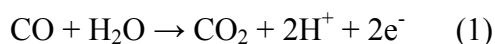
Not all bacteria possess HOs; however, there does seem to be a higher incidence of this enzyme in pathogenic or haemolytic species (Davidge *et al.*, 2009a). For example, *Neisseria* species have HemO (Zhu *et al.*, 2000a), while *Campylobacter jejuni* has the HO Cj1613c (Ridley *et al.*, 2006), which shares similarity with HugZ in *Helicobacter pylori* (Guo *et al.*, 2008). In addition, the opportunistic pathogen *Pseudomonas aeruginosa* has two HOs: PigA, which has 37% similarity to HemO from *Neisseria* (Ratliff *et al.*, 2001), and BhpO, which is a typical HO, but may also have a role in the production of phytochromes (Wegele *et al.*, 2004). Other pathogenic species of *Shigella* and *Enterobacter* also have HOs. Further evidence to support this generalisation is the absence of HO in *E. coli* K12 strains, but the presence of the HO, ChuS, in the enterohemorrhagic strain 0157:H7 (Suits *et al.*, 2005).

The proposed roles of HO in bacteria include iron acquisition, the production of chromophores and the establishment and maintenance of an anaerobic environment (reviewed by Davidge *et al.*, 2009a). With regards to the last, the HO HemT has been found in pathogenic species of *Clostridium* that colonise wounds in which anaerobiosis is beneficial, but not in non-pathogenic *Clostridium* species (Bruggemann *et al.*, 2004). The requirement of a functional HO for growth when haem is the only source of iron, for example during pathogenesis, has led to the identification of HOs as potential targets for antimicrobial therapy (Furci *et al.*, 2007) (see section 1.2.8 below).

There is a second, seemingly smaller, group of bacterial HOs that do not resemble mammalian HOs. Examples have been found in *Staphylococcus aureus*, designated IsdI and IsdG (Skaar *et al.*, 2004), *Listeria monocytogenes* (Wu *et al.*, 2005) and *Bacillus anthracis* (Skaar *et al.*, 2006) amongst others (Puri and O'Brian, 2006). Such HOs are regulated by iron and the utilisation of haem as a source of iron is a major role of these enzymes (Skaar *et al.*, 2004; Skaar *et al.*, 2006).

#### **1.1.4.2 Bacterial metabolism of CO**

Despite the propensity of CO to inhibit aerobic respiration, many bacteria, both aerobic and anaerobic, use CO as their main carbon and energy source (Ragsdale, 2004). Indeed the CO/CO<sub>2</sub> pair has a favourably low redox potential of -524 to 558 mV (Oelgeschlager and Rother, 2008). As seen in equation (1), the oxidation of CO to CO<sub>2</sub> generates two protons and two electrons through the simultaneous reduction of water.



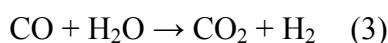
The metabolism of CO by some bacterial species (known as carboxidotrophic bacteria) has been comprehensively reviewed (King and Weber, 2007; Oelgeschlager and Rother, 2008; Ragsdale, 2004). This process requires a CO dehydrogenase (CODH) enzyme, the active site of which contains iron along with either nickel in anaerobic bacteria, or molybdenum in aerobic bacteria (reviewed by Ragsdale and Kumar, 1996).

The ability of aerobic bacteria, such as *Oligotropha carboxidovorans* and *Pseudomonas thermocarboxydovorans*, to use CO relies on a CO-insensitive respiratory chain involving ubiquinone and cytochromes, such as cytochrome  $b_{561}$  in *P. thermocarboxydovorans* (Jacobitz and Meyer, 1989). Anaerobic bacteria that can utilize CO include sulfate reducers, acetogens and hydrogenogens (Oelgeschlager and Rother, 2008). Many CO utilizing, sulfate reducers are thought to convert CO to CO<sub>2</sub> in order to detoxify the CO as well as to produce reducing power (Sipma *et al.*, 2006); however *Desulfotomaculum carboxydivorans* is remarkable in its ability to grow in 100% CO and in the absence of sulfate (Parshina *et al.*, 2005). Acetogenic bacteria are obligate anaerobes, which use CO to form acetic acid and CO<sub>2</sub>, according to equation (2).



This process provides a mechanism for autotrophic carbon assimilation (Oelgeschlager and Rother, 2008), and the formation of an ion motive force, which thereby allows ATP generation (Muller, 2003).

Another group of anaerobic carboxidotrophs are the hydrogenogens (Svetlitchnyi *et al.*, 2001). These oxidise CO and concomitantly reduce protons from H<sub>2</sub>O to produce molecular hydrogen, as shown in equation (3).



The best studied of this group, the facultative anaerobe *Rhodospirillum rubrum*, is able to generate energy by aerobic respiration, fermentation or photosynthesis depending on the oxygen tension of the surroundings. In the absence of both oxygen and light, *R. rubrum* can use CO as a terminal electron acceptor (Kerby *et al.*, 1995) using CO dehydrogenase (CooS), which deprotonates water at a Ni-Fe-S centre forming hydroxide which then attacks CO (Ragsdale and Kumar, 1996). A CO hydrogenase (CooH), with a CO-insensitive Ni/Fe center, then transfers the electrons produced to H<sup>+</sup> to form molecular hydrogen (Bonam *et al.*, 1989). This process translocates protons across the membrane, allowing the subsequent generation of ATP (Fox *et al.*, 1996; Maness *et al.*, 2005). The expression of the *coo* operon in this bacterium is regulated by

the haem-containing protein CooA, which senses CO as described below (Aono *et al.*, 1996). *Carboxydotherrmus hydrogenoformans* is another example of a bacterium that undergoes carboxidotrophic hydrogenogenesis, although it can also grow on other electron donors and acceptors. It is a strict anaerobe and is able to grow more rapidly on CO than many other species (Svetlitchnyi *et al.*, 1991).

#### 1.1.4.3 Bacterial sensing of CO

The two main types of bacterial CO sensors use haem in order to detect this gas. Such sensors are similar to the CRP/FNR transcription factors and globin coupled sensors (GCS) as they have a regulatory globin-like domain and a transducer domain (Thijs *et al.*, 2007). CooA, from *R. rubrum* is a typical example of a haem-based CO sensor (Aono *et al.*, 1996). It regulates the expression of CO-utilising genes (Shelver *et al.*, 1995), including the *coo* operon (Bonam *et al.*, 1989). Mutants of *cooA*, which were devoid of haem, were found to be constitutively active (Youn *et al.*, 2006). CooA is able to discriminate between CO and NO; although NO is able to bind to CooA, forming a 5-coordinate NO-haem complex, this does not trigger the binding of this sensor to DNA (Reynolds *et al.*, 2000). CO binds to CooA only when the haem is in the ferrous form, as the distal ligand is displaced when the iron is reduced, thereby allowing preferential binding of CO (Clark *et al.*, 2007). The binding of CO to CooA forms a 6-coordinate complex (Aono, 2003; Aono *et al.*, 1996; Aono *et al.*, 1998; Shelver *et al.*, 1997). This stabilises the CooA dimer, which allows the binding of DNA to a specific sequence of DNA (Roberts *et al.*, 2001) and thus transcription of the CODH genes. Histidine at residue 77 is required for the CO-responsiveness of this sensor (Youn *et al.*, 2006). Other haem-based CO sensors include the two component system FixLJ in *Rhizobium meliloti* (Gilles-Gonzalez *et al.*, 1991; Rodgers and Lukat-Rodgers, 2005), RcoM from *Burkholderia xenovorans* (Kerby *et al.*, 2008) and HemAT in *B. subtilis* (Hou *et al.*, 2000). In *Mycobacterium tuberculosis*, the haem-containing sensor kinases DosS and DosT are able to bind CO (Kumar *et al.*, 2007), which induces the Dos regulon, thereby inducing dormancy in this organism (Kumar *et al.*, 2008).

In *E. coli*, the direct oxygen sensor, DOS, is also able to bind to CO, although the purpose of this binding is not understood (Delgado-Nixon *et al.*, 2000) The  $K_d$  of DOS for oxygen is 340  $\mu\text{M}$ , while that of CO is 3.1  $\mu\text{M}$  (Taguchi *et al.*, 2004). The haem

binding domain of DOS has 60% sequence similarity to the PAS (signal transducing domain) of FixL, while the C-terminal domain is similar to phosphodiesterases (Delgado-Nixon *et al.*, 2000). The ferrous form of DOS has phosphodiesterase activity, but this is inhibited by CO, NO and etazolate (Sasakura *et al.*, 2002).

## **1.2 Carbon Monoxide-Releasing Molecules (CO-RMs)**

### **1.2.1 An introduction to CO-RMs**

When the beneficial physiological roles of CO became apparent, it was realised that molecules that could release CO in a controlled, targeted manner would facilitate research into the physiological effects of CO, and could potentially have therapeutic applications (Motterlini *et al.*, 2002). Such molecules would allow CO to be stored in a solid form and then solubilised to allow injection directly into target sites in the body, thereby avoiding the need to inhale CO for therapeutic purposes (see section 1.2.8.1).

Initial proponents of this idea, Brian Mann and Roberto Motterlini, realised the potential of transition metal carbonyls as stable CO carriers; however those that were commercially available were insoluble in water, and many required photolysis in order to release the CO. These molecules were shown to have some striking vasoactive properties (Motterlini *et al.*, 2002). However, in order to be therapeutically useful, CO-RMs need to be non-toxic, be sufficiently water-soluble, pure and stable, and to release CO at an adequate rate (Davidge *et al.*, 2009a). Table 1.2 Shows the structure of several commonly used CO-RMs and lists their properties, CO release mechanisms and some physiological effects.

Common initial tests to identify potentially therapeutically useful CO-RMs are the ability to cause vasodilation in pre-contracted aortic rings (Clark *et al.*, 2003; Motterlini *et al.*, 2002; Motterlini *et al.*, 2005b) and the ability to decrease levels of pro-inflammatory markers in response to lipopolysaccharides (LPS) (Crook *et al.*, 2011; Hewison *et al.*, 2010; Sawle *et al.*, 2005).

CO-RM	Structure	Solubility	CO release mechanism and stoichiometry	Physiological effects	Toxicity against mammalian cells	Reference
CORM-1 [Mn <sub>2</sub> (CO) <sub>10</sub> ]		Insoluble in water, Soluble in DMSO	Photolysis stoichiometry of CO release has not been reported.	Reduces vasoconstriction in rat hearts and reduces acute hypertension in vivo.	≤ 100 μmol l <sup>-1</sup> had no major cytotoxicity on smooth muscle cells detected after exposure for 24 h in complete medium.	(Motterlini <i>et al.</i> , 2002).
CORM-2 [Ru(CO) <sub>3</sub> Cl <sub>2</sub> ] <sub>2</sub>		Soluble in DMSO	Ligand substitution, promoted by dithionite.  Releases 0.7 mol CO / mol CO-RM	causes sustained vasodilation in precontracted rat aortic rings, attenuates coronary vasoconstriction in rat hearts, and significantly reduces acute hypertension in vivo.	420 μM not toxic to vascular smooth muscle cells over 3 hours, however, after 24 h exposure to high concentrations, 400 μmol l <sup>-1</sup> , there was >50% loss of cell viability	(Motterlini <i>et al.</i> , 2002) (McLean <i>et al.</i> , 2012)
CORM-3 (Ru[CO] <sub>3</sub> Cl (glycinate))		Soluble in water	Promoted by dithionite.  Releases 1 mol CO / mol CO-RM	Causes vasodilation. Protects myocardial cells and isolated rat hearts from ischemia-reperfusion injury. Prevents cardiac allograft rejection in mice.	500 μM not toxic to mammalian cells.	(Foresti <i>et al.</i> , 2004) (Clark <i>et al.</i> , 2003) (Vadori <i>et al.</i> , 2009)
CORM-A1 (Na <sub>2</sub> [H <sub>3</sub> BCO <sub>2</sub> ])		Soluble in water	Spontaneous, but rate of CO release is pH- and temperature-dependent. Half- life 21 min at pH 7.4	Slow acting and sustained vasodilation of precontracted aortic rings	Not documented	(Motterlini <i>et al.</i> , 2005b)
CORM-401 [Mn(CO) <sub>4</sub> (S <sub>2</sub> CNMeCH <sub>2</sub> CO <sub>2</sub> H)]		Soluble in phosphate buffered saline	1 CO released spontaneously by a reversible, dissociative process. Promoted by dithionite, pyridine and phosphorus ligands.	100 μM reduced nitrite production, a marker of inflammatory response induced by LPS in macrophages, show that 1 has potential to be developed as a pharmaceutical.	low toxicity - 100 μM gave a 25% decrease in cell viability.	(Crook <i>et al.</i> , 2011) (McLean <i>et al.</i> , 2012)

**Table 1.2 The structures of several commonly used CO-RMs and their properties**



## **1.2.2 Early CO-RMs**

### **1.2.2.1 CORM-1**

The first Carbon Monoxide-Releasing Molecule (CO-RM) to be investigated for biological effects was  $[\text{Mn}_2(\text{CO})_{10}]$  (CORM-1) (Motterlini *et al.*, 2002). CORM-1 was found to cause a reduction in vasoconstriction in rat hearts following photo-excitation, providing the first evidence of a pharmacological effect caused by CO from a transition metal carbonyl. These effects mimic those of the HO-1/CO pathway. However, CORM-1 had many problems that made it less than ideal as a potential therapeutic; it was not water-soluble and required photolysis to trigger CO release. However, promisingly, low concentrations of this compound (100  $\mu\text{M}$ ) were not toxic to vascular smooth muscle cells over a period of 24 h.

### **1.2.2.2 CORM-2**

The second CO-RM to be identified was tricarbonyldichlororuthenium (II) dimer  $[\text{Ru}(\text{CO})_3\text{Cl}_2]_2$  (CORM-2) (Motterlini *et al.*, 2002). Such ruthenium-based compounds were thought to have great potential as CO-RMs as many ligands can bind to this metal allowing manipulation of the CO release kinetics (Forresti *et al.*, 2004). In contrast to CORM-1, CO release is not induced by photo-excitation, but spontaneously by substitution of the ruthenium coordinated CO for DMSO from the solvent. When dissolved in DMSO, the CORM-2 dimer immediately dissociates to form tri-carbonyl and di-carbonyl monomers (Motterlini *et al.*, 2002). CO release occurs in the presence of dithionite-reduced myoglobin; each mole of  $[\text{Ru}(\text{CO})_3\text{Cl}_2]_2$  releases 0.7 moles of CO with a half-life of approximately 1 min. Recent evidence suggests that sulfite species such as dithionite dramatically increase the release of CO from several CO-RMs including CORM-2 (see section 1.2.3.1 below) (McLean *et al.*, 2012). CORM-2 is commercially available and by early 2012, approximately 150 papers had been published describing its biological effects (Mann, 2012).

## **1.2.3 Water soluble CO-RMs**

### **1.2.3.1 CORM-3**

One disadvantage of the CO-RMs mentioned so far is their lack of solubility in water. This prompted Motterlini and colleagues to synthesise a range of water soluble CO-

RMs, the most promising of which was tricarbonylchloro(glycinato)ruthenium(II), known as CORM-3 ( $\text{Ru}[\text{CO}]_3\text{Cl}(\text{glycinate})$ ) (Clark *et al.*, 2003). As mentioned above, ruthenium is particularly amenable to chemical modification as it can exist in many oxidation states. CORM-3 is derived from CORM-2, but with the addition of a glycine coordinated to the ruthenium. Glycine was chosen as an ideal ligand as it does not contain a chiral center and therefore avoids the formation of diastereomers (Mann, 2012).

When CORM-3 is dissolved in water,  $[\text{HO}]^-$  groups attack the CO group forming an acidic solution of pH 2.5 – 3 (Davidge *et al.*, 2009a). CORM-3 releases CO rapidly at physiological pH with each CORM-3 molecule releasing 1 molecule of CO, leaving 2 carbonyl groups attached to the ruthenium moiety. Subsequently, the glycinato group becomes monodentate and is lost from the compound (Johnson *et al.*, 2007).

CORM-3 has a very complex solution chemistry, which makes it difficult to fully elucidate the mechanism of CO release (Davidge *et al.*, 2009a). It was initially thought that electron-withdrawing ligands found endogenously in the cellular environment, such as thiol compounds or imidazole, combined with physiological pH, was sufficient to trigger CO release from CORM-3 (Alberto and Motterlini, 2007). In addition, the Cl<sup>-</sup> ligand of CORM-3 is very labile, and the exchange of this ligand for another in solution is thought to favour subsequent CO release (Davidge *et al.*, 2009a). It was known that CO was released from CORM-3 in the presence of dithionite-reduced myoglobin, but no spontaneous CO release could be detected using a CO electrode. It was therefore assumed that CO release from such CO-RMs required an acceptor, such as reduced myoglobin in order to trigger CO release. However, a recent study by McLean and co-workers (2012) has advanced our understanding of the mechanisms by which CO is released from such CO-RMs. It was found that reduced myoglobin alone was not sufficient to cause CO release from CORM-3, but that dithionite, a necessary component of the myoglobin assay used to detect CO release from CO-RMs, or other sulfite species, greatly facilitated CO release. Based on this new evidence, it is thought that *in vivo*, endogenous sulfite species, or other similar intracellular components, trigger CO release (McLean *et al.*, 2012). This has implications for how CO release from CO-RMs is measured, as the myoglobin assay can only measure CO release in the

presence of dithionite. An alternative ‘haemoglobin assay’ has been proposed in which the spectroscopic changes that occur when oxy-ferrous haemoglobin (which is stable in the absence of dithionite) binds to CO are measured (McLean *et al.*, 2012). It is of great importance for the future use of CO-RMs that intracellular CO release can be measured and understood.

Another recent study investigated the effects of the interactions of proteins with CORM-3 on CO loss (Santos-Silva *et al.*, 2011). The authors note that no CO is detected in the headspace of a closed vial of a solution of CORM-3 using a gas chromatography thermal conductivity detector (GC-TCD), which, in agreement with McLean *et al.* (2012), suggests that CO is not released spontaneously from CORM-3. They suggest instead that interactions between proteins and CORM-3 may cause the chloride ion, glycinate group and one CO group to be lost from this CO-RM. If correct, this has important implications for the use of CO-RMs as therapeutic agents, as it suggests that CO-RMs would become deactivated by plasma proteins before reaching their target site. An X-ray structure of hen egg white lysozyme soaked with CORM-3 was obtained, and revealed that the remaining fragment of CORM-3 binds to the protein at three exposed sites by interacting with histidine and aspartate groups. A further study by this group investigated the CO release profile of CORM-3 and Ru(CO)<sub>3</sub>Cl<sub>2</sub>(1,3-thiazole), which is structurally similar to CORM-3, and found that there was only marginal CO loss from this compound or CORM-3 in the presence of a range of serum proteins. They did however find that when lysozyme was soaked with Ru(CO)<sub>3</sub>Cl<sub>2</sub>(1,3-thiazole), protein–Ru(CO)<sub>2</sub> adducts were formed leading to the hypothesis that such CO-RMs deliver CO *in vivo* through the decay of their adducts with plasma proteins (Santos *et al.*, 2012).

### 1.2.3.2 CORM-A1

CORM-A1, also known as sodium boranocarbonate (Na<sub>2</sub>[H<sub>3</sub>BCO<sub>2</sub>]), is a water-soluble CO-RM that does not contain a transition metal and loses CO by becoming protonated at physiological pH. CORM-A1 releases CO at a much slower rate than CORM-3, with a half-life of 21 min at pH 7.4; however, lower pH leads to faster CO release to myoglobin. Temperature also affects the rate of CO release from CORM-A1, with lower temperatures causing slower release. The slow CO-release rate may be beneficial

in allowing the CO to reach biological targets and to elicit long-acting effects, thereby mimicking endogenous CO produced by HO-1 (Motterlini *et al.*, 2005b).

### 1.2.3.3 CORM-401

Due to the potential difficulties of using ruthenium as a therapeutic agent, attention was turned to developing manganese-based CO-RMs. Of these, CORM-401 [ $\text{Mn}(\text{CO})_4(\text{S}_2\text{CNMeCH}_2\text{CO}_2\text{H})$ ], had low cytotoxicity and was considered to have much potential. CORM-401 is water-soluble at pH 7.4 and this molecule releases more than 3 CO groups to dithionite-reduced myoglobin from each CO-RM molecule, a desirable property of efficient CO-RMs (Crook *et al.*, 2011). CORM-401 releases some CO spontaneously by a reversible, dissociative process, although it is now known that dithionite is able to accelerate the rate of CO release from CORM-401 (McLean *et al.*, 2012). The presence of pyridine and phosphorus ligands and myoglobin also promote CO release from CORM-401 in a concentration-dependent manner. This is because these compounds either react with the CO-RM backbone or with CO, thereby preventing reassociation with CO (Mann, 2012).

### 1.2.3.4 Iron indenyl carbonyls

A group of CO-RMs have been developed based on iron indenyl carbonyls, which are made water-soluble by the addition of functional groups to the cyclopentadienyl ring. The most promising is  $[\text{Fe}(\eta^5\text{-C}_9\text{H}_7)(\text{CO})_2(\text{NCMe})][\text{BF}_4]$  as it is not toxic and has a half-life for CO release of 210 min; however, it only slightly reduces the production of nitrite (a marker of inflammation) in macrophages stimulated with LPS. The X-ray structures have been obtained for several of these compounds (Hewison *et al.*, 2010).

### 1.2.4 PhotoCO-RMs

The term 'photoCO-RM' (photoactivated carbon monoxide-releasing moiety) (Rimmer *et al.*, 2010) describes a compound that releases CO when exposed to a specific wavelength and intensity of light (Schatzschneider, 2011). Indeed, as outlined above (section 1.2.1 and 1.2.2), many of the early CO-RMs to be investigated released CO upon irradiation (Motterlini *et al.*, 2002). The theoretical benefit of this mechanism of CO release is that it can be precisely controlled by the administrator of the CO-RM and therefore circumvents some of the problems faced with other CO-RMs that release CO

according to the physiological environment. There are of course disadvantages to the requirement for a particular light source in order to trigger CO release, including potential damage to tissues caused by certain wavelengths.

The use of light to modify drugs *in situ* is not without precedent; examples of photodynamic therapy include the use of light to generate singlet oxygen ( $^1\text{O}_2$ ) with the aim of destroying malignant cells (Brown *et al.*, 2004), and the activation of pro-drugs in anti-cancer treatment (Farrer and Sadler, 2008). PhotoCO-RMs must be stable in the dark in order for the compound to accumulate in target tissues prior to photoexcitation, after which CO will be released, and ideally will not rebind to a high degree, but rather bind a solvent molecule in order to stabilise the remaining molecule (Schatzschneider, 2011).

The next group of compounds to be thoroughly explored for their potential as therapeutically relevant photoCO-RMs were those based on monocationic manganese(I) tricarbonyls  $[\text{Mn}(\text{CO})_3(\text{tmp})]^+$  (Niesel *et al.*, 2008). The potential for modification of the tmp ligand at the pyrazole ring and at the central methane carbon atom adds to the usefulness of this group (Schatzschneider, 2010). Such compounds are stable in the dark and, in the absence of light, do not affect the viability of HT29 human colon cancer cells, but typically release 2 CO groups per molecule upon irradiation at around 360 nm, and in this activated form, significantly reduce the viability of such cells (Niesel *et al.*, 2008). In order to allow such photoCO-RMs to be targeted to specific cancer cells, the  $[\text{Mn}(\text{CO})_3(\text{tmp})]^+$  compound was conjugated to a targeting peptide (Pfeiffer *et al.*, 2009). An interesting development in the design of photoCO-RMs was the linkage of  $[\text{Mn}(\text{CO})_3(\text{tmp})]^+$  to silicium dioxide nanoparticles which have the potential to deliver CO-RMs into solid tumours, without adversely affecting CO release (Dordelmann *et al.*, 2011).

Another group of photoCO-RMs are based on the sodium salts of the water soluble tungsten carbonyl complex  $\text{Na}_3[\text{W}(\text{CO})_5(\text{TPPTS})]$  (Rimmer *et al.*, 2010). These are stable in aerated media, but release approximately 1 CO upon irradiation; further CO is then released due to aerobic oxidation. These photoCO-RMs have been suggested as suitable for topical applications using UVA as an excitation source.

Recently, a manganese-based photoCO-RM has been described that has therapeutic potential (Ward *et al.*, 2012). Particular advantages of this CO-RM are that it releases 3 CO molecules from each CO-RM molecule, is activated by light from a LED (light emitting diode) at 400 nm, and is not toxic to RAW 264.7 murine macrophages before and after irradiation. Further investigation of the biological activities of photoCO-RMs is now needed. PhotoCO-RMs that release CO at wavelengths near to IR are desirable for therapeutic purposes.

### **1.2.5 Recently designed CO-RMs with modified CO release or delivery mechanisms**

#### **1.2.5.1 Enzyme-Triggered CO releasers**

A number of enzyme-triggered CO-RMs have been described (Romanski *et al.*, 2011). These are acyloxybutadiene-iron tricarbonyl complexes, and are stable in solution but are activated to release CO after entry into the cell by cleavage of the ester group by intracellular esterases. By varying the dienylester ligand, it is possible to manipulate the biological and pharmacological properties of such CO-RMs and it is hoped that, after further development, this type of CO release mechanism will allow precise, tissue controlled delivery of CO.

#### **1.2.5.2 Carbon monoxide-releasing micelles**

A novel idea to enable the delivery of CO-RMs therapeutically is the incorporation of CO-RMs into carbon monoxide-releasing micelles (Hasegawa *et al.*, 2010). These are based on existing ruthenium-based CO-RMs, conjugated to a polymeric micelle forming a spherical structure 30 - 40 nm in diameter. The micelles are stable in buffer and serum, but interestingly, release CO in the presence of cysteine and other thiol compounds (see Chapter 5). The micelles release CO at a slower rate than CORM-3, and yet they were able to prevent NF- $\kappa$ B activation in human monocytes that had been stimulated with LPS while CORM-3 was not. Interestingly, the micelles were significantly less toxic than CORM-3. They also have the advantage of slowing the diffusion of the CO-RM into tissues, which is particularly advantageous for the targeting of CO-RMs to distal tissue drainage sites.

### 1.2.5.3 Other modifications of interest

Much current work is focusing on how to modify CO-RMs to allow them to be targeted to specific cell or tissue types or to alter the rate of CO loss in order to render them more suitable for therapeutic applications. One such example is the modification of CORM-A1 to reduce the CO release rate to allow this compound to reach the target cells prior to the release of CO (Pitchumony *et al.*, 2010). This is achieved by adding histamine, morpholine, aniline or ethylene-diamine groups to the [H<sub>3</sub>BCO] moiety. Another example is the conjugation of CO-RMs to a polymeric carrier system to facilitate the passive transport of the CO-RM to tumours or to sites of inflammation (Bruckmann *et al.*, 2011). This involves the addition of an organometallic fac-Mn(CO)<sub>3</sub> moiety, to a methacrylate or methacrylamide polymer backbone. These complexes are triggered to release CO by light and are of the appropriate size and weight to allow passive drug delivery.

### 1.2.6 The future of CO-RM development

Future design of CO-RMs and work to characterise them should pay special attention to understanding the mechanism of CO release from CO-RMs. It is desirable for CO-RMs to have high CO release ratios, so that less drug needs be administered in order to achieve a therapeutic effect. In addition, future CO-RM design needs to focus on making CO-RMs more suitable for use as a medical drug. Currently we have water-soluble, bioactive CO-RMs such as CORM-3 and CORM-A1, but in order for CO-RMs to be a realistic therapy they must have highly attuned absorption into tissues and excretion from them, have higher biocompatibility and contain no potentially harmful components (Motterlini and Otterbein, 2010).

It is also important that we gain a better understanding of how CO from CO-RMs enters cells (Mann, 2012). For example, it is not known whether CO-RM enters via specific transporters, or by passive diffusion. Furthermore, little is known about the fate of the CO-RM backbone or the released CO after it has entered cells (Mann, 2012). However, Raman microscopy has shown that when HT29 human colon cancer cells are exposed to CO-RM, most of the CO-RM localises around the nucleolous (Meister *et al.*, 2010).

It is also vital that future CO-RMs are designed with the importance of the availability of reliable control molecules in mind. Currently, despite the reported use of three different control molecules for CORM-3: inactive CORM-3 (iCORM-3), myoglobin inactivated CORM-3 (miCORM-3) and  $\text{RuCl}_2(\text{DMSO})_4$ , there is no control molecule for this compound for which the chemistry is completely understood, or that mimics the *in vivo* breakdown products of this CO-RM precisely. Recent work in the field of photoCO-RMs aims to avoid the problems associated with uncharacterised and potentially unstable break-down products following the release of CO by carrying an additional ‘pendant ligand arm’ for each labile CO, which is able to replace the CO group following its release (Nagel, Mclean *et al.*, unpublished). Well-defined iCO-RMs such as these could be synthesised and used as control compounds.

### 1.2.7 Methods of detecting CO

It is also important that better techniques are developed to monitor CO release from CO-RMs, particularly now that it is known that the CO release rates measured by the widely used myoglobin assay are affected by the presence of dithionite. Furthermore, a recent paper by Atkin *et al.* (2011), highlighted problems associated with the processing of data from myoglobin assays and inaccuracies that arise from shifts in the isosbestic points upon CO-RM addition. Alternative methods of CO detection include measuring spectroscopic changes when CO binds to haemoglobin (McLean *et al.*, 2012) or other overexpressed intracellular globins (Lauren Wareham and Mariana Tinajero Trejo, unpublished), the use of gas chromatography to detect CO in the gas phase of a closed system (Santos-Silva *et al.*, 2011), or the detection of redox changes in a haemin modified electrode (Obirai *et al.*, 2006). A recent paper has described a novel means of intracellular CO detection based on the genetic insertion of a fluorescent probe into the *coo* operon (Wang *et al.*, 2012). This operon is under the control of *CooA*, a highly selective CO sensor (see section 1.1.4.3). This technique has the potential to allow the distribution of CO to be monitored within a living cell. An electrochemical microsensor able to detect CO and NO has also been reported (Lee and Kim, 2007). The sensor consists of a platinum electrode and a Ag/AgCl reference electrode covered with a gas-permeable membrane, and has a detection limit of < 5 nM and is therefore sufficient for analysing physiological levels of NO and CO.



### **1.2.8 The therapeutic effects of CO and CO-RMs**

As discussed above, CO is capable of initiating myriad beneficial effects within mammalian systems, which has led to research into ways that CO can be harnessed as a therapeutic agent to treat cardiovascular disease, sepsis, acute injury of the kidney, liver and lung, and to prevent organ transplant rejection (Motterlini and Otterbein, 2010). While there are obvious concerns regarding the administration of a 'toxic' compound to patients, there are some advantages of the therapeutic use of CO: it is relatively unreactive and therefore does not undergo undesirable reactions with intracellular compounds, and is a natural compound that is not metabolised by the body to produce harmful breakdown products.

There are currently three main approaches to the administration of CO as a therapeutic. The first is by the induction of HO-1 expression. This can be achieved through the administration of haem or protoporphyrins and has been shown to have beneficial effects in pathologies such as hyperoxia-induced lung injury, nephrotoxicity and sickle cell disease (Belcher *et al.*, 2006; Nath *et al.*, 1992; Otterbein *et al.*, 1999). The second involves the inhalation of gaseous CO, and the third the delivery of CO using CO-RMs, both of which are described below.

#### **1.2.8.1 CO inhalation therapy**

There have been several clinical trials into the use of CO gas inhalation therapy. These involve the inhalation of air containing CO, usually at a dose of 100 – 250 ppm. One phase II trial investigated the use of CO gas to prevent the development of postoperative obstructions of the bowel following colon surgery, while another investigated the use of CO to improve the toleration of donor kidneys in transplant patients (reviewed by Mann, 2010). Many questions must be answered before CO inhalation can be considered as a credible therapy. These include questions about the dose of CO required, and whether this is best delivered in multiple, low dose sessions, or in less frequent, larger doses (Motterlini and Otterbein, 2010).

A recent study with cynomolgus macaques investigated the efficacy of inhaled CO in reducing LPS-induced lung inflammation and found that exposure to 500 ppm CO over 6 h decreased tumour necrosis factor- $\alpha$  (TNF- $\alpha$ ) production, but did not affect levels of

IL-6 or IL-8. Lower concentrations of CO (250 ppm, 6 h) were less effective at inducing these effects in primates, despite being effective in rodent models. Treatment with relatively high levels of CO (500 ppm over 6 h) increased COHb levels by more than 30% (Mitchell *et al.*, 2010). The propensity of CO to bind to haemoglobin poses a significant danger and limitation, particularly as other cellular targets have lower affinities for CO. However, despite similar reservations regarding the pharmacological use of NO, which also has toxic effects, inhaled NO is currently used to treat premature babies with pulmonary hypertension (Bloch *et al.*, 2007).

### **1.2.8.2 The therapeutic effects of CO-RMs**

CO-RMs were developed to provide a means by which CO could be stored in a stable, solid form and then solubilised prior to administration via intravenous or subcutaneous injection. This has the advantage of allowing CO to be delivered directly to the site at which it is required, thus bypassing haemoglobin in the blood and lowering the necessary dose, as well as reducing the likelihood of systemic side effects. Studies into the therapeutic effects of CO and CO-RMs are now numerous, and this area has been extensively reviewed (Johnson *et al.*, 2003; Motterlini and Otterbein, 2010; Romao *et al.*, 2012). Consequently, only a brief overview of this work will be given here. Table 1.3 summarises some of the preminent findings in this field, while Figure 1.3 presents some of the biological targets known to interact with CO in order to mediate these physiological effects. The beneficial effects of therapeutically applied CO mimic those of endogenous CO, such as the modulation of vascular tone and attenuation of inflammation, and many of the same pathways are involved in the mediation of these effects.

#### **1.2.8.2.1 Vasoactive properties**

CO-RMs are considered to have great potential in regulating vasoactive processes in a variety of diseases (Motterlini and Otterbein, 2010). CORM-2 causes vasodilation and reduces hypertension in rat aorta, whereas the control molecule  $\text{RuCl}_2(\text{DMSO})_4$ , which is structurally similar to  $[\text{Ru}(\text{CO})_3\text{Cl}_2]_2$ , but with the carbonyl groups replaced

CO-RM	Evidence of pharmaceutical potential	Reference
CORM-1 [Mn <sub>2</sub> (CO) <sub>10</sub> ]	Reduces vasoconstriction and maintains coronary perfusion pressure in isolated rat hearts, yet is not toxic to vascular smooth muscle cells after 24 hrs.	(Motterlini <i>et al.</i> , 2002)
	Causes <i>in vivo</i> dilation of porcine cerebral arteriole smooth muscle cells via activation of large conductance, calcium dependent potassium channels.	(Xi <i>et al.</i> , 2004)
	Increases renal blood flow by 54%, glomerular filtration by 38%, and urinary cGMP excretion by 128%.	(Arregui <i>et al.</i> , 2004)
	Reduces neutrophil migration, leukocyte rolling and adhesion to endothelial cells in acute inflammation.	(Freitas <i>et al.</i> , 2006)
CORM-2 [Ru(CO) <sub>3</sub> Cl <sub>2</sub> ] <sub>2</sub>	Causes vasodilation and reduces hypertension in aorta from rats through activation of sGC.	(Motterlini <i>et al.</i> , 2002)
	Reduces proliferation of human smooth muscle cells by increased mitochondrial ROS production and subsequent decreased phosphorylation of ERK1/2 and cyclin D1 expression.	(Taille <i>et al.</i> , 2005)
	CO from this compound causes production of ROS by complex III of the electron transport chain. This affects the redox state of key cysteine residues in cardiac L-type Ca <sup>2+</sup> channels, inhibiting ion transport, which has cardioprotective effects.	(Scragg <i>et al.</i> , 2008)
	Reduces inflammation by attenuating LPS-induced production of ROS and NO by preventing expression of intracellular adhesion molecule-1 and activation of NF-κB.	(Cepinskas <i>et al.</i> , 2008)
	Protects against acute renal failure caused by ischemia.	(Vera <i>et al.</i> , 2005)
CORM-3 (Ru[CO] <sub>3</sub> Cl(glycinate))	Prevents cardiac allograft rejection and protects against ischemia reperfusion injury in mice. This involves the activation of HO-1, sGC and ATP-dependent potassium channels.	(Clark <i>et al.</i> , 2003)
	Prevents human platelet aggregation.	(Chlopicki <i>et al.</i> , 2006)
	Reduction of microglia activity in strokes and other neuroinflammatory diseases.	(Bani-Hani <i>et al.</i> , 2006)
CORM-A1	Causes significant but slow-acting and sustained vasodilation of precontracted aortic rings, mimicking the effects of endogenous CO.	(Motterlini <i>et al.</i> , 2005b)
	Increases renal blood flow and the rate of glomerular filtration.	(Ryan <i>et al.</i> , 2006)
CORM-401	Reduces nitrite production in RAW 264.7 macrophages by 70% following stimulation with LPS.	(Crook <i>et al.</i> , 2011)
[Mn(CO) <sub>3</sub> (tmp)] <sup>+</sup> with targeting peptide	Such photoCO-RMs have the potential to be targeted to specific cancer cells.	(Pfeiffer <i>et al.</i> , 2009).
[Mn(CO) <sub>3</sub> (tmp)] <sup>+</sup> nanoparticles	Such photoCO-RM nanoparticles have the potential to deliver CO-RMs into solid tumours.	(Dordelmann <i>et al.</i> , 2011)

**Table 1.3 The pharmacological effects of CO-RMs.** This table summarises key literature into the effects of CO-RMs on mammalian systems.

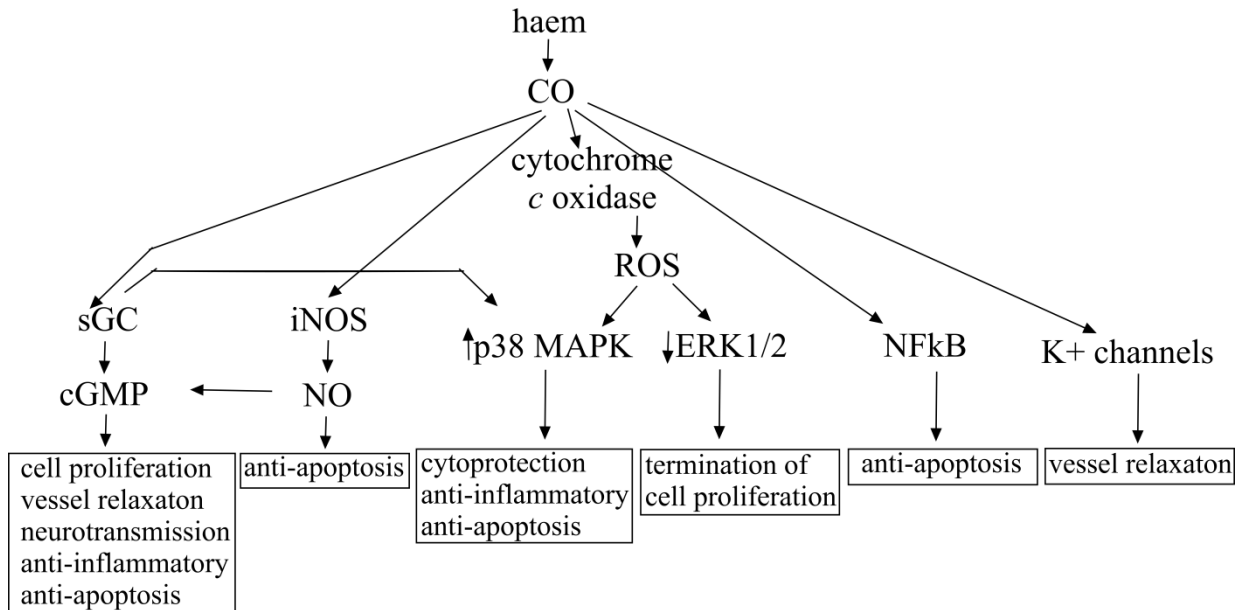


**Figure 1.3 The interaction of CO with biological targets and the subsequent effects**

CO mediates its biological effects by binding to haem-containing proteins such as soluble guanylate cyclase (sGC), which produces cyclic guanosine monophosphate (cGMP), inducible nitric oxide synthase (iNOS), or cytochrome *c* oxidase, or to transition metals such as Fe<sup>2+</sup> in potassium (K<sup>+</sup>) channels. Inhibition of respiration, due to CO binding to cytochrome *c* oxidase produces reactive oxygen species (ROS), which is a messenger for downstream signalling via mitogen activated protein kinases (MAPK) and extracellular-regulated-signal kinase (ERK1/2).

This is a simplified representation of the interaction of CO with a selection of biological targets. The precise mechanism by which CO exerts its effects on many of these targets is not fully understood, nor is the interplay between many of these pathways, or the complex interactions with NO. The information used to generate this figure was obtained from Boczkowski *et al.*, (2006), Dulak and Jozkowicz (2003) and Mann and Motterlini (2007).

with DMSO, is unable to cause these effects, suggesting that CO, rather than the CO-RM backbone is the causative agent (Motterlini *et al.*, 2002). Importantly, no cytotoxicity was experienced in vascular smooth muscle cells treated with up to 420  $\mu\text{M}$  CORM-2 over 3 h. CORM-3 also has significant vasodilatory properties, which are induced at concentrations of CORM-3 as low as 25 – 50  $\mu\text{M}$  (Foresti *et al.*, 2004). CORM-3 is also able to protect myocardial cells and isolated rat hearts from ischemia-reperfusion injury and can prevent cardiac allograft rejection in mice (Clark *et al.*, 2003). A major advantage of CORM-3 is that it has relatively low toxicity: concentrations less than 500  $\mu\text{M}$  are not toxic to porcine aortic endothelial cells or to primate peripheral blood mononuclear cells *in vitro* (Vadori *et al.*, 2009). Furthermore, the non-metal CO-RM, CORM-A1 causes significant but slow-acting and sustained vasodilation of precontracted aortic rings, thereby mimicking endogenous CO, while the inactive compound (iCORM-A1) does not.

The main mechanism by which CO-RMs (and indeed CO gas) mediate their vasoactive properties is by the activation of the haem-containing protein, soluble guanylate cyclase (Foresti *et al.*, 2004; Motterlini *et al.*, 2002; Motterlini *et al.*, 2005b) and the subsequent production of cGMP, an important second messenger with wide reaching effects (Kharitonov *et al.*, 1995). Both CO and NO activate sGC, but NO does so to a much greater extent (30 – 100-fold more than CO). However, the effects of CO on cGMP production can be increased by the benzyloid derivative YC-1 (Friebe *et al.*, 1998).

The activation of potassium channels by CO has also been implicated in the vascular activities of CO-RMs (Clark *et al.*, 2003; Foresti *et al.*, 2004). One mechanism by which CO may modulate the activity of such channels is by interacting with an associated haem group. Calcium-dependent Slo BK channels, interact with a haem group via a conserved haem-binding sequence motif. The association of haem with the channel inhibits the transport of  $\text{K}^+$  across the membrane and therefore reduces the frequency of channel opening (Tang *et al.*, 2003). Interestingly, HO-2 is part of the large-conductance,  $\text{Ca}^{2+}$ -sensitive potassium BK channel complex and CO was shown to be involved in regulating the activity of this channel (Williams *et al.*, 2004).

Haem-independent mechanisms may also be involved in the activation of such channels. There have been two separate reports of CO interacting with histidine and or aspartate residues to open such channels (Wang and Wu, 1997; Hou *et al.*, 2008). There is also evidence that reactive oxygen species (ROS) generated from the inhibition of respiration by CORM-3 can transduce signals to K<sup>+</sup> channels (Clark *et al.*, 2003) (see section 1.2.8.2.4).

#### **1.2.8.2.2 Anti-Inflammatory properties**

CO-RMs are also considered to have great potential as anti-inflammatory agents (Motterlini and Otterbein, 2010). Several CO-RMs have been shown to decrease levels of anti-inflammatory intermediaries and to reduce levels of TNF- $\alpha$  and NO in LPS stimulated macrophages (Sawle *et al.*, 2005).

CO delivered by CO-RMs may also be beneficial in the treatment of inflammation associated with arthritis. CORM-3 reduced levels of inflammatory cytokines in joint tissues and reduced the recruitment of inflammatory cells, joint inflammation and degradation of cartilage in animal models of arthritis (Ferrandiz *et al.*, 2008). In addition, CORM-2 has been shown to substantially reduce the inflammatory response induced by cytokines in human colonic epithelial cells. This includes reduced expression of nitric oxide synthase-2 (NOS-2) and subsequent production of nitrite as well as differential-regulation of inflammatory genes involved in intestinal inflammation and cancer progression (Megias *et al.*, 2007).

Many of the anti-inflammatory effects of CO and CO-RMs involve activation of the mitogen-activated protein kinase (MAPK) pathway. This pathway allows the transduction of signals via a series of serine/threonine-specific protein kinases and is involved in the regulation of proliferation, differentiation, gene expression, mitosis, cell survival, and apoptosis in a wide variety of eukaryotic cells (Johnson and Lapadat, 2002). It is well established that CO activates p38 MAPK and down-regulates extracellular-signal-regulated kinases, ERK1 and ERK2, but it is not understood how this is achieved. There is evidence that CO prevents ERK1/2 activation by CO gas after lung ischemia-reperfusion in rats, and that this involves the activation of sGC (Mishra *et al.*, 2006). Alternatively, it is possible that CO affects the MAPK pathway directly, by

interaction with  $Mn^{2+}$  in the serine/threonine phosphatase, protein phosphatase 2C, which is important in regulating stress responses in eukaryotes (Das *et al.*, 1996).

The regulation of NO production by CO also mediates the anti-inflammatory properties of CO-RMs. CO binds to haem in inducible nitric oxide synthase (iNOS), suppressing NO production (White and Marletta, 1992). This has important implications for the use of CO in antimicrobial therapies as NO is a key mediator of host defences against microbial infection (Motterlini and Otterbein, 2010) (see section 1.3.1). NO also has important roles in the regulation of vascular tone (Furchgott and Jothianandan, 1991), platelet aggregation (Sylman *et al.*, 2013) and smooth muscle relaxation (Sharma *et al.*, 2013). Interestingly, NO is a major regulator of sGC and, consequently, there is much interplay between the pathways involving iNOS and sGC.

#### **1.2.8.2.3 The effects of CO and CO-RMs on organ transplantation**

Much research has been undertaken into the protective potential of CO in organ transplant systems, and it has been found to have significantly beneficial effects (Akamatsu *et al.*, 2004). An early study into the biological activity of CORM-3 investigated cardiac allograft rejection in mice and found that treatment of recipients with CORM-3, but not an inactive control compound, greatly increased the survival rate of transplanted hearts (Clark *et al.*, 2003). CO-RMs have also been shown to prevent ischemia reperfusion injury in intestinal grafts via a sGC-dependent mechanism (Nakao *et al.*, 2006b). The reduction of pro-inflammatory cytokines by CO-RMs is also thought to be important in increasing the survival rate of transplant patients (Nakao *et al.*, 2006a). In addition, CO-RMs and saturated solutions of CO added to the organ preservation solution have been shown to greatly benefit the health of the transplanted organ (Musameh *et al.*, 2007; Pizarro *et al.*, 2009; Sandouka *et al.*, 2006). The mechanisms by which CO and CO-RMs induce these effects is not fully understood, but there is evidence that sGC (Nakao *et al.*, 2003), cytochrome p450 (Nakao *et al.*, 2008) and the reduction of inflammatory cytokine levels (Nakao *et al.*, 2006a) are involved.

#### **1.2.8.2.4 The effects of CO and CO-RMs on cell proliferation and apoptosis involves MAPK signalling and ROS production**

CO can both promote and prevent apoptosis. For example, CO from HO-1 or CORM-A1 has been shown to contribute to neuronal cell death following bradykinin-induced neuronal dysfunction (Yang *et al.*, 2013). In contrast, CO has been shown to prevent apoptosis in hepatocytes by inhibiting mitochondrial membrane permeabilization, which would otherwise release pro-apoptotic factors into the cell (Queiroga *et al.*, 2011). CO also prevents apoptosis by activating MAPK signalling. Administration of CORM-3 to a mouse model of peritonitis-induced sepsis elevated levels of ROS, which stimulated mitochondrial biogenesis and expression of peroxisome proliferator-activated receptor  $\gamma$  co-activator-1 $\alpha$  (Lancel *et al.*, 2009). Mitochondrial ROS and subsequent signalling involving ERK1/2 has also been implicated in the inhibition of proliferation of airway smooth muscle cells by CORM-2 (Taille *et al.*, 2005). CO has also been attributed an important role in mitochondrial biogenesis (Suliman *et al.*, 2007). Again, the production of ROS by inhibition of respiration is implicated in the increased expression of specific transcription factors that initiate transcription of mitochondrial proteins.

The binding of CO to cytochrome *c* oxidase in the eukaryotic respiratory chain inhibits respiration and therefore causes an accumulation of reduced components along the electron transport chain. ROS form when this reducing power is transferred to O<sub>2</sub> at ubiquinol forming superoxide (O<sub>2</sub><sup>-</sup>) (Poderoso *et al.*, 1999). ROS are known to be involved in diverse intracellular signalling processes, and therefore constitute second messengers of CO signalling (Gutterman *et al.*, 2005). Indeed, CO has been found to increase the production of ROS in RAW 264.7 cells, which initiates signalling pathways, including p38 MAPK, and therefore has anti-inflammatory effects (Zuckerbraun *et al.*, 2007). It should be noted however, that inhibition of cytochrome *c* oxidase by endogenous CO is only thought to occur at very low levels (D'Amico *et al.*, 2006), in part because of the propensity for haemoglobin and myoglobin to sequester free CO.

NADPH oxidase is widely distributed, but particularly important in phagocytes where it produces superoxide, which is an important host defence (Babior *et al.*, 2002). This protein contains haem and thus is susceptible to inhibition by CO, and consequently,



CO is also able to reduce levels of ROS (Taille *et al.*, 2005), although, this same work also showed that inhibition of respiration by CO delivered by CORM-2 increased the production of ROS, which then decreased cyclin D1 expression, preventing muscle proliferation. This exemplifies the complex balance that controls the biological effects of CO.

#### **1.2.8.2.5 Limitations to the therapeutic use of CO-RMs**

Despite the many potential advantages of CO-RMs compared to CO gas as a therapeutic agent, they also have some disadvantages. For example, consideration must be given to the fate of the CO-RM backbone following the release of CO. It is important that the resulting compound, and any residual breakdown products are not toxic, and that they are not metabolised by the body to subsequently produce toxic products. CORM-2 and CORM-3, which have potent therapeutic effects, both contain ruthenium, which is not found naturally in the body and therefore accumulation in cells and tissues would be undesirable.

### **1.3 Antimicrobial activity of CO and CO-RMs**

#### **1.3.1 The effects of CO and CO-RMs on the clearance of bacteria by the innate immune response**

Carbon monoxide is thought to be a key anti-inflammatory molecule involved in the resolution of inflammation and the prevention of sepsis; indeed, during infection, many host stress response genes are induced, including HO-1, which, as detailed above (section 1.1.3.4), catalyses the production of several anti-inflammatory molecules, including CO (Otterbein *et al.*, 2000; Zhou *et al.*, 2004). CO is anti-inflammatory, in part due to inhibition of haem-containing nitric oxide synthase (NOS), which prevents the production of NO, an inflammatory mediator. CO also increases the expression of interleukin-10 (IL-10) an anti-inflammatory molecule and decreases the expression of the pro-inflammatory cytokines, ICAM-1 and TNF- $\alpha$  through activation of a MAPK pathway (Otterbein *et al.*, 2000).

There is much evidence that CO plays an important role in host survival following bacterial infection (reviewed by Chung *et al.*, 2009). When challenged with endotoxin from the cell wall of gram negative bacteria, HO-1-deficient mice experienced

exacerbated organ injury and mortality caused by oxidative stress, compared to wild type mice (Wiesel *et al.*, 2000). However, treatment of such mice with exogenous CO reduced the inflammation experienced and increased the survival rate (Otterbein *et al.*, 2000). Furthermore, HO-1 deficient mice suffered increased lethality compared to wild type mice in a cecal ligation and puncture (CLP) model of abdominal sepsis, but this was ameliorated by the administration of CO, either by overexpression of HO-1, or delivery of CO by CO-RMs (Chung *et al.*, 2008). CORM-2 and CORM-3 have also been shown to reduce the inflammatory response caused by application of LPS to RAW 264.7 murine macrophages (Sawle *et al.*, 2005).

Inhalation of 250 ppm CO for 1 h before exposure to a lethal dose of LPS increased survival in rats by 86% compared to those without CO treatment (Sarady *et al.*, 2004). Moreover, treatment with this amount of CO for 3 h prior to LPS administration reduced levels of the pro-inflammatory cytokines (IL-6 and TNF- $\alpha$ ) and increased production of IL-10 in a rat macrophage cell line. Similar results were found with CO-RM treatment of human umbilical vein endothelial cells (Cepinskas *et al.*, 2008), suggesting that endogenous CO can modulate the inflammatory response and protect cells and organisms by the restoration of homeostasis.

Paradoxically, the anti-inflammatory role of CO might suggest that this gas could inhibit the innate immune response against microbial infections; indeed, there is evidence that administration of CORM-2 decreases the production of superoxide and NO in macrophages and blocks the oxidative burst, the first defence of macrophages against pathogens (Srisook *et al.*, 2006). This led to the suggestion that the anti-inflammatory properties of CO may be sufficient to resolve inflammation in inflammatory models of disease, but not to clear live pathogens from the host (Chin and Otterbein, 2009).

However, there is evidence that CO is also able to promote bacterial clearance, and that it does not suppress host defences. For example, over-expression of HO-1 was found to reduce death following *E. faecalis* infection, but not during *E. coli* infection, without the suppression of circulating inflammatory cells (Chung *et al.*, 2008). Furthermore, CO has been shown to increase phagocytosis of heat killed *E. coli* by RAW 264.7 macrophage

cells, by increased expression of Toll-like receptor 4 (TLR-4) (Otterbein *et al.*, 2005), while, more recently, CORM-3 (Desmard *et al.*, 2009) and CORM-2 (Desmard *et al.*, 2012) have been shown to increase survival and antimicrobial response following bacterial infection in mice.

This previously unappreciated role of CO in promoting the innate host response to infection has significant implications for the potential use of CO and CO-RMs as antimicrobial agents. Importantly, the finding that CO can eradicate bacterial infections in immuno-compromised mice (Desmard *et al.*, 2009) suggests that CO may have a direct bactericidal effect, as discussed below.

### **1.3.2 The effects of CO-RMs on bacterial growth and viability**

Until recently, very little research has been done into the effects of CO on bacterial growth and viability. Despite this, CO gas has been used for many years to reduce bacterial growth in the meat packaging industry. CO reacts with myoglobin on the surface of the meat to produce carboxymyoglobin, which has a bright red colour, making the meat more visually appealing to consumers (El-Badawi *et al.*, 1964). It was later found that CO could extend the shelf-life of packaged beef by inhibiting microbial growth (Clark *et al.*, 1976). Another early observation of the deleterious effects of CO on bacteria (Weigel and Englund, 1975), reported that this gas inhibited DNA replication in aerobically grown *E. coli* cells, which they suggested could be caused by a reduction in the amount of ATP available.

Significant new research has provided evidence that CO and CO-RMs can have a direct bactericidal effect (Davidge *et al.*, 2009b; Desmard *et al.*, 2009; Nobre *et al.*, 2009; Nobre *et al.*, 2007). Work by Saraiva and colleagues found that CORM-2 and CORM-3 and the CO-RMs ALF021 and ALF062 could significantly reduce the viability of both *E. coli* and *S. aureus* cells, providing the first evidence that CO from CO-RMs is bactericidal towards both Gram-positive and Gram-negative bacteria. CO was shown to be the causative agent of these effects as CO-RMs had no effect in the presence of haemoglobin a CO-scavenger, and inactive control compounds, also had no effect on cell viability (Nobre *et al.*, 2007).

The potential of CORM-3 as an antimicrobial therapeutic was also demonstrated by the ability of very low concentrations (0.5 – 10  $\mu\text{M}$ ) to inhibit the growth of an antibiotic resistant strain of *P. aeruginosa in vitro* at concentrations of that were 50-fold lower than concentrations that were toxic to eukaryotic cells (Desmard *et al.*, 2009). Moreover, 10  $\mu\text{M}$  CORM-3 was as effective at reducing the bacterial count *in vitro* as the established antibiotics amikacine (50 mg  $\text{l}^{-1}$ , or 0.8 mM) and ticarcilline (50 mg  $\text{kg}^{-1}$ ). CORM-2 is also effective at preventing *P. aeruginosa* biofilm maturation and at killing cells within established biofilms (Murray *et al.*, 2012). Interestingly, CORM-2 was found to be more effective when combined with tobramycin, an established antibiotic used to treat *P. aeruginosa* pulmonary infections.

Davidge *et al.* (2009b) found both aerobic and anaerobic cultures of *E. coli* to be sensitive to CORM-3; however, they demonstrated that CORM-3 completely prevented the growth of aerobic cultures at lower concentrations (100  $\mu\text{M}$ ) than was needed to prevent the growth and viability of anaerobic cultures (200  $\mu\text{M}$ ). Moreover, 30  $\mu\text{M}$  CORM-3 reduced the number of viable cells 10-fold in 2 h in aerobic conditions, whereas 100  $\mu\text{M}$  CORM-3 had no effect on the viability of anaerobic cultures within this time. The greater susceptibility of aerobic cultures concurs with our understanding of CO as a known inhibitor of aerobic respiration; however as CO is known to be a competitive inhibitor with oxygen, it is surprising that CO is inhibitory even at high oxygen concentrations. In contrast, Nobre *et al.* (2007) found CO-RMs to be more toxic towards anaerobic cells than aerobic cells, which they suggest may be due to CO binding to the ferrous form of haemoproteins, which are abundant at low oxygen concentrations. They propose that the stronger effect of CO-RMs on anaerobically grown cells implies the existence of significant targets of CO other than the cytochrome-containing terminal oxidases of aerobic respiration. The reasons for the different findings with regards to aerobic and anaerobic cultures of these two groups are not clear, but may be due to the type and concentration of CO-RM used: Davidge *et al.* used CORM-3, whereas Nobre *et al.* used high concentrations of ALF 021, ALF 062 and CORM-2. It is possible that CORM-2 and CORM-3 have different mechanisms of toxicity, as is discussed in Chapter 5. Inspection of the results of Nobre *et al.* (2007) reveals that, after 30 min, the viability of aerobic cultures was much more affected by

the addition of CORM-2 than that of anaerobically grown cultures, but that by 1 h after the addition of CORM-2, this trend has reversed, although to a lesser extent.

Interestingly, CO-RMs are more effective at preventing bacterial growth than the equivalent concentration of CO-saturated solution (Davidge *et al.*, 2009b, Nobre *et al.*, 2007). This was unexpected as CO gas delivered in solution is expected to be highly membrane-permeable, but may indicate that CO-RMs deliver CO directly to intracellular targets, a hypothesis confirmed by assaying for the presence of CO in the extracellular medium using myoglobin. In the absence of *E. coli*, CO from CORM-3 rapidly bound to Mb; however in the presence of *E. coli*, only 28% of the initial CO was found to be present in the extracellular medium after 10 min, suggesting it had been taken up by the cells and was therefore no longer accessible to the Mb. Further evidence of the direct delivery of CO by CO-RMs is that ruthenium from CORM-3 (Davidge *et al.*, 2009b) and molybdenum from ALF062 (Nobre *et al.*, 2007) were found to accumulate inside *E. coli* cells. Accumulation of ruthenium was greater in aerobic cells (where the concentration of ruthenium was 7-fold greater than that in the culture) compared to that in anaerobic cells (in which the concentration of ruthenium was 2.1-fold greater than in the culture), which may partly explain the greater sensitivity of aerobic cells to CORM-3 (Davidge *et al.*, 2009b). Table 1.4 presents a comparison of the effects of CO and CO-RMs on bacteria.

### **1.3.3 The effects of CO-RMs on bacterial respiration**

It has been known for nearly 90 years that CO inhibits bacterial respiration (reviewed by Keilin, 1966). As described previously (section 1.2.3.2), CO mediates this inhibition by binding to ferrous iron in the haem groups of terminal oxidases in the aerobic respiratory chain. This led to the assumption that bacterial respiration was a major target of CO from CO-RMs (as discussed in Chapter 3). For example, CO gas is known to bind to cytochrome *c* oxidase in *P. aeruginosa* (Parr *et al.*, 1975) and, more recently, aerobic cultures of *P. aeruginosa* treated with CORM-3 have been shown to exhibit reduced oxygen uptake followed by a reduced growth rate (Desmard *et al.*, 2009). Furthermore, when cultures of *E. coli* were stressed with 30  $\mu$ M CORM-3 for 2 h and then washed before respiration was measured, respiration rates were significantly diminished (although this effect was not immediate) (Davidge, 2009). Spectroscopic

analysis of several bacterial species, including *E. coli* (Davidge *et al.*, 2009b), *P. aeruginosa* (Desmard *et al.*, 2009) and *C. jejuni* (Smith *et al.*, 2011), treated with CORM-3 has confirmed that CO from such compounds binds rapidly to the terminal oxidases of the respiratory chain, as discussed in Chapter 3.

A recent publication has provided a detailed study of the effects of CORM-3 on microbial respiration (Wilson *et al.*, 2013). Addition of CORM-3 to cultures of *E. coli* resulted in a period of respiratory stimulation followed by inhibition, while higher concentrations of CORM-3 resulted in increased stimulation for a shorter time period, followed by more marked inhibition. It was concluded that the initial increase in respiration rate upon CORM-3 addition is not due to a direct stimulatory effect of CORM-3 on oxidase activity, or to the uncoupling of electron transport from the generation of the proton motive force as is true of classical respiratory uncouplers such as CCCP (Lou *et al.*, 2007). Instead, it is hypothesised that CORM-3 enables the movement of potassium or sodium ions into the cell, which results in less back pressure from positive charges outside of the cell, and therefore favours proton extrusion coupled to respiration (Wilson *et al.*, 2013). It was also found that incubation of CORM-3 with the bacterial suspension under anoxic conditions for increased time periods resulted in greater inhibition. Respiratory inhibition was also observed in *P. aeruginosa*, *Salmonella enterica* serovar Typhimurium and the yeast *Candida albicans*, although a higher concentration of CORM-3, 250  $\mu\text{M}$  instead of 100  $\mu\text{M}$ , was needed to see these effects in yeast.

It was initially assumed that the inhibition of respiration by CO from CO-RMs was a major cause of killing by these compounds (Davidge *et al.*, 2009b; Desmard *et al.*, 2009). However, the fact that cultures grown anaerobically also experience decreased viability in the presence of CO (Nobre *et al.*, 2007, Nobre *et al.*, 2009 and Davidge *et al.*, 2009b), suggests that aerobic respiration is not the only site of action of CO in bacteria. Further evidence that the inhibition of respiration may not be the main cause of killing by CO-RMs is provided by a study on the effects of CORM-3 on the growth and respiration of *C. jejuni* (Smith *et al.*, 2011). In this bacterium, 100  $\mu\text{M}$  CORM-3 diminished the rate of respiration, but had no effect on the growth rate. This was unexpected, as it was assumed that CO-RMs would be more inhibitory to *C. jejuni* as it

grows under microaerobic conditions, which could be expected to favour competitive inhibition by CO. It was suggested that *C. jejuni* may be better able to tolerate CO, due to its ability to grow on haem as an iron source consummate with its pathogenic lifestyle (Smith *et al.*, 2011).

#### **1.3.4 The effects of CO-RMs on gene expression**

To date, three studies have investigated the effects of CO-RMs on transcriptional regulation in *E. coli*. Nobre *et al.* (2009) concluded that CORM-2 has a greater effect on gene expression in anaerobic cultures as genes belonging to eight functional classes were down-regulated anaerobically, but not affected aerobically; this is in agreement with the findings of this group that anaerobic cultures are more sensitive to this compound. This work showed that the expression of the redox sensors OxyR and SoxS, which activate the expression of Fur, a repressor of ferric ion uptake, is up-regulated by CORM-2. The gene *oxyR* was up-regulated in aerobic conditions in the presence of CORM-2, whereas the expression of *soxS* was up-regulated at all oxygen tensions. Evidence was also presented that CORM-2 affects methionine metabolism and biofilm formation.

In contrast, Davidge *et al.* (2009b) found transcription in aerobic cultures to be affected more by CORM-3 than that in anaerobic conditions. They found CORM-3 to up-regulate 63 genes and down-regulate 183 genes aerobically compared to the up-regulation of 29 genes and down-regulation of 41 genes anaerobically. Many of the down-regulated genes encode important aerobic respiratory complexes confirming that aerobic respiration is a major target of CORM-3 (Davidge *et al.*, 2009b). Most notable was the 10 - 22-fold reduction in transcription of the *cyo* operon, which encodes the cytochrome *bo'* terminal oxidase involved in aerobic respiration; the *sdh* operon that encodes succinate dehydrogenase, which links the citric acid cycle to the electron transport chain and the *nuo* operon, which encodes NADH dehydrogenase-1. In contrast, cytochrome *bd-I*, which has a high affinity for oxygen was up-regulated by CORM-3. The increase in cytochrome *bd-I* levels and the reduction in cytochrome *bo'* was confirmed spectrophotometrically (Davidge *et al.*, 2009b). Anaerobically, although fewer genes were affected, there was still down-regulation of some of the genes

involved in respiration, including those encoding some of the subunits of cytochrome *bo'* and cytochrome *bd-I* (Davidge *et al.*, 2009b).

Both groups found genes involved in regulating transition metal metabolism, homeostasis and transport within the cell to be differentially expressed, particularly those involved with iron, zinc and copper. This is consistent with the propensity of CO to bind to transition metals (Boczkowski *et al.*, 2006).

The most affected gene in the presence of CORM-3 was *spy*, an envelope-stress-induced periplasmic protein that is regulated by the transcription factors BaeSR and CpxAR and is induced by zinc and copper. The *spy* gene was up-regulated more than 100-fold anaerobically, and 26-fold aerobically, although the reason for this dramatic up-regulation is not understood. Other zinc-related genes were also affected leading to the suggestion that CORM-3 adversely affects zinc release (Davidge *et al.*, 2009b). This gene was also up-regulated by CORM-2, and was affected more in aerobic conditions than in anaerobic conditions (Nobre *et al.*, 2009).

Interestingly, genes encoding transporters were affected, which could suggest attempts by the cell to prevent entry of CORM-3, or to increase efflux. The genes encoding the methyl-galactoside transporter (*mglABC*) were down-regulated, while those encoding the *mdtABC* operon, which is involved in a multi-drug export system, were up-regulated by 8 - 13-fold (Davidge *et al.*, 2009b).

This work used statistical modelling of the array data to identify 8 transcription factors that are significantly affected by CORM-3: ArcA, FNR, CRP, Fis, Fur, BaeR, CpxR and IHF (Davidge *et al.*, 2009b). It is difficult to envisage how most of these are affected by CO, although the response of ArcA is understood. The two-component system, ArcAB responds to changes in the redox state of the respiratory chain. Inhibition of respiration by CO from CORM-3 would lead to accumulation of reduced ubiquinone, which allows auto-phosphorylation of ArcB and the subsequent phosphorylation of ArcA, which inhibits the transcription of ArcA-regulated genes, including those encoding components of the aerobic respiratory chain (Davidge *et al.*, 2009b).



A subsequent time-resolved transcriptional analysis compared the effects of a sub-lethal concentration of CORM-3 (40  $\mu$ M) with the control compound iCORM-3 on gene expression in aerobically grown *E. coli* (McLean *et al.*, 2013). The control compound evoked a much smaller transcriptomic response than CORM-3, with only 2% of the genome significantly affected, compared to 23% at 40 min in the presence of CORM-3.

Both CORM-3 and iCORM-3 altered the expression of several genes involved in energy metabolism, amino acid metabolism and ABC (ATP-binding cassette) transport. The expression of genes involved in sulfate transport and utilization were also affected by both. However CORM-3 had a wider range of effects than iCORM-3, and also affected the expression of genes involved in signal transduction, carbohydrate metabolism and cell motility. That motility is affected by CO was confirmed by swarming assays, in which significantly less swarming occurred in an atmosphere of 50% CO compared to control conditions. Following the discovery that the *dppABCDF* operon, which encodes a dipeptide permease, is down-regulated, growth and ruthenium uptake analysis was performed to assess whether this transporter is responsible for CO-RM uptake; however this was not found to be the case. This transporter is also capable of acting as a haem permease (Letoffe *et al.*, 2006), which could indicate a role in the acquisition of haem to replace haem centers that have been damaged by CO.

#### **1.4 The aerobic respiratory chain of *Escherichia coli***

Respiration is an essential process that allows the generation of a proton motive force across a proton-impermeable membrane, by the net movement of protons from the cytoplasm to the periplasm in gram negative bacteria (Poole and Cook, 2000). This proton gradient can be used for the production of ATP or other processes that require energy, such as solute transport or motility.

Aerobic respiration in bacteria involves the transfer of electrons from an electron-donating substrate through a series of electron carriers that are sequentially oxidised and reduced, before the final transfer of the electrons to O<sub>2</sub>, and the formation of H<sub>2</sub>O. The complete reduction of O<sub>2</sub> to H<sub>2</sub>O requires 4 electrons. Aerobic respiration is favourable compared to anaerobic energy production, as the redox potential of oxygen reduction to water is + 815 mV and therefore results in more ATP generation than other terminal

electron acceptors such as the reduction of  $\text{NO}_3^-$  to  $\text{NO}_2^-$  (with a redox potential of +430 mV), or that of fumarate to succinate (+33 mV) (Poole and Cook, 2000). However, the use of oxygen as an electron acceptor requires its activation by a metal center, generally provided by two haem groups or a haem-copper center in the active site of terminal oxidases.

Most bacteria have a degree of redundancy in their respiratory chains, which allows them to respond to, and survive in, many different environmental conditions (reviewed by Poole and Cook, 2000). *E. coli* is a particularly good example of this. As exemplified above, not only can *E. coli* respire both aerobically and anaerobically using a variety of different substrates (and in the case of anaerobic respiration; using a range of electron acceptors), its aerobic respiratory chain can consist of 5 possible NADH:quinone oxidoreductases and 3 possible terminal oxidases. NADH dehydrogenase 1 (NDH-1) (Ohnishi *et al.*, 1994) translocates 4 protons across the membrane for each pair of electrons that it accepts (Calhoun *et al.*, 1993), while NDH-2 (Bjorklof *et al.*, 2000) is not electrogenic (Calhoun *et al.*, 1993). The other three NADH:quinone oxidoreductases; WrbA (Patridge and Ferry, 2006), YhdH (Sulzenbacher *et al.*, 2004) and QOR (Thorn *et al.*, 1995), are also not thought to contribute to the generation of the proton motive force. A diagrammatic representation of the main components of the branched aerobic respiratory chain of *E. coli* is shown in Figure 1.4.

By using different combinations of these respiratory chain components, different amounts of ATP can be produced for each molecule of oxygen that is reduced. This flexibility may allow the cell to respond to the varying rate at which electrons enter the respiratory chain, and allow more efficient production of products from the carbon source by minimising ATP and therefore biomass production (Calhoun *et al.*, 1993). The expression of respiratory chain components is precisely regulated and depends on several factors, including growth rate and the environmental conditions such as pH.

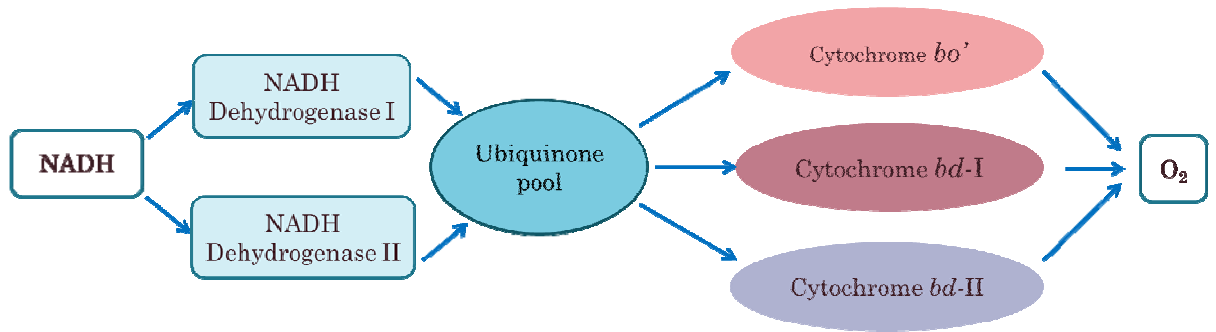


**Figure 1.4 The branched aerobic respiratory chain of *E. coli*.** The arrows represent the flow of electrons through the respiratory chain. The information used to generate this figure was obtained from (Borisov *et al.*, 2011b).

### 1.4.1 The terminal oxidases of the aerobic respiratory chain

The three terminal oxidases that can be expressed in *E. coli* are cytochrome *bo'*, cytochrome *bd-I* and cytochrome *bd-II*. All three catalyse the oxidation of ubiquinol and the reduction of oxygen to water, yet each have distinctive properties, outlined below. Each oxidase has a different affinity for oxygen (D'mello *et al.*, 1996), contribution to proton translocation (Calhoun and Gennis, 1993) and pattern of expression as a result of transcriptional regulation (Gunsalus, 1992; Tseng, 1996). A diagrammatic representation of cytochrome *bo'* and cytochrome *bd*-type oxidases can be seen in Figure 1.5.

#### 1.4.1.1 Cytochrome *bo'*

Cytochrome *bo'* is a haem-copper oxidase containing the redox centres haem *b*, haem *o'* and Cu<sub>B</sub>. It is expressed at high oxygen concentrations as it has a relatively low affinity for oxygen ( $K_m = 0.016 - 0.35 \mu\text{M}$  (D'mello *et al.*, 1995)), but a high affinity for ubiquinol. Cytochrome *bo'* is a proton pump and actively translocates up to 4 protons across the bacterial membrane for each pair of electrons that it accepts (Puustinen *et al.*, 1989). A low-spin six-coordinate haem (haem *b*) oxidises ubiquinol and transfers electrons to the binuclear centre, which is composed of a five-coordinate high-spin haem *o'* and a copper ion (Cu<sub>B</sub>). It is at this binuclear centre that oxygen is reduced to water (Mogi *et al.*, 1994).

Cytochrome *bo'* is encoded by the *cyo* operon, the expression of which is repressed under anaerobic conditions by the ArcA/ArcB two-component system and the transcriptional regulator, Fnr (Gunsalus and Park, 1994). The expression of this oxidase is also affected by the available carbon source used for growth and is up-regulated by iron limitation.

#### 1.4.1.2 Cytochrome *bd-I*

Cytochrome *bd-I* has 3 redox centres, low-spin haem *b*<sub>558</sub> and high-spin haem *b*<sub>595</sub> and haem *d* (Borisov, 1996; Junemann, 1997; Trumppower and Gennis, 1994). Oxygen binds to haem *d* and is reduced to water by a unique di-haem site comprising haems *b*<sub>595</sub>, and *d*. Cytochrome *bd-I* has an exceptionally high affinity for oxygen ( $K_m$  of 3-8 nM

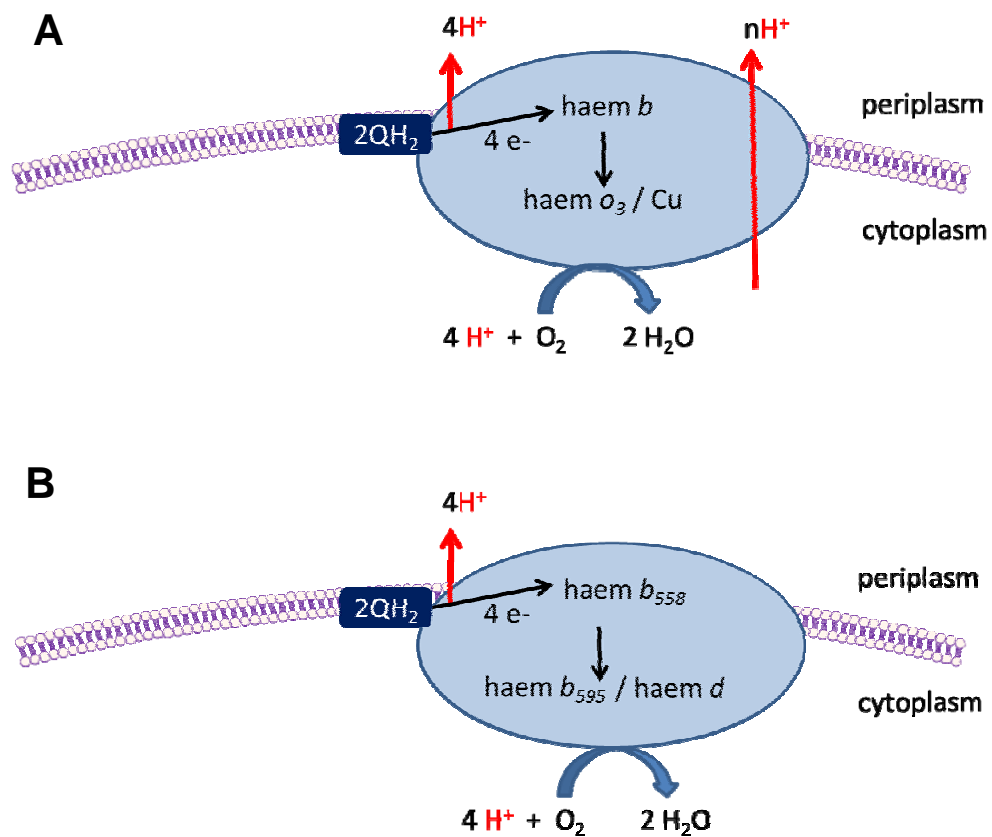


**Figure 1.5 The terminal oxidases of *E. coli*** This scheme shows the transfer of protons and electrons from 2 quinols and the ultimate reduction of 1 molecule of oxygen. Four electrons are required for this process and 4 protons are extruded from the ubiquinol. In the case of cytochrome *bo'* (**A**), a variable number of protons are also pumped through the membrane by this oxidase, although this does not occur for cytochromes *bd-I* or *bd-II* (**B**). The information used to generate these figures came from (Borisov *et al.*, 2011b; Jasaitis *et al.*, 2000).

(D'mello *et al.*, 1996)) and a relatively low affinity for ubiquinol. Unlike cytochrome *bo'*, cytochrome *bd-I* does not actively pump protons across the membrane; however, the oxidation of ubiquinol at the periplasmic side of the membrane releases protons, while the reduction of oxygen to water occurs at the cytoplasmic face of the membrane and requires the consumption of protons, therefore resulting in a net translocation of 2 protons for each pair of electrons transferred to O<sub>2</sub> (Puustinen *et al.*, 1991).

Cytochrome *bd-I* is encoded by the *cydAB* operon, and like cytochrome *bo'*, expression of this oxidase is repressed by Fnr anaerobically (Gunsalus and Park, 1994); however, in contrast, expression is induced under low oxygen conditions by the ArcA/ArcB two-component system. This leads to maximal gene expression under microaerobic conditions. Arc also regulates the expression of this operon in response to heat shock.

In addition to the role of cytochrome *bd-I* in enabling aerobic respiration in microaerobic conditions, it has also been suggested that this oxidase may be required to help *E. coli* survive when faced with unfavourable growth conditions (Avetisyan *et al.*, 1991) and environmental stresses (Poole and Cook, 2000; Poole *et al.*, 1989), and that high levels of cytochrome *bd-I* may be related to increased virulence of certain pathogens (Borisov *et al.*, 2007). Additionally, cytochrome *bd-I* may protect *E. coli* from NO-induced growth inhibition (Mason *et al.*, 2009). Exposure of *E. coli* to NO up-regulates expression of *cydAB* and causes greater inhibition of growth and respiration in a strain containing cytochrome *bo'* as the only terminal oxidase (see section 3.3.3).

#### **1.4.1.3 Cytochrome *bd-II***

The third, more recently recognised terminal oxidase, cytochrome *bd-II* (Sturr *et al.*, 1996), is able to reduce oxygen to water, but was initially suggested to be non-electrogenic, and therefore was thought to provide a route by which catabolism could be uncoupled from ATP synthesis (Bekker *et al.*, 2009). However, a more recent paper has disputed this and presents evidence that cytochrome *bd-II* does generate a proton motive force and thus contributes to the synthesis of ATP and the transport of nutrients (Borisov *et al.*, 2011b). This work shows that cytochrome *bd-II* generates this proton gradient in the same way as cytochrome *bd-I*, and that it too extrudes approximately 2 H<sup>+</sup> for each pair of electrons transferred to O<sub>2</sub>.

Cytochrome *bd*-II has a lower affinity for ubiquinol than the other terminal oxidases of *E. coli*, while the affinity of this oxidase for O<sub>2</sub> is under dispute. Measurements made using a membrane-covered Clark electrode suggested the  $K_m$  of cytochrome *bd*-II for oxygen was 2  $\mu$ M (Bekker *et al.*, 2009), although this method is insufficiently sensitive to accurately measure such values. A recent paper calculated the oxygen affinity of this oxidase using leghaemoglobin deoxygenation measurements and reported a  $K_m$  value almost 10-fold lower (0.24  $\mu$ M) (Jesse *et al.*, 2013). Irrespective of this discrepancy, it is clear that cytochrome *bd*-II has a lower oxygen affinity than cytochrome *bd*-I.

The amino acid sequences of both subunits of cytochrome *bd*-I and *bd*-II are highly homologous (approximately 60% identity). Cytochrome *bd*-II is encoded by the *appBC* operon (Dassa *et al.*, 1991), which is regulated by the transcriptional activator AppY (Atlung and Brondsted, 1994). Expression of this operon is induced by anaerobic conditions, upon entry into the stationary phase and by carbon or phosphate starvation.

#### **1.4.1.4 Kinetics of CO binding to and dissociation from the terminal oxidases of *E. coli***

In cytochrome *bd*-I, CO binds predominantly to haem *d*, however, at high concentrations (mM) some CO binds to haem *b*<sub>558</sub>, despite this being a low-spin haem (Borisov, 2008). The  $K_d$  value for cytochrome *bd*-I in membranes is fast as compared to heme-copper oxidases, 70 nM for cytochrome *bd*-I, as measured using myoglobin (Borisov, 2008), compared to 1.7  $\mu$ M for cytochrome *bo*' (Cheesman *et al.*, 1993). For cytochrome *bd* - I, the  $k_{off}$  is 6 or 1.6 s<sup>-1</sup> according to the method used (Borisov *et al.*, 2007). The experimentally determined  $K_d$  is consistent with the faster off rate of 6 s<sup>-1</sup> (Borisov, 2008). However, there are disagreements in the literature; Cheesman *et al.* (1993) report a  $K_{off}$  (CO) value of < 10 s<sup>-1</sup> for cytochrome *bo*', but the dependence of the pseudo-first-order rate upon CO concentration suggests a value around 1 s<sup>-1</sup>. Subsequent citing of these data, however, gives a  $K_{off}$  (CO) value of 0.1 s<sup>-1</sup> (Hill, 1994). This suggests that the different sensitivities of cytochrome *bo*' and *bd*-I for CO cannot be explained by the respective CO off-rates (Jesse *et al.*, 2013). The affinity of cytochrome *bd*-II for CO has not been reported.

#### **1.4.2 An exception to the rule: the alternative oxidase (AOX)**

In contrast to the terminal oxidases described above, some bacteria, notably the marine organism *Vibrio fischeri*, contain a functioning terminal oxidase that does not contain haem. This oxidase will be discussed in detail in Chapter 4.

#### **1.5 Conclusions and scope of thesis.**

Despite the established perception of CO as a respiratory inhibitor and ‘toxic’ molecule, appreciation has grown in recent years of the importance of this endogenous molecule in mammalian physiology, not least as a regulator of vascular tone and the inflammatory response to infection, as well as its vital role in maintaining cellular homeostasis. Preclinical and clinical trials into the use of CO as a therapeutic agent are underway, and CO, delivered through inhalation or through administration as a CO-RM, is hoped to have wide-reaching potential (Motterlini *et al.*, 2005a).

Many bacteria can utilize CO as a carbon source and many bacteria, particularly pathogenic and commensal species, possess HOs, and therefore produce this gas endogenously. There is a long history of the addition of CO to meat packaging in order to improve appearance, and reduce microbial growth (Clark *et al.*, 1976). However, it is only in the past six years, following the advent of CO-RMs, that CO has been investigated as a potential bactericidal agent. CORM-3 has been shown to be bactericidal to clinical isolates of *P. aeruginosa* at concentrations 50-fold lower than those that cause cytotoxicity to mammalian cells (Desmard *et al.*, 2009). Several CO-RMs have been shown to be bactericidal to numerous species of Gram-positive (Nobre *et al.*, 2007) and Gram-negative (Davidge *et al.*, 2009b) bacteria, although as yet, the mechanism(s) of killing by these compounds is not clear.

CO-RMs are particularly promising as novel antimicrobial agents for several reasons. Firstly, the rapid rise in antibiotic-resistant microbes is limiting the usefulness of traditional antibiotics, which is likely to have devastating consequences within the next few years unless alternative therapeutically safe bactericidal drugs can be established. Secondly, CO-RMs provide ideal means of storing CO and facilitating its delivery, with the potential to control CO release, directly to the site at which it is needed. A variety of CO-RMs are available, with a wide array of properties, and much research and several



clinical trials are underway into the use of many of these as therapeutic agents. Thirdly, CO-RMs have been shown to be much more effective at killing bacterial cells than the equivalent concentration of CO gas (Davidge *et al.*, 2009b; Nobre *et al.*, 2007). This potentiation of the bactericidal effects of CO is hypothesised to be due to the delivery of CO into bacterial cells, causing an accumulation of CO at the micro-domains at which it acts, although this is still unproven.

However, many questions remain in this new field. It is not well understood how CO-RMs kill bacteria. Initially, inhibition of respiration was considered to be a likely cause of the bactericidal properties of CO-RMs, and several pieces of evidence support this hypothesis. CO from CORM-3 has been shown to bind rapidly to the terminal oxidases of the aerobic respiratory chains of *E. coli* (Davidge *et al.*, 2009b) and *P. aeruginosa*, and a reduction in oxygen consumption in the later has been observed following treatment with this compound, prior to a decrease in viability (Desmard *et al.*, 2009). In contrast, there is evidence that inhibition of respiration is not the main cause of killing by CO-RMs. In *C. jejuni*, CO-RMs have been shown to inhibit respiration, without adversely effecting growth or viability (Smith *et al.*, 2011), and transcriptomic analysis of *E. coli* treated with CORM-3 suggests that while respiratory genes are greatly affected by this compound, the expression levels of a wide variety of non-respiratory genes are also significantly affected (Davidge *et al.*, 2009b). Furthermore, the growth and viability of anaerobic cultures is also adversely affected by treatment with CORM-3 (Davidge *et al.*, 2009b) and CORM-2 (Nobre *et al.*, 2009).

An alternative hypothesis is that CO-RMs are bactericidal because they generate ROS (Tavares *et al.*, 2011). Again there are several pieces of evidence both for and against this suggestion. Research has shown that CORM-2 generates hydroxyl radicals *in vitro*, and that *E. coli* mutants unable to resist oxidative stress are hypersensitive to killing by this compound (Tavares *et al.*, 2011). However, other work has found no evidence of ROS formation by CORM-3 (Desmard *et al.*, 2009; Desmard *et al.*, 2012) or CORM-2

(Murray *et al.*, 2012). Figure 1.6 shows a diagrammatic representation of our understanding of the effects of CO-RMs on bacterial cells.

The work presented in this thesis therefore aims to investigate the mechanisms of bacterial killing by CO-RMs, particularly by water-soluble CORM-3. Initial work focused on investigating the effects of CO-RMs on bacterial respiration, and particularly on the interaction of CO from CORM-3 with the terminal oxidases of the aerobic respiratory chain of the model organism *E. coli* (Chapter 3). Important differences between the behaviour of CO gas and CO from CO-RMs necessitated a thorough comparison of the effects of these two compounds on respiration. This work was extended through an investigation of the effects of CORM-3 on the growth and respiration of a mutant strain of the marine bacterium *Vibrio fischeri* (Chapter 4). This bacterium naturally contains a non-haem oxidase, AOX (alternative oxidase); therefore it was hypothesised that, if inhibition of haem-containing terminal oxidases is the primary cause of killing by CO-RMs, a strain of *V. fischeri* containing AOX as the only oxidase should be resistant to killing by this compound.

Another unanswered question with regards to the mechanisms of CO-RM action is why thiol-containing compounds such as *N*-acetyl cysteine (NAC), cysteine and reduced glutathione (GSH) prevent the bactericidal action of CO-RMs. There is conflicting evidence as to whether it is the anti-oxidant properties of these molecules that ameliorate the effects of CO-RMs (Desmard *et al.*, 2012; Tavares *et al.*, 2011). Therefore, a thorough investigation was undertaken into the mechanisms by which thiol compounds prevent killing by CO-RMs, and into whether CORM-3 causes the production of reactive oxygen species (Chapter 5).

Finally, uncertainty surrounding the mechanisms of action of CO-RMs on bacteria led to a search for new bacterial targets of CO-RMs. Consequently, random transposon mutants of *E. coli* were generated and then screened for CORM-2-resistance (Chapter 6).

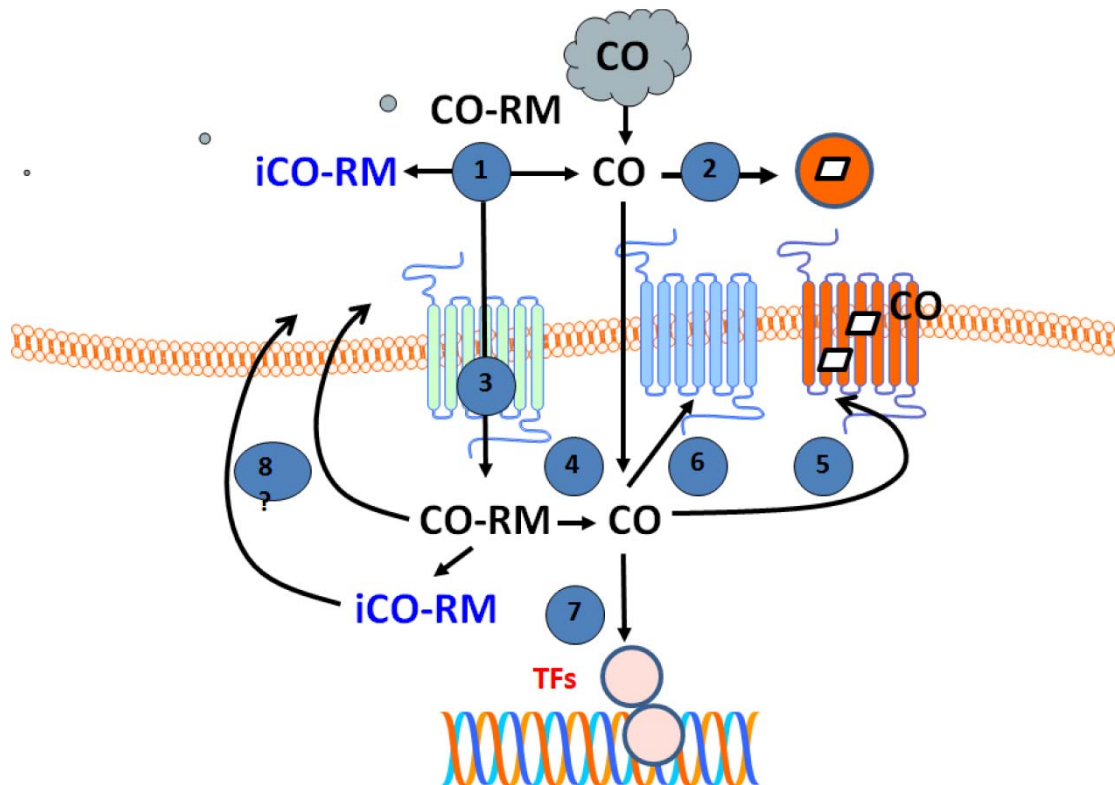


**Figure 1.6 The effects of CO-RMs on the bacterial cell.** CO-RMs may release CO extracellularly (1); external CO could then be detected using myoglobin (2). Alternatively, CO-RMs may be transported into the cell (3) by unknown pathways (possibly via a membrane importer as shown). Once inside the cell, the CO dissociates (4) from the CO-RM (with formation of iCO-RM, the inactive form). CO will then react with biological targets, including the haem centres of terminal oxidases in the cell membrane (5). Other targets include membrane transporters (6) and transcription factors (7) that regulate gene expression. The fate of CO-RM or iCO-RM in the cell is unknown but it is possible that the compounds are exported (8).

## Chapter 2

### Materials and Methods

#### 2.1 Bacteriological Methods

##### 2.1.1 Strains

The bacterial strains used in this work are described in Table 2.1

##### 2.1.2 Media

All media were prepared with distilled, deionised water and sterilised by autoclaving at 121 psi for 15 min. Unless stated otherwise, all chemicals were purchased from Sigma Aldrich and solutions were filter-sterilised as needed using Millipore filters with a pore size of 0.2  $\mu\text{m}$ .

###### 2.1.2.1 Luria Bertani broth (LB)

Into 1 l of  $\text{H}_2\text{O}$  was dissolved tryptone (10 g), yeast extract (5 g) (both from Oxoid) and NaCl (10 g) (BDH). The pH was then adjusted to 7.0 (Sambrook and Russell, 2001).

###### 2.1.2.2 Defined minimal medium

Into 990 ml of  $\text{H}_2\text{O}$  was dissolved  $\text{K}_2\text{HPO}_4$  (4 g),  $\text{NH}_4\text{Cl}$  (1 g),  $\text{CaCl}_2$  (10 mg),  $\text{K}_2\text{SO}_4$  (2.6 g) and glycerol (5 g). To this, 10 ml of trace element solution was added. The pH was then brought to 7.4 and the media was autoclaved. Before use, 1 ml  $\text{l}^{-1}$  of 1 M  $\text{MgCl}_2$  was added.

###### 2.1.2.3 Trace element solution for defined minimal medium

Into 700 ml of  $\text{H}_2\text{O}$  was added EDTA (5 g) and the pH adjusted to 7.4. Then  $\text{FeCl}_3 \cdot 6\text{H}_2\text{O}$  (0.5 g), ZnO (50 mg),  $\text{CuCl}_2 \cdot 2\text{H}_2\text{O}$  (10 mg),  $\text{H}_3\text{BO}_3$  (10 mg), ammonium molybdate (0.12 mg) and sodium selenite (17 mg) were added. The volume was brought up to 1 l with  $\text{H}_2\text{O}$  and the media was filter-sterilised (Flatley *et al.*, 2005).

	Phenotype	Genotype	Source/Reference
<i>Escherichia coli</i>			
MG1655	Wild type, K12	Wild type	(Blattner <i>et al.</i> , 1997)
TBE023	Cyd <sup>+</sup> App <sup>+</sup> Cyo <sup>+</sup>	F <sup>-</sup> lambda <sup>-</sup> <i>ilvG rfb-50 rph-1</i> MG1655 $\Delta$ <i>nuoB</i> ::kan	Kindly given by Alex Ter Beek, University of Amsterdam
TBE025	Cyo <sup>+</sup>	MG1655 $\Delta$ <i>cydB nuoB appB</i> ::kan	Kindly given by Alex Ter Beek, University of Amsterdam
TBE026	App <sup>+</sup>	MG1655 $\Delta$ <i>cydB nuoB cyoB</i> ::kan	Kindly given by Alex Ter Beek, University of Amsterdam
TBE037	Cyd <sup>+</sup>	MG1655 $\Delta$ <i>appB nuoB cyoB</i> ::kan	Kindly given by Alex Ter Beek, University of Amsterdam
<i>frvB</i> mutant		<i>frvB</i> ::kan From the Keio collection	Kindly given by Simon Andrews, The University of Reading.
<i>manX</i> mutant		<i>manX</i> ::kan From the Keio collection	Kindly given by Simon Andrews, The University of Reading.
<i>sgaU</i> mutant		<i>sgaU</i> ::kan From the Keio collection	Kindly given by Simon Andrews, The University of Reading.
<i>I</i> <sup>H</sup> Express competent <i>E. coli</i>		BL21 MiniF <i>lacI</i> <sup>H</sup> (Cam <sup>R</sup> ) / <i>fhuA2 [lon] ompT gal sulA11</i> <i>R(mcr-73::miniTn10--Tet<sup>S</sup>)2</i> <i>[dcm] R(zgb-210::Tn10--Tet<sup>S</sup>)</i> <i>endA <math>\Delta</math>(mcrC-mrr)114::IS10</i>	New England Biosciences
<i>gshA</i> mutant		MG1655 $\Delta$ <i>gshA</i> ::kan	This work
<i>Vibrio fischeri</i>			
ES114		Wild type <i>V. fischeri</i>	(Boettcher and Ruby, 1990)
AKD788		ES114 $\Delta$ <i>aox <math>\Delta</math>ccoNOQP</i>	(Dunn <i>et al.</i> , 2010)
AKD789		ES114 $\Delta$ <i>cydAB <math>\Delta</math>ccoNOQP</i>	(Dunn <i>et al.</i> , 2010)

**Table 2.1 Bacterial strains used in this work**

#### **2.1.2.4 Evans medium**

The following solutions were added to 1 l H<sub>2</sub>O to the stated final concentrations: NaH<sub>2</sub>PO<sub>4</sub>·2H<sub>2</sub>O (10 mM), KCl (10 mM), MgCl<sub>2</sub>·6H<sub>2</sub>O (1.25 mM), NH<sub>4</sub>Cl (100 mM), Na<sub>2</sub>SO<sub>4</sub> (2 mM) and CaCl<sub>2</sub>·2H<sub>2</sub>O (20 μM). Evans trace elements solution (5 ml) and 10 μl of a 3 mg ml<sup>-1</sup> solution of Na<sub>2</sub>SeO<sub>3</sub>·5H<sub>2</sub>O was then added along with nitrilotriacetic acid (0.38 g). The pH was adjusted to 7.5 with the addition of NaOH and the solution was autoclaved. Once cool, 20 ml of 1 M sterile glucose was added (Evans, 1970).

#### **2.1.2.5 Trace element solution for Evans medium**

Into 990 ml of H<sub>2</sub>O was added 8 ml of 37% HCl, ZnO (0.412 g), FeCl<sub>3</sub>·6H<sub>2</sub>O (5.4 g), MnCl<sub>2</sub>·4H<sub>2</sub>O (2 g), CuCl<sub>2</sub>·2H<sub>2</sub>O (0.172 g), CoCl<sub>2</sub>·6H<sub>2</sub>O (0.476 g), H<sub>3</sub>BO<sub>3</sub> (64 mg) and Na<sub>2</sub>MoO<sub>4</sub>·2H<sub>2</sub>O (4 mg). The solution was then filter-sterilised.

#### **2.1.2.6 LBS medium**

To 1 l H<sub>2</sub>O was added bactotryptone (10 g), yeast extract (5 g), NaCl (20 g) and 20 ml of a 1 M solution of Tris HCl. The pH was then adjusted to 7.5 and the medium was autoclaved. When solid LBS was required, 15 g l<sup>-1</sup> of agar was added before autoclaving (Stabb *et al.*, 2001).

#### **2.1.2.7 Artificial sea water (ASW)**

To make 1 l of medium, KCl (1.5 g) and NaCl (23.38 g) was dissolved in 809 ml H<sub>2</sub>O. To this 100 ml of 1 M MgSO<sub>4</sub>, 20 ml of 1 M CaCl<sub>2</sub>, 1 ml of 5.4% (w/v) K<sub>2</sub>HPO<sub>4</sub>, 50 ml of 1 M Tris HCl (pH 7.5) and 20 ml of 0.5 M *N*-acetyl glucosamine was added. The medium was then filter-sterilised (Reichelt and Baumann, 1973).

#### **2.1.2.8 SOC medium**

To 1 l H<sub>2</sub>O was added bactotryptone (20 g), yeast extract (5 g), NaCl (0.5 g) and 10 ml of a 250 mM solution of KCl. The pH was then adjusted to pH 7 and the medium was autoclaved. Before use, 10 ml of 1 M MgCl<sub>2</sub> and 20 ml of sterile 1 M glucose was added.

#### **2.1.2.9 TY medium**

To 100 ml H<sub>2</sub>O was added bactotryptone (1.6 g), yeast extract (1 g) and NaCl (1 g), the medium was then autoclaved (Sambrook and Russell, 2001).

#### **2.1.2.10 TB medium**

To 100 ml H<sub>2</sub>O was added bactotryptone (0.8 g) and NaCl (0.5 g). The medium was then autoclaved.

#### **2.1.2.11 TB soft agar**

To make TB soft agar, agar (0.7 g) was added to TB medium (100 ml) prior to autoclaving.

#### **2.1.2.12 Nutrient agar (NA).**

Nutrient agar (Oxoid) was dissolved at 2.8% w/v in H<sub>2</sub>O.

#### **2.1.2.13 Phage lysate plates**

To 500 ml H<sub>2</sub>O was added bactotryptone (4 g), yeast extract (2.5 g), NaCl (2.5 g), glucose (1 g) and agar (6 g). This was then autoclaved and cooled to approximately 50 °C before the addition of 5 ml of 0.5 M CaCl<sub>2</sub>, 5 ml 1 M MgCl<sub>2</sub>.6H<sub>2</sub>O and 0.5 ml 10 M FeCl<sub>3</sub> (all of which had been filter-sterilized), (Miller, 1972). Plates were refrigerated immediately after pouring to ensure a moist atmosphere.

#### **2.1.2.14 LBS Plates**

To make LBS plates, agar (7.5 g) was added to LBS medium (500 ml) prior to autoclaving (Stabb *et al.*, 2001).

### **2.1.3 Buffers and Solutions**

#### **2.1.3.1 Phosphate buffered saline (PBS)**

To 1 l of H<sub>2</sub>O was added NaCl (8 g), Na<sub>2</sub>HPO<sub>4</sub> (1.15 g), KCl (0.2 g) and K<sub>2</sub>HPO<sub>4</sub> (0.2 g). The pH of this solution was the adjusted to 7.4 before autoclaving.

### **2.1.3.2 KPi buffer**

Potassium phosphate buffer was made using 1 M stock solutions of  $K_2HPO_4$  and  $KH_2PO_4$ . These were mixed together in the appropriate ratios to give the desired pH. For a solution of pH 7.0, 61.5 ml  $K_2HPO_4$  and 38.5 ml  $KH_2PO_4$  were mixed, for a solution of pH 7.4, 80.2 ml  $K_2HPO_4$  and 19.8 ml  $KH_2PO_4$  were mixed together and for a solution of pH 7.8, 90.8 ml  $K_2HPO_4$  and 9.2 ml  $KH_2PO_4$  were mixed together; each of these stocks was then diluted 1 in 10 to 0.1 M.

### **2.1.3.3 Sonication buffer**

To 1 l  $H_2O$  was added 50 mM Tris HCl (7.88 g), 2 mM  $MgCl_2$  (395.8 mg) and 1 mM EGTA (380.35 mg). The pH of this solution was the adjusted to 7.4 and then filter-sterilised.

### **2.1.3.4 *Vibrio* phosphate buffer**

To 900 ml  $H_2O$  was added 100 ml of 0.2 M potassium phosphate buffer (pH 7.8), 10 mM  $MgSO_4$  (2.46 g) and 0.2 M NaCl (11.69 g).

### **2.1.3.5 TAE buffer (50x)**

To 843 ml  $H_2O$  was added 242 g Trisma base, 57.1 ml glacial acetic acid and 100 ml  $Na_2EDTA$  (0.5 M, pH 7.8). This was then diluted 1:50 with  $H_2O$  before use to give 1x TAE buffer.

### **2.1.3.6 Phage lysate buffer**

To 500 ml  $H_2O$  was added Tris base (0.61 g),  $MgSO_4 \cdot 7H_2O$  (1.23 g),  $CaCl_2 \cdot 2H_2O$  (0.37 g) and NaCl (1.47 g). The pH was adjusted to 7.5 and the solution autoclaved (Miller, 1972).

### **2.1.3.7 Sodium dithionite solution**

A fresh solution of sodium dithionite (0.1 M) was made immediately prior to use in 5 ml KPi (0.1 M, pH 7.0, previously degassed by bubbling with  $N_2$  from a cylinder (BOC) for 10 min) in a sealed 7 ml Bijoux bottle fitted with a Suba-Seal and vent. This solution was further degassed after addition of the sodium dithionite by bubbling with  $N_2$  for 10 min.



#### **2.1.3.8 CO-saturated solution**

CO-saturated solutions were made by bubbling the appropriate buffer with CO gas from a cylinder (BOC, Guildford) in a 7 ml Bijoux bottle fitted with a Suba-Seal and gas escape needle at room temperature for 15 min. This generates a solution of approximately 1 mM, as verified spectroscopically by a myoglobin assay (section 2.3.1.1).

#### **2.1.3.9 N<sub>2</sub>-saturated solution**

N<sub>2</sub>-saturated solutions were made by bubbling the appropriate buffer with N<sub>2</sub> gas from a cylinder (BOC, Guildford) in a 7 ml Bijoux bottle fitted with a Suba-Seal and gas escape needle at room temperature for 15 min.

### **2.1.4 Strain Storage**

#### **2.1.4.1 *E. coli***

Strains were cultured on NA plates and stored at 4 °C and, when necessary, subcultured onto fresh plates. Glycerol stocks were made by adding 2 ml sterile LB medium containing 25% (v/v) glycerol onto a lawn of bacteria grown on NA. The bacteria were resuspended and removed using a sterile 1 ml pipette. This slurry was dispensed into a cryovial (Nalgene) and stored at - 80 °C.

#### **2.1.4.2 *V. fischeri***

Strains were cultured on LBS plates and stored at 4 °C. Fresh plates were made directly from the glycerol stock prior to each experiment. Glycerol stocks were made by adding 2 ml sterile LB medium containing 25% (v/v) glycerol onto a lawn of bacteria grown on NA. The bacteria were resuspended and removed using a sterile 1 ml pipette. This slurry was dispensed into a cryovial (Nalgene) and stored at - 80 °C.

#### **2.1.4.3 Bacteriophage**

P1 *vir* phage lysates were stored at 4 °C in air-tight vials containing a few drops of chloroform.

#### **2.1.4.4 Antibiotics**

Kanamycin and ampicillin stock solutions (both  $50 \mu\text{g ml}^{-1}$ ) were prepared in  $\text{H}_2\text{O}$  and filter-sterilised using a  $0.2 \mu\text{m}$  filter (Sartorius Stedim Biotech). Antibiotics were stored at  $-20 \text{ }^\circ\text{C}$ .

#### **2.1.5 Culture conditions**

All cultures were grown aerobically with shaking at 200 rpm to ensure even oxygen distribution.

##### **2.1.5.1 Cultures for *E. coli* growth and viability studies**

*E. coli* starter cultures of the appropriate strain were grown in 10 ml LB broth for 7 h and then the LB removed by centrifugation at 5500 rpm for 5 min. The cells were then washed in aerobic defined minimal medium and pelleted once more, before being resuspended in defined minimal medium (10 ml) and a 0.1 % v/v inoculum added to 30 ml aerobic defined minimal medium in side arm conical flasks. The cultures were kept at  $37 \text{ }^\circ\text{C}$  and were shaken at 200 rpm. For growth studies, CO-RM was added after the OD of the cultures reached 30 Klett units at the concentration specified in the appropriate Figure legends, whereas for viability studies, CORM-3 was added at 50 Klett units.

##### **2.1.5.2 Cultures for *V. fischeri* growth studies**

To measure the sensitivity of a strain to a range of CO-RM concentrations (0-100  $\mu\text{M}$ ), starter cultures were grown in 10 ml LBS for 6 h. The LBS was removed by centrifugation at 4500 rpm for 5 min. The cells were then washed in ASW and pelleted once more, before being resuspended in ASW. An inoculum (20  $\mu\text{l}$ ) was added to 5 ml ASW in 20 ml Sterilin tubes with the appropriate volume of CO-RM. Cultures were incubated at  $28 \text{ }^\circ\text{C}$  overnight and then  $\text{OD}_{600}$  measured using a Jenway spectrophotometer.

### **2.1.5.3 Cultures for the preparation of *E. coli* membrane particles**

To produce large quantities of cells from which to isolate membranes, starter cultures were grown in 5 ml LB broth and incubated at 37 °C with shaking at 200 rpm for 16 h. Each starter culture was then added to 995 ml of LB broth in 2 l baffled flasks, which were also kept at 37 °C, with shaking, until mid-exponential phase was reached. For each membrane preparation, 6 l of culture was grown.

### **2.1.5.4 Cultures for the preparation of *V. fischeri* membrane particles**

Starter cultures were grown in 5 ml LBS broth and incubated at 28 °C for 16 h. An aliquot of this culture (2 ml) was then added to 1 l of LBS broth in 2 l conical flasks, which were also kept at 28 °C and shaken at 200 rpm until the culture reached an OD<sub>600</sub> of 1.0. For each membrane preparation, 5 l of culture was grown.

### **2.1.5.5 Growing and sampling bacterial cells for ruthenium analysis (ICP-MS)**

Evans medium (200 ml) supplemented with glucose (4 ml of a 1 M stock solution) was transferred to a sterile 500 ml conical flask and inoculated with 10 µM starter culture of the appropriate strain, which had been grown for 8 h in LB and then pelleted and resuspended in double the volume of Evans medium. This was incubated overnight at 37 °C with shaking at 200 rpm. When the cells reached an OD<sub>600</sub> of approximately 0.4, a 20 ml sample was removed. Where appropriate, 40 µM CORM-3 or 20 µM CORM-2 in combination with a 10 fold molar excess of NAC was added and the culture placed back in the incubator. Samples (20 ml) were taken at 2.5, 5, 10, 20, 40 and 80 min following the addition of CORM-3. The OD<sub>600</sub> of the culture was read at each time-point. Each sample was centrifuged for 20 min at 5,500 rpm at 4 °C. The supernatant was reserved. The cell pellet was resuspended in 0.5 ml nitric acid (0.5%) and this was centrifuged at 13,000 rpm for 5 min. This wash step was repeated twice more and the supernatant from each wash was retained along with the final pellet. This method was adapted from that described by (Davidge *et al.*, 2009b; Graham *et al.*, 2009). The protocol for ICP-MS is described in section 2.3.2.4.

### **2.1.6 Culture turbidity measurements**

In order to measure the growth of a culture, the optical density was measured using a Klett-Summerson photoelectric colourimeter (Klett Manufacturing Co., New York)

with a number 66 red filter. A blank containing the sterile medium was used. Cultures were grown in conical side arm flasks, which allowed the optical density reading to be taken without removing any culture from the flask.

## **2.1.7 Screening a library of *E. coli* transposon mutants**

### **2.1.7.1 The initial CORM-2 screen**

Cells treated with transposon (250  $\mu$ l) were inoculated into 30 ml defined minimal medium in each of 3 Klett flasks. These cultures were incubated at 37 °C with shaking at 250 rpm until they reached approximately 25 Klett units (early exponential phase). CORM-2 (40  $\mu$ M) or the equivalent concentration of the vehicle DMSO, was added, and the cultures incubated for a further 30 min at 37 °C with shaking at 250 rpm. The cultures were then washed by centrifugation at 4500 rpm for 4 min at 4 °C and then resuspended in 10 ml of defined minimal medium and then the centrifugation step repeated before finally resuspending in 500  $\mu$ l defined minimal medium. This was then plated onto nutrient agar containing 30  $\mu$ g ml<sup>-1</sup> kanamycin.

### **2.1.7.2 The second stage of the screen**

Each of the 288 kanamycin and putatively CORM-2 resistant colonies obtained in the initial CORM-2 screen was inoculated into 200  $\mu$ l defined minimal medium in wells of a 96-well plate and grown for 8 h until a typical OD<sub>600</sub> of between 0.1 and 0.3 was reached. CORM-2 (40  $\mu$ M) was then added to each well and incubated at 37 °C with shaking for 16 h. OD<sub>600</sub> was measured on a multilabel reader (Victor™ X3, Perkin Elmer). Mutants were regarded as interesting if they had an increase in OD<sub>600</sub> > 0.2, 16 h after treatment with CORM-2.

### **2.1.7.3 CORM-2 susceptibility assay**

To measure the sensitivity of a strain to a range of CORM-2 concentrations (0-1.5  $\mu$ M), starter cultures were prepared as described above (section 2.1.5.1) and a 20  $\mu$ l inoculum added to 5 ml defined minimal medium in 20 ml Sterilin tubes with the appropriate volume of CORM-2. Cultures were incubated at 37 °C overnight with shaking at 200 rpm and then OD<sub>600</sub> measured using a spectrophotometer (Jenway).

#### **2.1.7.4 The growth of transposon mutants of interest on plates containing CORM-2**

Overnight cultures of each transposon mutant of interest were grown in LB (10 ml). The cultures were harvested by centrifugation at 5000 rpm at 4 °C for 5 min, and the pellets resuspended in 10 ml defined minimal medium. An aliquot of each culture (50 µl) was added to 2.95 ml of molten defined minimal medium with 0.7% agar and maintained at 50 °C, before the addition of various concentrations of CORM-2 (20 - 40 µM). This was mixed and poured onto a base layer of defined minimal medium with 1.5% agar and incubated overnight.

#### **2.1.7.5 Gradient plates**

Gradient plates consisting of two layers of agar were made as described by Gerhardt (1994) and used by Poole *et al.* (1989). The first layer consisted of defined minimal medium containing 1.5% agar, which was set at an angle (achieved by balancing the plate on the edge of a plate lid). The second layer consisted of defined minimal medium containing 0.7% agar, to which (after cooling to approximately 50 °C) 60 µM CORM-2 was added. This agar containing CORM-2 was poured on to the first layer, resulting in a level agar plate, which had a maximal quantity of CORM-2 at one apex of the plate, which decreased gradually across the plate (for a diagrammatic representation of the construction of this plate, see Figure 6.5A and B). Cultures of each transposon mutant of interest, and the parent strain, were grown overnight in LB (10 ml) at 37 °C with shaking at 250 rpm; these cultures were then harvested by centrifugation at 5000 rpm at 4 °C for 5 min, washed by resuspending in defined minimal medium, harvested once more and finally resuspended in 200 µl defined minimal medium. An aliquot of this suspension (50 µl) was streaked onto the CORM-2 gradient plates using a Gilson pipette to release the cell suspension along the concentration gradient, starting at the apex that had the least CORM-2. Care was taken to apply the suspension evenly and consistently between strains. The plates were then incubated at 37 °C overnight and then growth observed by eye.

### **2.1.8 Viability Studies**

#### **2.1.8.1 Viability Studies with *E. coli***

Cultures were prepared as described above (section 2.1.5.1). In the case of CORM-3, samples were taken immediately prior to addition of CORM-3 or iCORM-3 (both at 30

$\mu\text{M}$ ) and at 10, 20, 30, 45, 60, 90 and 120 min thereafter, whereas in the case of CO-RM-2, samples were taken immediately prior to addition of the CO-RM or  $\text{RuCl}_2(\text{DMSO})_4$  (20 - 50  $\mu\text{M}$ ) and after 30 min. Samples were diluted ( $10^{-5}$ - $10^{-8}$ ) and plated on to nutrient agar thus allowing the  $\text{cfu ml}^{-1}$  to be calculated. The experiments were performed with 3 independent cultures.

#### **2.1.8.1.1 Measuring the effect of photolysis on the viability of *E. coli***

To evaluate the effect of photolysis of the haem-CO bond on bacterial viability, wild-type MG1655 *E. coli* was grown to mid-exponential phase (50 Klett units) and 2 ml of culture transferred into each of two glass chambers (Strathkelvin instruments); one dark chamber (foil-wrapped) and one light chamber, on which a beam of light from a 150 W projector bulb was focused using a magnifying glass. Cultures were held at 37 °C and stirred magnetically at 260 rpm. Viable counts were performed as described above (section 2.1.8.1).

#### **2.1.9 Isolation of bacterial membrane particles**

Cells grown as described in section 2.1.5.1 and 2.1.5.2 were harvested by centrifugation at 12,000 g for 10 min at 4 °C. The pellets were then washed by resuspending in 8 ml of sonication buffer (for *E. coli*) or *Vibrio* phosphate buffer (for *V. fischeri*) and pelleting by centrifugation at 5500 rpm for 10 min at 4 °C. The cells were then resuspended in 4 ml buffer to make a thick slurry and then broken by sonication at 12  $\mu\text{m}$  amplitude for 5 intervals of 30 s with a 15 s rest between each. The cells were kept on ice throughout this process. The sonicate was then centrifuged at 12000 g for 15 min at 4 °C in order to remove the unbroken cells. These unbroken cells were sonicated once more as above in order to ensure maximal cell breakage. The sonicate was centrifuged again at 12000 g for 15 min at 4 °C. The supernatant was then spun in an ultracentrifuge at 225,000 g for 60 min at 4 °C in order to remove the membranes from the cytoplasm. The pellet obtained was resuspended in buffer using a glass homogeniser and the ultracentrifugation step repeated in order to wash the membranes. Finally, the pellets were resuspended in 3 ml buffer, frozen in liquid nitrogen and stored at – 70 °C in 200  $\mu\text{l}$  aliquots until required. This protocol is based on that of Poole (1993).

## **2.2 Biochemical Methods**

### **2.2.1 Carbon monoxide-releasing molecules (CO-RMs)**

#### **2.2.1.1 Synthesis of CORM-3**

CORM-3 was either provided by Dr. Roberto Motterlini and Professor Brian Mann (Hemocorm), or synthesised by the following method as published by (Johnson *et al.*, 2007). CORM-2 ( $[\text{Ru}(\text{CO})_3\text{Cl}_2]_2$ , 0.129 g) and glycine (0.039 g) were placed under nitrogen in a round bottomed flask. Methanol (75 ml) and sodium ethoxide (0.034 g) were added and the reaction progressed for 18 h at room temperature while being magnetically stirred. The solvent was then removed under pressure and the residue redissolved in tetrahydrofuran. This was filtered and diethyl ether was added, followed by an excess of 40 - 60 light petroleum. The yellow solution was then evaporated under reduced pressure to give a pale yellow solid (typically 0.142 g, 96% yield). The purity of the CORM-3 preparation was assessed by infrared Anvel cell spectrophotometry performed by Dr. Robert Hanson and  $^1\text{H}$  NMR in methanol performed by Dr. Brian Taylor (both in the Chemistry Department of The University of Sheffield). CO-release by each CORM-3 preparation was measured spectroscopically by a myoglobin assay (Johnson *et al.*, 2007) (see section 2.3.1.1).

#### **2.2.1.2 Preparation of CO-RM stock solutions and control compounds**

##### **2.2.1.2.1 CORM-2**

CORM-2 was purchased from Sigma Aldrich. Fresh 10 mM stock solutions were made each hour by dissolving in DMSO and wrapped in foil to exclude light.

##### **2.2.1.2.2 CORM-3**

CORM-3 (tricarbonylchloro(glyinato)ruthenium(II)) was obtained from Professor Brian Mann (Alfama, previously Hemocorm). Stock solutions (10 mM or 100 mM) were made by dissolving in water and stored on ice. Stocks were used fresh or on the following day after overnight storage at 4 °C.

##### **2.2.1.2.3 CORM-401**

CORM-401  $[\text{Mn}(\text{CO})_4(\text{S}_2\text{CNMeCH}_2\text{CO}_2\text{H})]$ , was obtained from Professor Brian Mann (Alfama, previously Hemocorm). Stock solutions (5 mM) were made by dissolving in PBS (pH 7.4, section 2.1.3.1).

#### **2.2.1.2.4 Preparation of RuCl<sub>2</sub>(DMSO)<sub>4</sub>**

RuCl<sub>2</sub>(DMSO)<sub>4</sub> was provided by Dr. Tony Johnson (Chemistry Department, University of Sheffield). A solution of this compound (100 mM) was prepared fresh for each experiment in distilled H<sub>2</sub>O.

#### **2.2.1.2.5 Preparation of iCORM-3 (inactive CORM-3)**

CORM-3 was dissolved in PBS to give a 5 mM solution. This was bubbled with nitrogen for 5 min immediately after it was made and then for 5 min every 2 h the following day (Clark *et al.*, 2003; McLean *et al.*, 2012). On the day of use, the solution was bubbled once more with nitrogen for 5 min. The lid was left off during the day, but closed overnight. Immediately prior to use, a myoglobin assay was performed (see section 2.3.1.1) to confirm that no CO was released from the iCORM-3.

#### **2.2.1.2.6 Preparation of miCORM-3**

miCORM-3 was prepared by treating CORM-3 twice with a 2-fold excess of ferrous myoglobin, reduced by adding sodium dithionite solution (2.2 mM final concentration in 0.1 M potassium phosphate, pH 7) to 1 mM metmyoglobin. Carbonmonoxy myoglobin was separated from the inactivated CORM-3 by centrifugation in a Vivaspin 20 concentrator (Sartorius Stedim Biotech) with a molecular weight cut-off of 5 kDa (Wilson *et al.*, 2013). Immediately prior to use, a myoglobin assay was performed (see section 2.3.1.1) to confirm that no CO was released from the miCORM-3.

### **2.2.2 Determination of protein concentration**

The concentration of protein in whole cell and membrane samples was determined using the protocol established by Markwell *et al.* (1978). Cell and membrane samples were diluted as appropriate, typically by a factor of 20 initially, followed by 1 in 100, 5 in 100, or 1 in 10 dilutions. Reagent A (100 parts) containing Na<sub>2</sub>CO<sub>3</sub> (20 g l<sup>-1</sup>), NaOH (4 g l<sup>-1</sup>), sodium tartrate (1.6 g l<sup>-1</sup>) and sodium dodecyl sulphate (SDS, 10 g l<sup>-1</sup>) was mixed with 1 part reagent B (CuSO<sub>4</sub>.5H<sub>2</sub>O, 40 g l<sup>-1</sup>); 3 ml of this was then added to each sample dilution. This was left to incubate at room temperature for 1 h, after which, 0.3 ml Folin-Ciocalteu (Lowry) reagent (diluted 1:1 with H<sub>2</sub>O) was added to the samples and incubated at room temperature for a further 45 min. The absorbance of each sample



at 660 nm was then measured using a spectrophotometer (Jenway) against a H<sub>2</sub>O blank. The standard curve of protein amount against A<sub>660</sub> was plotted and the equation of the line obtained. Protein concentrations (mg ml<sup>-1</sup>) were determined using a standard curve constructed using a range of dilutions of bovine serum albumin (BSA, 20 µg ml<sup>-1</sup> to 200 µg ml<sup>-1</sup>).

### **2.2.3 DTNB thiol assay**

Ellman's reagent (DTNB, 5,5'-dithiobis-[2-nitrobenzoic acid]) is reduced by free thiol groups causing the production of 5-thio-2-nitrobenzoic acid, which has a spectroscopic feature at 412 nm.

#### **2.2.3.1 The DTNB assay with variation of thiol concentration**

In an assay to investigate whether a range of CO-RMs and control molecules are able to react with thiol groups, various concentrations (10 – 200 µM) of NAC were incubated for 5 min with 100 µM of each of the following: CORM-3, CORM-2, iCORM-3, RuCl<sub>2</sub>(DMSO)<sub>4</sub>, CO-saturated solution or CORM-A1. DTNB (0.8 mM) was then added and incubated for 15 min. The OD<sub>412</sub> was measured using a spectrophotometer (Jenway).

#### **2.2.3.2 The DTNB assay with variation of CO-RM concentration**

In an additional experiment, the thiol containing compounds cysteine, reduced glutathione and sodium hydrosulphide were incubated for 15 min with various concentrations (25 – 1000 µM) of either CORM-3, iCORM-3, or CO-saturated solution in KPi (0.1 M pH 7.0). DTNB (0.5 mM) was then added and incubated for 15 min. The OD<sub>412</sub> was measured using a Jenway spectrophotometer.

#### **2.2.3.3 The DTNB assay to determine intracellular thiol concentration**

Starter cultures of wild type MG1655 *E. coli* and the *gshA* mutant in an MG1655 background were grown for 8 h in 5 ml LB and 100 µl used to inoculate 20 ml LB in a 250 ml conical flask, which was then incubated at 37 °C for 16 h with shaking at 200 rpm. Cells were harvested by centrifugation at 5500 rpm for 5 min and then resuspended in 2 ml sonication buffer. Cells were broken by sonication at 12 µm amplitude for 5 intervals of 30 s with a 15 s rest between each, and the unbroken cells

removed by centrifugation (5500 rpm, 5 min). DTNB (0.8 M) was added to the cell free extract, which had been diluted by a factor of 4, and the  $A_{412}$  measured after 15 min incubation. Three technical and three biological replicates were performed. The concentration of thiol compounds in the sample was established by comparing the  $A_{412}$  of the samples to a standard curve (0 – 0.1 mM NAC). This method is adapted from Goldman *et al.* (1996).

#### **2.2.4 Superoxide Assay**

Cytochrome *c* (20  $\mu$ M) was added to the CO-RM or control molecule (1 mM), or CORM-3 pre-incubated for 5 min with NAC (1 mM) in KPi, pH 7.8. The  $OD_{550}$  was then read over a time course, as the reduction of cytochrome *c* causes an increase in absorbance at this wavelength. Superoxide dismutase (SOD, 250 units) was included as a control to determine whether the increase in absorbance detected is caused by superoxide. This method is adapted from Korshunov and Imlay (2006).

#### **2.2.5 Amplex red assay for hydrogen peroxide**

Hydrogen peroxide production by *E. coli* treated with CORM-3 was assayed using the Amplex Red Hydrogen Peroxide / Peroxidase Assay Kit (Invitrogen), which uses 10-acetyl-3,7-dihydroxyphenoxazine to react with  $H_2O_2$  in a 1:1 stoichiometry to produce the fluorescent oxidation product resorufin, which has excitation and emission maximum of approximately 571 nm and 585 nm respectively. This assay is extremely sensitive and can detect as little as 10 picomoles  $H_2O_2$  in 100  $\mu$ l.

A starter culture of wild type MG1655 *E. coli* was grown in 10 ml defined minimal medium for 17 h and then harvested by centrifugation (5500 rpm, 5 min, 4 °C) and then resuspended in 2 ml (1x) reaction buffer, which gave an  $OD_{600}$  of 9.2. This was then further diluted with reaction buffer to give a final  $OD_{600}$  of 0.09. The Amplex red reaction mixture was made up according to the manufacturer's protocol and contained the amplex red reagent dissolved in DMSO, reaction buffer and horse radish peroxidase. An aliquot of this mixture (to give a final total volume of 50  $\mu$ l) was added to wells of a 96-well plate along with 5  $\mu$ l cell suspension alone or with either CORM-3 (100  $\mu$ M), CORM-3 with glycerol (5 mM) or glycerol alone. A standard curve was generated using a series of dilutions of  $H_2O_2$  (0 – 10  $\mu$ M). The absorbance at 560 nm was measured

spectrophotometrically (Victor™ X3, Perkin Elmer). Method adapted from Seaver and Imlay (2001).

### **2.2.6 Oxygen electrode for measurement of respiration rates**

Respiration was measured using a Clark-type oxygen electrode (OXY041A, Rank Bros Ltd., Bottisham, CB25 9DA) operating at a polarising voltage of 0.6 V. This consists of a chamber separated from an electrode by an oxygen-permeable Teflon membrane. The oxygen is reduced at the cathode and creates a potential difference, which is recorded by a chart recorder (REC112, Amersham Pharmacia Biotech). The chamber is kept at a constant temperature by connection to a water bath, and the reaction mixture is constantly stirred magnetically (Gilberthorpe and Poole, 2008). The oxygen electrode was calibrated using air-equilibrated buffer appropriate for the sample type to establish maximal dissolved oxygen tensions; a few grains of sodium dithionite were added to remove all oxygen for the chamber to calibrate for 0% dissolved oxygen. A photograph of the oxygen electrode is shown in Figure 2.1.

#### **2.2.6.1 Closed electrode experiments**

A small amount of bacterial membrane suspension (adjusted to give a final protein concentration typically between 60 and 275  $\mu\text{g ml}^{-1}$ ) was added to sonication buffer (used with *E. coli* membrane particles) or *Vibrio* phosphate buffer to a final volume of 2 ml. The lid was then replaced and the system was left for several minutes to allow the amount of oxygen in the chamber to stabilise. Respiration was stimulated by the addition of 6.25 mM NADH, and then the compound of interest (for example CO-RM, CO-saturated solution, or control compound), was added at an oxygen tension of approximately 150  $\mu\text{M}$ . The precise concentrations of compounds added are detailed in each experimental chapter. Where appropriate, thiol compounds, antioxidants or SOD were added to the chamber 1 min prior to the addition of CO-RM. Compounds were added through a hole in the lid using a Hamilton syringe to prevent additional oxygen from being added to the chamber. Respiration rates were calculated as nmol O<sub>2</sub>

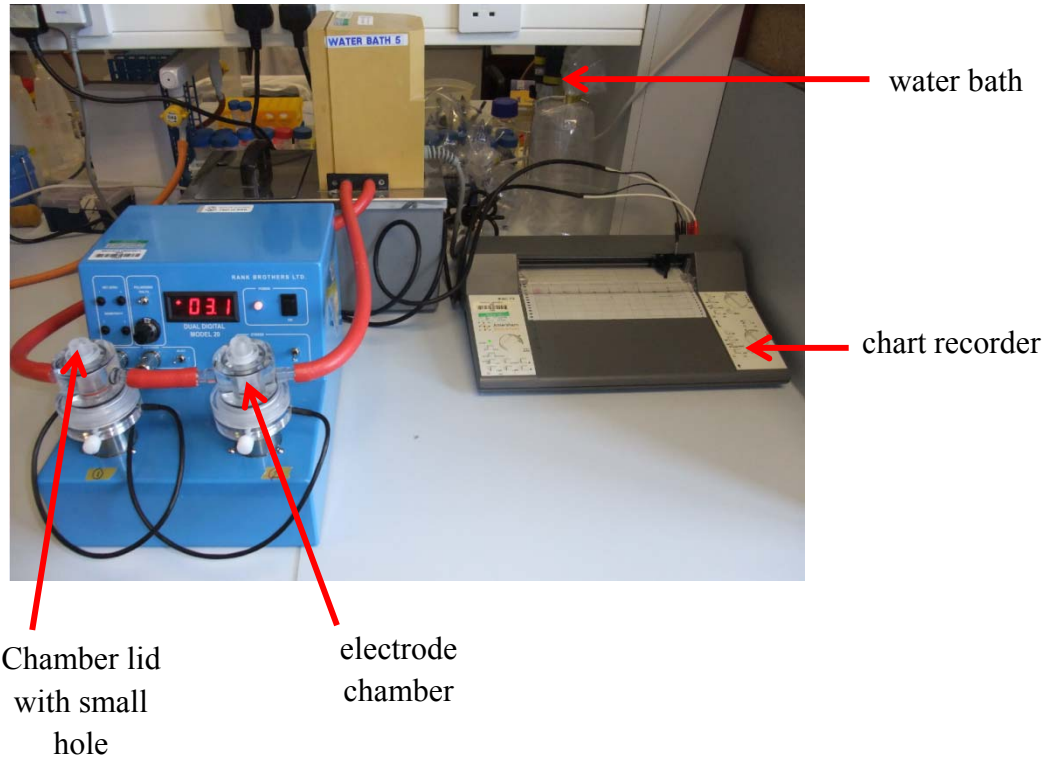


**Figure 2.1 Oxygen electrode for measurement of respiration rates.**

consumed per min per mg of protein (measured using the Markwell assay described in section 2.2.2).

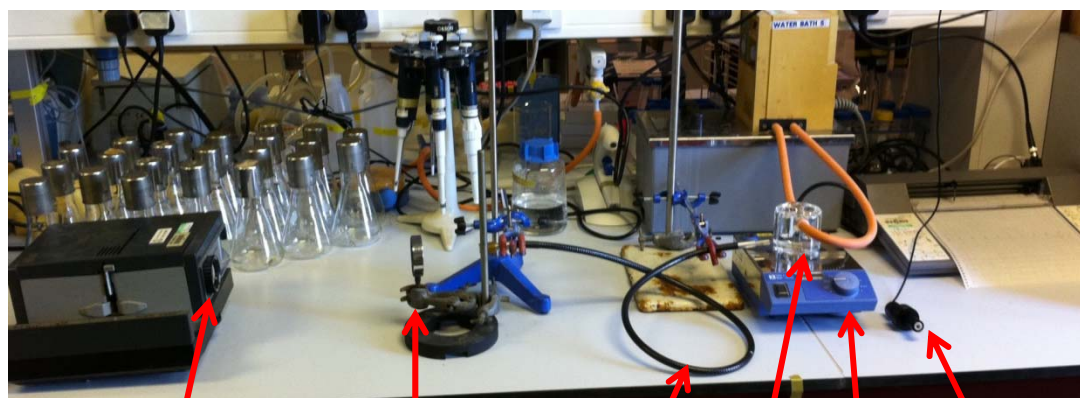
#### **2.2.6.2 Photolysis of the haem – CO bond**

Membranes were prepared from each *E. coli* single oxidase-containing strain as described in (Poole, 1993) and resuspended in 1.95 ml N<sub>2</sub>-saturated sonication buffer mixed with 50 µl air-saturated sonication buffer and placed in a glass chamber held at 37 °C (Strathkelvin instruments) and stirred magnetically at a moderate speed. CORM-3 (300 µM) was added and respiration was stimulated by addition of 12.5 mM NADH. A microcathode O<sub>2</sub> electrode (SI130; Strathkelvin Instruments Limited) connected to an O<sub>2</sub> meter (Model 781) was placed in the chamber. Prior to use, the electrode was calibrated using air-saturated buffer and by the addition of sodium dithionite (50 µl of a 0.1 M solution, section 2.1.3.7) to remove all oxygen from the system. A 150 W projector bulb was used as a source of white light, and the beam focused on the wall of the glass chamber using a magnifying glass and an optical light guide. The intensity of light at the vessel surface was measured as 175,000 lux. The light was switched on and off at 1 or 2 min intervals. The oxygen level in the chamber was recorded using Data-Trax™ software using a Lab-Trax-4/16 recorder (World Precision Instruments). A photograph of the apparatus used in this experiment is shown in Figure 2.2.

#### **2.2.6.3 Open electrode experiments**

##### **2.2.6.3.1 Respiratory studies utilising membranes subjected to various oxygen tensions**

Membranes were prepared from wild-type *E. coli*, MG1655 as described previously (Poole, 1993). Membranes (175 µg ml<sup>-1</sup>, resuspended in 2 ml of sonication buffer) were transferred to an open, stirred chamber fitted with a Clark-type polarographic oxygen electrode (Rank Brothers) and held at 37 °C. Respiration was stimulated by the addition of 12.5 mM NADH. The speed of stirring was manipulated so that a steady state was achieved at either a high (approximately 75% of air saturation), low (approximately 15% of air saturation) or very low (approximately 3% of air saturation) oxygen level. CORM-3 or RuCl<sub>2</sub>(DMSO)<sub>4</sub> at 50 µM were added 2 min after the oxygen equilibrium had been reached. Respiration rates were calculated for both the CORM-3-inhibited and



Projector  
(150 W  
bulb)

magnifying  
glass

light  
guide

glass  
chamber

magnetic  
stirrer

Oxygen  
electrode in  
chamber lid,  
connected to an  
oxygen meter

**Figure 2.2 Apparatus to measure oxygen consumption following photolysis.**

control cultures (with either RuCl<sub>2</sub>(DMSO)<sub>4</sub> or nothing added) at 10 and 20 min after the addition of compound.

#### **2.2.6.3.2 Measuring the time taken for the electrode chamber to reoxygenate**

The extent of respiratory inhibition of bacterial membrane particles was determined using an open electrode system in which the time taken for a sample to begin to re-accumulate oxygen following a period of anoxia is measured as previously described (Hendgen-Cotta *et al.*, 2008; Shiva *et al.*, 2007). In this experimental design, the sample is open to the atmosphere and is stirred magnetically allowing continuous O<sub>2</sub> diffusion from the vortex surface into the sample with a typical K<sub>L</sub>a value of 0.35 min<sup>-1</sup>. K<sub>L</sub>a is the gas transfer coefficient from gas to liquid and is dependent on reaction volume, surface area and temperature (Pirt, 1985). The respiration of more sensitive strains will be inhibited to a greater extent and so will not be able to utilise the oxygen in the chamber as quickly, leading to a shorter time to reoxygenation.

In order to compare the sensitivity of the terminal oxidase of *E. coli* to respiratory inhibition, membranes prepared from mutants containing only one of the three terminal oxidases of *E. coli* were added to the chamber to a final concentration of approximately 370 µg ml<sup>-1</sup> and stimulated to respire by the addition of 12.5 mM NADH. The stirring speed was set to 5 as, in the absence of compound, this maintained the oxygen level in the chamber at 0 for an extended period of time after the lid had been removed. Either CORM-3 or miCORM-3 (100 µM) was added 2 min after the oxygen in the chamber had reached 0, and the lid was then immediately removed. The time taken for the oxygen levels in the chamber to rise above 0 was recorded.

In order to compare the sensitivity of the terminal oxidase of *V. fischeri* to respiratory inhibition, membranes prepared from wild type *V. fischeri* or mutants containing either AOX or cytochrome *bd* as the only terminal oxidase were resuspended in *Vibrio* phosphate buffer to a final concentration of approximately 40 mg ml<sup>-1</sup>, added to the electrode chamber, which was stirred magnetically at speed 5. The sample was stimulated to respire by the addition of 12.5 mM NADH. CORM-3 or iCORM-3 (both at 25 µM) or CN<sup>-</sup> (100 µM) were added 1 min after the dissolved oxygen tension in the

chamber reached 0% and the lid removed 1 min later. The time taken for the oxygen levels in the chamber to rise above 0 was recorded.

In order to assess whether NAC is able to protect bacterial respiration from inhibition by CORM-3, wild-type *E. coli* membrane particles were resuspended in sonication buffer (2 ml) to a final concentration of approximately 1.5 mg ml<sup>-1</sup> and placed in an electrode chamber, which was stirred magnetically at speed 5. Respiration was initiated by the addition of NADH (6.25 mM). Where appropriate, NAC (400 µM) was added to the chamber 1 min before the addition of CORM-3 (400 µM); after a further minute, the lid was removed and the time taken for the chamber to reoxygenate was recorded.

## **2.3 Spectroscopic methods**

### **2.3.1 Measurement of CO release from CO-RMs**

#### **2.3.1.1 Myoglobin assay for the measurement of CO loss from CORM-3**

CO release from CORM-3 and control molecules to ferrous myoglobin was assayed as before (Clark *et al.*, 2003), using an SDB4 dual-wavelength scanning spectrophotometer (The Johnson Foundation, University of Pennsylvania Biomedical Instrumentation Group and Current designs Inc., Philadelphia, PA, USA). This spectrophotometer scans samples from 400 to 700 nm in 0.5 nm increments. The data was analysed using *SoftSDB* software and then plotted using Sigma Plot (Systat Software Inc.). Horse heart Mb (10 µM) in 0.1 M KPi (pH 7.4) was reduced by the addition of a few grains of sodium dithionite, and this was scanned in triplicate as a baseline.

In order to assess CO release from CORM-3 and control compounds, CORM-3 (8 µM) (pre-incubated for 5 min with various concentrations of NAC where appropriate) was added to the reduced myoglobin (10 µM), in a cuvette with 10 mm path length, and rapidly mixed before recording CO reduced *minus* reduced difference spectra in triplicate. Data were averaged and the spectrum of reduced myoglobin was subtracted from that of the CO-RM treated, reduced myoglobin. The change in absorbance was calculated as the difference between the peak and trough in the Soret region (426 – 441 nm) of this difference spectrum, using Excel software. Where appropriate, the extinction coefficient of Mb-CO (177 mM<sup>-1</sup> cm<sup>-1</sup>) was used to calculate the concentration of Mb-CO formed over time (Wood, 1984).



### 2.3.1.2 Haemoglobin assay

This assay measures the release of CO from CO-RMs without the presence of dithionite, which has been shown to facilitate CO loss from some CO-RMs including CORM-2 and CORM-3 (McLean *et al.*, 2012).

Haemoglobin (Sigma, grade P90%) was dissolved in 0.1 M KPi (pH 7.4) and reduced by the addition of a few grains of sodium dithionite. This was then passed down a PD MiniTrap G-25 column (GE Healthcare) to remove the excess dithionite and generate oxyferrous-haemoglobin. The concentration of reduced oxy-hamoglobin was measured spectrophotometrically using the known extinction coefficient for bovine muscle haemoglobin ( $133 \text{ mm}^{-1} \text{ cm}^{-1}$ , at 430 nm). CORM-3 (8  $\mu\text{M}$ ) (pre-incubated for 5 min with 80  $\mu\text{M}$  NAC when appropriate) was added to 10  $\mu\text{M}$  oxyferrous-haemoglobin. Scans were taken every 30 s for 10 min, then every 1 min for the next 10 min and every 5 min for the next 20 min using a scanning kinetics program (Cary 50). Difference spectra were then obtained by subtracting the oxyferrous-haemoglobin spectrum from the CORM-3 treated spectra in Excel, followed by plotting of the data in Sigma Plot.

### 2.3.1.3 Measurement of CO binding to cytochromes

For *E. coli*, membrane particles (prepared as described above, section 2.1.9) were suspended in sonication buffer to a final protein concentration of 8 – 33  $\text{mg ml}^{-1}$  whereas, for *V. fischeri*, samples were suspended in *Vibrio* phosphate buffer to a final protein concentration of 2 - 4  $\text{mg ml}^{-1}$  for membrane particles, or 12 - 14  $\mu\text{g ml}^{-1}$  for whole cell samples grown to  $\text{OD}_{600}$  1.0, as described above (section 2.1.5.4). Samples were transferred to a cuvette of 10 mm path length and reduced with sodium dithionite and spectra recorded in a Johnson Foundation SDB4 dual-wavelength spectrophotometer as detailed above (2.3.1.1) at room temperature (Kalnenieks *et al.*, 1998). This reduced sample spectrum was recorded in triplicate and assigned as the baseline, before the addition of CO-saturated solution, CORM-3 (pre-incubated with 1 mM NAC where appropriate), iCORM-3 or  $\text{RuCl}_2(\text{DMSO})_4$  (each at 100 $\mu\text{M}$ ). The CO treated samples were scanned in triplicate and spectra were viewed using *SoftSDB* software. Data were averaged and the spectrum of reduced myoglobin was subtracted from that of the CO-treated, reduced myoglobin to produce what is termed a CO reduced *minus* reduced, or CO difference spectra. Where appropriate, the change in

absorbance was calculated as the difference between the peak and trough in the Soret region (426 – 441 nm) of this difference spectrum, using Excel software, and then plotted in Sigma Plot. Where stated, data have been smoothed in Sigma plot graphing software with a sampling proportion of 0.1 and a polynomial degree of 9.

#### **2.3.1.4 ICP-MS**

Pellets were digested with 1 ml nitric acid (Aristar, 69% v/v) for 60 min and then diluted to 5 ml with 1% nitric acid. Analysis of ruthenium (mass 101) was done using an Agilent 7500CE ICP-MS (inductively coupled plasma-mass spectrometer) instrument using rhodium (mass 103) as an internal standard. Calibration standards were made up in 20% nitric acid to match the samples (blank, 25, 50 and 250  $\mu\text{g l}^{-1}$  ruthenium). With each batch of samples a sample blank was prepared comprising 1 ml nitric acid diluted to 5 ml with 1% nitric acid. This work was done at the Centre for Analytical Sciences (CAS, University of Sheffield) (Davidge *et al.*, 2009b; Graham *et al.*, 2009).

#### **2.3.1.5 Electron paramagnetic resonance (EPR) spectroscopy**

The spin trap BMPO (5-tert-butoxycarbonyl 5-methyl-1-pyrroline N-oxide) (Enzo Life Sciences) was used to allow superoxide and hydroxyl radicals to be detected, identified and quantified. Superoxide and hydroxyl adducts of BMPO were generated to provide reference spectra for comparison with the CO-RM spectra. The components for each sample are described in the relevant figure legends. Samples were loaded into an AquaX cell and EPR spectra were recorded, at room temperature, on a Bruker EMX spectrometer at 9.47 GHz microwave frequency, 3.18 mW microwave power, 100 kHz modulation frequency and 9.54  $\text{G s}^{-1}$  scan rate. Spectra were analysed using WINEPR, Version 2.11 (Bruker). This work was done in collaboration with Dr. Dimitri Svistunenko at the University of Essex.

### **2.4 Genetic and molecular techniques**

#### **2.4.1 Generalised transduction with bacteriophage P1 vir**

This was done to transfer the *gshA* mutation into an MG1655 background, and to transfer the mutated genes identified as important in the CORM-2 resistance screen

from independently sourced strains from the Keio collection (Simon Andrews, The University of Reading) into an MG1655 background.

#### **2.4.1.1 Preparation of lysates**

Donor cells were grown overnight at 37 °C in TY medium with CaCl<sub>2</sub> (5 mM) with antibiotic where necessary. A P1 stock was diluted to 10<sup>8</sup>, 10<sup>7</sup> and 10<sup>6</sup> PFU ml<sup>-1</sup>, and each was mixed with donor cells (100 µl) and incubated at 37 °C for 20 min. This phage / cell mixture was then added to TB medium (1 ml) and TB soft agar (1.5 ml) both at 50 °C, and then poured onto phage lysate plates, which were incubated in a wet atmosphere at 37 °C until plaques appeared giving the plates a ‘lacy’ appearance. The plates were then chilled at 4 °C for 20 min before cold phage dilution buffer was carefully added to the surface of the plates. These were then stored overnight at 4 °C, and then the overlay liquid was harvested using a Pasteur pipette and filtered through a 0.45 µm filter to exclude any bacterial cells. Phage lysates were stored over a drop of chloroform in sterile, screw capped tubes at 4 °C.

#### **2.4.1.2 P1 *vir* transduction of the recipient strain**

Recipient cells were grown overnight at 37 °C in 2.5 ml TY medium with CaCl<sub>2</sub> (5 mM). P1 lysates containing the DNA of the donor strain were diluted by 10- and 100-fold and these dilutions as well as the neat lysate (100 µl) were mixed with the recipient cells (100 µl) and incubated at 37 °C for 20 min. The cells were then spread onto nutrient agar plates containing kanamycin (50 µg ml<sup>-1</sup>) and NaP<sub>2</sub>O<sub>7</sub> (0.125 mM) and incubated at 37 °C overnight. A control plate with non-transformed recipient cells, and another with the phage lysate was also made. Surviving colonies from the transduced cultures were then re-plated on selective medium containing kanamycin (50 µg ml<sup>-1</sup>) and PCR carried out to confirm the mutation.

#### **2.4.2 Transposon mutagenesis**

Transposon mutagenesis was performed using the EZ-Tn5™ <R6K<sub>γori</sub>/KAN-2>Tnp Transposome™ Kit from Epicentre Biotechnologies, according to the manufacturer’s instructions. Briefly, the transposome complex (1 µl) was transformed into *I*<sup>q</sup> Express chemically competent *E. coli* (50 µl) using the high efficiency transformation protocol (known as heat shock) as described in section 2.4.3.

### **2.4.3 High Efficiency Transformation Protocol**

A tube of NEB Express *I*<sup>q</sup> Competent *E. coli* cells was thawed on ice for 10 min, then mixed gently and 50 µl of cells mixed with 1 µl transposon. The tube was flicked 4-5 times to gently mix the cells and DNA. The mixture was placed on ice for 30 min and placed in a water bath at 42 °C for exactly 20 s, then placed on ice for 5 min. SOC (950 µl) that had been heated to 37 °C was added and then the mixture incubated at 37 °C for 60 min with shaking at 250 rpm. The cells were then mixed thoroughly but gently, then several 10-fold serial dilutions were performed in SOC. An aliquot (100 µl) of each dilution was spread onto a nutrient agar plate containing kanamycin (30 µg ml<sup>-1</sup>), which had been pre-warmed to 37 °C. The plates were then incubated overnight at 37 °C.

### **2.4.4 Primer design and cloning**

Primers were designed based on the DNA sequences of the target genes using Primer 3 software (V.0.4.0). Primers were designed to be 18 – 24 bp in length and to have a melting temperature (T<sub>m</sub>) of 57 – 65 °C and a GC content of 20 – 80 %. Primers that had the potential to form secondary structures were eliminated and redesigned. Primers were synthesised by Sigma Aldrich and were supplied as desiccated oligonucleotides that were then resuspended in super-pure H<sub>2</sub>O to a final concentration of 100 µM. The primers used in this work are described in Table 2.2.

### **2.4.5 Genomic DNA extraction**

The Blood and Tissue Kit (Qiagen) was used to extract genomic DNA according to the manufacturer's protocol, from 1 ml culture grown to late-exponential phase in LB medium. Instructions for pre-treatment of Gram-negative bacteria, then those describing the purification of total DNA from animal tissues were followed. Super-pure water (50 µl) was pipetted directly onto the membrane; this was incubated at room temperature for 1 min, then spun for 1 min at 8000 rpm to elute the DNA.

### **2.4.6 Restriction enzyme digestion**

Genomic DNA (17 µl) from mutants of interest was digested using the restriction enzyme *Rsa*I (1 µl, NEB), which recognises the sequence 5'GTAC 3' and cuts between the T and the A to generate blunt ends. The reaction mixture also included buffer 4 (2

µl, NEB). The digested DNA was purified using Qiaquick PCR purification kit (Qiagen) according to the manufacturer's protocol.

#### 2.4.7 Ligation of Fragmented DNA

Previously digested DNA (100 ng or 1 µl) was ligated by incubating with T4 DNA ligase (1 µl, NEB) and ligase buffer (1 µl, NEB) in super-pure water (7 µl) at room temperature for 6 h.

#### 2.4.8 PCR

PCR was conducted in order to amplify the DNA adjacent to the transposon in the mutant strains. The primers used were KAN-2 FP1 Forward Primer (EZ-Tn5 <R6Kγori/KAN-2>Tnp Transposome™ Kit, Epicentre Biotechnologies) and a primer internal to the *RsaI* site of the EZ-Tn5 transposon (designed by Iain Kean), the sequences of which are given in Table 2.2

The reaction mixture contained genomic DNA (0.5 µl) as a template, forward and reverse primers (0.1 µl of each), Dream Taq (2x) Green PCR mastermix (25 µl) (Thermo Scientific) and 24.3 µl super-pure water.

A PCR machine was used to heat the mixture according to the following thermal cycle:

95 °C	1 cycle
95 °C	} 35 cycles
55 °C	
68 °C	
72 °C	1 cycle

Primer name	Primer Sequence	Source
KAN-2 FP1 Forward Primer	5' ACCTACAACAAAGCTCTCTCATCAACC 3'	EZ-Tn5 <R6Kγori/KAN-2>Tnp Transposome™ Kit, Epicentre Biotechnologies
Primer internal to the <i>Rsa</i> I site of the EZ-Tn5 transposon	5' GTAACCATGCATCATCAGG 3'	Designed by Iain Kean
frvB forward primer	5' CAAACCCTCAGCTCATAAGGAAG 3'	Designed for this work using Primer3 Version 0.4.0
frvB reverse primer	5' GTTATCAGAATGTCGCGAACTTC 3'	Designed for this work using Primer3 Version 0.4.0
manX forward primer	5' GTGTTAACGATAATAAAGGAGGTAGC 3'	Designed for this work using Primer3 Version 0.4.0
manX reverse primer	5' CTCATTGTACTTCTCCTGTTTACG 3'	Designed for this work using Primer3 Version 0.4.0
sgaU forward primer	5' ATCGCTGAACTGTGGGGCTAAGGA 3'	Designed for this work using Primer3 Version 0.4.0
sgaU reverse primer	5' CCA TGT TGG CTT CAA ATA CCT GCT G 3'	Designed for this work using Primer3 Version 0.4.0
gshA forward primer	5' CAGTTCGTTTTCCAATCTGCAAC 3'	Designed by Mariana Tinajero Trejo
gshA reverse primer	5' ATTTTGACAGGCGGGAGGT 3'	Designed by Mariana Tinajero Trejo

**Table 2.2 List of Primers.** Synthetic oligonucleotides used as primers for the sequencing of transposon insertion sites or PCR amplification of DNA fragments.

#### **2.4.9 Agarose gel electrophoresis**

DNA samples were separated and visualised using agarose gel electrophoresis. Agarose (1 g) was dissolved in 100 ml 1 x TAE buffer by heating and then poured into a plastic mould containing a comb to form the sample wells. Hyperladder 1 (Bioline) was typically loaded alongside the DNA samples to provide a reference of the fragment size and concentration. The gel was covered with 1 x TAE buffer and 3  $\mu$ l of 10 mg ml<sup>-1</sup> ethidium bromide solution (Promega) was added to the buffer in order to allow visualisation of the DNA. The gels were run at 100 V for approximately 45 min and then the DNA visualised under UV light using the GeneGenius Gel Imaging System (Syngene).

#### **2.4.10 Purification of DNA samples**

Following amplification of a region of DNA by PCR, samples were purified using Qiaquick PCR purification kit (Qiagen) according to the manufacturer's protocol.

#### **2.4.11 DNA sequencing**

Samples were sent for nucleotide sequencing (Beckman Coulter Genomics) with the KAN-2 FP1 Forward Primer.

#### **2.4.12 Sequence and database analysis for identification of genes inactivated by transposon mutagenesis**

The sequence of the DNA adjacent to the transposon (sequenced using the KAN-2 FP1 Forward Primer) was entered into a BLASTN search in the NCBI (The National Center for Biotechnology Information) database (<http://blast.ncbi.nlm.nih.gov/Blast.cgi>) against the *E. coli* K12 genome sequence.

## Chapter 3

### CO-RMs as inhibitors of the terminal oxidases of *E. coli*

The haem-containing cytochromes of bacterial aerobic respiratory chains are thought to be important targets of CO from CORM-3, although there is mounting evidence that there are several other bacterial targets of this compound (as discussed in section 1.3.4 and section 4.3). UV- visible spectroscopy of bacterial suspensions, including *E. coli* (Davidge *et al.*, 2009b), *P. aeruginosa* (Desmard *et al.*, 2009), and *C. jejuni* (Smith *et al.*, 2011) show the formation of CO-bound cytochromes upon treatment with CORM-3. In *E. coli*, CO from CORM-3 binds rapidly to cytochrome *d*, followed by the slower formation of another CO-adduct, which is thought to be cytochrome *bo'* (Davidge *et al.*, 2009b). Transcriptional analysis of *E. coli* treated with CORM-3 also implicates aerobic respiration as a major target of this compound. CORM-3 down-regulates the *cyo* operon, which encodes the terminal oxidase cytochrome *bo'* and slightly up-regulates *cydAB*, which encodes cytochrome *bd-I* (Davidge *et al.*, 2009b).

While there have been many detailed studies of the interaction of CO gas with respiratory cytochromes (Borisov, 2008; Borisov *et al.*, 2007; Borisov *et al.*, 2001; Chance *et al.*, 1953; Keilin, 1966), several key discrepancies between the effects of CO gas and CORM-3 on bacterial growth and respiration necessitate a thorough investigation of the nature of the interaction of CO from CORM-3 with the aerobic respiratory chain. These discrepancies include the finding that CO from CORM-3 is inhibitory to growth when present at concentrations equal to atmospheric oxygen levels (Davidge *et al.*, 2009b), whereas historically, it has been understood that CO has a lower affinity for respiratory cytochromes than O<sub>2</sub> and thus must be present in a significant excess, typically in a ratio of 19:1 (Poole *et al.*, 1973), in order to be inhibitory. Nobre *et al.*, (2007) have also reported that CO-RMs are more potent antibacterial agents than CO gas. More recent work has found that CORM-3 is more inhibitory to the respiration of *E. coli* cells than the equivalent concentration of CO gas (Wilson *et al.*, 2013).



The work described in this chapter aims to compare the effects of CORM-3, and where appropriate CORM-2, on respiration in the model organism *E. coli* with the well-established effects of CO gas. It was hoped that in doing so, a better understanding would be gained of the mechanism(s) by which CO-RMs inhibit respiration, and in turn, further our understanding of one of the key questions regarding the antibacterial properties of CO-RMs: to what extent does inhibition of respiration by CO-RMs contribute to the bactericidal properties of these compounds (see section 1.3.3).

Specifically, it was investigated whether the three quinol oxidases of the aerobic respiratory chain of *E. coli*: cytochrome *bd-I*, cytochrome *bd-II* and cytochrome *bo'* differ in their sensitivity to CO from CORM-3. Work was also done to investigate the photosensitivity of the CO-haem bond in CORM-3 treated bacterial membranes, and to assess whether the oxygen tension at which CORM-3 is added affects the extent of respiratory inhibition.

### **3.2 Results CORM-2, CORM-3 and CO gas inhibit respiration in *E. coli* membrane particles**

When this work began, there were only two published reports of the effects of CORM-3 on bacterial respiration. These reported incubation of CORM-3 with cultures of *E. coli* for an extended period, followed by the measurement of oxygen consumption (Davidge *et al.*, 2009b) and the treatment of *P. aeruginosa* cultures with CORM-3 prior to respiration rates being measured over a 40 min time-course (Desmard *et al.*, 2009). Both pieces of work also provided spectroscopic evidence of the formation of CO-adducts of cytochromes following treatment with CORM-3. Two papers have since been published on this subject, one of which demonstrates that CORM-3 inhibits respiration in *C. jejuni* without inhibiting growth (Smith *et al.*, 2011), and the other presents a comprehensive study of the effects of CORM-3 on bacterial respiration in several bacteria and the yeast *Saccharomyces cerevisiae* (Wilson *et al.*, 2013).

The respiratory studies described in the present work differ from previous published reports as they study the effects of CO-RMs on bacterial membrane particles created by disrupting *E. coli* suspensions by ultrasonication (Poole, 1993). Measuring respiratory inhibition of *E. coli* membrane particles allowed the direct measurement of the effects of CORM-3 on respiratory components, without interference from other cellular components, or the effects of trans-membrane ion gradients.

The work described in this chapter predominantly used CORM-3 as a model CO-RM as it is chemically well characterised and is water soluble, a property that will be important in future therapeutically relevant CO-RMs. In some experiments, CORM-2, which is soluble only in organic solvents, was also used in order to confirm whether the effects observed with CORM-3 were shared by other CO-RMs. The chemical structure of both of these compounds can be seen in Table 1.2. It was important to begin by comparing the sensitivities of membrane particles to CORM-2, CORM-3 and equivalent concentrations of CO-saturated solution. *E. coli* membrane particles were suspended in fully aerated sonication buffer in a stirred Perspex chamber fitted with a Clark-type polarographic oxygen electrode (OXY041A, Rank Bros Ltd.) held at 37 °C, with a lid placed on the chamber to prevent the entry of additional oxygen into the sample (Gilberthorpe and Poole, 2008). NADH (6.25 mM) was added to stimulate respiration and the CO-RM compound or CO-saturated solution was added, through a small hole in the lid using a Hamilton syringe, when the dissolved oxygen tension in the chamber reached approximately 155  $\mu\text{M}$  (75% of air saturation).

Previous published reports had not studied the immediate effect of CORM-3 on bacterial respiration in the closed oxygen electrode, as inhibition could not be observed for intact *E. coli* cells in the limited time this experimental design allowed (Davidge *et al.*, 2009b), however, the present study used fragmented membrane particles, which allowed an immediate inhibition of respiration to be observed when CORM-3 was added to the chamber. CO gas (100  $\mu\text{M}$ ) significantly inhibited respiration of membrane particles (by 38%), and to a greater extent than the equivalent concentration of CORM-3 (12%; Figure 3.1A and B, blue short dash line). High concentrations of CORM-3 (400  $\mu\text{M}$ ) were required to inhibit respiration in wild type membrane particles by 54.6%. CORM-2 was found to be more inhibitory to respiration than CORM-3 (100  $\mu\text{M}$  inhibited respiration by 85%; Figure 3.1B and C). Importantly, the control compounds iCORM-3 (Figure 3.1B, red dot dash line) and  $\text{RuCl}_2(\text{DMSO})_4$  (Figure 3.1C, red dot dash line) caused little (6%) or no inhibition respectively. This confirms that CO is the

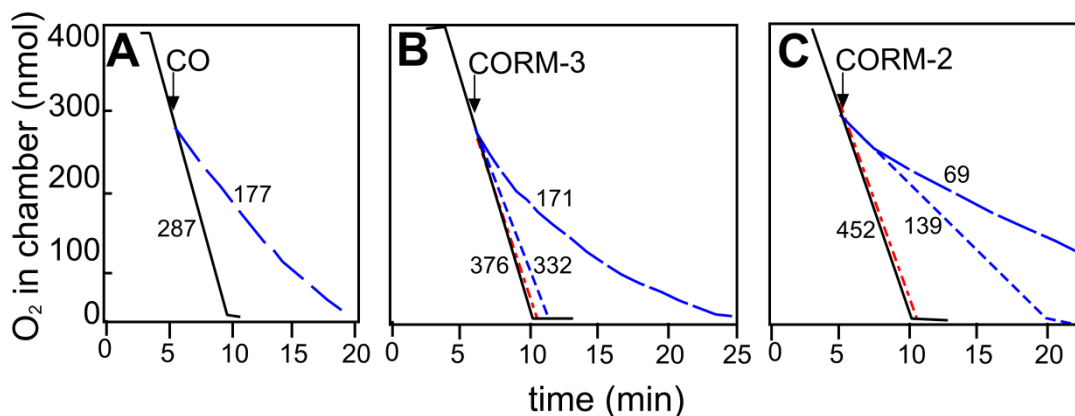


**Figure 3.1 CO gas, CORM-3 and CORM-2 inhibit respiration in wild type *E. coli* membrane particles.** Wild type *E. coli* membrane particles were added to an oxygen electrode chamber in sonication buffer (2 ml) to a final concentration of approximately 60  $\mu\text{g ml}^{-1}$  (**in A**), 170  $\mu\text{g ml}^{-1}$  (**in B**) and 100  $\mu\text{g ml}^{-1}$  (**in C**). A lid was placed on the chamber and respiration was initiated by the addition of 6.25 mM NADH. Traces show dissolved oxygen in the chamber as follows: (**A**) control (black solid line) and 100  $\mu\text{M}$  CO (blue broken line); (**B**) control (black solid line), 100  $\mu\text{M}$  iCORM-3 (red dot dash line), 100  $\mu\text{M}$  CORM-3 (blue short dash line), 400  $\mu\text{M}$  CORM-3 (blue long dash line); (**C**) control (black solid line), 100  $\mu\text{M}$  RuCl<sub>2</sub>(DMSO)<sub>4</sub> (red dot dash line), 50  $\mu\text{M}$  CORM-2 (blue short dash line), 100  $\mu\text{M}$  CORM-2 (blue long dash line). CO and CO-RMs were added at approximately 75% of oxygen saturation (310 nmol O<sub>2</sub>). These data are representative of at least 3 technical and 2 biological replicates. Respiration rates (nmol min<sup>-1</sup> mg<sup>-1</sup> protein) 2 min following the addition of CO-RM are shown adjacent to each trace. This figure was published in Jesse *et al.* (2013).

causative agent of respiratory inhibition by CO-RMs, and that the inactive metal-containing structure of the CO-RM does not contribute substantially to respiratory inhibition. Typical respiration rates for each of these conditions are given in Figure 3.1.

### **3.2.2 The oxygen tension at which CORM-3 is added does not affect the degree of respiratory inhibition.**

It has been known for several decades that CO gas is a competitive inhibitor of the terminal oxidases of aerobic respiration as it binds to haem in place of oxygen, thereby preventing the reduction of oxygen to water (Wikstrom *et al.*, 1981). Because of this, CO gas is a more potent inhibitor of respiration when oxygen concentrations are low (Poole *et al.*, 1973). It has recently been reported that endogenously produced, but artificially induced CO can inhibit respiration, and that it does so more potently following a period of hypoxia (D'Amico *et al.*, 2006). It is expected that CO from CO-RMs inhibits aerobic respiration in the same way as CO gas; however this cannot be taken for granted as CO-RM-derived CO is known to elicit some strikingly different effects than CO gas, such as being inhibitory to growth (Davidge *et al.*, 2009b) and respiration at substantially lower concentrations (Smith *et al.*, 2011; Wilson *et al.*, 2013), even when present at concentrations much lower than surrounding oxygen tensions (Davidge *et al.*, 2009b; Smith *et al.*, 2011).

It was therefore important to assess whether CO from CO-RMs inhibits aerobic respiration in a competitive manner. Wild type *E. coli* membranes were stimulated to respire in an open electrode using 12.5 mM NADH, and the speed of stirring was manipulated so that a steady state was achieved at either a high (approximately 75% of air saturation), or low (approximately 9% of air saturation) oxygen levels. 50  $\mu$ M CORM-3 was then added two min after the oxygen equilibrium had been reached, and the respiration rates calculated 10 and 20 min after the addition of compound. Respiration rates at the corresponding time points in a control experiment in which no compound was added were also calculated. At both time points, there was no significant difference in the percentage inhibition induced by CORM-3 with regards to the oxygen level at which it was added (Figure 3.2). It was then investigated whether there was a difference in the degree of respiratory inhibition when CORM-3 was added at either low

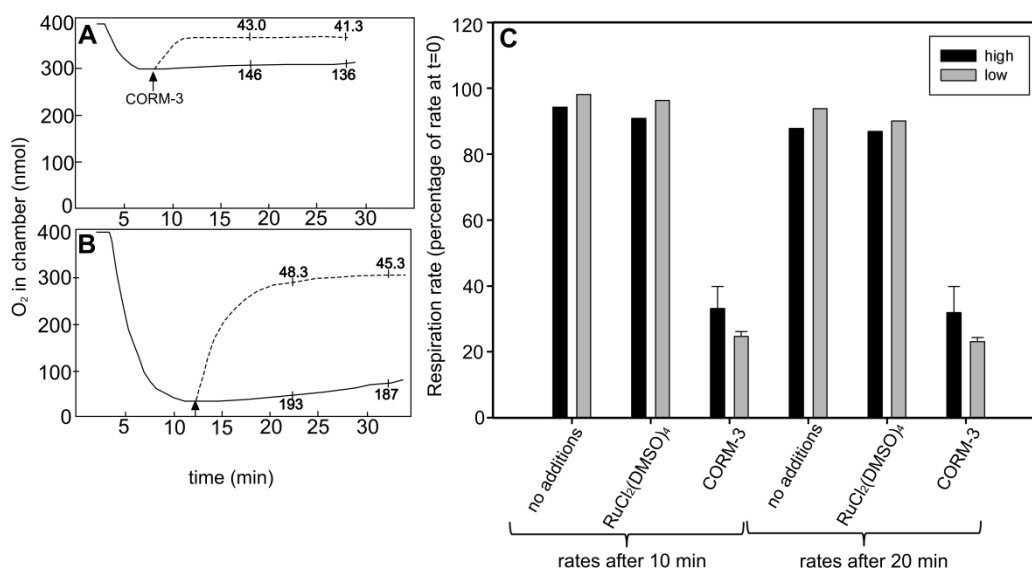


**Figure 3.2 The oxygen tension at which CORM-3 is added does not affect the degree of respiratory inhibition.** Wild type membrane particles were added to sonication buffer to a final concentration of approximately 175  $\mu\text{g ml}^{-1}$  in an open system oxygen electrode chamber. A magnetic stirrer bar was used to mix the suspension and to introduce oxygen into the sample. The rate of stirring was manipulated to achieve a constant dissolved oxygen tension for an extended time period. A stirrer speed of 9 achieved a plateau at high oxygen tensions (approximately 75.0% of air saturation), shown in (A), while a stirrer speed of 5 achieved a plateau at low oxygen tensions (approximately 9.3% of air saturation), shown in (B). NADH (12.5 mM) was added to initiate respiration and 50  $\mu\text{M}$  CORM-3 (broken line) was added at the point indicated by the arrow ( $t = 0$ ). No compound was added to the control (solid line). The numbers shown on the traces are the respiration rates ( $\text{nmol min}^{-1} \text{mg}^{-1}$  protein) 10 and 20 min following the addition of compound, or at the equivalent point in the control. Data are from one representative experiment. (C) Respiration rates 10 and 20 min following the addition of CORM-3, or the control compound  $\text{RuCl}_2(\text{DMSO})_4$  (both at 50  $\mu\text{M}$ ) are expressed as a percentage of the respective rates at  $t=0$ . Data are the mean and standard deviations of 3 biological replicates.

(13%) or very low (3%) oxygen tensions. Again, no significant difference was found between these conditions (Figure 3.3).

### **3.2.3 Cytochrome *bd*-I is the most resistant oxidase of *E. coli* to respiratory inhibition by CORM-3 and a strain containing only this oxidase is partially protected from growth inhibition by this compound.**

As mentioned previously, terminal oxidases are thought to be one of the major targets for CO-RM inhibition and may be important in determining sensitivity to CO-RMs in antimicrobial therapy. It was therefore important to study the interaction of CO from CORM-3 with each individual terminal oxidase of *E. coli* and to ascertain whether these differed in sensitivity to CORM-3. It could not be taken for granted that the oxidases would behave the same with CORM-3-derived CO as with CO gas due to the many differences in the effects of CO and CORM-3 described above (section 3.1). Additionally, there are no published reports of the interaction of CO or CORM-3 with the more recently identified cytochrome *bd*-II of *E. coli*. This work therefore constitutes the first comparison of the effects of a CO-RM on the individual terminal oxidases of a bacterial respiratory chain.

The *E. coli* strains used in this work were each able to express only one of the three quinol oxidases of the aerobic respiratory chain of *E. coli*. For example, the strain containing only cytochrome *bd*-I had the phenotype  $\text{Cyd}^+ \text{App}^- \text{Cyo}^-$  (see Table 2.1). To simplify the nomenclature in this work, this strain will be referred to by the phenotype,  $\text{Cyd}^+$ , the strain containing only cytochrome *bd*-II will be referred to as  $\text{App}^+$  and the strain containing only cytochrome *bo*' will be referred to as  $\text{Cyo}^+$ . The single oxidase mutants also had a deletion in the *nuo* gene rendering them unable to produce NADH dehydrogenase-I, an electrogenic component upstream of the quinol oxidases in the respiratory chain of *E. coli*. The control strain used in this work was able to express all three oxidases, but had a *nuo* deletion and is referred to throughout this work as the parent strain.

Growth of each of the single oxidase strains was monitored in the presence of 12.5  $\mu\text{M}$  CORM-3, which was added during early exponential phase (at approximately 30 Klett units) (Figure 3.4 A-D). This concentration of CORM-3 had only a slightly deleterious

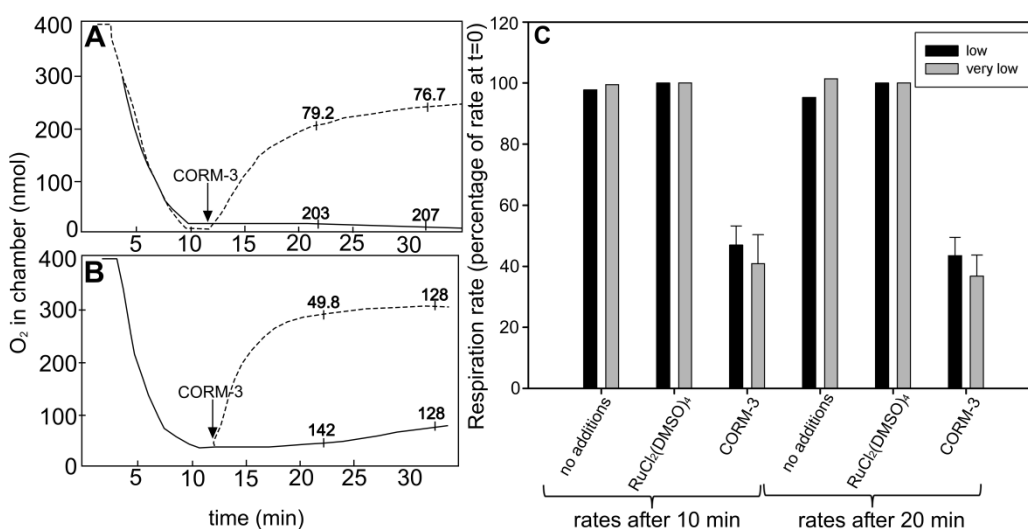


**Figure 3.3** The degree of respiratory inhibition experienced by wild type *E. coli* membrane particles treated with CORM-3 is not exacerbated at very low oxygen tensions. Wild type membrane particles were added to sonication buffer to a final concentration of  $175 \mu\text{g ml}^{-1}$  in an open system oxygen electrode chamber, as described in Figure 3.2. A stirrer speed of 7 achieved a plateau at low oxygen tensions (approximately 13.4% of air saturation), shown in (A), while a stirrer speed of 5 achieved a plateau at very low oxygen tensions (approximately 3.1% of air saturation), shown in (B). NADH (12.5 mM) was added to initiate respiration and  $50 \mu\text{M}$  CORM-3 (broken line) was added at the point indicated by the arrow ( $t = 0$ ). No compound was added to the control (solid line). The numbers shown on the traces are the respiration rates ( $\text{nmol min}^{-1} \text{mg}^{-1} \text{protein}$ ) 10 and 20 min following the addition of compound, or at the equivalent point in the control. Data are from one representative experiment. (C) Respiration rates 10 and 20 min following the addition of CORM-3, or the control compound  $\text{RuCl}_2(\text{DMSO})_4$  (both at  $50 \mu\text{M}$ ) are expressed as a percentage of the respective rates at  $t = 0$ . Data are the mean and standard deviation of 3 biological replicates.

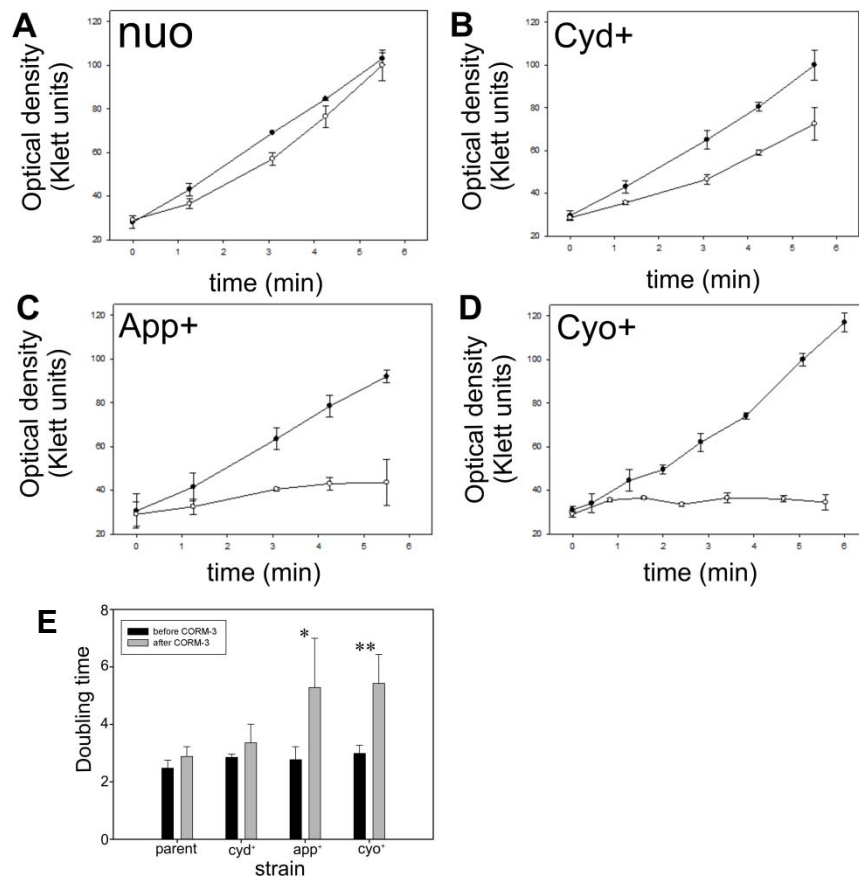


**Figure 3.4. A strain containing only cytochrome *bd-I* is resistant to growth inhibition by CORM-3.** CORM-3 (12.5  $\mu$ M) was added at early exponential phase to cultures of *E. coli*: (A) parent strain; (B) expressing cytochrome *bd-I* only; (C) expressing cytochrome *bd-II* only and (D) expressing cytochrome *bo'* only. Nothing was added to the controls. Data in (A) – (D) show growth in the absence (closed symbols) and presence (open symbols) of CORM-3. (E) Shows the doubling times of these strains, for the two hours before (black bars) and after (grey bars) the addition of CORM-3. All data are averages and standard deviations of three biological repeats. Student's t-test was done in order to establish whether the doubling times before and after CORM-3 were significantly different for each strain. \*,  $p = 0.0564$ , \*\*,  $p = 0.0214$ . This figure was published in Jesse *et al.* (2013).



effect on the growth rate of the parent strain. The single oxidase mutants were all affected to a greater extent than the control strain, however, the doubling time of the  $Cyd^+$  mutant was inhibited much less than that of both  $App^+$  and  $Cyo^+$  (Figure 3.4 E). The doubling time of the parent strain was affected by a factor of 1.19 by 12.5  $\mu$ M CORM-3, 1.16 for  $Cyd^+$ , 1.98 for  $App^+$  and 1.81 for  $Cyo^+$ . Student's t-test was performed to establish whether the changes in doubling time following the addition of CORM-3 were statistically significant for each single oxidase containing strain. The doubling times of the parent strain and the strain containing cytochrome *bd-I* as the only oxidase were not significantly changed by the addition of 12.5  $\mu$ M CORM-3, whereas that of the strains containing either cytochrome *bd-II* or cytochrome *bo'* as the only oxidase were significantly decreased by this concentration of CORM-3.

In order to further investigate this finding, membrane particles prepared from these single oxidase-expressing *E. coli* mutants were assessed for their susceptibility to respiratory inhibition by CORM-3. The extent of respiratory inhibition was determined by measuring the time taken for oxygen re-accumulation to begin after removal of the chamber lid, in the presence of CORM-3 or the control compound miCORM-3. miCORM-3 is a control compound developed by Jayne Louise Wilson (Wilson *et al.*, 2013), which is prepared by treating CORM-3 with dithionite and myoglobin in order to remove any labile CO from the compound. It has an advantage over another commonly used control compound iCORM-3, as it has been exposed to biological ligands. While both compounds have been used in published work, the precise chemical structure of neither is known.

In this experimental design, the respiration of more sensitive strains will be inhibited to a greater extent and so will not be able to utilise the oxygen in the chamber as quickly, leading to a shorter time to reoxygenation. This is an established method for comparing the sensitivity of respiring samples to inhibitors (Hendgen-Cotta *et al.*, 2008; Shiva *et al.*, 2007). The chamber was initially closed and NADH (12.5 mM) was added to stimulate respiration. Compound(s) were added 1 min after the dissolved oxygen tension in the chamber reached 0 and the lid removed 1 min later. This allowed continuous  $O_2$  diffusion from the vortex surface into the sample with a typical  $K_La$  value of  $0.35 \text{ min}^{-1}$ .  $K_La$  is the gas transfer coefficient from gas to liquid and is

dependent on reaction volume, surface area and temperature (Pirt, 1985), all of which were quantified and controlled. The extent of respiratory inhibition was determined by measuring the time to oxygen re-accumulation after removal of the chamber lid, as previously described (Shiva *et al.*, 2007). This method has the advantage that prolonged measurements can be made without exhaustion of oxygen.

When respiring membrane particles containing either cytochrome *bd-II* or all three oxidases (parent strain) were treated with 100  $\mu\text{M}$  CORM-3, the time taken for the chamber to reoxygenate was significantly reduced (by 80 - 84%) (Figure 3.5A) compared to treatment with the control compound, miCORM-3 (Figure 3.5B). Thus, CORM-3 significantly inhibits respiration in these strains. However, when membrane particles prepared from a strain expressing only cytochrome *bd-I* were treated with 100  $\mu\text{M}$  CORM -3, the time to reoxygenation of the electrode chamber was reduced by only 9% compared to that when miCORM-3 was present. Figures 3.5A and B show the electrode traces of one representative experiment. Figure 3.5C shows the means and standard deviations of 2 technical and 2 biological replicates of these data. Mean times to reoxygenation in min for each experimental condition were as follows: parent strain with miCORM-3 ( $65.8 \pm 2.99$ ) and with CORM-3 ( $13.2 \pm 2.56$ ); App<sup>+</sup> with miCORM-3 ( $55.5 \pm 6.28$ ) and with CORM-3 ( $9.42 \pm 3.84$ ); Cyd<sup>+</sup> with miCORM-3 ( $65.7 \pm 4.51$ ) and with CORM-3 ( $59.8 \pm 4.84$ ). This confirms that cytochrome *bd-I* is the most resistant oxidase of *E. coli* to CORM-3.

#### **3.2.4 A spectroscopic study of the binding of CO from CORM-3 to each of the terminal oxidases of *E. coli***

UV-visible spectroscopy was performed using a dual-beam spectrophotometer, in order to identify the haems present in membrane particles prepared from each single oxidase mutant and therefore confirm the oxidase composition of the mutants used in this work (Figure 3.6). CORM-3 difference spectra (i.e. the difference between the spectrum of a reduced sample treated with 100  $\mu\text{M}$  CORM-3 *minus* the spectrum of a reduced sample (Wood, 1984)) were recorded for membrane particles prepared from the single oxidase-expressing strains and resuspended in sonication buffer to a final concentration of between 8 and 16  $\text{mg ml}^{-1}$ . In each strain, the Soret feature consisting of a peak near 420

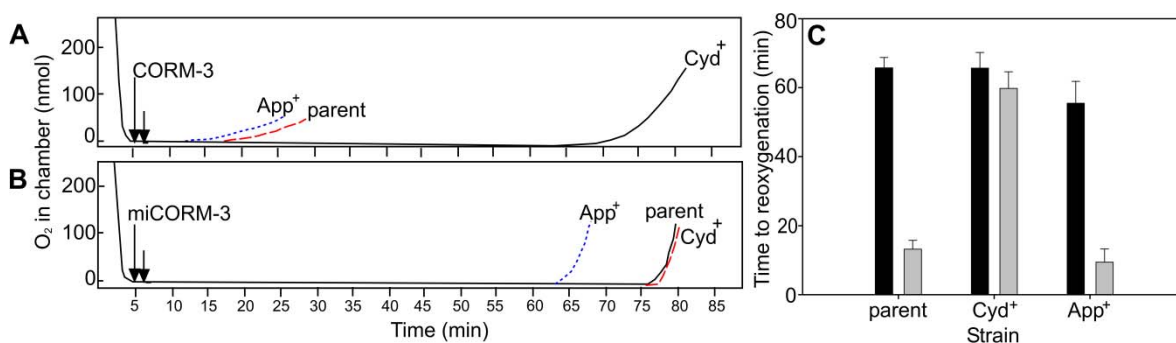


**Figure 3.5 Cytochrome *bd-I* is resistant to respiratory inhibition by CORM-3.**

Membranes prepared from mutants containing only one of the three terminal oxidases of *E. coli* were added to an oxygen electrode chamber in sonication buffer (2 ml) to a final concentration of approximately 370  $\mu\text{g ml}^{-1}$  and stimulated to respire by the addition of NADH (12.5 mM). The point at which either CORM-3 (shown in **A**) or the control compound miCORM-3 (shown in **B**, both at 100  $\mu\text{M}$ ) were added is indicated by the first, longer arrow in each panel. The lid was removed from the chamber 1 min later, indicated by the second arrow. These traces show dissolved oxygen in the chamber and indicate the times taken for the chamber to begin to reoxygenate for the strains containing cytochrome *bd-I* only (black lines), cytochrome *bd-II* only (blue dotted lines) and the parent strain (red dashed lines). The times taken for the chamber to reoxygenate (min) in each condition were as follows: parent strain with miCORM-3 (70) and with CORM-3 (14); App<sup>+</sup> with miCORM-3 (54) and with CORM-3 (7); Cyd<sup>+</sup> with miCORM-3 (70) and with CORM-3 (63). These data are representative of 2 technical and 2 biological replicates. **(C)** Shows the time to reoxygenation for each strain with CORM-3 (grey bars) or miCORM-3 (black bars). These data are the means and standard deviations of 2 technical and 2 biological replicates. This figure was published in Jesse *et al.* (2013).

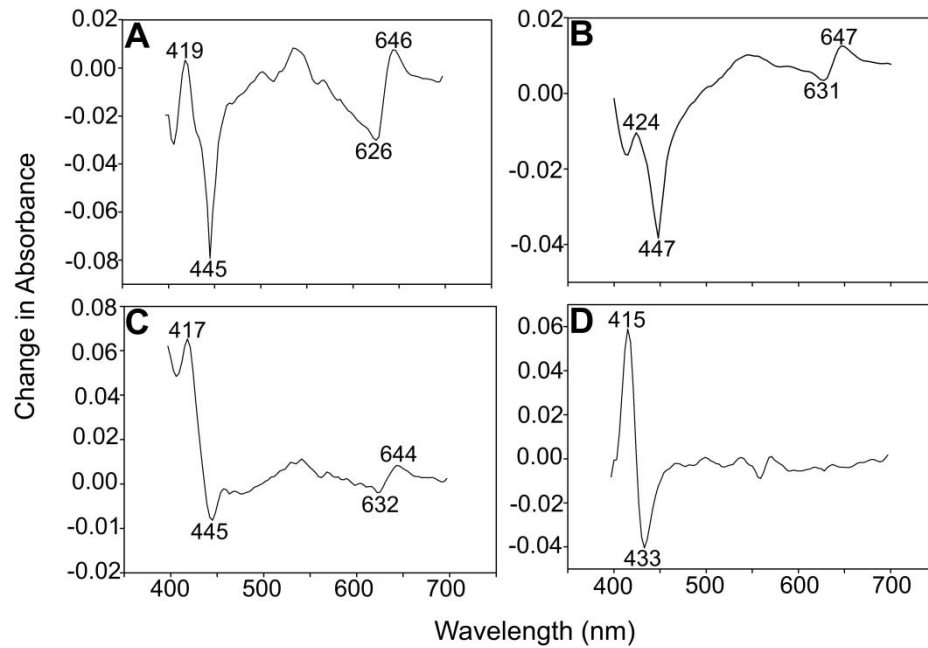


**Figure 3.6 Difference spectra of single oxidase membrane particles.** Membranes were prepared from *E. coli* respiratory mutants and diluted with sonication buffer to a final protein concentration of 8 - 19 mg ml<sup>-1</sup>. Spectra were obtained 10 min after the addition of CORM-3 to membranes from the following strains: **(A)** wild type; **(B)** cytochrome *bd-I* only; **(C)** cytochrome *bd-II* only; **(D)** cytochrome *bo'* only. Data were plotted using a scanning dual wavelength spectrophotometer as the difference between the spectrum of a dithionite reduced sample incubated with 100 μM CORM-3 minus the spectrum of a reduced sample. Data have been smoothed in Sigma plot graphing software with a sampling proportion of 0.1 and a polynomial degree of 9. This figure was published in Jesse *et al.* (2013).

nm and the trough near 445-459 nm demonstrate the binding of CO from CORM-3 to a mixture of cytochromes including cytochrome *b*, and in the case of Cyo<sup>+</sup> cytochrome *o'* (Figure 3.6D). The peak in the  $\alpha$ -region, between 645 - 647 nm, is indicative of the binding of CO to cytochrome *d* (Figures 3.6A-C). Importantly, this feature is absent in the CORM-3 difference spectrum of Cyo<sup>+</sup> (Figure 3.6D).

Work was done to obtain CORM-3 difference spectra over a time-course in order to gain time-resolved data regarding the rate of CO binding to the respiratory cytochromes. Here, membrane particles prepared from wild type *E. coli* were resuspended in buffer to a final protein concentration of approximately 32 mg ml<sup>-1</sup>. The samples were reduced by the addition of a few grains of sodium dithionite and then treated with 100  $\mu$ M CORM-3. Spectra were recorded after 5 and 10 s, then every 10 s until 5 min, every 30 s until 10 min, every 5 min until 40 min and then at 60 min. The main spectral features are shown in Figure 3.7A (the Soret region) and Figure 3.7B (the  $\alpha$ -region). The magnitude of the peak at 423 nm and trough at 440 nm increase over time. These features are characteristic of CO binding to cytochrome *b*<sub>595</sub>. Cytochrome *o'* bound to CO also has spectral features in this region, but this typically has a peak at 415 nm and a trough at 430 nm (Wood, 1984). The absorbance minima of this feature (at 440 nm) was subtracted from the absorbance maxima (at 423 nm) and this difference in absorbance plotted against time (Figure 3.7C). This confirms that CO from CORM-3 binds rapidly to cytochrome *b*<sub>595</sub> from *E. coli*, reaching saturation 10 min after CORM-3 treatment. The half-time of CO binding to cytochrome *b*<sub>595</sub> was calculated as 0.44 min ( $\pm$  0.13; 2 biological replicates). The peak at 643 nm (Figure 3.7B) is indicative of CO-bound haem *d*. This change in intensity of this peak over time (calculated as the absorbance at 643 nm minus the absorbance at 658 nm) is shown in Figure 3.7D. This shows that CO from CORM-3 binds extremely rapidly to haem *d* in *E. coli* membrane particles. The half-time of CO binding to this cytochrome was calculated as 0.17 min ( $\pm$  0.011; 2 technical replicates), although it should be noted that this spectroscopic method is not ideal for calculating accurate kinetic data for such a rapid process.

For comparison, spectra of CO gas (from a saturated solution) bound to wild type membrane particles were also recorded over a time-course (Figure 3.8). The Soret region has a peak at 424 nm and a trough at 438 nm (Figure 3.8A), almost identical in

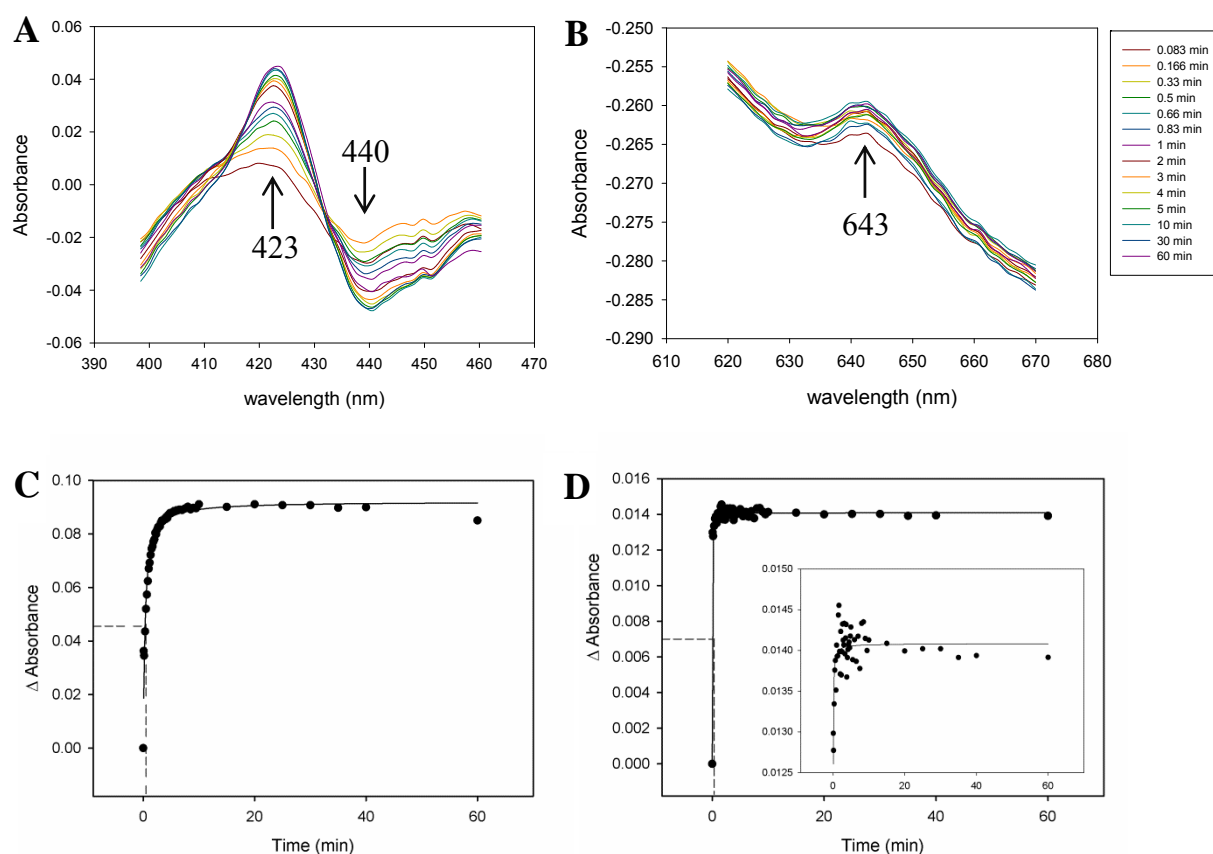


**Figure 3.7. Binding of CO from CORM-3 to haem *d* and haem *b*<sub>595</sub> of the terminal oxidases of *E. coli*.** Membranes were prepared from wild type *E. coli* and diluted with sonication buffer to a final protein concentration of 32.6 mg ml<sup>-1</sup>. The samples were treated with 100 μM CORM-3. CORM-3 reduced *minus* reduced difference spectra were recorded. (A) shows the Soret region of the spectrum and (B) the α-region over a time course. (C) shows the change in absorbance in the Soret region (absorbance at 423 nm minus the absorbance at 440 nm) plotted against time and (D) shows the change in the α-region (absorbance at 643 nm minus the absorbance at 658 nm plotted against time. In both cases, the absorbance at time 0 (ie. at the point of CORM-3 addition) has been assigned as zero, although technical limitations prevent a spectrum from being recorded at this point. The dashed horizontal lines in (C) and (D) indicate half the maximal absorbance change and the dashed vertical lines indicate the half time of CO binding to each cytochrome. The inset figure in (D) shows the same data as in the main figure, but without the data point for time zero allowing greater resolution of the data. Data are from one technical replicate but are representative of 2 technical replicates.

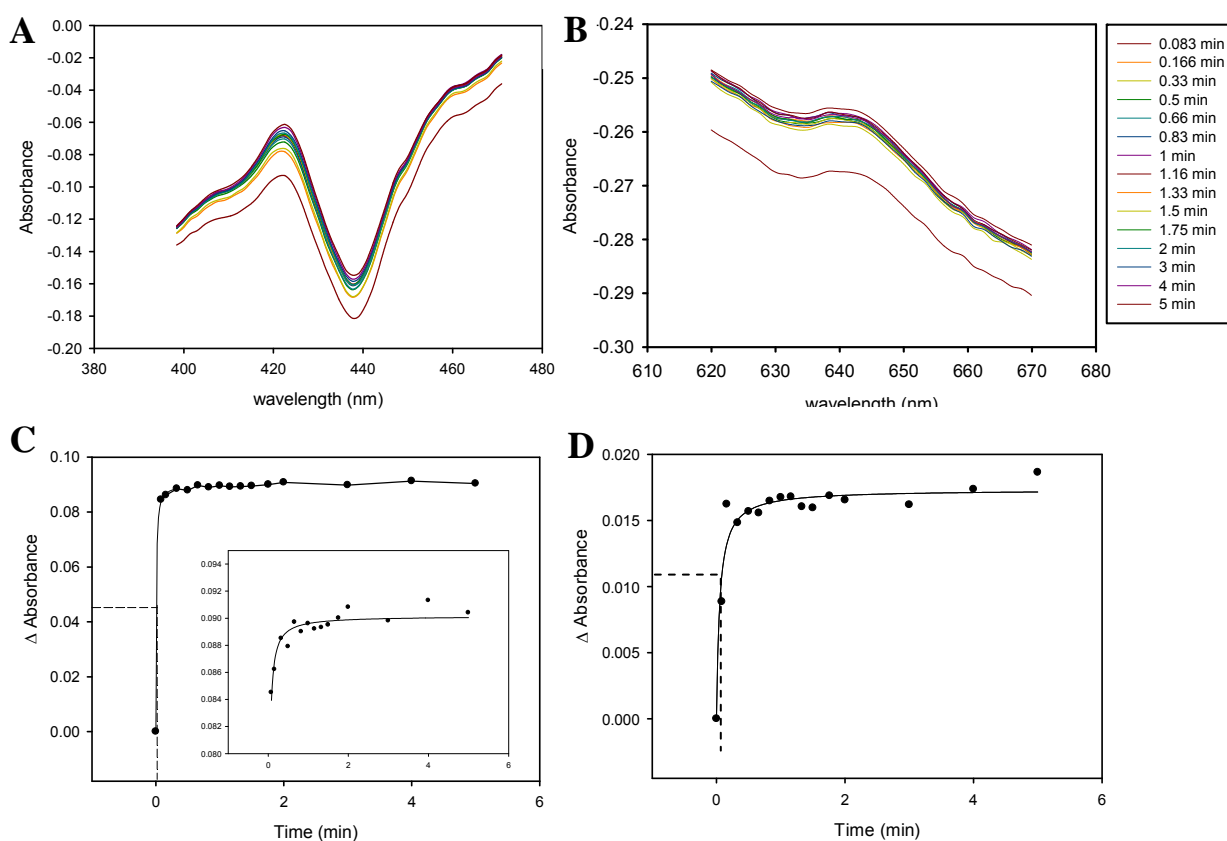


**Figure 3.8 Binding of CO from a saturated solution to haem *d* and haem *b*<sub>595</sub> of the terminal oxidases of *E. coli*.** Membranes were prepared from wild type *E. coli* and diluted with buffer to a final protein concentration of 32.6 mg ml<sup>-1</sup>. The samples were treated with 100 μM CO from a saturated solution. CO reduced *minus* reduced difference spectra were recorded. (A) shows the Soret region of the spectrum and (B) the α-region over a time course. (C) shows the change in absorbance in the Soret region (absorbance at 423 nm minus the absorbance at 440 nm) plotted against time and (D) shows the change in the α-region (absorbance at 643 nm minus the absorbance at 658 nm) plotted against time. In both cases, the absorbance at time 0 (ie. at the point of CORM-3 addition) has been assigned as zero, although technical limitations prevent a spectrum from being recorded at this point. The inset figure in (C) shows the same data as in the main figure, but without the data point for time zero allowing greater resolution of the data. The dashed horizontal lines in (C) and (D) indicate half the maximal absorbance change and the dashed vertical lines indicate the half time of CO binding to each cytochrome. Data are from one technical replicate but are representative of 2 technical replicates.

wavelength and magnitude to those in the difference spectra generated following treatment with CORM-3. However, this spectral feature formed much more rapidly following treatment with CO gas compared to CORM-3, with a half-time of CO binding of 0.020 min (Figure 3.8C), which is more than 5-fold lower than that for CORM-3. CO bound to haem *d* so rapidly, that almost no changes could be detected over time (Figure 3.8B).

### **3.2.5 Photolysis alleviates the inhibition of respiration by CO from CORM-3 and reduces killing by CORM-3**

Over 100 years ago, in 1896, Haldane and Smith noted that carbonmonoxy-haemoglobin dissociates in the light, and reassociates in the dark (Keilin, 1966). Then in 1926, Warburg demonstrated that a mixture of 95% CO and 5% O<sub>2</sub> caused the respiration of yeast to be inhibited by 71% in the dark, but that this was greatly alleviated in the light, with respiration inhibited by only 14%. The photo-reversibility of CO inhibition of respiration was later used to identify terminal oxidases (Castor and Chance, 1955). In the early 1970s it was shown that the inhibition of respiration by CO in yeast, for example, *Schizosaccharomyces pombe* was light-reversible, confirming that CO was inhibiting respiration by binding to haem in the cytochromes of the terminal oxidases of this organism (Poole *et al.*, 1973).

The current work aimed to establish whether the binding of CO from CORM-3 to the terminal oxidases of the aerobic respiratory chain of *E. coli* could also be reversed by light in order to ascertain to what extent CO from CORM-3 mimics CO gas applied as a solution. Initially, work was done to confirm that photolysis of the haem-CO bond could be observed as a change in respiration rate upon illumination of respiring wild type membrane particles. White light from a 150 W bulb was focused on the wall of a glass chamber using a convex lens; the light was switched on and off at 1 min intervals.

In the presence of a solution of CO gas, an increase in respiration rate was evident immediately following the application of light, followed by an instant decrease in respiration rate upon removal of the light (Figure 3.9A, respiration rates for the first two light / dark cycles are given in Table 3.1). This confirms that the experimental design used here is suitable for observing the effects on respiration caused by the photolysis of



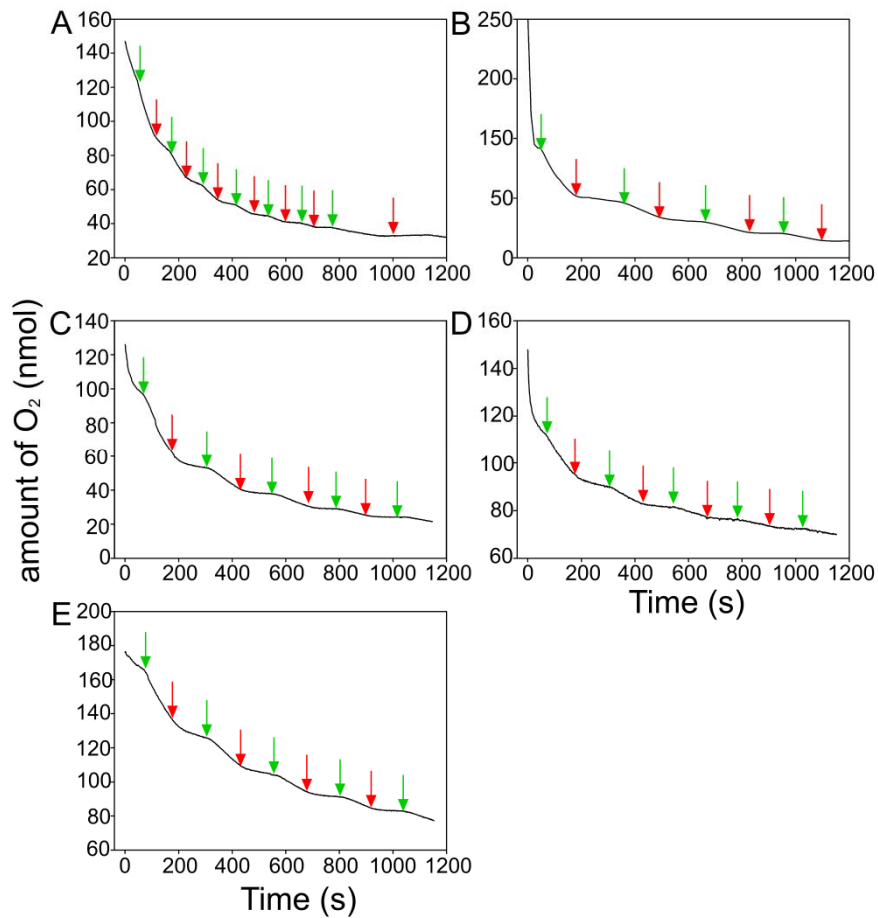


**Figure 3.9** Photolysis of CORM-3 treated membrane particles confirms that the heme-CO bond is photolabile in each terminal oxidase of *E. coli*. Oxygen consumption of *E. coli* membrane particles prepared from (A) and (B) wild type, (C) cytochrome *bd-I* only, (D) cytochrome *bd-II* only and (E) cytochrome *bo'* only strains in the presence of (A) a solution of CO gas and (B) – (E) 300  $\mu\text{M}$  CORM-3. The membrane particles were resuspended in sonication buffer to a final protein concentration of approximately 0.1  $\text{mg ml}^{-1}$ . Respiration was started by the addition of 12.5 mM NADH. White light focused on the glass chamber was switched on and off at 1 min intervals (A), and 2 min intervals (B-E); green arrows indicate where the light was switched on and red arrows where it was switched off. These traces are representative of at least 2 technical replicates. Respiration rates for the first 2 light / dark cycles for each condition can be found in Table 3.1.

<b>Respiration rates (nmol O<sub>2</sub> min<sup>-1</sup> mg<sup>-1</sup>)</b>					
	Wild type with CO *	Wild type with CORM-3	Cytochrome <i>bd</i> -I with CORM-3	Cytochrome <i>bd</i> -II with CORM-3	Cytochrome <i>bo</i> ' with CORM-3
Rate 1 (light on)	157.5	82.0	88.5	52.7	15.0
Rate 2 (light off)	51	13.7	12.3	10.5	4.0
Rate 3 (light on)	78	31.9	36.8	21.0	8.6
Rate 4 (light off)	21	7.18	6.1	3.6	2.5

**Table 3.1 The respiration rates calculated from the gradients of the traces at four different time points.** For CORM-3 treated membranes, rate 1 refers to the rate of respiration between 1 min and 3 min when the light is on, rate 2 is that between 3 and 5 min when the light is off, rate 3 between 5 and 7 min when the light is on and rate 4 between 7 and 9 min when the light is off. This experiment was conducted three times for each oxidase, the data shown is from one representative experiment. \*The rates for wild type membranes with CO gas were recorded between the following time intervals: rate 1: 1 and 2 min when the light is on, rate 2: 2 and 3 min when the light is off, rate 3 3 and 4 min when the light is on and rate 4: 4 and 5 min when the light is off.

the bond between CO gas and the haem groups of the terminal oxidases of the respiratory chain of *E. coli*.

In order to establish whether CO from CORM-3 binds to CO in a 'classical' photolabile manner, this experiment was repeated with membranes prepared from wild type *E. coli* and from each single oxidase strain in the presence of 300  $\mu$ M CORM-3. Membrane particles were suspended in sonication buffer, which had been bubbled with nitrogen gas for 15 min in order to reduce the amount of dissolved oxygen in the buffer to between 60 - 90  $\mu$ M, to obtain a dissolved oxygen tension similar to that in the experiment with CO-saturated solution described above. The light was switched on and off at 2 min intervals. Addition of CORM-3 inhibited respiration significantly in all strains, but this inhibition was immediately alleviated during illumination of the sample, and these effects were observed repeatedly over several light dark cycles (Figure 3.9B-E).

Table 3.1 shows the rates of respiration for each strain after the first four light changes. The initial inhibited rate is very similar for both wild type and *Cyd*<sup>+</sup> membranes treated with CORM-3, and in both cases there is approximately a 3-fold increase in the rate of respiration when the light is switched on (between rate 2 and rate 3). In contrast, the respiration rates for both the *App*<sup>+</sup> and the *Cyo*<sup>+</sup> membranes increased by approximately 2-fold in the presence of white light compared to the CORM-3 inhibited rate in the dark (between rates 2 and 3).

Following the demonstration that respiratory inhibition by CORM-3 could be reversed by white light, it was hypothesised that light may also be able to rescue *E. coli* cultures from killing by CORM-3. To investigate whether this was the case, wild type cultures of *E. coli* were grown to an optical density of 50 Klett units and then a 2 ml aliquot of this culture was placed into a glass chamber wrapped in foil so that no light could enter, while a second 2 ml aliquot was placed in an identical glass chamber on which a beam of light was focused. The cultures in each chamber were stirred magnetically and samples were taken before the addition of 30  $\mu$ M CORM-3 and at 10, 20, 30, 45 and 60 min after. These samples were diluted and plated out on to nutrient agar, incubated overnight and then counted. The cfu ml<sup>-1</sup> values of the cultures grown in the light were

calculated and compared to those of the dark cultures. The light incubated CORM-3 treated culture experienced approximately 70% killing in the first hour following treatment, however, the viability loss was significantly greater in the dark; 95% of the population was killed in 60 min. Statistical analysis of the data was done using a Student's *t* test, which revealed that survival of the CORM-3 treated cultures grown in the light was significantly higher than that of the cultures grown in the dark at 30 ( $P < 0.001$ ), 45 ( $P = 0$ ) and 60 min ( $P = 0$ ) following CORM-3 addition (Figure 3.10).

### **3.3 Discussion**

#### **3.3.1 CORM-2, CORM-3 and CO gas inhibit respiration in *E. coli* membrane particles**

Inhibition of bacterial respiration by CORM-3 had been reported when the work described in this thesis was undertaken, including preliminary evidence that CORM-3 treated *E. coli* cells contained CO-bound cytochromes (Davidge *et al.*, 2009b; Desmard *et al.*, 2009). However the details of respiratory inhibition by CORM-3 remained elusive and it was uncertain as to what extent inhibition of the terminal oxidases by CO from CORM-3 contributed to the bactericidal nature of these compounds. As outlined in the Introduction to this chapter (section 3.1) several key differences between the behaviour of CO gas and CORM-3 were evident, which necessitated a thorough investigation into the similarities and differences between respiratory inhibition by CO-RMs with the established knowledge of the mechanisms by which CO gas inhibits respiration, in order to ascertain to what extent CO from CORM-3 mimics CO applied as a saturated solution. The work presented in this chapter investigated the nature of the inhibition of the terminal oxidases of *E. coli* with the aim of better understanding the mechanism of respiratory inhibition by CORM-3

The respiratory studies presented in this thesis utilize bacterial membrane particles rather than whole cells. This was done to allow the investigation of respiration alone, without interference from other cellular components. The utilization of membrane particles allowed the immediate inhibitory effect of CO-RMs on the terminal oxidases to be observed without interference from the phenomenon of respiratory stimulation seen in whole cells treated with CORM-3, which is thought to arise from the transport of  $K^+$  and  $Na^+$  ions across the cell membrane as described in section 1.3.3.

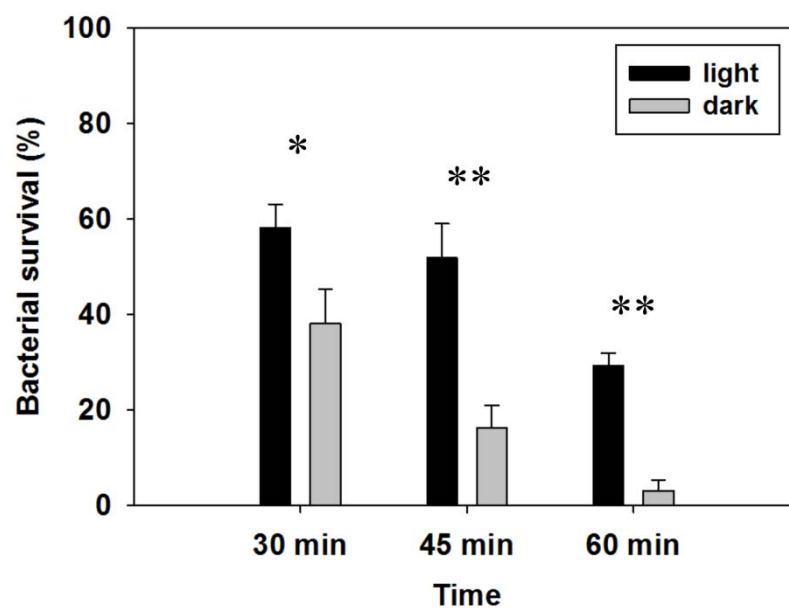


**Figure 3.10 Light can reduce the toxic effect of CORM-3 by photolysing the haem – CO bond.** *E. coli* was grown aerobically to an OD of 50 Klett units, and 2 ml culture was added to both a light and dark chamber. Samples were taken before addition of 30  $\mu$ M CORM-3 and at regular intervals after and viability counts performed. The mean percentage survival of 5 technical replicates at 30, 45 and 60 min compared to the viability before the addition of CORM-3 is shown. Asterisks indicate statistically significant decreases in viability of cultures grown in the dark compared to cultures grown in the light as measured using Student's *t* test (\*,  $P < 0.001$ ; \*\*,  $P < 0$ ). These data are representative of 3 biological replicates.

These data have been published in Wilson *et al.* (2013)

(Wilson *et al.*, 2013). Indeed the demonstration that respiration rates are not stimulated in fragmented membrane samples is evidence that CORM-3 does not directly stimulate oxidase activity as has been reported with cytochrome *c* oxidase activity in mitochondria, in which low doses of CO (10  $\mu$ M) transiently stimulate respiration (Queiroga *et al.*, 2011).

The use of membrane particles in respiratory studies also has the advantage of providing a more stable sample, whereas when whole cells samples were prepared their ability to respire deteriorated over several hours. It also allowed rapid measurements to be made in the closed system of the oxygen electrode, which is not possible with whole cell samples.

While inhibition of respiration of *E. coli* membranes particles by CORM-3 is reported in this work as occurring on a faster time scale than that of whole cells as reported in Wilson *et al.* (2013), much higher concentrations of CORM-3 (400  $\mu$ M) were required in order to give substantial inhibition (55%, Figure 3.1B). In the current work, 100  $\mu$ M CORM-3 added at 75% of air saturation inhibited respiration by only 12%, while this concentration of CORM-3 inhibited intact *E. coli* cell suspensions by approximately 40% (Wilson *et al.*, 2013). While it would be unwise to try to make quantitative comparisons between these two findings, due to several inherent differences in the methodology used in each study, including differences in the amount of protein used, the oxygen tension at which the CO-RM compound was added and the use of the closed, compared to the open electrode system, it can be qualitatively concluded that over an extended time period, CORM-3 is more inhibitory to respiration in whole cells than in membrane particles. This is particularly evident when the effects of CORM-3 are compared to those of CO gas in each system. CO gas (100  $\mu$ M) administered as a solution has been shown not to inhibit bacterial respiration in whole cells Wilson *et al.* (2013), whereas work presented in this chapter shows CO gas to be more inhibitory to respiration of *E. coli* membrane particles than the equivalent concentration of CORM-3 (38% inhibition following treatment with 100  $\mu$ M CO gas, Figure 3.1A).

Although it may initially seem counterintuitive that CORM-3 would be more inhibitory to whole cells than to membrane particles, as it could be expected that CO from CORM-

3 would be better able to access its respiratory targets in fractured membrane particles compared to intact cells (as indeed it appears to with regards to exhibiting immediate inhibition upon addition of CORM-3), it may be that the low levels of cellular components available with washed membrane particles may reduce the rate or extent of CO release from CORM-3. This hypothesis is consistent with the findings of (McLean *et al.*, 2012) who showed that CORM-3 requires the presence of compounds such as sulfites in order to release CO. It is thought that CORM-3 releases CO once it has entered the cell, but not when in buffer, due to the presence of intracellular species similar to sulfites, which trigger this release.

CORM-2 was used in addition to CORM-3 in these initial experiments to provide a comparison with CORM-3 and to ascertain the effects of this compound on respiration of *E. coli* membrane particles as a precursor to other work using this compound throughout this thesis. The finding that CORM-2 was more inhibitory to respiration than the same concentration of CORM-3 is in agreement with the findings of Nobre *et al.*, (2007) who found that higher concentrations of CORM-3 than CORM-2 were required to decrease viability in *E. coli* and *S. aureus* cultures.

### **3.3.2 The oxygen tension at which CORM-3 is added does not affect the degree of respiratory inhibition.**

An interesting finding of the current work is that the oxygen tension at which CORM-3 is added does not determine the extent of respiratory inhibition experienced by *E. coli* membrane particles. This is contrary to our established knowledge that CO gas is preferentially inhibitory to respiration when present in concentrations in excess of dissolved oxygen (Keilin, 1966) and therefore provides additional evidence that CO from CORM-3 does not merely mimic CO gas. It is known from the work described in this thesis (section 3.2.1) and from the published work of others (Davidge *et al.*, 2009b; Wilson *et al.*, 2013), that CO is the agent of CORM-3 that causes inhibition of respiration, as control molecules, including the CORM-2 precursor  $\text{RuCl}_2(\text{DMSO})_4$ , inactive iCORM-3 and myoglobin inactivated miCORM-3, do not perturb respiration. Therefore it is hypothesised that the differing effects of CORM-3 and CO applied as a saturated solution are caused by the ability of CO-RMs such as CORM-3 to deliver CO into the cell, perhaps directly to the micro-domain of the respiratory chain resulting in

concentrations of CO at these sites that exceed concentrations applied outside the cell, and consequently, that greatly exceed the local oxygen concentrations (Davidge *et al.*, 2009b). Further evidence in support of this hypothesis is that ruthenium from CORM-3 is known to accumulate inside cells to concentrations approximately 8-fold that applied to the culture medium (McLean *et al.*, 2013), and results described in Chapter 5).

The finding that CORM-3 is not more inhibitory to respiration of *E. coli* membrane particles when applied at low oxygen tensions differs from the findings of Wilson *et al.* (2013) who found that incubation of whole cell suspensions of *E. coli* and CORM-3 under anoxic conditions for an extended period of time resulted in a shorter period of respiratory stimulation and a greater degree of inhibition when oxygen was allowed to re-enter the system. These differences may result from differences in experimental design between the two studies, particularly variations in the behaviour of CORM-3 with whole cells and membrane particles. It is also possible that the greater inhibition seen when CORM-3 is incubated with whole cells under extended conditions of anoxia is in part due to the longer time period in which the cells were exposed to CORM-3, rather than a specific consequence of the oxygen tension at which this incubation occurred.

A limitation of the experimental design used in this work is that the oxygen tension achieved may not have been sufficiently low considering the very high affinity of respiratory cytochromes for oxygen. In the ‘very low’ oxygen condition, the oxygen tension will have been approximately 6.2  $\mu\text{M}$ , however, the  $k_m$  of cytochrome *bo'* for oxygen is reported to be between 0.2 and 0.46  $\mu\text{M}$ , depending on the globin used in the measurement (D’mello *et al.*, 1996), while that for cytochrome *bd-I* is between 3 – 8 nM (D’mello *et al.*, 1996). Furthermore, the cytochrome composition of the wild type membranes used in this work was not quantified. It is likely therefore likely that even in the very low oxygen condition, the cytochromes were able to bind oxygen efficiently, therefore out competing CO from the CO-RM.

### **3.3.3 Cytochrome *bd-I* is the most resistant oxidase of *E. coli* to CORM-3**

The data presented in Figure 3.3 and 3.4 clearly demonstrate that cytochrome *bd-I* is significantly more resistant to inhibition by CO from CORM-3 than the other two



quinol oxidases of *E. coli* and that when expressed as the sole respiratory oxidase it is able to partially protect this organism from growth inhibition caused by CORM-3. The notion that cytochrome *bd-I* may have a role as a cellular protector against stressors is well established in the literature. This oxidase is known to protect bacteria from various environmental stresses such as azide and divalent metal ions. Moreover, cytochrome *bd-I* null mutants are more sensitive to hydrogen peroxide than wild type *E. coli* (Poole and Cook, 2000). Cytochrome *bd-I* is more resistant to haem group inhibitors than haem-copper oxidases such as cytochrome *bo'*, including cyanide (Pudek and Bragg, 1974), NO and CO (Poole *et al.*, 1989).

More recently, cytochrome *bd-I* has been shown to protect *E. coli* cultures from NO-induced growth inhibition by virtue of the fast dissociation rate of NO from this oxidase (Mason *et al.*, 2009). Evidence for this stems from the findings that *cydA* and *cydB*, the genes that encode cytochrome *bd-I*, are up-regulated by exposure to NO (Pullan *et al.*, 2007). It was found that there was greater inhibition of respiration by NO of a strain containing cytochrome *bo'* as the only terminal oxidase, and that the growth of this strain was also more restricted during NO stress. The authors concluded that these negative effects were not caused by a reduction in the amount of terminal oxidase in this strain (caused by the down-regulation of cytochrome *bo'* in response to NO) but that cytochrome *bo'* is more sensitive to NO than cytochrome *bd-I*. Measuring the O<sub>2</sub>- and NO-binding kinetics of each terminal oxidase allowed the authors to conclude that it is the rapid rate at which NO dissociates from cytochrome *bd-I* (5 times faster than that of cytochrome *bo'*) that causes this resistance (Mason *et al.*, 2009). The resistance of cytochrome *bd-I* to NO may confer an advantage to pathogenic bacteria such as *M. tuberculosis* (Shi *et al.*, 2005) and *S. aureus* (Richardson *et al.*, 2006), both of which increase expression of this oxidase in response to low concentrations of NO. In support of this hypothesis, cytochrome *bd* mutants of several pathogenic bacteria are significantly less virile than their wild type counterparts (Endley, 2001; Shi *et al.*, 2005; Way, 1999).

Cytochrome *bd-I* also has a very high dissociation constant for CO ( $K_d = 70$  nM for membrane bound enzyme (Borisov, 2008) compared to 1.7  $\mu$ M for cytochrome *bo'* (Cheesman *et al.*, 1993)), which could explain the resistance of this oxidase to CO from

CORM-3. That the genes encoding cytochrome *bd*-I are up-regulated upon exposure to CORM-3 (Davidge *et al.*, 2009b; McLean *et al.*, 2013), provides further evidence that this oxidase provides a modest cellular defence against this compound. The increased transcription of *cydAB* was shown using a gene profiling microarray and then confirmed spectroscopically; a mutant containing only cytochrome *bd*-type oxidases exhibited increased levels of this oxidase following treatment with CORM-3 (Davidge *et al.*, 2009b). The published work also found a 10 - 22-fold reduction in the transcription of the genes in the *cyo* operon that encode cytochrome *bo*'. This is consistent with the finding in the current work that a strain expressing this cytochrome as the only terminal oxidase is the most sensitive to growth inhibition following treatment with CORM-3.

### **3.3.4 Time-resolved spectra of CO from CORM-3 binding to each of the terminal oxidases of *E. coli***

The data presented in Figure 3.7 confirm that CO is released rapidly from CORM-3 in the presence of *E. coli* membrane particles and sodium dithionite, and that it binds rapidly to haem *b*<sub>595</sub> and even more so to haem *d*. This is consistent with the findings of Davidge *et al.* (2009b), which provided evidence of the binding of CO from CORM-3 to cytochromes in *E. coli* whole cells, however, the current work provides more detailed and time-resolved data. The substantially longer half-time of CO (from CORM-3) compared to that of a CO-saturated solution, binding to the respiratory cytochromes of *E. coli* membrane particles is consistent with CO needing to dissociate from the CORM-3 molecule before it can bind to the oxidases.

It is acknowledged that kinetic data cannot be accurately determined for such fast processes using this experimental technique. The use of stopped-flow spectroscopy would allow much more accurate kinetic data to be collected, although this is not trivial due to limitations with regards to the optical density of the samples used in this method. The data reported here do however confirm that, like CO gas (Figure 3.8), CO from CORM-3 binds most rapidly to haem *d* and that the majority of haem *d* becomes CO-bound within the first 5 seconds following the addition of CORM-3.

A limitation of both studies is the use of dithionite, which is added in order to reduce the haem proteins, thereby allowing CO binding, as this compound is now known to

promote CO release from several CO-RMs including CORM-3 (McLean *et al.*, 2012). Therefore, while this method allows the relative rates of binding of CO from CORM-3 to be measured, it does not allow conclusions to be drawn as to the un-facilitated rate of CO release from CORM-3 to the respiratory cytochromes. For this to be achieved, whole cell, or membrane particles should be treated with glucose, or another respirable substrate, to promote respiration to render the sample anoxic prior to the addition of CORM-3. This would allow *in vivo* measurements of CO release from CORM-3 to the terminal oxidases to be made.

Cytochrome *bd-I* from *E. coli* has a  $K_m$  ( $O_2$ ) value of 3-8 nM, which is the highest reported oxygen affinity for a respiratory oxidase. In this oxidase, it is haem *d* that binds  $O_2$  and reduces it to  $H_2O$ , and it is known that this is also the site of CO binding (Borisov, 2008). Studies of the binding of CO gas to cytochrome *bd* from *Azotobacter vinelandii* have shown that haem *d* has an affinity for CO approximately 20-fold higher than that of haem *b<sub>595</sub>* (Borisov *et al.*, 2001).

### **3.3.5 Photolysis alleviates the inhibition of respiration by CO from CORM-3 and reduces killing by CORM-3.**

When this work began, one of the major questions surrounding the bactericidal activity of CO-RMs was to what extent the inhibition of respiration is the major cause of killing by these compounds. The work described in this chapter aimed to investigate the mechanism by which CO from CORM-3 binds to respiratory cytochromes, and to answer this question by investigating the relationship between the alleviation of respiratory inhibition and the effect this has on the viability of CORM-3 treated cultures.

It is shown here for the first time that CO from CORM-3 inhibits respiration in a ‘classical’ photo-sensitive manner. This is an important finding and confirms that, despite having many properties distinct from CO gas (Davidge *et al.*, 2009b; Nobre *et al.*, 2007; Wilson *et al.*, 2013), the mechanism of respiratory inhibition is similar.

Most significantly, this work has directly demonstrated that, by alleviating CORM-3 induced inhibition of respiration through photolysis of the haem-CO bond, the viability

of CORM-3 treated cultures can be preserved. This provides strong evidence that the binding of CO to haem proteins, including those in respiratory cytochromes, is a key contributor to the bactericidal properties of CORM-3. This is in agreement with the work of Desmard *et al.* (2009), who showed that inhibition of respiration precedes the loss of viability of *P. aeruginosa* caused by CORM-3, but is in contrast to the findings of Wilson *et al.* (2013), who measured respiration rates and viability concurrently in CORM-3 treated *E. coli* cultures and found a significant loss of viability of *E. coli* cultures before respiratory inhibition began. The conflicting evidence suggests that respiration is a significant target of CO from CORM-3, and that, by relieving this inhibition by photolysing the CO-haem bond in CORM-3-treated cultures, viability can be significantly protected. However, this does not exclude other important mechanisms by which CORM-3 exerts its toxicity. Such mechanisms may include the binding of CO from CORM-3 to other non-respiratory haem proteins, which based on the findings of this work, would be expected to be relieved by light, or indeed the effects of CORM-3 on non-haem proteins (as described in section 4.3).

Further evidence that inhibition of respiration is not the main mechanism by which CO-RMs exert their bactericidal effects is provided by the work of Desmard *et al.* (2012), which compared the effects of two fast CO-releasing, ruthenium based CO-RMs (CORM-2 and CORM-3) with those of the slow releasing CO-RMs, CORM-371, which is manganese based, and CORM-A1, which does not contain a metal moiety. This work found that CORM-2, CORM-3 and CORM-371 decreased oxygen consumption to a similar extent, but that CORM-371 had a more transient effect on loss of viability. Furthermore, CORM-A1 only had a slight effect on O<sub>2</sub> consumption and no adverse effect on viability. These differences in bactericidal effect suggest that it is unlikely that inhibition of respiration, is the cause of viability loss, but rather that the metal component of CO-RMs may have a larger effect on the toxicity of these compounds than was previously thought.

The greater increase in respiration rate when light is applied to wild type and *Cyd*<sup>+</sup> membranes treated with CORM-3 compared to that of *App*<sup>+</sup> and *Cyo*<sup>+</sup> membranes could suggest that CO is either bound more strongly to cytochrome *bd*-II and cytochrome *bo*' or that it associates more rapidly with these oxidases reducing the stimulatory effects of

photolysis in these strains. This is consistent with the data presented earlier in this chapter, which suggest that cytochrome *bd*-II and cytochrome *bo*' are more sensitive to respiratory inhibition by CORM-3. The data also support the work of Borisov (2008), which shows CO to dissociate more rapidly from cytochrome *bd*-I than from cytochrome *bo*'.

Overall, this work provides the first evidence that the biological consequences of CO release from a CO-RM can be reversed by light and has been published in part in Wilson *et al.*, (2013). There is much current work developing CO-RMs that release CO upon irradiation; see section 1.2.4 and the recent review by Schatzschneider (2011). The findings of the current work have important implications for future therapeutic applications of CO-RMs, particularly regarding photoCO-RMs.

## Chapter 4

### The non-haem oxidase AOX from *Vibrio fischeri* is sensitive to inhibition by CORM-3

#### 4.1 Introduction

*Vibrio fischeri* is a bioluminescent bacterium, which is able to live freely in fresh or salt water or to live symbiotically in the light organ of the Hawaiian bobtail squid *Euprymna scolopes*. This bacterium is of interest to the present work as it encodes the non-haem alternative oxidase AOX (Visick and Ruby, 2006), haems being prime targets of CO.

##### 4.1.1 Respiration in *V. fischeri*

*V. fischeri* is able to conserve energy by aerobic and anaerobic respiration (Ruby *et al.*, 2005) and by mixed acid fermentation (Doudoroff, 1942). Anaerobically, it is able to use several terminal electron acceptors, including trimethylamine N-oxide (TMAO), nitrate, nitrite and fumarate (Dunn and Stabb, 2008; Ruby *et al.*, 2005). Aerobically, *V. fischeri* can express three terminal ubiquinol oxidases; cytochrome *bd-I*, encoded by *cydAB*, a *cbb<sub>3</sub>* type oxidase, encoded by *ccoNOQP* and an alternative oxidase, encoded by *aox*. Cytochrome *bd-I* and the *cbb<sub>3</sub>* type oxidase are both haem-based oxidases, whereas AOX is unique as it does not contain haem, but instead possesses a di-iron catalytic center (Berthold *et al.*, 2002). Figure 4.1 shows a diagrammatic representation of the respiratory chain of *V. fischeri*.

##### 4.1.2 Alternative oxidase

Alternative oxidase was originally discovered in the mitochondria of plants and is also found in some fungi, bacteria and protozoa (Vanlerberghe and McIntosh, 1997). Most of the knowledge of the structure, regulation and function of AOX comes from studies of the plant oxidase, although it is not known whether bacterial AOX shares all of these properties. Bacterial homologs of plant *aox* were discovered by genome sequencing (McDonald and Vanlerberghe, 2005; Stenmark and Nordlund, 2003) and it is notable that many bacteria that possess *aox*, including *V. fischeri*, are marine organisms

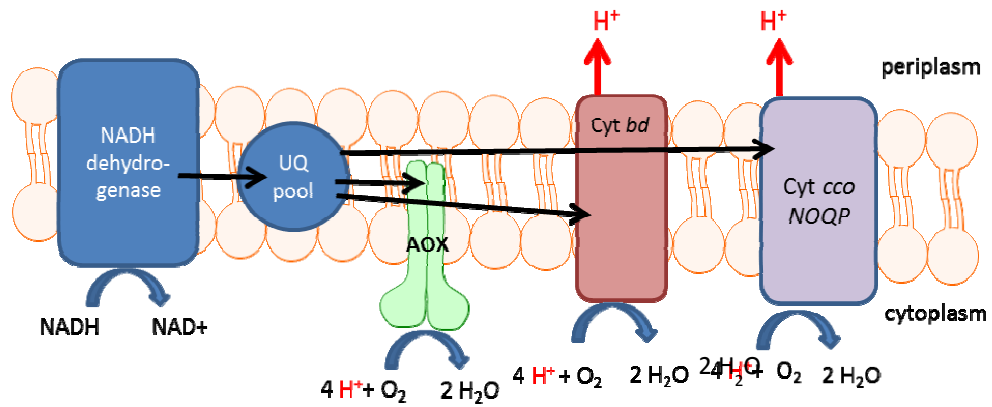


**Figure 4.1 AOX and the respiratory chain of *V. fischeri*.** The black arrows represent the flow of electrons through the respiratory chain from NADH dehydrogenase to the ubiquinone pool and then to either AOX or the haem-containing terminal oxidases cytochrome *bd* and cytochrome *ccoNOQP*. The information used to generate this figure was obtained from (Vanlerberghe and McIntosh, 1997).

(Rusch *et al.*, 2007). As a functioning ubiquinol oxidase, AOX catalyses the four electron reduction of oxygen to water in aerobic respiratory chains, with oxygen binding to the di-ferrous form of the enzyme (Berthold and Stenmark, 2003). In plants, AOX does not directly contribute to the generation of a proton motive force, but may contribute indirectly when coupled to proton-pumping by NADH dehydrogenase (reviewed by Vanlerberghe and McIntosh, 1997).

#### **4.1.2.1. Structure of plant AOX**

Relatively little is known about the structure of AOX due to difficulties in purifying this protein. Work investigating the plant AOX indicates that it is a monotopic integral membrane protein (Berthold and Stenmark, 2003) with a dicarboxylate di-iron active site (Berthold *et al.*, 2002). Recent work by Moore *et al.* (2008) used EPR spectroscopy to confirm that this is also true of trypanosomal AOX. The iron atoms are located within a bundle of 4 helices (Andersson and Nordlund, 1999; Berthold and Stenmark, 2003) and are bound by four carboxylate groups and two histidine residues (Berthold and Stenmark, 2003).

#### **4.1.2.2 Regulation of AOX activity and expression**

In *V. fischeri aox* is not expressed under normal laboratory conditions (Dunn, 2012). AOX activity is regulated at both the gene and protein levels. The expression of AOX is regulated by many stressors including low temperature, oxidative stress, pathogens and by inhibitors of cytochrome-mediated respiration (Slayman, 1977). Reduced sulfur compounds such as cysteine and methionine are known to induce AOX expression in the yeast *Hansenula anomala* (Minagawa *et al.*, 1990).

AOX activity is also regulated by post-transcriptional and post-translational modifications. The activity of plant AOX has been shown to increase when levels of reduced ubiquinone are high, implicating it as a useful respiratory pathway when the cytochrome oxidases are saturated (Lambers, 1982). However, AOX does not merely constitute an ‘overflow’, as it is known to compete with cytochrome oxidases for electrons (Hoefnagel *et al.*, 1995). In plants, AOX activity is known to depend on direct interaction of a key cysteine residue, Cys I (Berthold *et al.*, 2000) with certain alpha-keto acids, particularly pyruvate (Day *et al.*, 1994; Millar *et al.*, 1993). High levels of



pyruvate occur with rapid glycolytic flux and when ADP levels are high, ensuring AOX is not active when respiratory substrates are limited. Recent studies in the plant *Arum maculatum* have elucidated the mechanism of AOX activation by pyruvate, which has been shown to stabilise the active conformation of AOX, directly increasing  $V_{\max}$  (Carre *et al.*, 2011). AOX can exist as a monomer or dimer linked by disulfide bonds, with the dimer being the less active form (Umbach and Siedow, 1993). AOX must be in the reduced monomeric form in order to be activated by pyruvate and this reduced, activated form of AOX has a higher affinity for ubiquinone (Umbach *et al.*, 1994). Figure 4.2 summarises factors that affect AOX activity.

#### 4.1.2.3 The role of AOX

In thermogenic plants, AOX is involved in heat generation, which is important for pollination and temperature regulation (Meeuse, 1975); however the specific role of this oxidase in other species is less well understood. There is some evidence that AOX is involved in the maintenance of metal homeostasis (Rasmusson *et al.*, 2009), protection from oxidative stress (Gupta *et al.*, 2009; Wagner and Moore, 1997) and in virulence (Akhter *et al.*, 2003). Plant AOX is not directly involved in the generation of the proton motive force, and is therefore not subject to back pressure from this force, however, AOX may be important in maintaining turnover of the Krebs cycle and allowing synthesis of carbon skeletons (Lambers, 1982).

AOX may also confer a selective advantage to *V. fischeri*, enabling it to exclusively colonise the squid *Euprymna scolopes*. This symbiotic relationship is well studied as a model for beneficial host - microbe interactions. *V. fischeri* readily colonises the light organ of *E. scolopes*, where it receives a plentiful supply of nutrients, while the squid benefits from the bioluminescence produced by the bacteria in a process called ‘counterillumination’, which reduces the visibility of the squid to predators (Jones and Nishiguchi, 2004). *V. fischeri* produces light via the enzyme luciferase, which requires oxygen in order to convert a reduced flavin mononucleotide and an aldehyde to a carboxylic acid. The reaction forms an excited hydroxyflavin intermediate, which emits blue-green light of  $\lambda_{\max}$  490 nm upon dehydration (Fisher *et al.*, 1996). Strains unable to generate light have a colonisation defect (McFall-Ngai *et al.*, 2012; McFall-Ngai and Ruby, 2000; Visick *et al.*, 2000). Luciferase has an affinity for oxygen in the nanomolar

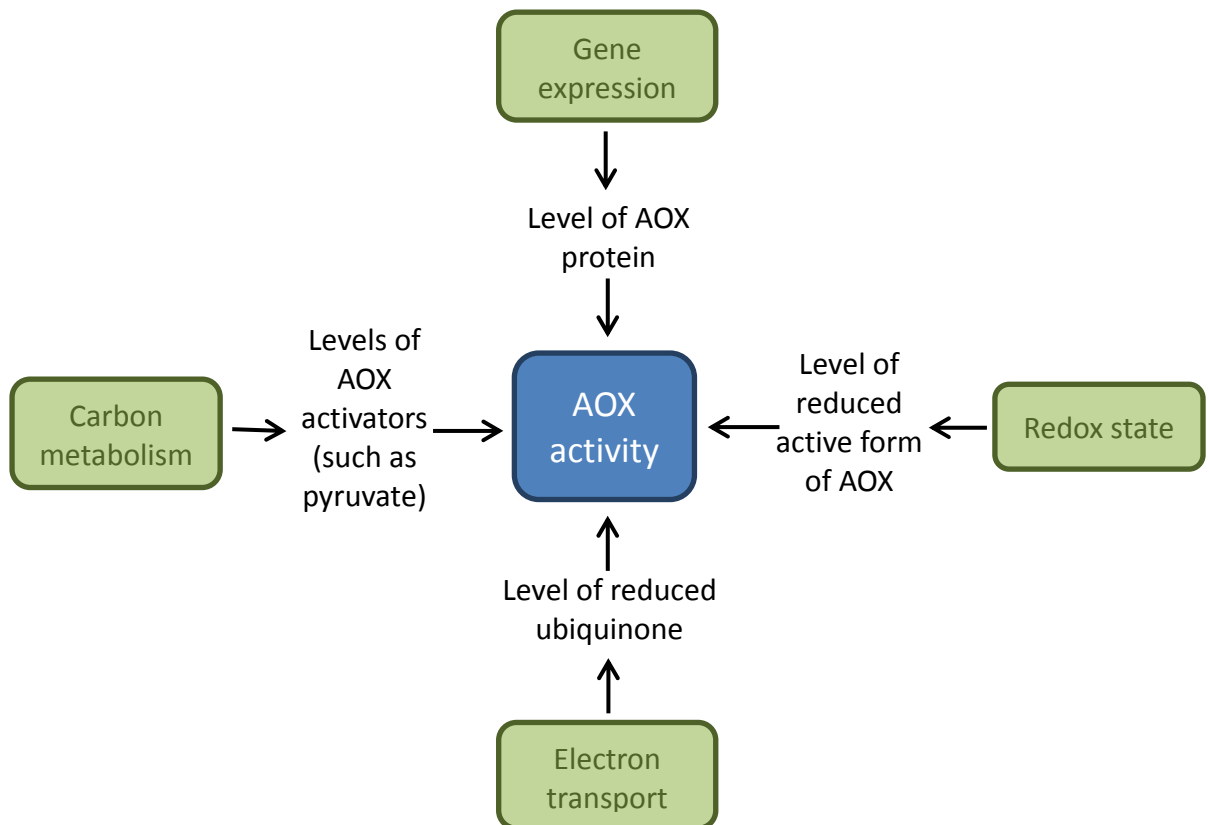


**Figure 4.2 Factors that affect the activity of plant AOX.** Major factors that control the partitioning of respiratory electrons to the non-energy-conserving alternative oxidase may include coarse control of the amount of AOX enzyme present as well as fine metabolic control of the activity of pre-existing AOX enzyme. The information used to generate this figure was obtained from (Vanlerberghe and McIntosh, 1997).

range (Lloyd *et al.*, 1985), therefore the process of light generation is in competition with aerobic respiration, which may be problematic at later stages of colonisation when oxygen may be limited (Ruby and McFall-Ngai, 1999). The low oxygen affinity of AOX (see below) may enable it to continue catalysing aerobic respiration, without compromising essential luciferase activity.

#### **4.1.2.4 Interaction of AOX with gaseous ligands**

The affinity of AOX for oxygen has long been known to be lower than that of cytochrome based oxidases (Kano and Kageyama, 1977). Studies of cytochrome oxidases similar to those encoded by *V. fischeri* suggest that cytochrome *bd* has a Michaelis constant of between 3 – 8 nM (D'mello *et al.*, 1996), while CcoNOQP is thought to have a  $K_m$  value of 7 nM (Preisig *et al.*, 1996). These oxidases have considerably higher affinities for oxygen than plant AOX, which has a  $K_m$  in the micromolar range (Ribas-Carbo *et al.*, 1994).

It is well established that AOX from plants is a cyanide-resistant oxidase (reviewed by Laites, 1982) due to the absence of haem, which is at the center of the catalytic mechanism of traditional cytochrome oxidases. Indeed, the existence of cyanide-resistant respiration in plants such as that in potato tubers, has been known since before the discovery of AOX (Hanes and Barker, 1931). The ability to undergo cyanide-resistant respiration is an important property in plants as approximately 800 species of plant are known to produce cyanide when wounded or attacked by pathogens (Mansfield, 1983).

It has recently been shown that a strain of *V. fischeri* containing AOX as the sole terminal oxidase was significantly less sensitive to the respiratory inhibitor NO than a strain containing cytochrome *bd* as the only terminal oxidase (Dunn *et al.*, 2010). As AOX is up-regulated by NO via the negative regulator NsrR, it has been suggested that AOX is important in protecting *V. fischeri* from host-derived NO during colonisation, enabling the symbiotic relationship between the bacterium and squid to be established. Contrary to this, *aox* mutants have been shown to be capable of colonizing squid with the same efficiency as wild type, which may suggest that AOX has a role at later stages of symbiosis (Dunn *et al.*, 2010).

There is currently no literature describing the relationship between CO and AOX, but this oxidase is assumed to be CO insensitive by analogy with cyanide and NO, which inhibit haem-based oxidases, but not AOX (Dunn *et al.*, 2010; Lambers, 1982).

#### **4.1.3 The aim of this work**

The aim of the work in this chapter was to assess the effects of CO-RMs on the non-haem oxidase AOX from *V. fischeri* through respiratory studies and spectroscopic methods. It was hypothesised that this oxidase would be resistant to respiratory inhibition by CO-RMs, as it lacks haem, which is believed to be a major target of CO from CO-RMs.

## **4.2. Results**

### **4.2.1 The growth of *V. fischeri* in rich medium**

In this work, mutants were obtained that were each able to express only one of the terminal oxidases of *V. fischeri*. AKD788 has the genotype  $\Delta aox \Delta ccoNOQP$  and therefore expresses CydAB (cytochrome *bd-I*) as the only ubiquinol oxidase; AKD789 has the genotype  $\Delta cydAB \Delta ccoNOQP$  and expresses AOX (alternative oxidase) as the only terminal oxidase (Dunn *et al.*, 2010). *CydAB* is known to be essential for aerobic growth; however, when such mutants were switched from anaerobic to aerobic growth, many developed suppressor mutations, which often affected AOX expression and allowed these mutants to grow normally in aerobic conditions (Dunn *et al.*, 2010). AKD789 contains the suppressor mutation OG1-10, which disrupts the putative NsrR binding site and results in NO-independent AOX expression (Dunn *et al.*, 2010). The wild type *V. fischeri* strain used as a control in this work was ES114 (Boettcher and Ruby, 1990), from which the mutant strains and were derived.

Initially, the growth of these strains was assessed in rich LBS medium (Figure 4.3). The strain AKD789 (AOX-only) grew at a much slower rate than both the wild type and AKD788 strains, which had similar growth rates.

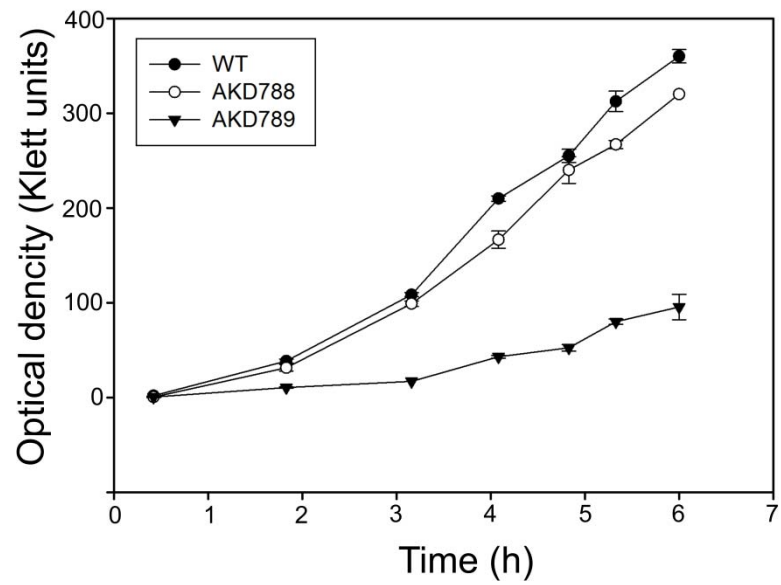


**Figure 4.3 The growth of three strains of *V. fischeri* in LBS medium.** The growth of wild type *V. fischeri* ES114 (closed circles), the mutant expressing only cytochrome *bd* (AKD 788, open circles) and the mutant expression only AOX (AKD 789, closed triangles) was measured spectroscopically using a Klett meter. Data are the means and standard deviations of 2 technical replicates and are representative of 2 biological replicates.

#### **4.2.2 The effects of CO gas and CO-RMs on the terminal oxidases of *V. fischeri***

In order to investigate the effects of CO-RMs on the terminal oxidases of *V. fischeri*, oxygen consumption of membrane particles prepared from cultures of each of the strains introduced in section 4.2.1 was measured using an oxygen electrode. Respiration was initially studied in a closed oxygen electrode (ie. a lid was placed on the electrode chamber to prevent the entry of oxygen into the system). The closed system allows oxygen consumption to be studied simply and directly for a short duration. A small amount of membrane preparation (typically 275  $\mu\text{g ml}^{-1}$ ) was added to the chamber and the respiratory substrate NADH (6.25 mM) was added to initiate respiration. As respiration proceeded, oxygen levels within the chamber rapidly decreased in a linear fashion. When the oxygen levels in the chamber reached 75% of air saturation (approximately 150  $\mu\text{M}$ ), the compound of interest (CO, CORM-401, CORM-3 or iCORM-3) was added to the chamber through a narrow hole in the lid, using a Hamilton syringe.

The addition of CORM-3 (50  $\mu\text{M}$ ) to both wild type and AKD788 (cytochrome *bd-I*-only) membranes reduced the rate of respiration to 84% and 74% respectively of the control rates in which no compound was added (data are the mean of at least 2 technical and 2 biological replicates). In contrast, the addition of CORM-3 (50  $\mu\text{M}$ ) to AKD 789 (AOX-only) membrane particles had a larger effect on the respiration rate, which was reduced to 27% of the control rate (Figure 4.4A and Figure 4.5).

The finding that membranes containing AOX as the sole terminal oxidase were hypersensitive to CORM-3 was contrary to expectations, as it was hypothesised that an oxidase without haem would be insensitive to respiratory inhibition by CO from CORM-3. In order to further investigate this finding, the above experiment was repeated with a CO-saturated solution used in place of CORM-3. CO reduced the rate of oxygen consumption by wild type, AKD788 and AKD789 membrane particles to 50, 60 and 79% of the control rates respectively (Figure 4.4B and Figure 4.5). The experiment was then repeated using the control compound iCORM-3. This had a minimal effect on the rates of oxygen consumption, altering respiration rates to 101, 94 and 90% of the control for wild type, AKD 788 and AKD 789 respectively (Figure 4.4C and Figure 4.5). Finally, the experiment was repeated using the manganese based CO-RM, CORM-

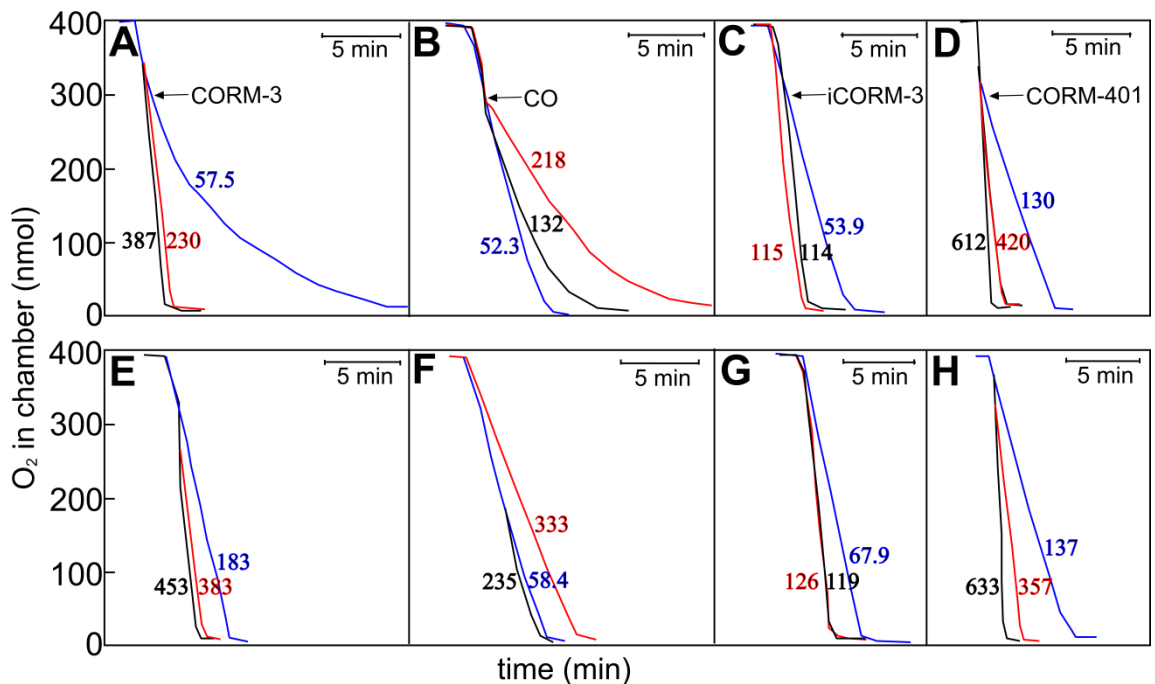


**Figure 4.4** AOX from *V. fischeri* is resistant to respiratory inhibition by CO-saturated solution, but hypersensitive to CORM-3 and CORM-401. Membrane particles resuspended in 2 ml *Vibrio* phosphate buffer to a final protein concentration of approximately 275 μg ml<sup>-1</sup>, and added to the closed oxygen electrode chamber. NADH (6.25 mM) was added to initiate respiration. Traces show oxygen consumption of membrane particles from wild type (black lines), cytochrome *bd-I*-only (red lines) and AOX-only (blue lines) in the presence of (A) CORM-3 (50 μM), (B) CO-saturated solution (100 μM), (C) iCORM-3 (50 μM) and (D) CORM-401 (50 μM), all added at approximately 150 μM O<sub>2</sub>, as indicated by the arrow. Traces (E - H) show the corresponding controls for the above experiments. Variations in respiration rate between control experiments are due to variation in the use of different batches of membrane preparation and variations of the quantity of protein added for different strains. The numbers on the traces are respiration rates 2 min following the addition of compound (nmol O<sub>2</sub> min mg<sup>-1</sup> protein<sup>-1</sup>). These traces are representative of at least 2 technical and 2 biological replicates.

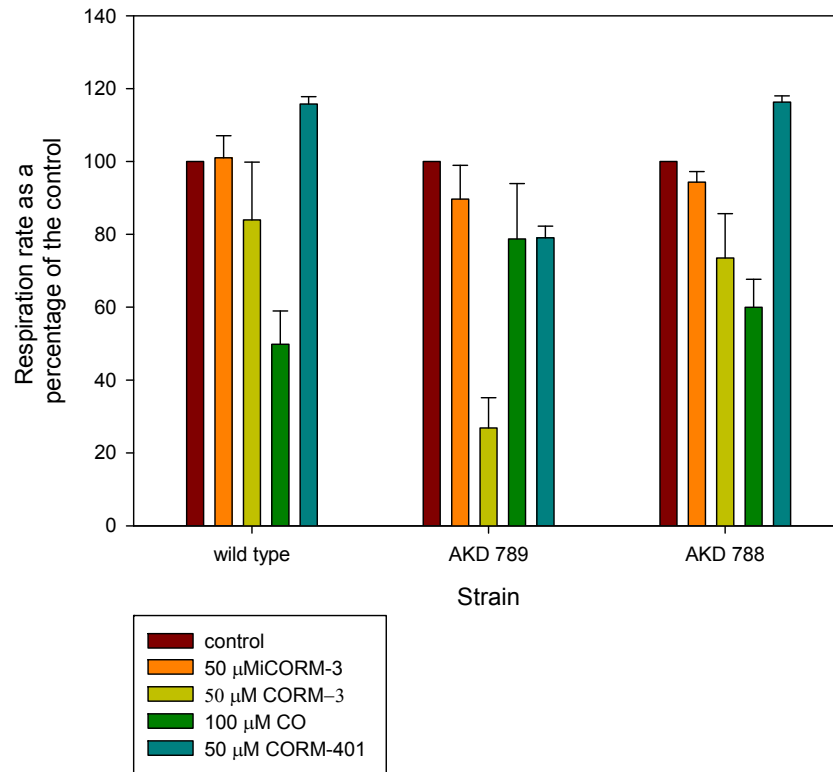


**Figure 4.5 Respiration rates of *V. fischeri* membrane particles treated with CO, CORM-3, iCORM-3 or CORM-401 as a percentage of the control rate.** This figure summarizes graphically the data shown in Figure 4.4. Respiration rates were calculated 2 min after the addition of compound, and at the corresponding point in the control experiment in which no compound was added. Rates were expressed as a percentage of the control rate and means and standard deviations calculated from at least 2 technical replicates of at least 2 biological replicates. Brown bars represent the control rate, which was set as default at 100%, orange bars show the data for iCORM-3 (50 μM), yellow bars for CORM-3 (50 μM), green bars for CO (100 μM) and blue bars for CORM-401 (50 μM).



401. This compound is able to release up to 3 CO equivalents from each CO-RM molecule under biological conditions (1.2.3.3). CORM-401 inhibited respiration to a lesser extent than CORM-3, consistent with the effects of this compound on *E. coli* membranes (Lauren Wareham, unpublished work). Oxygen consumption rates of wild type and AKD788 membranes were both increased by 116% in the presence of 50  $\mu\text{M}$  CORM-401 compared to the control in which no compound was added, whereas that of AKD789 was inhibited to 79% of the control (Figure 4.4D and Figure 4.5). Figures 4.4E – F show the oxygen consumption rates of the control experiments in each case. Numbers shown on each trace represent the respiration rates calculated at 2 min following the addition of compound (or the equivalent time point in the control experiments). In some cases, these numbers appear misleading; for example the respiration rate calculated for AKD789 membranes in Figure 4.2F is  $58.4 \text{ nmol O}_2 \text{ min}^{-1} \text{ mg}^{-1} \text{ protein}$ , however it appears to have a faster rate of oxygen consumption than AKD788 membranes in the same figure, which have a respiration rate of  $333 \text{ nmol O}_2 \text{ min}^{-1} \text{ mg}^{-1} \text{ protein}$ . This is because a larger amount of protein was added to the chamber in the case of AKD789 in order to achieve similar apparent rates of oxygen consumption for all three strains prior to the compound of interest being added. Variation between the various control respiration rates occurred between each preparation of membrane particles; however, the trends seen when the various compounds were added to the chamber were consistent between biological replicates as reflected by the small standard deviations of the percentage inhibition data (Figure 4.5).

Due to the unexpected nature of the results described above, work was also done to compare the sensitivities of the oxidases to inhibition by CORM-3 in the open oxygen electrode, by measuring the time taken for the chamber to reoxygenate, as described in Chapter 3. This method allows a comparison between the sensitivity of various strains to the inhibitor to be made; the respiration of more sensitive strains will be inhibited to a greater extent and so will not be able to utilise the oxygen in the chamber as quickly, allowing oxygen to accumulate in the chamber and be detected by the electrode.

In this experiment, conditions were established that allowed respiration to proceed at a sufficient rate to maintain an oxygen level of 0 in the chamber for an extended period of time. Eventually, the substrate NADH became exhausted, leading to reoxygenation of

the chamber. In the absence of an inhibitor, the time to reoxygenation of membranes from all three strains (wild type, AKD788 and AKD789) was very similar (between 40 and 48 min; Figure 4.6A). However, when CORM-3 (25  $\mu$ M) was added, while the time to reoxygenation of wild type and AKD789 was largely unaffected (wild type: 81% of control, AKD788: 87% of control), the chamber containing AKD789 membranes began to reoxygenate almost immediately, confirming that this oxidase is extremely sensitive to respiratory inhibition by CORM-3 (Figure 4.6B). Importantly, the control experiment using iCORM-3 gave times to reoxygenation for each membrane type similar to that of the control (Figure 4.6C; wild type: 93% of control, AKD788: 103%, AKD789: 94%).

Plant AOX is known to be resistant to cyanide (reviewed by Lambers, 1982). In order to validate the experimental design, the experiment was repeated using potassium cyanide (KCN) (Figure 4.6D). Indeed, it was found that the time taken for membranes containing AOX or cytochrome *bd-I* as the only terminal oxidase to begin to reoxygenate was largely unaffected by 50  $\mu$ M cyanide (with times to reoxygenation of 96% and 119% of the control times respectively). AKD788 membranes were able to maintain anoxia in the chamber for a significantly longer duration than wild type membranes, which is consistent with cytochrome *bd-I* having some cyanide resistance (Borisov *et al.*, 2011a; Voggu *et al.*, 2006) The control traces for this experiment, in which no cyanide was added, are shown in Figure 4.6E. The data described thus far in this chapter confirm that AOX is resistant to cyanide and CO, but hypersensitive to CO-RMs.

#### **4.2.3 The effects of CORM-2 and CORM-3 on the growth of *V. fischeri***

Next, it was investigated whether the sensitivity of the AOX protein to respiratory inhibition by CORM-3 led to an increased sensitivity of a strain of *V. fischeri* expressing AOX as the only ubiquinol oxidase to growth inhibition by this compound. Aliquots of CORM-2 or CORM-3 were added to 5 ml ASW medium in sterilin tubes with a small inoculum of primary culture (40  $\mu$ l of wild type and 120  $\mu$ l of AKD789), which had been grown in 5 ml LBS for 6 h.

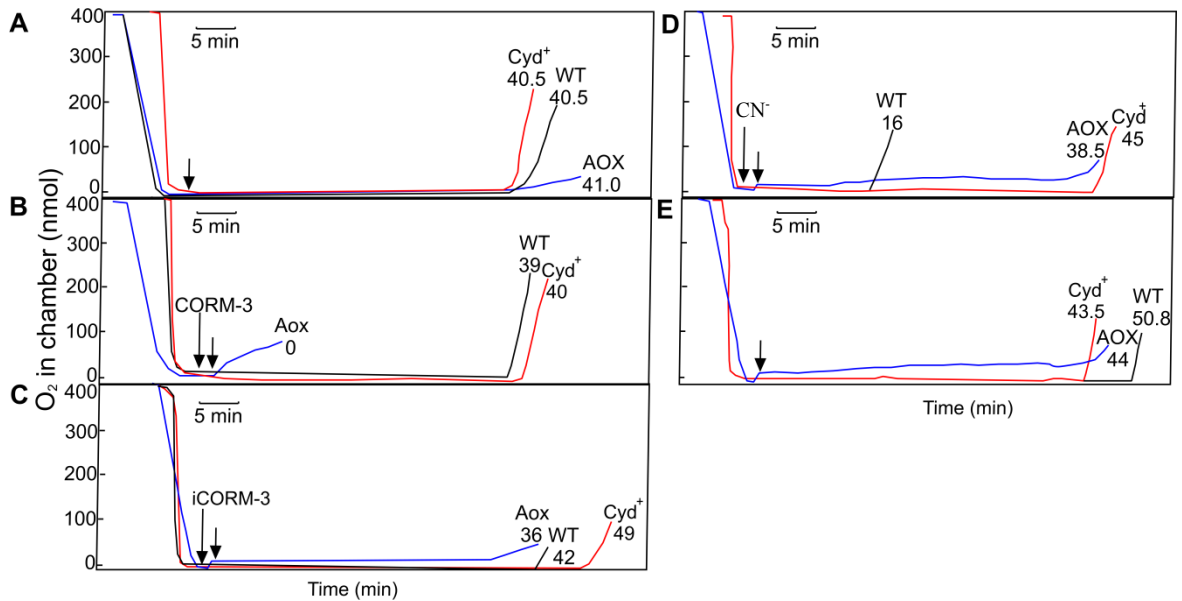


**Figure 4.6 AOX is the most sensitive oxidase of *V. fischeri* to respiratory inhibition by CORM-3.** Membranes prepared from either wild type *V. fischeri* or from mutants containing either AOX (AKD 789) or cytochrome *bd-I* (AKD 788) as the only terminal oxidase were added to the chamber to a final concentration of approximately 40 mg ml<sup>-1</sup> and stimulated to respire by the addition of 12.5 mM NADH. The black lines show the traces for the wild type strain, red lines show the traces for the strain containing cytochrome *bd-I* only and blue lines for the strain containing AOX only. (A) shows the control in which no compound was added for the CORM-3 experiment, (B) CORM-3 (25 μM) added at the long arrow, (C) iCORM-3 (25 μM) added at the long arrow, (D) CN<sup>-</sup> (100 μM) added at the long arrow, (E) shows the control in which no compound was added for the cyanide experiment. In each case, the lid was removed from the chamber at the time point indicated by the short arrow. The numbers with each trace show the time taken for the chamber to reoxygenate, following the removal of the lid, in minutes. Data are representative of at least 2 biological and 2 technical repeats.

These cultures were then incubated at 28 °C with shaking for 17 h and then the OD<sub>600</sub> measured using a spectrophotometer. One difficulty that arose when comparing the growth of AKD 789 with that of wild type *V. fischeri* in the presence of CO-RM, is that in the absence of an inhibitor, the former grows significantly slower than the later. In the absence of CO-RM, AKD789 reached an optical density (OD<sub>600</sub>) approximately 40% lower than that of wild type after 16 h (Figure 4.7A and C). For this reason, it was considered that the optical density values expressed as a percentage of the growth for each strain in the absence of CORM-3 (Figure 4.7B and D) gave more meaningful information than the raw optical density data (Figure 4.7A and C). The growth of AKD789 was inhibited by a lower percentage than that of wild type *V. fischeri* over a range of CORM-3 concentrations. CORM-2 had a more potent effect on the growth of *V. fischeri* than CORM-3, consistent with observations in other organisms (see Chapter 3 of this work and Nobre *et al.* (2007)). CORM-2 (50 µM) reduced the growth of wild type *V. fischeri* by 93%, whereas 50 µM CORM-3 reduced the growth of *V. fischeri* by only 65% (Figure 4.7B and D). At three of the four CORM-2 concentrations tested (12.5, 50 and 100 µM), the growth AKD789 appeared to be slightly less affected in terms of percentage than that of the wild type strain. Importantly, the control compound RuCl<sub>2</sub>(DMSO)<sub>4</sub>, a CORM-3 precursor that is also structurally similar to CORM-2, did not have any effect on the growth of either strain under the same experimental conditions (data not shown).

#### **4.2.4 Spectroscopic studies of *V. fischeri* cell suspensions and membrane preparations treated with CORM-3**

The haem content of the membrane particles used in the respiratory studies in this chapter was confirmed by generating reduced *minus* oxidised difference spectra (Figure 4.8). *V. fischeri* membrane particles were suspended in buffer to a final concentration of approximately 2 - 4 mg ml<sup>-1</sup>. The 'oxidised' sample was scanned in triplicate using a dual wavelength spectrophotometer (Kalnenieks *et al.*, 1998) using a 10 mm path

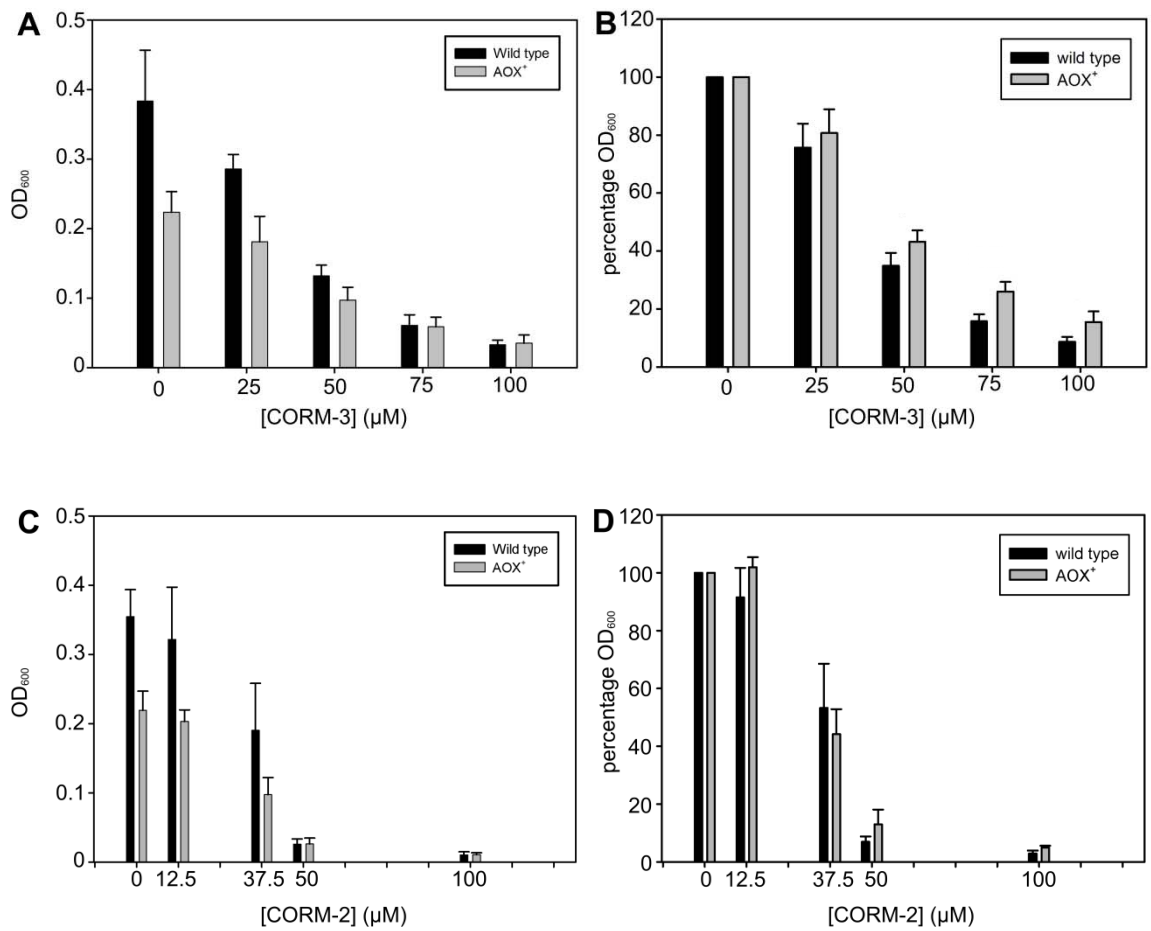


**Figure 4.7** The effect of various concentrations of CORM-2 and CORM-3 on the growth of *V. fischeri*. Cultures of *V. fischeri*; wild type (black bars) and AKD 789 (grey bars) were grown overnight in the presence of various concentrations of CORM-2 or CORM-3 (0 – 100 μM). OD<sub>600</sub> was then recorded for each strain (A and C) and expressed as a percentage of the OD<sub>600</sub> in the absence of CO-RM (B and D). Data are the means and standard deviations of 3 biological repeats.

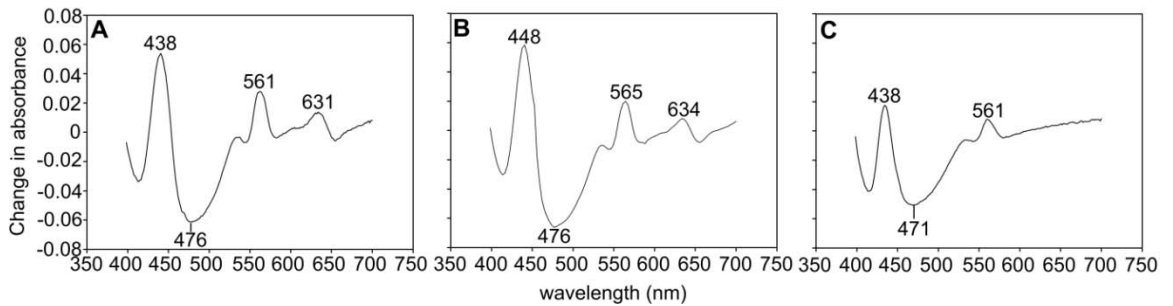


**Figure 4.8 Reduced minus oxidised spectra of *V. fischeri* membrane particles.** (A) wild type, (B) AKD788 (cytochrome *bd-I* only) and (C) AKD789 (AOX only) membranes were analysed using a dual-beam spectrophotometer to generate reduced minus oxidised difference spectra. Membrane preparations were diluted with vibrio buffer to a final concentration of 2 - 4 mg ml<sup>-1</sup>. These spectra are representative of 2 technical and 2 biological replicates.

length. Samples were then reduced by the addition of a few grains of sodium dithionite and spectra were again recorded in triplicate. Data were averaged in Excel and plotted as reduced *minus* oxidised difference spectra. The spectrum of each strain had a peak between 438 and 448 nm, which is indicative of various cytochromes, a trough at approximately 470 nm, which is probably attributable to flavin and a peak at approximately 560 nm caused by haem *b* (Jones and Poole, 1985). Importantly, there is a peak at approximately 634 nm in the wild type and cytochrome *bd-I*-only-containing cells that is not present in the AOX only cells confirming the absence of haem *d*.

CORM-3 difference spectra for *V. fischeri* whole cells (Figure 4.9) were then generated for each strain to further investigate their interaction with CO from CORM-3. Samples were suspended in buffer to a final concentration of approximately 12 - 14 mg ml<sup>-1</sup>, reduced by the addition of a few grains of sodium dithionite and then scanned in triplicate using a dual wavelength spectrophotometer as described above. Samples were then treated with CORM-3 (300 μM). Spectra were recorded in triplicate, averaged and plotted as a CO reduced minus reduced difference spectra. The whole cell CORM-3 difference spectra confirmed that CO from CORM-3 binds to components of all three strains, including AKD789, which expresses AOX as the only terminal oxidase.

In order to investigate more directly the interaction of CO from CORM-3 with the terminal oxidases of *V. fischeri*, CO difference spectra were also generated as described above by treating membrane particles (final concentration 2 - 4 mg ml<sup>-1</sup>) prepared from wild type *V. fischeri* (Figure 4.10A, C, E), or the strain expression AOX as the only terminal oxidase (Figure 4.10B, D, F) with CO (Figure 4.10A, B, bubbled for 5 min) CORM-3 (Figure 4.10C, D; 300 μM) or iCORM-3 (Figure 4.10E, F; 300 μM), or by bubbling with CO for 5 min. The spectra produced from the whole cell samples and the membrane preparations were very similar, confirming that membrane-based components are interacting with CO in all cases. CO and CORM-3 treatment also led to very similar spectra, indicating that CO released from CORM-3 was responsible for the spectral changes seen when the membrane particles were treated with this compound (Figure 4.10A and C, B and D). An important spectral difference between the two membrane types is the absence of a peak at 648 nm in the AOX only membranes. This

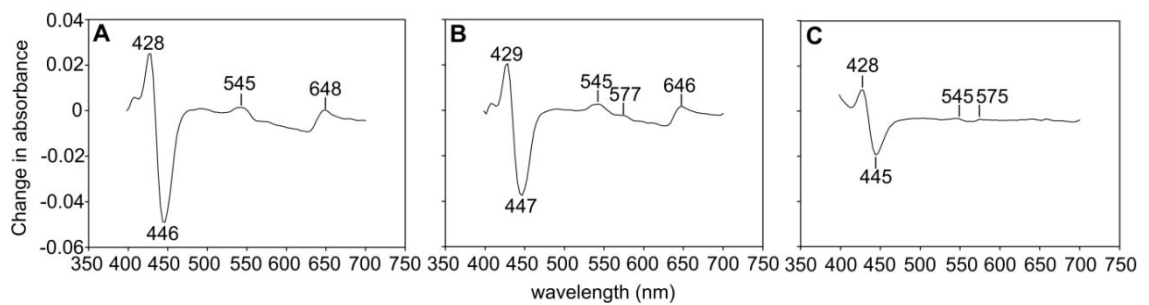


**Figure 4.9 CORM-3 difference spectra of *V. fischeri* whole cells.** A dual wavelength spectrophotometer was used to generate difference spectra (CORM-3 reduced minus reduced) of (A) wild type, (B) AKD788 (cytochrome *bd-I*-only) and (C) AKD789 (AOX only membranes). Cell suspensions were added to *Vibrio* phosphate buffer to a final concentration of between 12 - 14  $\mu\text{g ml}^{-1}$  and treated with CORM-3 (100  $\mu\text{M}$ ). These spectra are representative of 2 technical and 2 biological replicates.



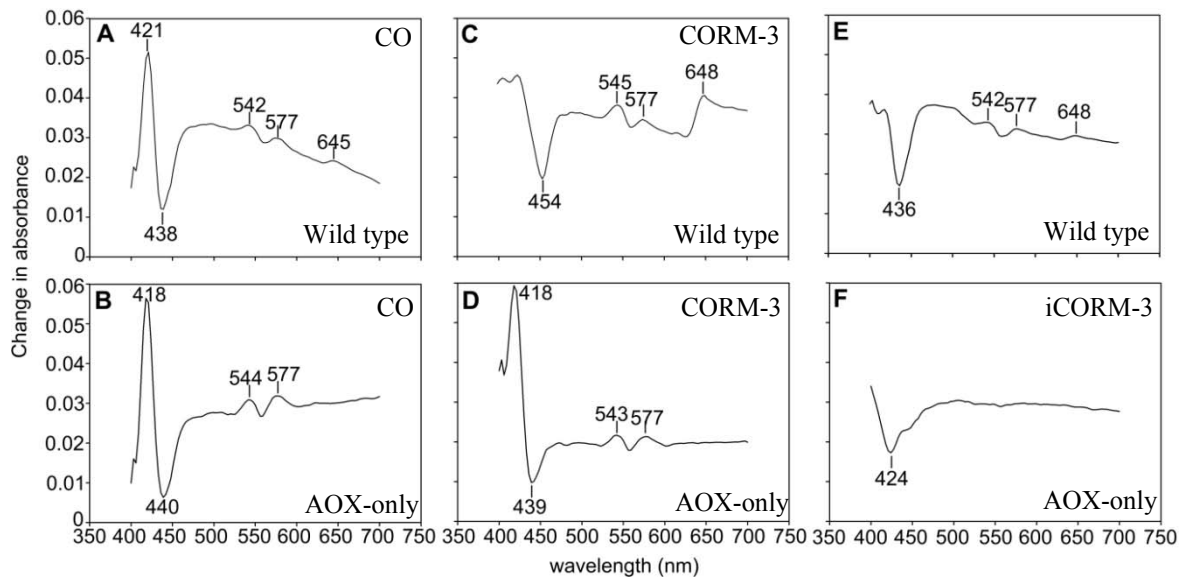


**Figure 4.10 CORM-3 difference spectra *V. fischeri* membrane particles** (reduced plus CORM-3 minus reduced) were recorded in a dual wavelength spectrophotometer. *V. fischeri* membrane particles from wild type (**A**, **C**, **E**) and AOX-only (**B**, **D**, **F**) strains were added to *Vibrio* buffer to a final concentration of between 2 - 4  $\mu\text{g ml}^{-1}$  and treated with either CO-saturated solution (**A** and **B**), CORM-3 (300  $\mu\text{M}$ ) (**C** and **D**) and iCORM-3 (300  $\mu\text{M}$ ) (**E** and **F**).

confirms that haem *d* is not present in these membranes (Figure 4.10B and D). It is clear however that there are some spectral features in the CO and CORM-3 difference spectra of the AOX-only membranes (Figure 4.10B and D), some of which are also present in the wild type membranes (Figure 4.10A and C). Difference spectra were produced for each membrane type treated with the control compound iCORM-3, which was verified to release very little CO to myoglobin (less than 1% compared with CORM-3, data not shown). The addition of iCORM-3 to wild type membranes resulted in oxidation of the membrane particles (seen by a trough at 436 nm, Figure 4.10E) as well the formation of a small peak at 648 nm indicating the binding of a small amount of CO to haem *d*. Interestingly, while the addition of iCORM-3 to AOX-only membranes appears to cause slight oxidation (shown by a small trough at 424 nm), no other distinct features are seen, suggesting that membranes devoid of haem are less able to trap the small amount of residual CO from iCORM-3.

### 4.3 Discussion

The work in this chapter constitutes the first investigation of the effects of CO and CO-RMs on a non-haem oxidase. Contrary to the expectation that AOX would be resistant to respiratory inhibition by CO-RMs, membranes containing only this oxidase were found to be hypersensitive to these compounds. Two different methods were used to measure respiration in membranes treated with CO-RMs because of the unexpected findings. These included closed electrode experiments, which measure respiration rates directly, and an open electrode method, used to compare the sensitivities of various strains to a respiratory inhibitor. Both methods experienced the same difficulty; that the respiration rate of AKD789 was significantly slower than that of AKD788 or wild type, which had similar oxygen consumption rates to one another (Dunn *et al.*, 2010). This necessitated a greater quantity of membrane preparation be used for AKD789 than the other two strains in order to achieve similar oxygen consumption rates. It is therefore possible that CORM-3 could be titrated by the additional membrane in this sample, thereby dampening the effects of the compound; however, the finding that CORM-3 is in fact more inhibitory to respiration in this strain negates this potential problem. Another concern caused by the differing respiration rates of the strains used was the possibility that the weak oxygen consumption rates of AKD 789 would render this strain sensitive to potent respiratory inhibition by any inhibitor. This led to the control

experiment in which cyanide (to which AOX is known to be resistant) was added to respiring membrane particles in the open electrode chamber (Figure 4.6D). The ability of AKD789 membrane particles to respire in the presence of cyanide acts as a positive control and confirms the validity of the finding that these membranes are hypersensitive to CORM-3. The experiment to measure time to reoxygenation is also validated by the finding that membranes containing only cytochrome *bd-I* were more resistant to CN<sup>-</sup> than wild type membranes, as is reported in the literature (Borisov *et al.*, 2011a).

The finding that the control compound iCORM-3 does not significantly inhibit respiration in any of the strains (Figure 4.4C and 4.6C) supports the conclusion that CO is the agent causing the inhibition, rather than the ruthenium-containing CO-RM backbone; however, the uncertain nature of iCORM-3, which was not fully appreciated at the time this work was carried out, complicates the interpretation of these results. This hypothesis is further supported by the finding that CORM-401, which contains manganese instead of ruthenium at its centre, is also more inhibitory to respiration in AKD789 membranes (Figure 4.4D). However, in contrast to this, AOX was shown to be resistant to CO delivered as a saturated solution (Figure 4.4B), suggesting that CO is not the causative agent of the inhibition of the enzymatic activity of this oxidase (Figure 4.4B).

Despite the finding that AOX oxidase activity is extremely sensitive to respiratory inhibition by CORM-3, the strain AKD 789 was less sensitive to growth inhibition by CORM-3. One difficulty in assessing the contribution of AOX to growth sensitivity in the presence of an inhibitor is that the strain AKD 789 grows at a much slower rate than wild type, which may affect the growth response to CORM-3. It should also be noted that the percentage of the optical density in the presence of CORM-3 compared to that in the absence of CORM-3 is quoted, and this will be affected to a different magnitude by an inhibitor because of the differing growth rates of the two strains. Another difficulty with the strain AKD789 is that the expression of AOX has been uncoupled from control by the NO response regulator NsrR and so AOX is being expressed under conditions in which it might not otherwise be, and perhaps in the absence of other proteins or conditions that are associated with its normal function. It is also possible that the *V. fischeri* cultures were able to ferment the carbon source in the medium (N-acetyl

glucosamine). As elucidating the effects of CO-RMs on the respiratory components of *V. fischeri* is the aim of this work, further studies should be done using a non-fermentable carbon source, such as glycerol to force the bacteria to respire.

It was considered important to investigate further the nature of the interaction between CO from CORM-3 and the terminal oxidases of *V. fischeri*. This process was hampered by the inherent difficulties of studying AOX, which, in plants, is notoriously difficult to purify and has no characteristic spectral features and no specific EPR signals (Laites, 1982).

Both the reduced minus oxidised and CO and CORM-3 difference spectra show that haem *d* is absent from both whole cell and membrane samples of the strain ADK789. Importantly though, CO applied as a saturated solution, or as CORM-3, was found to bind to components of membranes from all three strains of *V. fischeri*. The CO bound features of AKD789 membranes cannot yet be positively identified, however it is possible that they contribute to the sensitivity of this strain to CORM-3.

The peaks at 631 - 634 nm in the wild type and cytochrome *bd*-only reduced minus oxidised spectra (Figure 4.8A and B) are characteristic of cytochrome *d* as shown by Haddock *et al.* (1976) in *E. coli* and *A. vinelandii*, Jones and Redfearn (1966) in *P. aeruginosa* and Miller and Gennis (1986) in *E. coli*. This feature is absent from the AOX-only spectrum as expected (Figure 4.8C). The peaks between 561 and 565 nm are due to multiple *b* type cytochromes, with a contribution from cytochrome *c* (a component of *ccoNOQP*) in the case of the wild type and cytochrome *bd*-only membranes (Figure 4.8A and B). In the Soret region, the bands between 438 and 448 nm are again due to a composite of signals from cytochromes *b* and *d*. In Figure 4.8B, there is a greater contribution from cytochrome *bd*, shown by the shift of the peak to 448 nm. The features from the *c*-type cytochromes in the *cco* type oxidase would be expected at shorter wavelengths, but these are masked by other features.

These conclusions are supported by the CO and CORM-3 difference spectra in Figure 4.9 and 4.10, which show the presence of haem *d*, indicated by a peak at 645 – 648 nm (Jones and Poole, 1985) in the wild type and cytochrome *bd*-only strains, but not in the

AOX-only strain. In the Soret region of Figure 4.9A and B, the peak and trough can be attributed largely to CO binding cytochrome *b* (ie. cytochrome *b*<sub>595</sub>) and haem *d*. The identity of the spectral features seen in the CO spectra of AKD 789 is much less clear; the only oxidase reported in this strain is AOX and it has been reported that this oxidase has no spectral features (Laites, 1982).

Haemoproteins other than respiratory oxidases are capable of giving rise to spectral features. Indeed, a peak at approximately 420 nm can indicate CO binding to cytochrome P-420, while a peak at approximately 440 – 445 nm can be caused by CO binding to cytochrome *a*<sub>1</sub> or *a*<sub>3</sub> (Jones and Poole, 1985). There is no evidence that *V. fischeri* contains either of these cytochromes; however, it is known to contain cytochromes *c*<sub>551</sub> and *c*<sub>554</sub> (Petushkov and Lee, 1997), which have reduced absorption spectra similar to *c*-type cytochromes from *P. aeruginosa* and *Azotobacter* with a strong peak at 416 nm. There are other components of *V. fischeri* that absorb in the UV-visible region; blue fluorescence protein also has an absorption maximum at 417 nm and thioredoxin reductase has absorption features between 400 – 500 nm (Petushkov and Lee, 1997).

The binding of CO from CO-RMs to haem proteins and the subsequent inhibition of these proteins was initially considered to be a major cause of the bactericidal nature of these compounds. While this is still considered to be an important mechanism of CO-RM action, there is mounting evidence that CO-RMs have much wider reaching cellular effects. Transcriptomic profiling indicates that the metabolism and transport of many ions are greatly affected by CORM-3, as well as several global regulators of transcription (Davidge *et al.*, 2009b). There is also evidence that *E. coli* cultures treated with CORM-3 (100 µM) lose significant viability prior to the onset of respiratory inhibition (Wilson *et al.*, 2013). In addition, anaerobic cultures have been shown to be susceptible to killing by high concentrations of CO-RMs (Davidge *et al.*, 2009b; Nobre *et al.*, 2007). Recent work from this laboratory has found that both naturally occurring haem-deficient bacteria (*Lactococcus lactis*) and a strain of *E. coli*, which had been genetically modified to be haem-deficient, were both susceptible to growth inhibition and killing by CORM-3 (Wilson, 2012).

These findings, and the results presented in this chapter, suggest that there are significant targets of CORM-3 other than the haem-containing respiratory oxidases. There are examples of CO directly affecting the activity of non-haem proteins. CO is known to activate large-conductance  $\text{Ca}^{2+}$ - and voltage-gated  $\text{K}^+$  (Slo1 BK) channels, which are involved in oxygen sensing, vasodilation and the activation of signalling from neurones (Wang *et al.*, 1997). The interaction of CO with such channels is thought to involve sulfur from cysteine and nitrogen from histidine residues within the cytoplasmic domain of the channel. CO is thought to act as a partial agonist for the divalent cation sensor in the Slo1 BK channel (Hou *et al.*, 2008).

As yet, the mechanism of AOX inhibition by CO-RMs cannot be envisaged as there is no structural information available for the active site of bacterial AOX. CO is able to bind to iron in iron, iron-iron and iron-nickel hydrogenases (Armstrong, 2004) and to the iron-iron hydrogenases of *Chlamydomonas* (Stripp *et al.*, 2009), which could provide a precedent for the binding of CO to the di-iron active site of AOX. Furthermore, a cyanide-resistant but CO-sensitive hydrogenase has been reported (Lamrabet *et al.*, 2011). As some hydrogenases have di-iron centres that coordinate to both CO and cyanide in order to activate hydrogen, this may be a starting point for understanding the CO-RM sensitivity of the di-iron centre of AOX.

CO-RM has been reported to have activities distinct from those of CO gas; for example, CORM-2, but not CO gas, has been shown to obstruct ATP-gated human P2X4 receptors involved in the sensing of pain in mammalian systems (Wilkinson and Kemp, 2011). CORM-2 is thought to behave as an antagonist, reversibly inhibiting these receptors in a competitive manner independent of its CO releasing properties. Furthermore, CORM-3, but not CO gas or iCORM-3, has recently been shown to facilitate the transport of  $\text{K}^+$  and  $\text{Na}^+$  ions across the bacterial membrane, causing a stimulation of respiration (Wilson *et al.*, 2013). These findings could be analogous to the results obtained in the current study, in which it is possible that the whole CO-RM molecule is binding to and interfering with the activity of AOX, compatible with the finding that both CO gas and the control compound iCORM-3 do not inhibit the activity of AOX. It should be noted that the structure and redox properties of iCORM-3 are not well characterised, which poses difficulties in drawing firm conclusions from the results

gained when using this control compound (see section 7.2). CORM-3 has recently been reported to bind to proteins (Santos-Silva *et al.*, 2011; Santos *et al.*, 2012). It would therefore be interesting to investigate this hypothesis further by purifying AOX (although this would not be trivial) and then investigating whether CORM-3 is able to bind to this protein.

CO-RMs are known to be more potent than CO gas at inhibiting growth (Davidge *et al.*, 2009b), viability (Nobre *et al.*, 2007), and respiration (Wilson *et al.*, 2013). However, in such cases, it is assumed that CO-RMs deliver CO into the cell, dramatically increasing the concentration of this gas at the target sites (Davidge *et al.*, 2009b). In the case of AOX, CORM-3 is inhibitory, while CO is not, and there is no conceivable mechanism for how CO could inhibit this enzyme, even at high concentrations.

Although regulation of AOX activity is not well understood, it is known that in plants, certain carboxylic acids such as pyruvate and glyoxylate stabilize the active conformation of AOX and are essential for the activity of this oxidase (Carre *et al.*, 2011). Pyruvate is a fundamental component of metabolism. It is produced by glycolysis and is also converted into acetyl-coenzyme A, which is essential for the Krebs cycle. It could therefore be investigated whether CORM-3 interferes with the binding of pyruvate to AOX, thereby adversely affecting the activity of this oxidase.

The lack of detailed structural or sequence information for bacterial AOX, as well as the unavailability of the purified protein, have limited efforts to explain the unexpected finding that AOX is hypersensitive to respiratory inhibition by CORM-3. Ideally, Infrared or Resonance Raman spectroscopy would be performed to investigate whether CO interacts with AOX directly, or with another component of these membranes. There has been some success elucidating the nature of the active site of plant and trypanosomal AOX using EPR spectroscopy (Moore *et al.*, 2008), and so this technique could be used to investigate the binding of CO to this oxidase.

## Chapter 5

### The effects of thiol-containing compounds and antioxidants on the activities of CO-RMs

#### 5.1 Introduction

Almost a decade ago, it was noted that N-acetylcysteine (NAC) abolished the activities of CORM-2 and CORM-3 (Sawle *et al.*, 2005 and Taille *et al.*, 2005). Since then, several papers have been published describing this phenomenon, but none have comprehensively explained the mechanism by which these compounds exert their effects. It was initially shown that while CORM-2 and CORM-3 increased HO-1 expression and haem oxygenase activity in murine macrophages, these effects were abolished by NAC (Sawle *et al.*, 2005). NAC was also found to partially prevent the inhibitory effects of CORM-2 on the mitochondrial respiratory chain and NAD(P)H oxidase (Taille *et al.*, 2005). It was then reported that NAC (1 mM), reduced glutathione (GSH) (50  $\mu$ M) and cysteine (100  $\mu$ M) all completely prevent the effects of CORM-3 on the growth and oxygen consumption of *P. aeruginosa*. The authors concluded that this was not due to NAC preventing the liberation of CO from CORM-3, or causing the activation of the cysteine - glutathione pathway leading to increased levels of free glutathione. Instead, they hypothesised that NAC may interfere with the interaction of CO liberated from CORM-3 and the cytochromes of the bacterial respiratory chain, or that inhibition of oxygen consumption by CORM-3 may involve cysteine moieties strategically located in the enzymes of the respiratory chain (Desmard *et al.*, 2009). It was later reported that only the activity of metal-containing CO-RMs (especially those containing ruthenium) are affected by thiol compounds; therefore it is unlikely that NAC interferes with the binding of CO to terminal oxidases, as this is assumed to be a target of all CO-RMs (Desmard *et al.*, 2012). It was hypothesised that thiol compounds may favour a very rapid rate of CO release from transition metal carbonyls (Desmard *et al.*, 2012), causing them to mimic the application of CO gas (ie. CO release prior to the CO-RM entering the cell), and that this could abrogate the intracellular delivery capacity of CO-RMs. In support of this, there is some evidence that thiol-containing



compounds such as cysteine, can promote CO release from CO-RMs (Hasegawa *et al.*, 2010).

An alternative hypothesis suggests that thiol-containing compounds quench the activity of CO-RMs by virtue of their antioxidant properties (Tavares *et al.*, 2011). It was found that GSH was able to prevent the antibacterial effects of CORM-2 by approximately 95% and that cysteine prevented the growth inhibitory effects of the CO-RM ALF062 by approximately 85%. Evidence is presented that high concentrations of CORM-2 cause an increase in reactive oxygen species (ROS) as measured by the fluorescent probe 2',7'-dichlorofluorescein diacetate, and that application of exogenous glutathione reduces the amount of ROS detected, leading the authors to conclude that the antioxidant properties of GSH are responsible for this activity. It was also shown that CO is necessary for ROS production, as cultures treated with RuCl<sub>2</sub>(DMSO)<sub>4</sub> or with CORM-2 in media supplemented with haemoglobin, which scavenges CO, did not experience an increase in ROS (Tavares *et al.*, 2011).

It is important to note that another group had previously investigated the possibility that CORM-3 mediates its bactericidal effects by the production of ROS and concluded this was unlikely as not all antioxidants (for example ascorbic acid) were able to abolish the effects of CO-RMs and hydrogen peroxide production was not detected when *P. aeruginosa* was treated with 10 µM CORM-3, despite this concentration of CORM-3 significantly decreasing the viability of this organism (Desmard *et al.*, 2009).

In light of the uncertainty in the published literature as to how thiol compounds abrogate the effects of CO-RMs, and whether the production of ROS contributes to the deleterious effects of CO-RMs, the work presented in this chapter aimed to address the following questions. (1) Do thiol compounds affect the rate or amount of CO released from CORM-3? (2) If not, by what mechanism do thiol compounds abrogate the effects of CO-RMs? (3) Do endogenous thiol compounds protect bacterial cells from the deleterious effects of CO-RMs? (4) To what extent does the production of ROS by CO-RMs contribute to the bactericidal effects of these compounds?

## 5.2 Results

### 5.2.1 Thiol-containing compounds completely prevent the inhibitory effects of CORM-2 and CORM-3 on respiration

It was important to begin by establishing that under the standard experimental conditions used in this laboratory, thiol-containing compounds could prevent the inhibitory effects of CORM-3 on bacterial respiration as has been reported by others (Desmard *et al.*, 2009). Initially, a closed oxygen electrode system was used to measure the rate of respiration of wild type *E. coli* membrane particles in the presence of CORM-3 and the thiol-containing compounds NAC, cysteine and reduced glutathione. Membrane particles were added to 2 ml sonication buffer to a final concentration of between 60 and 100  $\mu\text{g ml}^{-1}$  and respiration was initiated by the addition of 6.25 mM NADH. The thiol compound was added when the dissolved oxygen tension in the chamber reached approximately 155  $\mu\text{M}$  (75% of air saturation) and the CO-RM was added 1 min later.

The respiration rate of membrane particles 2 min after the addition of CO-saturated solution to a final concentration of 100  $\mu\text{M}$  was 177  $\text{nmol min}^{-1} \text{mg}^{-1}$  compared to 287  $\text{nmol min}^{-1} \text{mg}^{-1}$  in the control in which no compound was added. NAC was unable to abrogate the inhibition caused by CO gas: respiration in the presence of both NAC and CO was inhibited to the same extent as when CO-saturated solution was added alone (Figure 5.1A).

This experiment was then repeated with CORM-3. The respiration rate of membrane particles 2 min after the addition of 400  $\mu\text{M}$  CORM-3 was 167  $\text{nmol min}^{-1} \text{mg}^{-1}$  compared to 442  $\text{nmol min}^{-1} \text{mg}^{-1}$  in the absence of inhibitor. However, in the presence of CORM-3 and an equimolar concentration of NAC, the respiration rate was restored to 418  $\text{nmol min}^{-1} \text{mg}^{-1}$  (Figure 5.1B). NAC also reduced respiratory inhibition of *E. coli* membrane particles by CORM-2; however a 10-fold excess of NAC was required in order to reduce the inhibitory effect of CORM-2 by approximately 45% (Figure 5.1C). The respiration rate of membrane particles 2 min after the addition of 50  $\mu\text{M}$  CORM-2 was 139  $\text{nmol min}^{-1} \text{mg}^{-1}$  compared to 452  $\text{nmol min}^{-1} \text{mg}^{-1}$  in the absence of inhibitor, and 276  $\text{nmol min}^{-1} \text{mg}^{-1}$  in the presence of CORM-2 and NAC. Figure 5.1D shows the oxygen consumption profile of *E. coli* membranes in which NAC was added

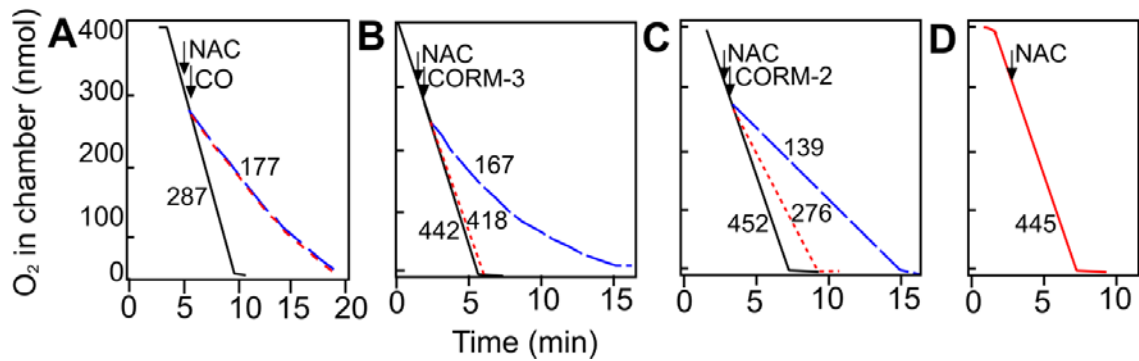


**Figure 5.1 NAC prevents CORM-2 and CORM-3 - dependent inhibition of respiration in *E. coli* membrane particles.** Wild type *E. coli* membrane particles were added to sonication buffer (2 ml) to a final concentration of approximately 60  $\mu\text{g ml}^{-1}$  (A) or 100  $\mu\text{g ml}^{-1}$  (B, C, D) and respiration was initiated by the addition of NADH (6.25 mM). In (A) arrows indicate the addition of 100  $\mu\text{M}$  NAC, or 100  $\mu\text{M}$  CO as a saturated solution; in (B), arrows indicate the addition of NAC or CORM-3 (both at 400  $\mu\text{M}$ ); in (C) arrows indicate the addition of NAC (500  $\mu\text{M}$ ) or CORM-2 (50  $\mu\text{M}$ ) and in (D), the arrow shows the addition of 400 mM NAC. The traces show dissolved oxygen in the chamber for uninhibited respiration (black solid lines) or oxygen consumption in the presence of CO or CO-RM (blue dashed lines) or CO-RM and NAC (red dotted lines). Respiration rates ( $\text{nmol min}^{-1} \text{mg}^{-1} \text{protein}$ ) 2 min following the addition of CO or CO-RM are shown adjacent to each trace. These data are representative of at least 3 technical and 2 biological replicates. This figure was published in Jesse *et al.* (2013).

alone when the oxygen in the chamber reached approximately 80%. The respiration rate here ( $445 \text{ nmol min}^{-1} \text{ mg}^{-1}$ ) was very similar to that when no compound was added, confirming that NAC alone has no effect on the rate of respiration. This investigation was extended to confirm that the thiol-containing compounds glutathione and cysteine were also able to abrogate the inhibitory effects of CORM-3. The respiration rate of wild type *E. coli* membrane particles 2 min after the addition of  $400 \text{ }\mu\text{M}$  CORM-3 was  $91.8 \text{ nmol min}^{-1} \text{ mg}^{-1}$  compared to  $197 \text{ nmol min}^{-1} \text{ mg}^{-1}$  in the absence of inhibitor and  $123 \text{ nmol min}^{-1} \text{ mg}^{-1}$  in the presence of CORM-3 and  $200 \text{ }\mu\text{M}$  reduced glutathione (Figure 5.2A). Similarly, in the case of GSH, the respiration rate of the membrane particles 2 min after the addition of  $400 \text{ }\mu\text{M}$  CORM-3 was  $72.6 \text{ nmol min}^{-1} \text{ mg}^{-1}$  compared to  $117 \text{ nmol min}^{-1} \text{ mg}^{-1}$  in the absence of inhibitor and  $115 \text{ nmol min}^{-1} \text{ mg}^{-1}$  in the presence of CORM-3 and  $400 \text{ }\mu\text{M}$  cysteine (Figure 5.2B). It is important to note that the addition of these thiol compounds alone did not affect significantly the rate of respiration (Figure 5.2 C and D).

The open electrode system in which the time taken for the oxygen electrode chamber to begin to reoxygenate is measured (as described in section 3.2.3 and 4.2.2) was also used to confirm that NAC protects respiration from inhibition by CORM-3. In this experiment, the balance between the oxygen entering the stirred system and the oxygen consumed by respiration is manipulated (by adjusting the speed of stirring) so that the oxygen detected by the electrode remains at 0 for an extended period of time. The presence of a respiratory inhibitor will reduce the rate at which oxygen is consumed, therefore allowing oxygen to be detected by the electrode leading to an upward deflection of the electrode trace (Figure 5.3).

The addition of  $400 \text{ }\mu\text{M}$  CORM-3 caused the chamber to reoxygenate immediately, indicating that respiration was inhibited (Figure 5.3, blue dashed line). However, when  $400 \text{ }\mu\text{M}$  NAC was added prior to CORM-3, respiration was protected so that the time taken for the chamber to reoxygenate was restored to 87% of the control time in which no inhibitor was added (Figure 5.3, red dotted line). NAC was added to the chamber in the absence of CORM-3 and found to cause reoxygenation in 74% of the time taken under control conditions. However, previous measurements in the closed oxygen

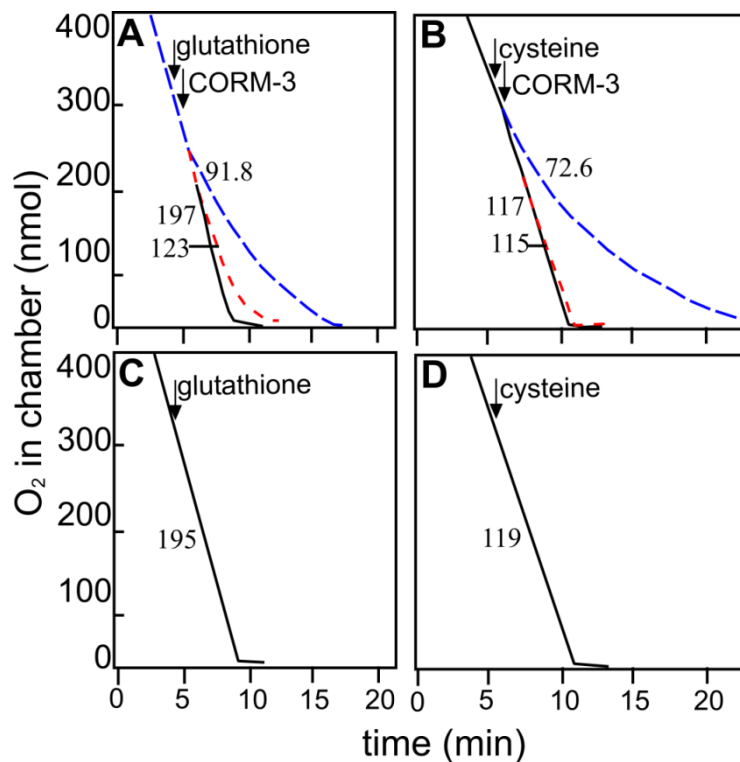


**Figure 5.2 Reduced glutathione and cysteine prevent CORM-3 dependent inhibition of respiration in *E. coli* membrane particles.** *E. coli* membrane particles were added to sonication buffer to a final concentration of  $\sim 60 \mu\text{g ml}^{-1}$  inside an oxygen electrode chamber. A lid was placed on the chamber and respiration was initiated by the addition of 6.25 mM NADH. The first arrow in each panel indicates the addition of either 200  $\mu\text{M}$  reduced glutathione (**A**) and (**C**), or 400  $\mu\text{M}$  cysteine (**B**) and (**D**), while the second arrow in (**A**) and (**B**) indicates the addition of 400  $\mu\text{M}$  CORM-3. In (**A**) and (**B**) the black solid lines indicate respiration in the absence of these compounds, the blue dashed lines show oxygen consumption in the presence of CORM-3 and the red dotted lines show oxygen consumption in the presence of CORM-3 and the thiol-containing compound. In (**C**) and (**D**) the black lines show oxygen consumption in the presence of 200  $\mu\text{M}$  reduced glutathione and 400  $\mu\text{M}$  cysteine respectively. Respiration rates ( $\text{nmol min}^{-1} \text{mg}^{-1} \text{protein}$ ) 2 min following the addition of CO or CO-RM are shown adjacent to each trace. These data are representative of 3 technical and 2 biological replicates for each condition. This figure was published in McLean *et al.* (2013).

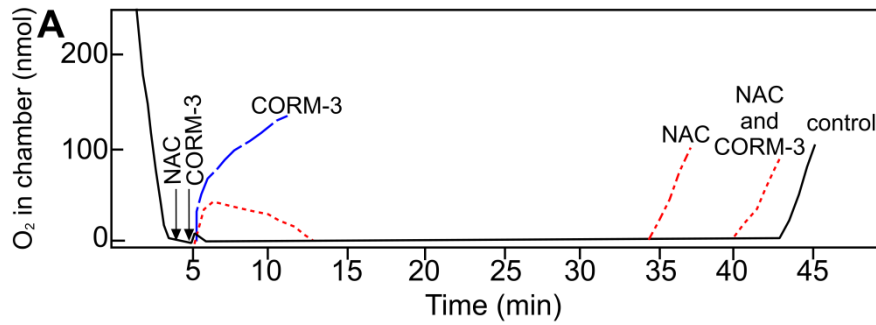


**Figure 5.3 NAC prevents CORM-3-dependent inhibition of respiration in *E. coli* membrane particles.** Wild type *E. coli* membrane particles were added to sonication buffer (2 ml) to a final concentration of approximately  $1.5 \text{ mg ml}^{-1}$  and respiration was initiated by the addition of NADH (6.25 mM). Arrows indicate the addition of NAC or CORM-3 (both at  $400 \text{ } \mu\text{M}$ ). The trace shows dissolved oxygen in the chamber for uninhibited respiration (black solid lines) or oxygen consumption in the presence of CORM-3 (blue dashed lines), CORM-3 and NAC (red dotted lines) or NAC alone (red dot-dash line). The lid was removed from the chamber 1 min after the addition of CORM-3 and the time taken for the chamber to reoxygenate (given in min in parentheses) was measured for the various conditions: with no additions (35); with CORM-3 (0); with NAC and CORM-3 (33); with NAC alone (28). These data are representative of at least 3 technical and 2 biological replicates. This figure was published in Jesse *et al.* (2013).

electrode had shown that the respiration rate of *E. coli* membrane particles was not affected when NAC was added on its own to the chamber (Figure 5.1D). These results confirm that NAC, in a 1:1 ratio with CORM-3, is able to protect the respiration of *E. coli* from inhibition by this CO-RM.

### **5.2.2 Investigating the hypothesis that thiol-containing compounds affect the rate or amount of CO released from CORM-3.**

In order to elucidate the mechanism by which thiol-containing compounds prevent the effects of CO-RMs, several hypothesis were considered. Initially it was investigated whether NAC affects the rate at which CO is released from CORM-3. The rate of CO release from CORM-3 was measured spectroscopically by assaying the rate of formation of carbonmonoxy-myoglobin (CO-Mb) in the presence and absence of NAC. A dual-beam spectrophotometer was used to record the spectra of a 10  $\mu$ M solution of myoglobin in phosphate buffer (pH 7.4) reduced with sodium dithionite. This was then subtracted from the spectra of this sample treated with either 8  $\mu$ M CORM-3, or 8  $\mu$ M CORM-3 pre-treated with a 10-fold molar excess of NAC.

The rate of CO release was slower and 21% less CO was released from CORM-3 in the presence of a 10:1 molar excess of NAC (Figure 5.4, open circles). The half-life of CO release from CORM-3 to dithionite-reduced myoglobin was calculated to be 2.5 min, whereas the half-life of CO release in the presence of NAC in a 10:1 molar excess was 2.8 min. It was then investigated whether higher ratios of NAC:CORM-3 led to diminished CO loss from CORM-3 to myoglobin. There was no concentration-dependent difference in the amount or rate of CO loss from CORM-3 when a 20-fold excess of NAC (Figure 5.4, closed triangles) was used instead of a 10-fold excess. However the use of both a 50-fold excess (Figure 5.4, open triangles) and a 100-fold excess (Figure 5.4, closed squares) of NAC did slightly reduce the rate and amount of CO release compared to the lower concentrations; however there was no difference between these higher concentrations.

The finding that the total amount of CO released to myoglobin was reduced in the presence of NAC, could imply that NAC acts by either preventing some CO loss from CORM-3, or by promoting the loss of CO, which could then be lost from solution prior

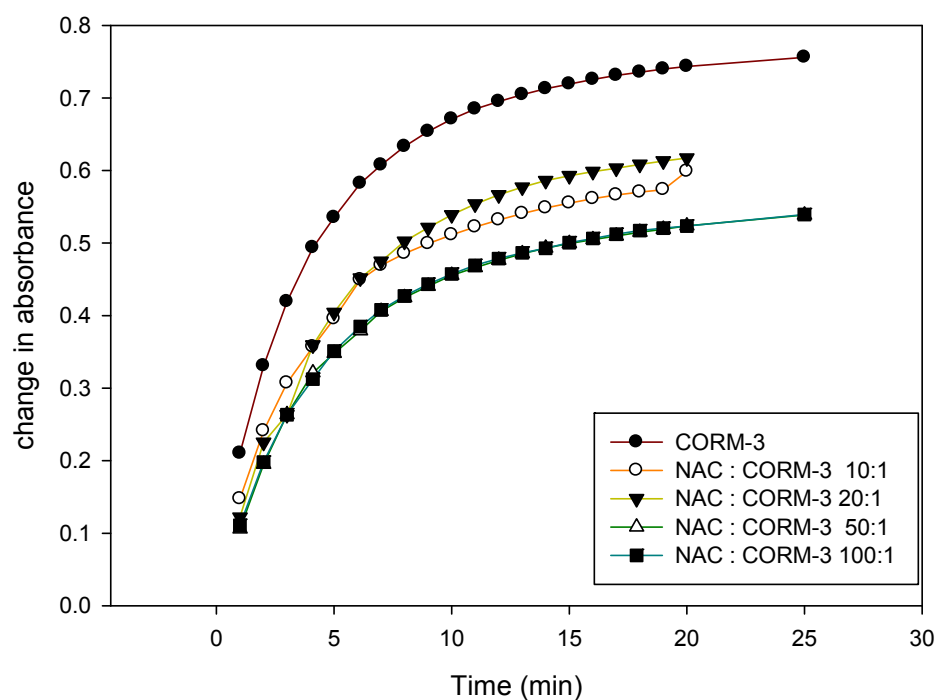


**Figure 5.4** Increasing the ratio of NAC to CORM-3 to some extent reduces the amount of CO lost to myoglobin up to a 50-fold NAC excess. The change in absorbance in the Soret region induced by the binding of CO from 8  $\mu\text{M}$  CORM-3 to 10  $\mu\text{M}$  of dithionite-reduced myoglobin was measured spectroscopically and plotted against time. This was done for CORM-3 alone (closed circles) and for CORM-3 preincubated for 5 min with NAC in either a 10:1 (open circles), 20:1 (closed triangles), 50:1 (open triangles) or 100:1 (closed squares) ratio. These data are representative of 2 technical replicates.



to the application of CORM-3 to myoglobin. Recent work from this laboratory has greatly advanced our understanding of the mechanisms by which CO is released from CORM-3 (McLean *et al.*, 2012). It is now known that sulfite species including dithionite (a necessary component of the myoglobin assay, which has been widely used to determine the rate of CO loss from CO-RMs (Atkin *et al.*, 2011; Davidge *et al.*, 2009b; Desmard *et al.*, 2012) cause CO loss from CO-RMs. The myoglobin assay is therefore not an ideal method by which to measure of the rate of CO release from these compounds. Haemoglobin has been proposed as an alternative to reduced myoglobin for this purpose (McLean *et al.*, 2012), as CO binds to oxyhaemoglobin much more avidly than oxygen (Sirs, 1974). In this assay, sodium dithionite is used to reduce the haem groups of haemoglobin, but is then removed by chromatography, producing oxyhaemoglobin, which, unlike oxymyoglobin, is stable in air. The spectroscopic changes that occur when oxyhaemoglobin is converted to carbonmonoxy-haemoglobin in the presence of CO-RMs can therefore be used as a measure of the rate of CO loss from these molecules in the absence of sodium dithionite (McLean *et al.*, 2012). In particular, the peak at 422 nm in the CO difference spectrum is indicative of CO binding to the haem in oxyhaemoglobin (see Figure 5.5B).

Haemoglobin was reduced with dithionite, then desalted on a PD-10 column, producing oxyferrous haemoglobin with no residual dithionite. This was diluted in phosphate buffer (100 mM, pH 7.4) to 10  $\mu$ M and the spectrum of this sample recorded in an OLIS spectrophotometer as described above (section 2.3.1.2). CO was added to the oxyhaemoglobin by bubbling the contents of the cuvette with CO from a cylinder for 2 min, and the spectrum of this sample was recorded. The absolute spectra of the oxyhaemoglobin and carbonmonoxyhaemoglobin are shown in Figure 5.5 A, while the difference spectrum of these samples (CO - treated oxyhaemoglobin minus oxyhaemoglobin) is shown in Figure 5.5B. The shift in the peak of the Soret region of the absolute spectra, from 414 nm to 419 nm (Figure 5.5A) and the corresponding peak at 422 nm in the difference spectrum confirms that CO has bound to haemoglobin; however, when oxyhaemoglobin is treated with CORM-3 (8  $\mu$ M), this shift was not seen (Figure 5.5C) and therefore, no peak was seen at 422 nm in the CORM-3 difference spectrum (Figure 5.5D). This confirms that when CORM-3 is exposed to a biological ligand in buffer, no CO loss occurs (McLean *et al.*, 2012). This experiment

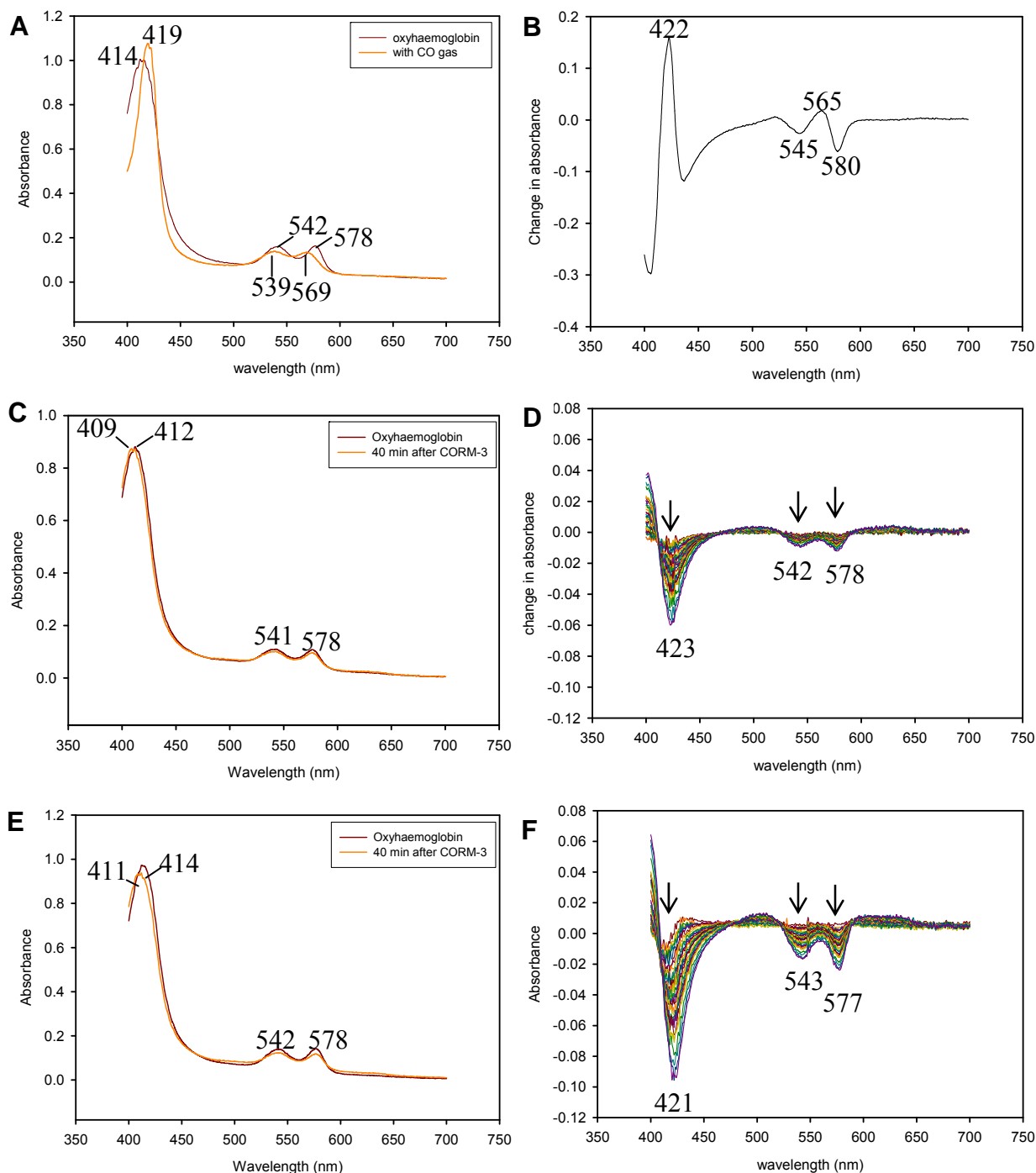


**Figure 5.5 The haemoglobin assay: NAC does not promote CO loss from CORM-3.**

Haemoglobin was reduced with sodium dithionite, then desalted on a PD-10 column, producing oxyferrous-haemoglobin with no residual dithionite. (A, C and E) show the absolute spectra (B, D and F) show the CO difference spectra (ie. the oxyhaemoglobin spectra minus the spectra of oxyhaemoglobin treated with CO (B), CORM-3 (D) or NAC and CORM-3 (F). The various coloured lines represent the spectra taken at time points from 0 to 40 min). In (A, C and E), the absolute spectrum of oxyhaemoglobin (10  $\mu$ M) is shown in burgundy, while the orange lines show the absolute spectrum in the presence of (A) CO (applied by bubbling the contents of the cuvette with CO from a cylinder for 2 min), (C) CORM-3 (8  $\mu$ M) and (E) CORM-3 (8  $\mu$ M) preincubated with NAC (80  $\mu$ M) for 5 min before the assay was begun.

was then repeated with CORM-3 pre-incubated for 5 min with a 10-fold excess of NAC (80  $\mu$ M) in order to investigate whether NAC was able to promote CO loss from CORM-3. As can be seen from the absolute spectra (Figure 5.5E) and the difference spectra (Figure 5.5F), CO does not bind to oxyhaemoglobin in the presence of NAC and CORM-3. This confirms that NAC does not cause CO loss from CORM-3. The troughs seen in the difference spectra (Figure 5.5D and F) indicate a small loss of the reduced form of oxyhaemoglobin, which may suggest that CORM-3 can act as an oxidising agent, as discussed in section 7.1.2.

### **5.2.3 NAC does not prevent the interaction between CO from CORM-3 and the terminal oxidases of the aerobic respiratory chain of *E. coli***

In order to assess whether NAC prevented the interaction of CO from CORM-3 with the terminal oxidases of the aerobic respiratory chain, difference spectra were recorded of wild type *E. coli* membrane particles treated with CORM-3 alone (Figure 5.6A) or with CORM-3 pre-incubated for 5 min with a 10-fold excess of NAC (Figure 5.6B). Both spectra show a peak at approximately 420 nm and a trough at approximately 446 nm in addition to a peak at approximately 644 nm. The later indicates the presence of CO-bound cytochrome *d* of *E. coli* (Wood, 1984), while the features in the Soret region can be attributed to CO binding to a mixture of haems, including haems *d* and *bs95*. Importantly, there was no reduction in the magnitude of these features in the presence of NAC, confirming that this compound does not interfere with the binding of CO released from CORM-3 with the terminal oxidases of *E. coli*.

### **5.2.4. A glutathione-deficient *E. coli* mutant is more resistant to killing than a wild type strain**

As thiol-containing compounds have been shown to protect bacteria from the deleterious effects of some CO-RMs (Desmard *et al.*, 2009; Desmard *et al.*, 2012; Tavares *et al.*, 2011), it was hypothesised that endogenous glutathione may constitute a cellular defence against CORM-3. It was therefore investigated whether a mutant strain of *E. coli* that was unable to produce glutathione was hypersensitive to killing by CORM-3.

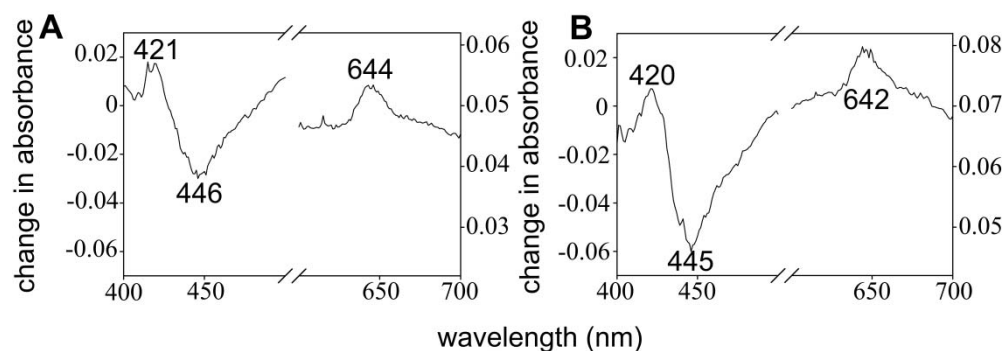


**Figure 5.6 Reaction of the terminal oxidases in wild type *E. coli* membrane particles with CORM-3.** Wild type *E. coli* membrane particles were added to sonication buffer to a final concentration of approximately 10 mg ml<sup>-1</sup> and incubated with (A) CORM-3 (100 μM) and (B) CORM-3 (100 μM) pre-incubated for 5 min with NAC (1 mM). Spectra were obtained 5 min after the addition of CORM-3 to membranes using a scanning dual-beam spectrophotometer. Data were plotted as the difference between the spectrum of a dithionite-reduced sample incubated with CORM-3 minus the spectrum of a reduced sample. Data have been smoothed in Sigma plot graphing software with a sampling proportion of 0.1 and a polynomial degree of 9. This figure was published in Jesse *et al.* (2013).

A mutation in the glutathione gene *gshA* was moved into a wild type MG1655 background by P1 *vir* phage transduction. The successful transduction was verified by an absence of a PCR product generated using primers specific to the *gshA* gene (described in Table 2.2) in the mutant, but the presence of an appropriately sized product in the MG1655 wild type. A 64.4% ( $\pm$  4.41) reduction in intracellular thiol content in the *gshA* mutant was confirmed by the DTNB assay (section 2.2.3.3). The viability of this mutant was then studied in the presence and absence of CORM-3 and compared to that of wild type. Treatment with 30  $\mu$ M CORM-3 reduced the viability of wild type *E. coli* cultures to 56% of the initial viable cell count at 45 min, and 2.8% at 90 min, whereas the viability of the *gshA* mutant had only decreased to 68% of the initial viable cell count at 45 min, and 75% at 90 min (all percentages given are the means and standard deviations of 5 technical and 3 biological replicates). Figure 5.7A shows data from one representative biological replicate in which the *gshA* mutant is statistically significantly more resistant to killing than the wild type strain at 30, 45, 90 and 120 min ( $p < 0.02$ ). In each biological replicate, the *gshA* mutant had statistically greater viability than wild type 120 min following CORM-3 treatment (as determined by a Student's t test). In order to confirm that the effects seen in this experiment were due to CO released from CORM-3, the experiment was repeated using the control compound iCORM-3, which does not release CO. This compound did not reduce the viability of either strain within 120 min (Figure 5.7B).

### 5.2.5 CORM-2 and CORM-3 react with thiol groups

A recently published paper suggests that CORM-2 and the molybdenum-based CO-RM ALF062 generate ROS, specifically hydroxyl radicals, which are able to oxidise thiol groups (Tavares *et al.*, 2011). The authors propose that CO-RMs are bactericidal because of this ROS, and that thiol compounds are protective against the effects of CO-RMs because they quench these damaging species. The DTNB assay was used to show that in the presence of CORM-2, but not  $\text{RuCl}_2(\text{DMSO})_4$ , the amount of thiol groups detected in a solution of glutathione was diminished. DTNB (5,5'-dithiobis-2-nitrobenzoic acid) reacts quantitatively with thiol groups releasing 5-sulfido-2-nitrobenzoic acid which absorbs light at 412 nm (Ellman, 1959).

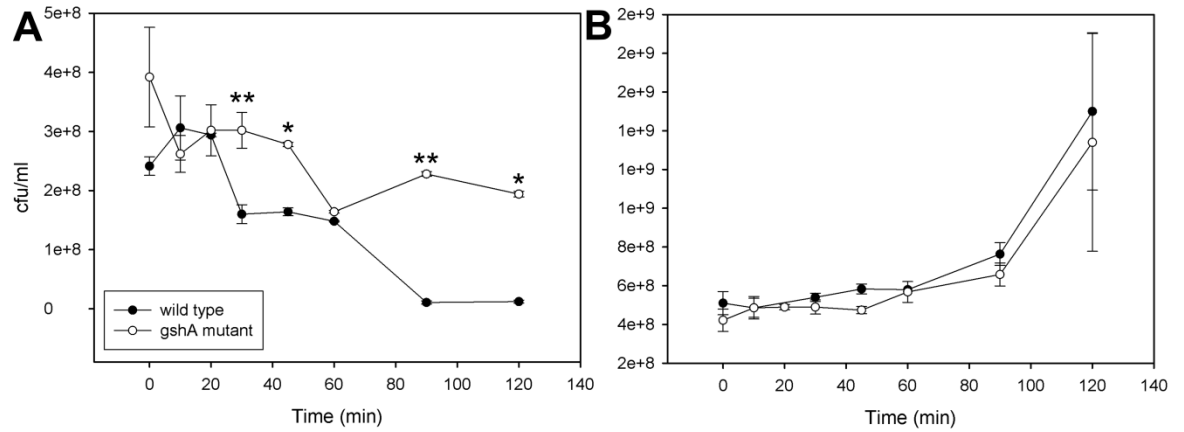


**Figure 5.7 A glutathione deficient *E. coli* mutant is more resistant to killing than a wild type strain.** The viability of wild type (closed circles) and a *gshA* mutant (open circles) in the presence of (A) CORM-3 and (B) iCORM-3, both at 30  $\mu$ M. Data are the means and standard deviations of 5 technical replicates and are representative of 3 biological replicates. Asterisks denote the degree of statistical significance for the data as determined by a Student's t test (\*,  $p < 0.02$ ), (\*\*,  $p < 0.001$ ).

In order to determine whether NAC is able to react with other CO-RMs, various concentrations (10 – 200  $\mu\text{M}$ ) of NAC were incubated for 5 min with CORM-3, CORM-2 and CORM-A1 or the control compounds iCORM-3,  $\text{RuCl}_2(\text{DMSO})_4$  or CO-saturated solution, all at 100  $\mu\text{M}$ . DTNB (0.8 mM) was then added and incubated for 15 min before the  $\text{OD}_{412}$  was measured using a Jenway spectrophotometer. This assay revealed that CORM-3 reacts with 16% of the thiol groups of NAC (Figure 5.8A) when present in equimolar amounts, while CORM-2 reacts with approximately 80% of the thiol groups in NAC when present at equimolar amounts. In contrast, the control compounds iCORM-3,  $\text{RuCl}_2(\text{DMSO})_4$  and CO gas did not react to a significant degree with thiol groups. The non-metal CO-RM, CORM-A1 reacted with only 4% of the thiol groups in NAC when present in a 2-fold excess.

It was then investigated whether CORM-3 could react with a range of thiol compounds, specifically cysteine, reduced glutathione and sodium hydrosulfide. Cysteine and glutathione were investigated as they are abundant within the cellular milieu, and sodium hydrosulfide in order to determine whether CORM-3 had different effects on an inorganic sulfide compound compared with organic thiol compounds. The DTNB assay was employed again, but here the concentration of thiol compound was kept constant (100  $\mu\text{M}$ ), while the concentration of CORM-3, iCORM-3 or CO-saturated solution was varied (0 – 100  $\mu\text{M}$ ). The presence of CORM-3 reduced the number of thiol groups in solution for each thiol compound (Figure. 5.9). The control compound iCORM-3 caused a less pronounced, yet still significant, decrease in the amount of free thiol groups, whereas exposure of the thiol compounds to CO-saturated solution had no significant effect on the free thiol groups (Figure 5.9).

#### **5.2.6 Superoxide is generated by CORM-2 and CORM-3 in solution**

As there are conflicting data in the literature as to whether CO-RMs generate ROS and therefore whether the protective effect of thiol compounds against CO-RMs is due to their antioxidant properties, superoxide production by CORM-2, CORM-3, the non-metal CO-RM, CORM-A1 and the control compounds  $\text{RuCl}_2(\text{DMSO})_4$  and iCORM-3 was assayed *in vitro*. Cytochrome *c* (20  $\mu\text{M}$ ) was added to a solution of each CO-RM (1 mM) in potassium phosphate buffer (pH 7.8). Spectrophotometric changes at 550 nm, which are indicative of the reduction of cytochrome *c* (Winterbourn, 1982),

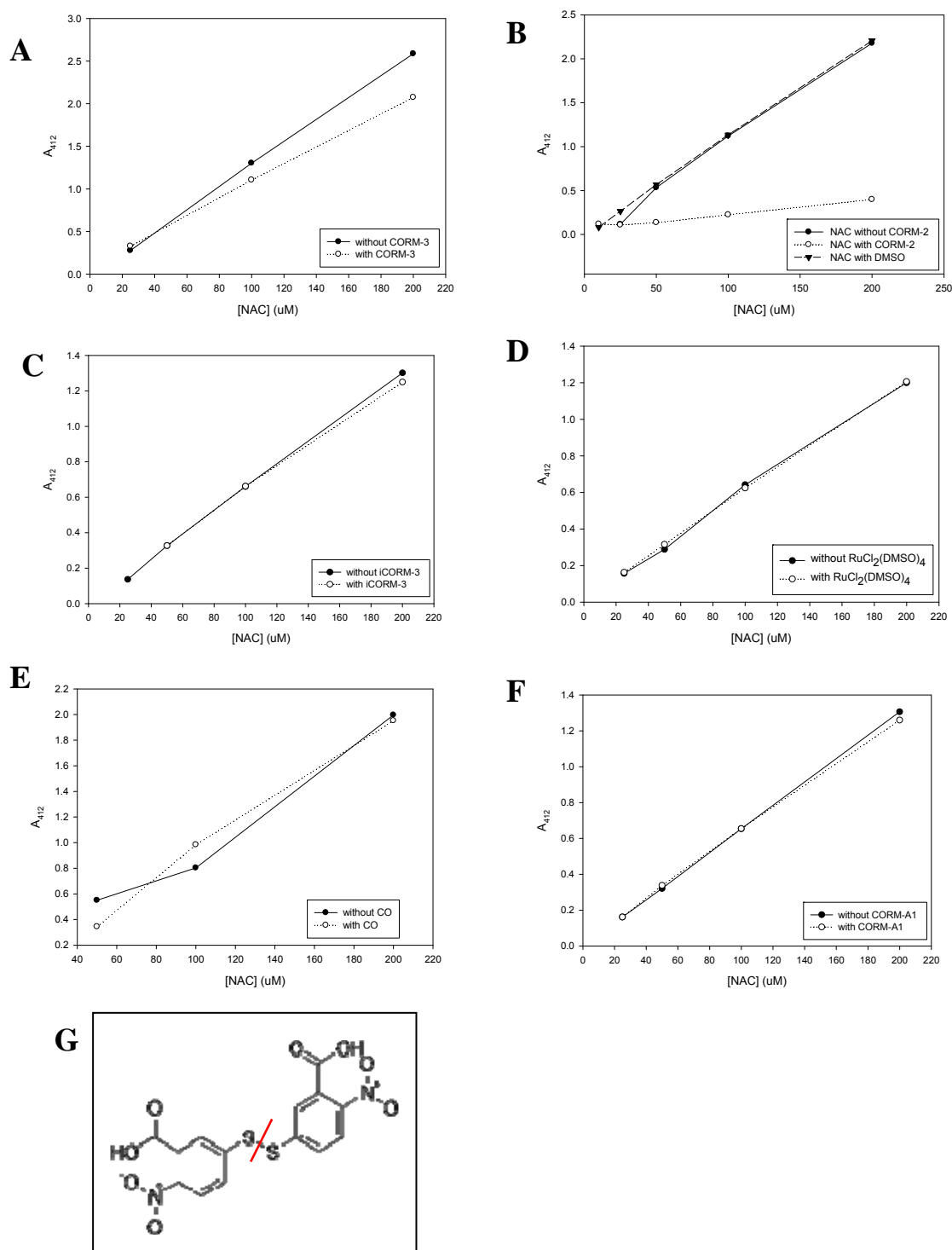


**Figure 5.8** CORM-2 and CORM-3, but not CORM-A1 or control compounds react with NAC. Various concentrations (10 – 200  $\mu\text{M}$ ) of NAC were incubated for 5 min with each of the following, all at 100  $\mu\text{M}$ : (A) CORM-3, (B) CORM-2, (C) iCORM-3, (D)  $\text{RuCl}_2(\text{DMSO})_4$ , (E) CO-saturated solution or (F) CORM-A1. DTNB (0.8 mM) was then added and incubated for 15 min. The  $\text{OD}_{412}$  was measured using a Jenway spectrophotometer. (G) Shows the structure of DTNB (5,5'-dithiobis(2-nitrobenzoic acid)). The red line shows the site of cleavage when DTNB reacts a thiol group.



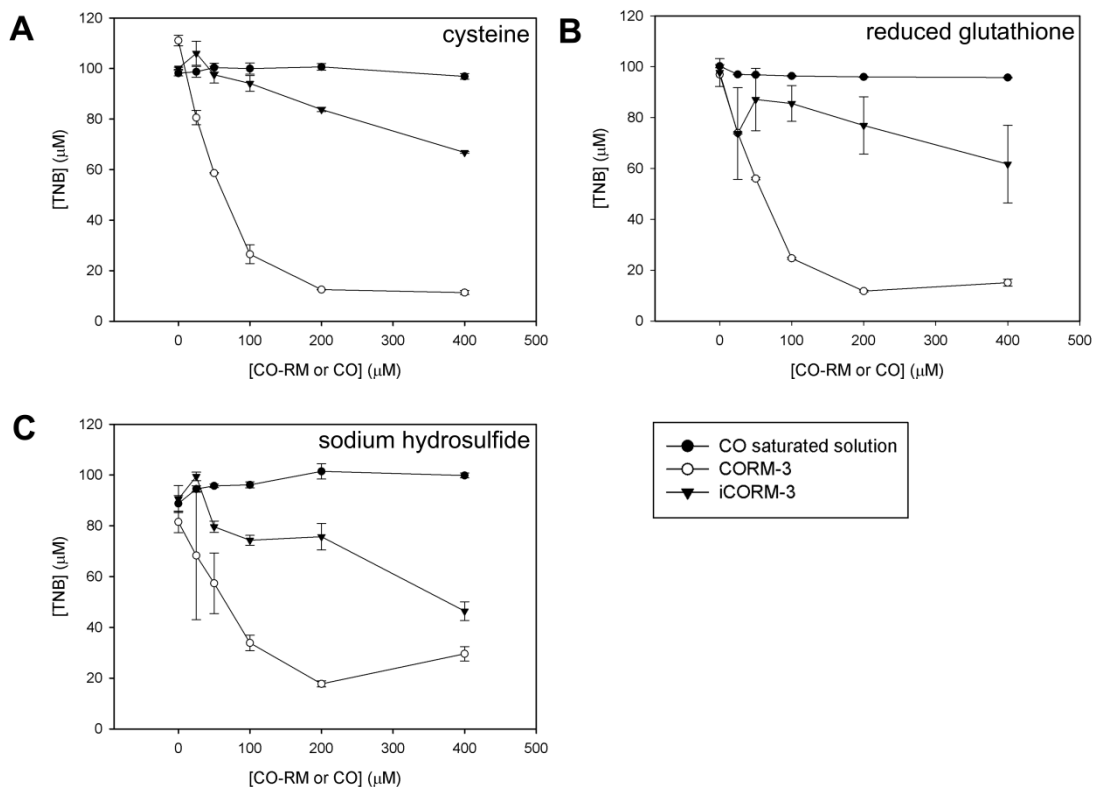


**Figure 5.9 CORM-3 reacts with glutathione, cysteine and sulfide.** Various concentrations (0 – 100 μM) of CORM-3 (closed circles), iCORM-3 (open circles) or CO-saturated solution (closed triangles) were incubated with 100 μM (A) cysteine, (B) reduced glutathione or (C) sodium hydrosulfide in phosphate buffer for 15 min at room temperature. 500 μM DTNB was added and the solution incubated for a further 15 min before the absorbance was measured at 412 nm. These data are the means and standard deviations of three separate experiments. This figure was published in McLean *et al.* (2013).

were then monitored over a time course. The abolition of the signal by superoxide dismutase (SOD) confirmed that the reduction of cytochrome *c* is caused by superoxide. CORM-3 (Figure 5.10A), CORM-2 (Figure 5.10B) and CORM-A1 (Figure 5.10C), all at 1 mM, were found to produce low levels of superoxide (equivalent to ~ 1% of the CO-RM concentration). CORM-2 produced superoxide at an initial rate approximately 10-fold faster than CORM-3 ( $1.9 \mu\text{M O}_2^- \text{ min}^{-1}$  and  $0.17 \mu\text{M O}_2^- \text{ min}^{-1}$  respectively); however the overall amounts of superoxide produced from CORM-2 and CORM-3 were similar. CORM-A1 generated a similar amount of superoxide as CORM-3 and did so at a similar rate. Interestingly, iCORM-3 was found to produce slightly more superoxide than CORM-3 over 2 h (Figure 5.10D), and at a slightly faster initial rate ( $0.624 \mu\text{M O}_2^- \text{ min}^{-1}$ ), whereas the control compound for CORM-2,  $\text{RuCl}_2(\text{DMSO})_4$ , produced only a very small amount of superoxide ( $0.0971 \mu\text{M O}_2^-$  in one hour; Figure 5.10E).

It was then investigated whether NAC altered the kinetics of superoxide production from CORM-3 (Figure 5.10F). Contrary to the expectation that this antioxidant would reduce the amount of superoxide detected, the rate of superoxide production from CORM-3 in the presence of NAC was greatly increased ( $1.17 \mu\text{M O}_2 \text{ min}^{-1}$ ).

### **5.2.7 Antioxidants do not consistently prevent the inhibitory effects of CORM-3 on respiration**

As mentioned previously, recent work has presented evidence that CORM-2 generates ROS, specifically hydroxyl radicals ( $\text{OH}^\cdot$ ), leading the authors to conclude that this accounts for the antibacterial properties of this CO-RM (Tavares *et al.*, 2011). However, it is important to note that very high concentrations of CORM-2 are used in these assays (up to 2 mM). This group had also previously reported the up-regulation of oxidative stress response genes such as *soxS* and *oxyR* when *E. coli* was subjected to  $250 \mu\text{M}$  CORM-2. Other groups have not seen the up-regulation of oxidative stress response genes in transcriptomic studies using low concentrations ( $30 \mu\text{M}$ ) CORM-3 (Davidge *et al.*, 2009b). It is therefore unlikely that the generation of ROS by CO-RMs is able to account for all of the deleterious effects that occur when bacteria are stressed with low concentrations of CORM-3.

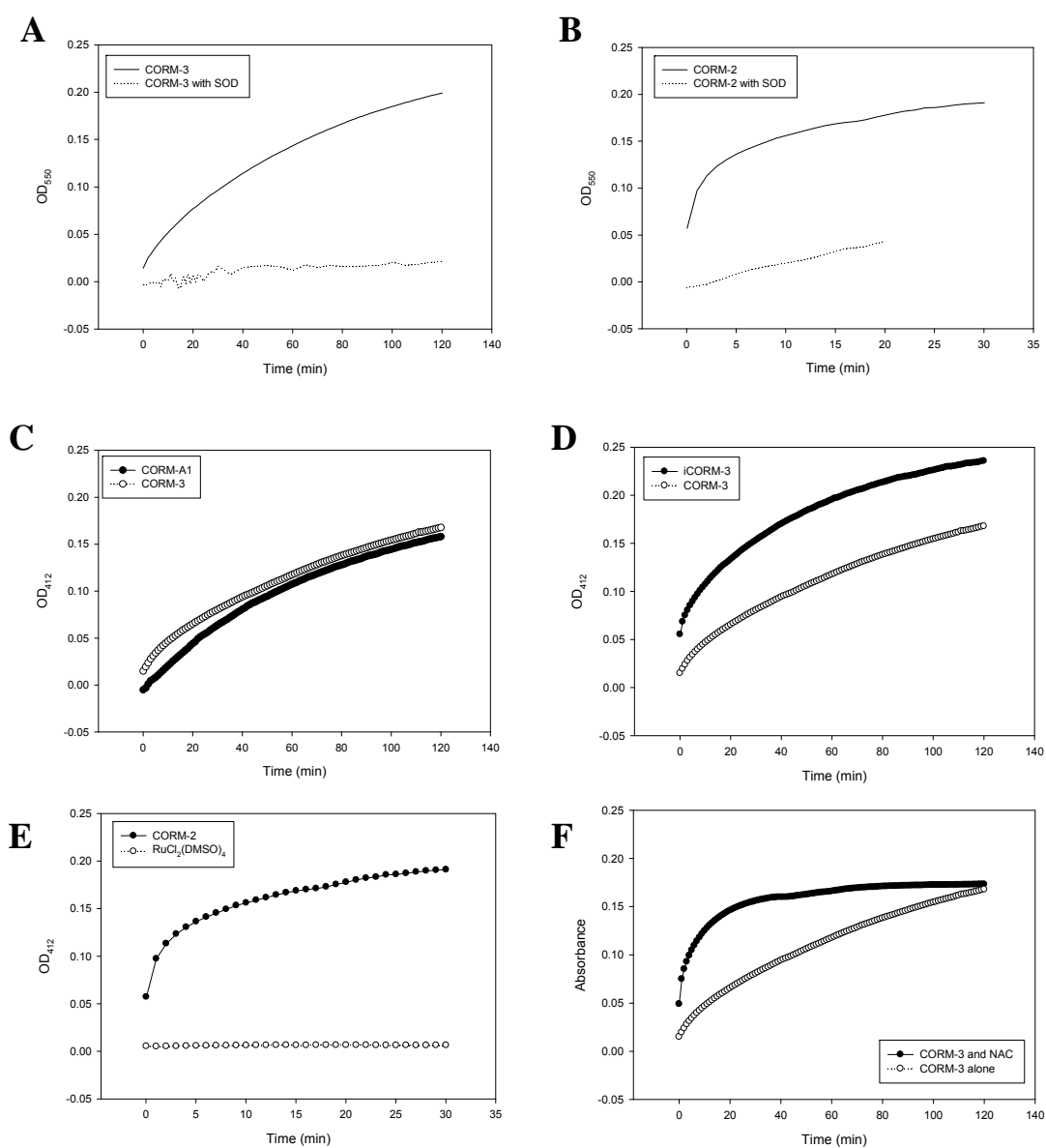


**Figure 5.10 Both CORM-2 and CORM-3 generate superoxide.** Cytochrome *c* (20  $\mu$ M) was added to the CO-RM (1 mM) in KPi, pH 7.8. The OD<sub>550</sub> was then read over a time course. Graphs show superoxide generated by (A) CORM-3 (solid line) and CORM-3 in the presence of SOD (250 units) (broken line), (B) CORM-2 (solid line) and CORM-2 in the presence of SOD (250 units) (broken line), (C) CORM-3 (open circles) and CORM-A1 (closed circles), (D) CORM-3 (open circles) and iCORM-3 (closed circles) (E) CORM-2 (closed circles) and RuCl<sub>2</sub>(DMSO)<sub>4</sub> (open circles), CORM-3 (open circles) and (F) CORM-3 in the presence of NAC (1mM) (closed circles). Part A of this figure was published in McLean *et al.* (2013).

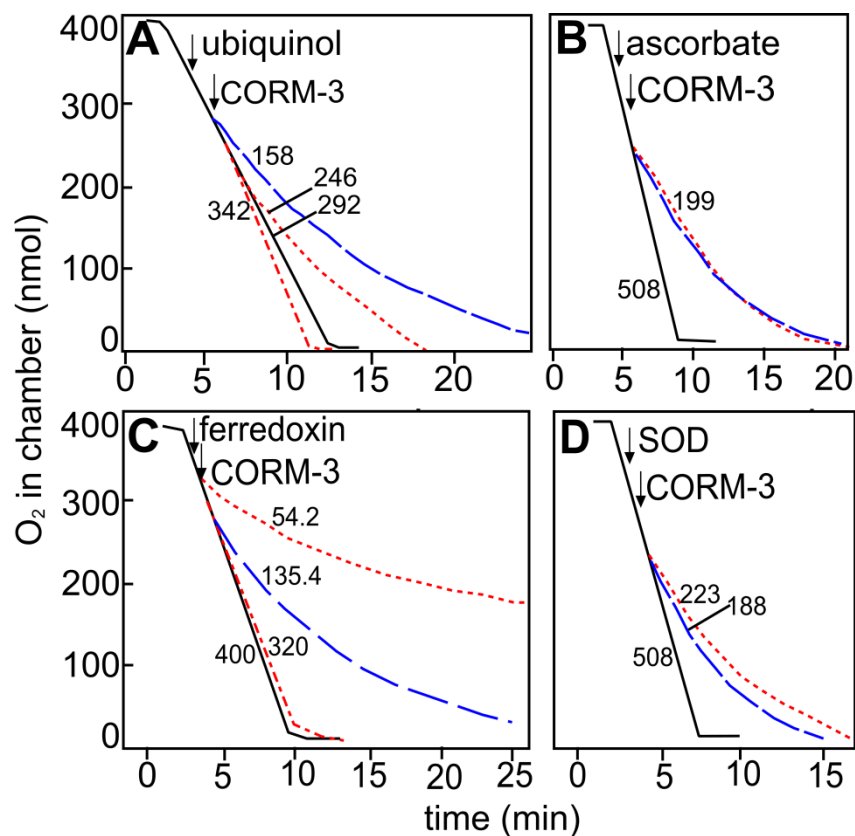


**Figure 5.11 Antioxidants and superoxide dismutase (SOD) do not prevent CORM-3-dependent inhibition of respiration to the same extent as thiol compounds.** Wild type *E. coli* membrane particles were added to the oxygen electrode in sonication buffer (2 ml) to a final concentration of approximately 60  $\mu\text{g ml}^{-1}$ . A lid was placed on the chamber and respiration was initiated by the addition of 6.25 mM NADH. The first arrows in each panel indicate the addition of the antioxidant or enzyme: **(A)** ubiquinol (100  $\mu\text{M}$ ); **(B)** ascorbate (1 mM); **(C)** ferredoxin (200  $\mu\text{g ml}^{-1}$ ) and **(D)** SOD (250 units) to the chamber, while the second arrows indicate the addition of CORM-3 (400  $\mu\text{M}$ ). The black solid lines show the uninhibited respiration rate, the blue dashed lines show oxygen consumption in the presence of CORM-3 and the red dotted lines show oxygen consumption in the presence of CORM-3 and the antioxidant **(A, B and C)** or SOD **(D)**. In **(A and C)**, the red dot dash line shows oxygen consumption in the presence of **(A)** ubiquinol or **(B)** ferredoxin alone. Respiration rates ( $\text{nmol min}^{-1} \text{mg}^{-1} \text{protein}$ ) 2 min following the addition of CO-RM are shown adjacent to each trace. Traces are representative of 2 biological replicates, each with 3 technical replicates. This figure was published in Jesse *et al.* (2013).

In order to examine this further, it was investigated whether non-thiol-containing antioxidants were capable of abolishing the inhibitory effects of CORM-3 on respiration (Figure 5.11). While the antioxidant ubiquinol (100  $\mu$ M) was capable of partially decreasing the degree of respiratory inhibition caused by CORM-3 (Figure 5.11A), ascorbic acid (1 mM) had no effect on respiratory inhibition by CORM-3 (Figure 5.11B). Interestingly, in the presence of CORM-3 and the antioxidant ferredoxin, respiration was inhibited more than it was in the presence of CORM-3 alone (despite ferredoxin having no significant effect on the respiration rate of these membranes when added alone (Figure 5.11C, red dot dash line). These results suggest that it is not the antioxidant nature of compounds such as NAC, reduced glutathione and cysteine that enable them to prevent metal-based CO-RMs from exerting their effects but, more likely, the chemical interaction of the thiol groups with the CO-RM. Additionally, when superoxide dismutase (SOD) was added to the electrode with CORM-3 (Figure 5.13D), there was no significant change in the degree of inhibition suggesting that superoxide plays no role in the inhibition of respiration by CORM-3.

### **5.2.8 The use of EPR spectroscopy and the spin trap BMPO to assess whether reactive oxygen species are generated from solutions of CORM-2 and CORM-3**

Electron Paramagnetic Resonance (EPR) spectroscopy is a sensitive method able to detect species with unpaired electrons and therefore has the potential to identify ROS. However, ROS are transient, which causes difficulties when recording EPR spectra; consequently, nitron spin traps are often used to stabilize these species (Frejaville *et al.*, 1995).

The spin trap BMPO (5-*tert*-butoxycarbonyl 5-methyl-1-pyrroline *N*-oxide) has the advantage over other spin traps that it is able to distinguish between hydroxyl radicals and superoxide anions (Zhao *et al.*, 2001). In comparison, the spin trap DMPO forms a superoxide adduct, which then decomposes to form the hydroxyl adduct (Finkelstein *et al.*, 1982).

Tavares *et al.*, (2011) recently reported the use of a BMPO spin trap with EPR spectroscopy to detect ROS generated from CORM-2, RuCl<sub>2</sub>(DMSO)<sub>4</sub> and CORM-2

incubated with reduced haemoglobin. They claim that the species detected is hydroxyl radicals ( $\text{OH}^\cdot$ ), yet they show a hyperfine splitting constant around both nitrogen and hydrogen of 1.1 mT or 11 gauss (G) (Figure 5.12). This does not match the EPR spectrum of the hydroxyl-BMPO adduct seen in Zhao *et al.* (2001), which has aN values of 13.37 G and 13.4 G and aH values of 9.42 G and 12.1 G. Therefore, independent EPR spin trapping measurements were undertaken to investigate whether hydroxyl radicals could be detected in solutions of CORM-2. This work was then extended to investigate whether CORM-3 was able to produce such species.

Initially, superoxide and hydroxyl adducts of BMPO were generated to provide reference spectra for comparison with the CO-RM spectra. Samples were loaded into an AquaX cell and EPR spectra were recorded, at room temperature, on a Bruker EMX spectrometer at 9.47 GHz microwave frequency, 3.18 mW microwave power, 100 kHz modulation frequency and 9.54 G/s scan rate. Spectra were analysed using WINEPR, Version 2.11 (Bruker).

Xanthine and xanthine oxidase were reacted in order to generate superoxide. Figure 5.13A shows the EPR spectrum of a mixture of 1 mM xanthine, 5 milliunits xanthine oxidase, the chelator DTPA (0.1 mM) and 25 mM BMPO, 2 min after mixing, while Figure 5.13B shows the spectrum of this mixture 80 min after mixing. This spectrum has a nitrogen hyperfine coupling constant (aN) of 11 G and a hydrogen hyperfine coupling constant (aH) of 13.4 G. This spectrum is similar to that for superoxide reported by Zhao *et al.*, (2001). Two values are given as there are two diastereomers of each spin adduct (Zhao *et al.*, 2001), each with their own hyperfine coupling constants for both nitrogen and hydrogen. There are however some slight differences between the spectra obtained in this work and those reported by Zhao *et al.*, (2001): the features circled in green in Figure 5.13B were slightly broader than expected when compared to the published spectrum and the feature circled in red was not as broad as that presented in Zhao *et al.*, (2001); this suggests that there are two contributions to this feature in the present work.

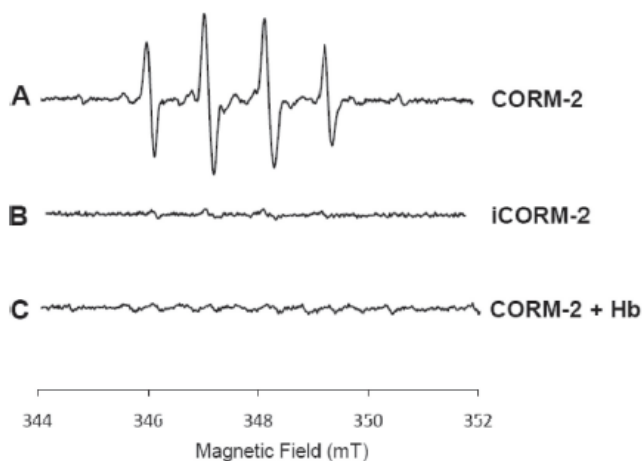
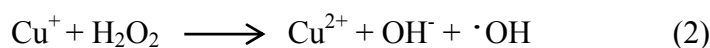
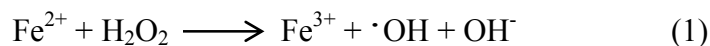


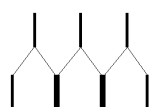
**Figure 5.12 EPR spectra** of samples containing (A) 2 mM CORM-2, (B) iCORM-2 and (C) CORM-2 plus hemoglobin (*Hb*.) acquired in the presence of the spin trap, BMPO.

This figure was originally published in *The Journal of Biological Chemistry*. Tavares, A.P.N., Teixeira, M., Romao, C.C. Seixas, J.D., Nobre, L.S. and Saraiva, L.M. Reactive Oxygen Species Mediate Bactericidal Killing Elicited by Carbon Monoxide-releasing Molecules. *The Journal of Biological Chemistry*. (2011) 286 (30):26708-26717. © The American Society for Biochemistry and Molecular Biology.

Attempts were then made to generate the hydroxyl-BMPO adduct using Fenton chemistry. This involves hydroxyl radicals being produced from H<sub>2</sub>O<sub>2</sub> in the presence of either Fe<sup>2+</sup> or Cu<sup>+</sup> according to the reactions below:



When 1 mM FeSO<sub>4</sub> was mixed with 1 mM H<sub>2</sub>O<sub>2</sub> in the presence of 8 mM BMPO, an EPR spectrum typical of the BMPO-hydroxyl adduct was observed (Figure 5.13 C; see also Zhao *et al.*, (2001)). The hyperfine splitting around nitrogen was 13.3 G, while that for hydrogen was 14.0 G; these values are consistent with those reported by Zhao *et al.*, (2001). However, when CuSO<sub>4</sub> was used to generate hydroxyl radicals, a different EPR spectrum was observed. CuSO<sub>4</sub> (1 mM) was mixed with 1 mM ascorbic acid (included to reduce the copper in CuSO<sub>4</sub> to Cu<sup>+</sup>) and 1 mM H<sub>2</sub>O<sub>2</sub> with 8 mM BMPO (Figure 5.13D; see also Zhao *et al.*, (2001)) and gave a spectrum that appears to be a doublet of overlapping triplets, i.e. the first, second and fourth features comprise the first triplet and the third, fifth and sixth features comprise the second. The hyperfine splitting for nitrogen was 15 G, while aH was measured as 21.4 G. When both hydrogen and nitrogen, interact with an electronic spin, the EPR line splits into a 1:1:1 triplet (on I<sub>N</sub> = 1, with a distance between the lines being the a<sub>N</sub> value), then each line splits into a 1:1 doublet (on I<sub>H</sub> = 1/2, with a distance between the lines being the a<sub>H</sub> value). Now, a spectrum exhibiting a quartet pattern 1:2:2:1 can be observed if a<sub>N</sub> ≈ a<sub>H</sub>, or, to be more precise, if the difference | a<sub>N</sub> - a<sub>H</sub> | is not notably greater than the individual line width (see below).



The FeSO<sub>4</sub> generated hydroxyl-BMPO spectrum (Figure 5.13C) is approximately a 1:2:2:1 spectrum, while that generated by CuSO<sub>4</sub> (Figure 5.12D) shows a well resolved 1:1 doublet of 1:1:1 triplets giving 6 lines in intensity 1:1:1:1:1:1. Both spectra seem to show the presence of two isomers.



The EPR spectrum generated from  $\text{CuSO}_4$ , ascorbic acid and  $\text{H}_2\text{O}_2$  (Figure 5.13D) shows a larger than expected aH, which indicates a slightly higher spin density on the hydrogen. It is possible that the BMPO molecule has either been oxidised or reduced as a result of the attack of the oxygen radical, leaving the O-N=CH fragment planar rather than the -CH existing in a tetrahedral conformation. The planar O-N=CH would allow a higher unpaired electron density at the H and therefore an increased aH. However, the  $\text{CuSO}_4$ -generated spectrum (Figure 5.13D) appears to show a small quantity of a second isomer is present, which would rule out the existence of a planar structure. An alternative possibility is that Cu or Ru could coordinate at either the NO or the OH/OOH oxygen of BMPO, which would modify the unpaired electron density distribution, resulting in a larger than expected aH (Brian Mann, personal communication).

The EPR spectrum of 4 mM CORM-2 in DMSO mixed with 10 mM BMPO was then recorded (Figure 5.14A). The resulting spectrum was not identical to either the superoxide or hydroxyl BMPO adducts reported in the literature (Zhao *et al.*, 2001), nor to the EPR spectrum reported by Tavares *et al.* (2001) for CORM-2 mixed with BMPO. The spectrum does however overlay the spectrum generated by a mixture of  $\text{CuSO}_4$ , ascorbic acid and  $\text{H}_2\text{O}_2$  mixed with BMPO and has a hyperfine splitting value for nitrogen of 15.2 G, while that for hydrogen is 21.2 G (Figure 5.14B). This suggests the EPR spectrum obtained for CORM-2 in this work could indicate the presence of hydroxyl radicals, although it is not clear why this spectrum differs from those reported in the literature for both the BMPO hydroxyl radical (Zhao *et al.*, 2001) and CORM-2 with BMPO (Tavares *et al.*, 2011). The EPR spectrum of  $\text{RuCl}_2(\text{DMSO})_4$  mixed with BMPO was generated, and no features were detected, suggesting that this control compound does not generate any ROS (Figure 5.14C). The relative intensity of the EPR spectrum generated by CORM-2 and BMPO was plotted against time (Figure 5.14D) and revealed that the BMPO adduct was short lived, with a maximum intensity occurring within the first 2 min following mixing.

EPR spectra were then recorded for a solution of CORM-3 (4 mM) with BMPO (8 mM) over time. Initially, no clear features could be seen, (Figure 5.15A and B); however, by recording multiple spectra and averaging the signals, the signal to noise ratio was

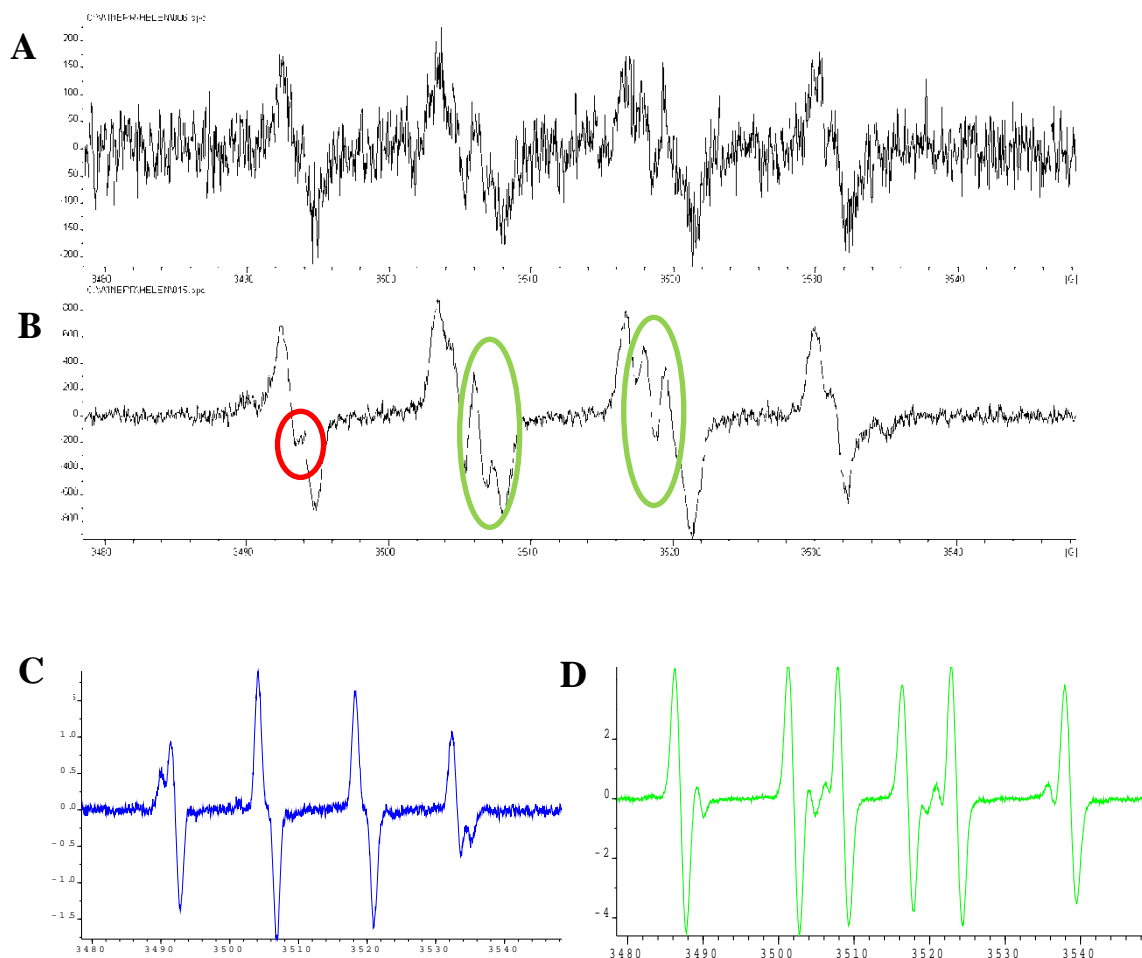


**Figure 5.13 Reference spectra of superoxide (A and B) and hydroxyl (C and D) radicals bound to BMPO.** EPR spectra were generated from the following samples including the spin trap BMPO (5-tert-butoxycarbonyl 5-methyl-1-pyrroline N-oxide). (A) and (B) xanthine (1 mM), xanthine oxidase (5 milliunits), DTPA (0.1 mM) and BMPO (25 mM), A) 2 min after mixing and (B) 80 min after mixing, (C) hydroxyl-BMPO adduct generated by  $\text{FeSO}_4$  (1 mM),  $\text{H}_2\text{O}_2$  (1 mM) and BMPO (8 mM) and (D) hydroxyl-BMPO adduct generated by  $\text{CuSO}_4$  (1 mM), ascorbic acid (1 mM),  $\text{H}_2\text{O}_2$  (1 mM) and BMPO (8 mM) 10 min after mixing. The features circled in green were slightly broader than expected when compared to the spectrum published by Zhao *et al.*, (2001), and the feature circled in red was not as broad.

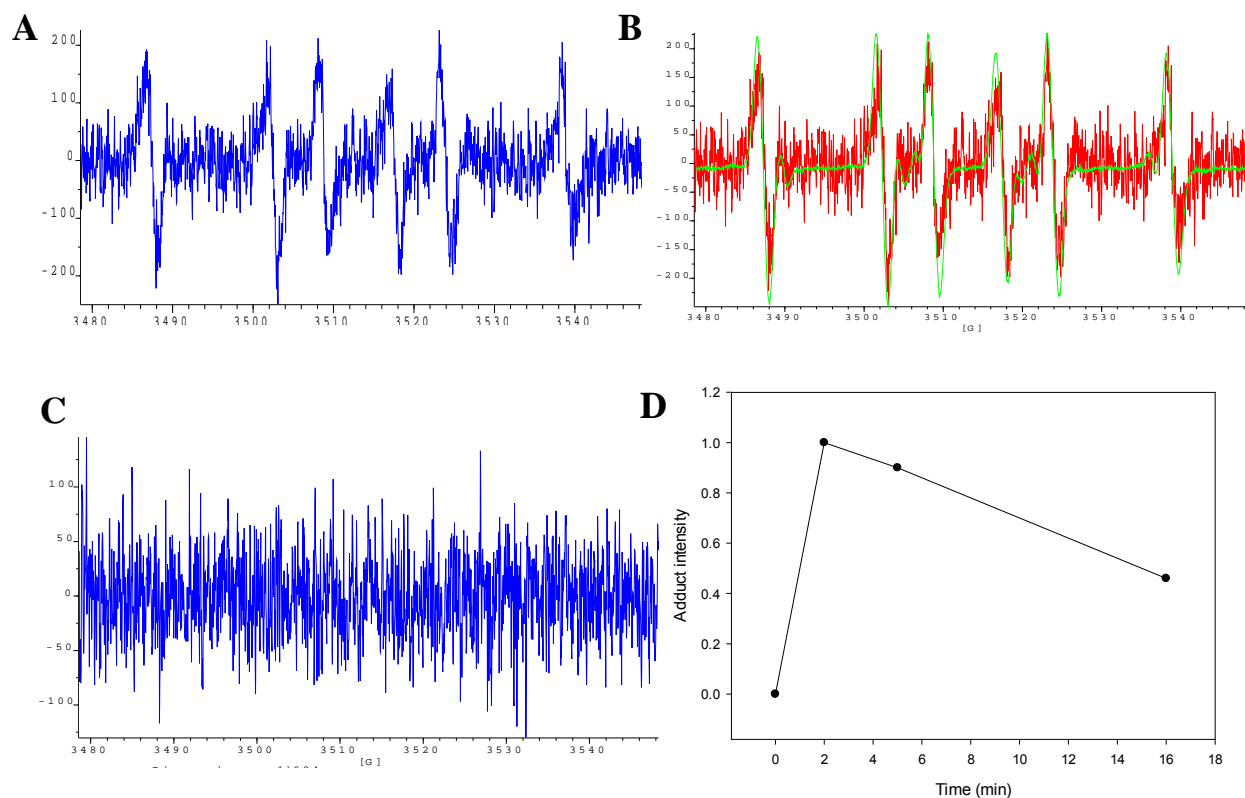


**Figure 5.14 CORM-2 EPR spectra.** Spectra were generated from the following samples including the spin trap BMPO (5-tert-butoxycarbonyl 5-methyl-1-pyrroline N-oxide). (A) shows the spectrum generated by CORM-2 (4 mM) in DMSO with BMPO (10 mM) 2 min after mixing, (B) shows an overlay of the copper generated hydroxyl radical bound to BMPO in green (Figure 5.12D) and the CORM-2 with BMPO spectra (red), (C) shows the spectrum of RuCl<sub>2</sub>(DMSO)<sub>4</sub> (4 mM) with BMPO (8 mM) and (D) shows the intensity of the CORM-2 adduct of BMPO over time.

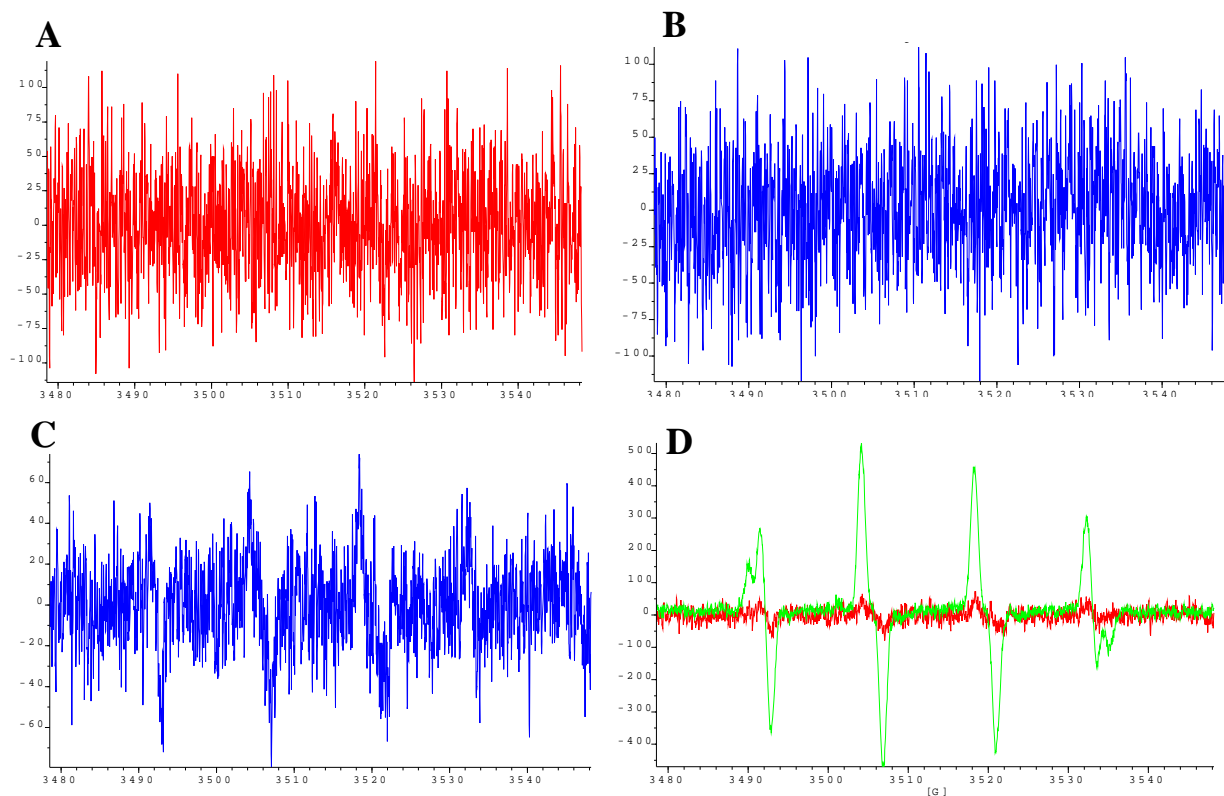


**Figure 5.15 CORM-3 EPR spectra.** (A) and (B) Spectra were generated from CORM-3 (4 mM) with the spin trap BMPO (5-tert-butoxycarbonyl 5-methyl-1-pyrroline N-oxide) (8 mM) (A) 2 min after mixing, (B) 6 min after mixing, (C) shows the average of 4 spectra generated from this sample and (D) shows an overlay of the iron-generated hydroxyl radical bound to BMPO and the averaged CORM-3 with BMPO spectrum.

improved allowing a distinct spectrum to be produced (Figure 5.15C). This spectrum bears great resemblance to the hydroxyl-BMPO spectrum generated from FeSO<sub>4</sub> in this work, with similar values for aH (14.5 G) and aN (13.8 G); however it is of very low intensity suggesting that only a small amount of hydroxyl radical is formed. Figure 5.15D shows an overlay of the CORM-3 - BMPO spectrum with the FeSO<sub>4</sub> generated hydroxyl-adduct of BMPO.

### **5.2.9 Assay of H<sub>2</sub>O<sub>2</sub> production *in vitro* by CORM-3 treated *E. coli***

It was also considered important to assess whether CORM-3 produced hydrogen peroxide *in vivo*; therefore an Amplex red assay (Invitrogen) was performed in CORM-3 treated cells. This assay uses 10-acetyl-3,7-dihydroxyphenoxazine, which reacts with H<sub>2</sub>O<sub>2</sub> in a 1:1 stoichiometry to produce the fluorescent oxidation product resorufin, which has excitation and emission maximum of approximately 571 nm and 585 nm respectively, and can also be detected spectrophotometrically at 560 nm. This assay is extremely sensitive and can detect as little as 10 picomoles H<sub>2</sub>O<sub>2</sub> in 100  $\mu$ l.

H<sub>2</sub>O<sub>2</sub> production was assayed in a suspension of wild type MG1655 *E. coli* cells alone (resuspended to a final OD<sub>600</sub> of 0.09) and with either CORM-3 (100  $\mu$ M), CORM-3 with glycerol (5 mM) or glycerol alone. Glycerol was added to ensure the samples were respiring. A standard curve was generated using a series of dilutions of H<sub>2</sub>O<sub>2</sub> (0 – 10  $\mu$ M). The absorbance at 560 nm was measured spectrophotometrically. No hydrogen peroxide was detected in any of the samples (data not shown). This could suggest that the cell concentration used was too dilute; however it is similar to that used by Seaver and Imlay (2001) who detected elevated H<sub>2</sub>O<sub>2</sub> production by *E. coli* mutants unable to express both alkyl hydroperoxide reductase and catalase. It therefore seems reasonable to conclude that a dilute *E. coli* cell suspension (OD<sub>600</sub> = 0.09) treated with 100  $\mu$ M CORM-3 produces less than 10 picomoles H<sub>2</sub>O<sub>2</sub> irrespective of whether the cells are respiring or not.

### **5.2.10 NAC significantly reduces CORM-2 and CORM-3 uptake of *E. coli* cells**

Finally, it was investigated whether the presence of NAC affects the uptake of CO-RMs into bacterial cells (Figure 15.16). ICP-MS is a technique that measures with great sensitivity the concentration of individual metals within a sample, and therefore was

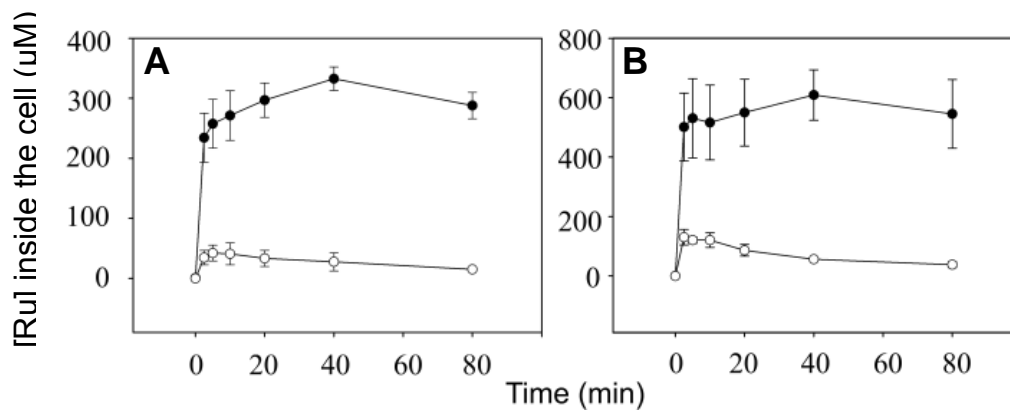


**Figure 5.16 NAC significantly reduces the uptake of CORM-2 and CORM-3 into bacterial cells.** Cultures of wild type *E. coli* were grown to mid-log phase ( $OD_{600} \sim 0.5$ ) prior to the removal of 20 ml samples both before and at regular intervals after the addition of CORM. In (A) ruthenium uptake as CORM-3 (40  $\mu\text{M}$ ) in the absence (closed symbols) or presence (open symbols) of 400  $\mu\text{M}$  NAC is shown. In (B) ruthenium uptake as CORM-2 (20  $\mu\text{M}$ ) in the absence (closed symbols) or presence (open symbols) of 200  $\mu\text{M}$  NAC is shown. Cell pellets were assayed for ruthenium content by inductively coupled plasma-mass spectrometry. Data are the means and standard deviations of 3 biological replicates. This figure was published in Jesse *et al.* (2013).

ideal for comparing the uptake of both CORM-2 and CORM-3 (measured as ruthenium) in the presence and absence of NAC. As ruthenium is not present in bacteria under normal conditions, it can be assumed that any ruthenium detected in the cell pellets following CO-RM treatment has come directly from the CO-RM. Bacteriostatic concentrations of each CO-RM were added to cultures of wild type *E. coli* grown in Evans medium to early exponential phase ( $OD_{600} = 0.5$ ) either alone, or in the presence of a 10-fold excess of NAC. Samples (20 ml) were taken before the addition of CORM-3 and at 2.5, 5, 10, 20, 40 and 80 min thereafter. Cells were harvested by centrifugation at 5500 rpm for 5 min in polypropylene tubes (50 ml). Culture supernatants were retained for analysis. Cell pellets were washed three times in 0.5%  $HNO_3$  (0.5 ml; Aristar nitric acid (69%, v/v)) to remove loosely bound elements. Supernatants collected from the washes were also retained for analysis. Samples were analyzed using a Spectro Ciros<sup>CCD</sup> (Spectro Analytical) inductively coupled plasma-mass spectrometer (ICP-MS). The percentage of ruthenium recovered from these samples was calculated to monitor the precision of this technique and revealed that between 74 to 90% of the ruthenium added to the culture was recovered in the cell pellet, wash steps or medium. To calculate intracellular ruthenium concentrations, published values for individual cell dry mass and volume were used (Graham *et al.*, 2009).

Treatment of cultures of *E. coli* with 40  $\mu M$  CORM-3 led to a rapid accumulation of ruthenium within the cells to approximately 8 times the concentration of ruthenium applied to the culture (Figure 5.16A). The striking discovery was made that in the presence of 400  $\mu M$  NAC, ruthenium from CORM-3 accumulated inside *E. coli* cells approximately 8-fold less, i.e. to a similar concentration to that applied to the culture.

A similar effect was true of CORM-2 treated *E. coli*: in the absence of NAC, ruthenium from CORM-2 (20  $\mu M$ ) accumulated inside the cells to concentrations approximately 30-fold higher than that applied to the culture, however in the presence of 200  $\mu M$  NAC, intracellular ruthenium concentrations were 5-fold lower, confirming that NAC dramatically reduces the uptake and intracellular accumulation of ruthenium-based CO-RMs.

### 5.3 Discussion

As detailed in the introduction to this chapter (section 5.1), this work aimed to ascertain the mechanism by which thiol compounds are able to prevent the inhibitory effects of CO-RMs, and specifically, to what extent the negation of the deleterious effects of ROS are responsible for these effects.

The finding presented in this chapter that an excess of NAC, cysteine or reduced glutathione is able to abolish the effects of CORM-3 on respiration is in agreement with the literature (Desmard *et al.*, 2009, Desmard *et al.*, 2012). However, the work presented here is the first demonstration that NAC is able to completely abolish the inhibitory effects of CORM-3 on respiration when present at an equimolar concentration to CORM-3 (Figure 5.1B). Furthermore, it is shown that thiol compounds are able to prevent or greatly reduce the inhibition of respiration induced by ruthenium based CO-RMs in *E. coli* membrane particles (Figure 5.1B and C, and Figure 5.2A and B), but have no effect on inhibition caused by CO gas (Figure 5.1A).

Importantly, it was shown that thiol compounds do not interfere with binding of CO from CORM-3 to the terminal oxidases (Figure 5.6). This concurs with the conclusions of Desmard *et al.* (2012), who found that only the activity of certain CO-RMs, specifically those containing metal, are affected by thiol-containing compounds such as NAC. They concluded that if thiol compounds elicited their effects by interfering with the downstream effects of CO-RMs, such as the binding to the terminal oxidases, they would affect all CO-RMs similarly.

#### 5.3.1 The effect of thiol compounds on the release of CO from CORM-3

The hypothesis that the rate of CO release from CORM-3 may be affected (either increased or decreased) by thiol compounds was investigated. CO release from CORM-3 was assayed by performing myoglobin assays in the presence of varying concentrations of NAC. The data obtained suggest that the rate of CO release from CORM-3 is slightly diminished and that the final amount of CO release is slightly less (21%) in the presence of a 10-fold excess of NAC (Figure 5.4), and that these effects are greater as the ratio of NAC to CORM-3 increased. However, as the majority of CO can still be released to Mb following incubation with NAC, these differences do not seem



sufficient to completely abolish the effects of CO-RMs on bacteria. In light of our current understanding of the ability of sulfite species, such as dithionite, to promote CO release from many CO-RMs, it is possible that thiol compounds do greatly reduce the ability of CO to be released from CO-RMs in cellular conditions, but that the ability of dithionite to promote CO loss then overrides this, resulting in relatively normal CO release kinetics to myoglobin (Figures 5.4).

The haemoglobin assay (Figure 5.5) was used as a measure of CO release from CORM-3 in the absence of dithionite, and in accordance with the findings of McLean *et al.* (2012), no CO release from CORM-3 was observed. Furthermore, CO release was not observed from CORM-3 pre-incubated with an excess of NAC, confirming that this compound does not promote CO loss from CORM-3.

These findings suggest that NAC stabilizes the CO-bound CORM-3 structure. It is possible that interaction between thiol compounds and CORM-3 causes a conformational change in the latter, thereby decreasing the rate of CO loss from CORM-3. It is known that CORM-3 and other *fac*-[Ru(CO)<sub>3</sub>]<sup>2+</sup> compounds are able to bind to hen egg white lysozyme resulting in a conformational change in the CO-RM that may decrease the rate of CO-release (Santos-Silva *et al.*, 2011; Santos *et al.*, 2012).

The finding that CORM-3 may cause slight oxidation of oxy-ferrous haemoglobin is interesting and is in agreement with observations of other researchers in this laboratory (Lauren Wareham, unpublished). Conversely, another researcher, Salar Ali (unpublished) has found some evidence that some CO-RMs are able to reduce tetrazolium dyes. It is becoming increasingly clear that the redox potential of CO-RMs, of which very little is currently known, may have important biological effects, and therefore should be a key area for future investigation.

There is a published report of thiol compounds promoting the release of CO from CORM-3 and carbon monoxide-releasing micelles (Hasegawa *et al.*, 2010); cysteine (10 mM) was found to cause the release of 0.12 equivalents of CO per molecule of CORM-3. However, lower concentrations of cysteine (100 μM) did not have this ability. These effects were also observed for glutathione. It is important to note that CO release was

measured using a CO detector that measured the CO concentration in the gas phase, and that only very low levels of CO were detected and the CO release occurred slowly (Hasegawa *et al.*, 2010).

It has been suggested that if thiol compounds promoted the release of CO from CO-RMs, it would cause the CO-RM to ‘act like CO gas’ (Desmard *et al.*, 2012) and therefore be less effective at inhibiting respiration in whole cells than CORM-3. The data presented in this chapter show that CO gas, at a concentration of 100  $\mu$ M, causes substantial inhibition of respiration in *E. coli* membranes particles (Figure 5.1A). Therefore, with regards to the inhibition of respiration of membrane particles, thiol compounds do not cause CORM-3 to behave like CO gas. Moreover, when CO is released from CORM-3 prior to a myoglobin assay being conducted, a characteristic jump in the myoglobin spectrum is seen upon addition of the CORM-3 mixture to the myoglobin (McLean *et al.*, 2012). This is not seen in the case of CORM-3 pre-treated with NAC (Figure 5.4).

Desmard *et al.* (2009) reported that NAC did not affect the rate of CO release from CORM-3 as measured by the myoglobin assay; however, while specific details were not provided in that paper, it is likely that they added NAC directly to the CORM-3 and myoglobin, without allowing a 5 min pre-incubation period as was done in the present work. In addition, the presence of dithionite in that study and in the present work adds a variable that contributes to CO release in a manner that was not understood when both pieces of work were undertaken.

### **5.3.2 The influence of endogenous thiol compounds on the bactericidal effects of CORM-3**

Glutathione is present in a wide variety of organisms including bacteria, yeast, plants and animals (Hopkins, 1921). It was shown to undergo reversible oxido-reduction and was believed to have an important role in respiration (Hopkins, 1923), for a recent review see Masip *et al.* (2006). Viability studies presented in the current work found that an *E. coli* mutant unable to produce endogenous glutathione was significantly more resistant to killing by CORM-3 than wild type cultures, particularly at 90 and 120 min following treatment (Figure 5.7). This provides further evidence that ROS is not a

significant cause of bacterial killing by this CO-RM. These findings are contrary to the expectation that glutathione would protect against damage from CORM-3. However the finding that CORM-3 is able to react with thiol groups (Figure 5.8 and 5.9) and that superoxide is generated from CORM-3 at a substantially faster rate in the presence of NAC (Figure 5.10F), could suggest that there are deleterious consequences of CORM-3 in the presence of glutathione. An alternative possibility is that the glutathione mutant has an altered redox potential, which may affect the ability of CORM-3 to release CO inside the cell. It is also important to note that there are many other endogenous proteins that stabilize the redox potential of a cell such as glutaredoxins and thioredoxins (Aslund *et al.*, 1997). In contrast, Tavares *et al.* (2011) found that exogenous glutathione protects against killing by CORM-2 and ALF062, while Nobre *et al.* (2009) found that *E. coli* mutants unable to synthesize methionine are hypersensitive to CORM-2.

The expression of several genes involved in the transport and metabolism of thiol-containing compounds are affected by treatment of *E. coli* with CORM-3 (McLean *et al.*, 2013). Genes affected include *cysPUWA*, which encodes the sulfate-thiosulfate transport system, *metQIN*, which are involved in methionine metabolism and transport and *ssuABCDE* and *tauABCD*, which respond to sulfur starvation. This indicates that *E. coli* cultures treated with CORM-3 have enhanced requirements for sulfur.

### **5.3.3 Could ROS account for the bactericidal effects of CO-RMs?**

As mentioned above, it has been suggested that the main mechanism by which CORM-2 induces bacterial cell death is by the generation of ROS, specifically hydroxyl radicals (Tavares *et al.*, 2011). There is a large body of evidence suggesting that CO (and in some cases CO-RMs) lead to increased ROS due to inhibition of respiration (Queiroga *et al.*, 2011; Smith *et al.*, 2011; Zuckerbraun *et al.*, 2007). Such ROS are thought to play an important role in mediating some of the downstream effects of CO, particularly in eukaryotic systems (Zuckerbraun *et al.*, 2007) (see section 1.2.8.2.4). However, there is evidence that low concentrations of CO can actually protect against oxidative stress in models of mouse lung hypoxia (Otterbein *et al.*, 1999) and that CO can actually decrease ROS production by NADPH oxidase (Taille *et al.*, 2005).

Tavares *et al.* (2011) suggest that, in addition to ROS produced by the inhibition of respiration, CORM-2 and ALF062 can also generate hydroxyl radicals directly. It is known that some transition metal carbonyls e.g. Na[Mo(CO)<sub>3</sub>(histidinate)] and Na<sub>3</sub>[Mo(CO)<sub>3</sub>(citrate)] can cause hydroxyl radical formation (Seixas, 2010). It is proposed that ALF062 produces hydroxyl radicals by reaction of the electron dense metal with H<sub>2</sub>O and O<sub>2</sub>, as ROS did not form in anoxic conditions (Tavares *et al.*, 2011). They propose that hydroxyl radicals are formed by CORM-2 via the reduction of oxygen by ruthenium species that are generated by the water gas shift reaction, which occurs when water reacts with one of the CO ligands of this CO-RM. They show that the control molecule RuCl<sub>2</sub>(DMSO)<sub>4</sub>, which they refer to as iCORM-2, did not produce ROS, and neither did CORM-2 in the presence of haemoglobin, as in these conditions, CORM-2 forms Ru<sup>II</sup>(CO)<sub>2</sub>, which is stable and does not react with water to form OH radicals. It is also important to remember that EPR is very sensitive and the radicals detected in the current work and in Tavares *et al.* (2011) may be the products of a minor side reaction, or even a contaminant in the CO-RM preparation.

The data collected in this current work, by biochemical assays (Figure 5.10) and EPR spectroscopy (Figure 5.14 and 5.15) indicate that while small amounts of ROS (both superoxide and hydroxyl radicals) are produced by high concentrations (1 - 4 mM) of both CORM-2 and CORM-3, this does not explain all of the effects of CO-RMs on bacteria. Indeed, neither CORM-2 nor CORM-3 (both at 100 μM) produced sufficient superoxide to be detected by the superoxide assay (data not shown). This is close to the concentration of CO-RMs used in biological studies and therefore it is unlikely that superoxide is responsible for the deleterious effects induced by low concentrations of these CO-RMs. Furthermore, no H<sub>2</sub>O<sub>2</sub> was detected *in vivo* by relatively high concentrations of CORM-3 (100 μM) in a dilute suspension of *E. coli* cells (data not shown). This concurs with the findings of Desmard *et al.* (2012) that 100 μM of CORM-2, CORM-3, CORM-371 and CORM-A1 did not cause any ROS production in *P. aeruginosa* within 1 h of treatment as measured by DCFH-DA, which measures oxidation of DCFA by ROS. This is in agreement with previous work from this group, which showed that CORM-3 did not produce ROS (Desmard *et al.*, 2009). Furthermore, while CORM-2 treatment has been shown to increase the production of ROS by *P. aeruginosa* biofilms, this increase did not correlate with bacterial cell death and addition

of the thiol compound and antioxidant L-cysteine in combination with 100  $\mu\text{M}$  CORM-2 reduced biofilm formation, but did not affect ROS production, suggesting that CORM-2 is preventing biofilm formation by a different mechanism (Murray *et al.*, 2012).

Therefore, our data support the previous observations that ROS production is not the major mechanism by which CORM-2 disrupts *P. aeruginosa* growth. There is, however, some evidence that inhibition of respiration by CORM-3 leads to ROS production in *C. jejuni* (Smith *et al.*, 2011). The addition of catalase to respiring *C. jejuni* cultures in the presence of 100  $\mu\text{M}$  CORM-3 resulted in an increase in the oxygen concentration in the chamber, indicating that respiratory inhibition by CORM-3 generates  $\text{H}_2\text{O}_2$ , most likely via the production of superoxide.

The possibility that the superoxide detected is generated from impurities in the CO-RM preparation cannot be discounted, particularly as the amount of superoxide generated by CORM-A1, CORM-2, CORM-3 and iCORM-3 was approximately 1% of the CO-RM concentration. That iCORM-3 generated more superoxide than CORM-3 suggests that superoxide is not caused by the CO release process. It is possible that superoxide is formed from the oxidation of ruthenium causing an electron to pass to oxygen, although this is unlikely as CORM-3 is known to be stable in water for several hours. Furthermore, if superoxide radicals were formed in this way, it is feasible that they would spontaneously dismutate to form peroxide, which could react with contaminating free iron or copper in the solution to form hydroxyl radicals, which would be detected by the BMPO spin trap. In this case, haemoglobin, used as a control in the EPR spectra shown by Tavares *et al.* (2011) would scavenge the peroxide and so decrease the signal, as is seen in the published work, rather than CO scavenging by haemoglobin being the cause of this decrease, as is proposed.

CORM-2, and to a lesser extent CORM-3, were found to react with the thiol groups of NAC (Figure 5.8). This is consistent with the findings of Tavares *et al.* (2011) that CORM-2 is able to diminish the thiol groups in reduced glutathione. They suggest that this indicates that CORM-2 generates species that promote oxidation of thiol groups. Contrary to expectations, incubation of NAC with CORM-3 was found to increase the

rate of superoxide generation by CORM-3 (Figure 5.10F). This could be due to the reaction of the thiol group of NAC with CORM-3 (section 5.2.4) generating electrons, which then produce superoxide. CORM-3 and iCORM-3, but not CO gas, decrease the amount of free thiol groups detected in cysteine, reduced glutathione and sodium hydrosulfate (Figure 5.9), which suggests that it is the ruthenium skeleton that reacts with thiol groups. It is possible that this involves the binding of a thiol group to ruthenium, which displaces a chloride ion on the (i)CORM-3 compound (McLean *et al.*, 2013).

The present work used EPR spin-trapping to show that ROS is formed by CORM-2, and to a much lesser extent by CORM-3, and that this species is likely to be hydroxyl radical. However, there are still uncertainties as to why the species generated here do not match the literature spectrum of hydroxyl bound to BMPO, and why the spectrum presented in Tavares *et al.* (2011) does not have aH and aN values that match those reported in the literature (Zhao *et al.*, 2001).

In order to further investigate the claim of Tavares *et al.* (2011) that it is the antioxidant properties of thiol compounds that abolishes the antibacterial effects of CO-RMs, the ability of a range of antioxidants that do not contain thiol groups were assessed for their ability to prevent inhibition of respiration by CORM-3 (Figure 5.11). Both ascorbic acid (Figure 5.11B; in accordance with the observations of Desmard *et al.* (2009)) and ferredoxin (Figure 5.11C), were unable to abolish the inhibitory effects of CORM-3 on respiration, while ubiquinol (Figure 5.11A) was only able to slightly reduce these effects. Ubiquinol and ascorbate have identical redox potentials (+ 60 mV), while ferredoxin has much lower reduction potential of - 430 mV. For comparison, glutathione has a reduction potential intermediate to these of - 172 mV (Nicholls and Ferguson, 2002). Therefore, the ability of ubiquinol to slightly diminish the apparent inhibition of respiration by CORM-3, is unlikely to be related to the reduction potential of this compound, as ascorbate, and the more potent reducing agent ferredoxin, do not have the same effects. When ubiquinol is added to respiring membrane particles in the oxygen electrode chamber in the absence of CORM-3, respiration appears to be stimulated slightly, consistent with the role of this compound in carrying electrons to the terminal oxidases, which is likely to explain why the respiration rate is slightly

faster in the presence of ubiquinol and CORM-3 than with CORM-3 alone. Taken together, these data suggest that it is the thiol group that is crucial in preventing the effects of CORM-2 and CORM-3 on respiration, and that not all antioxidants are capable of this.

While this work has shown that superoxide is produced by CORM-2 and CORM-3, the addition of SOD had no effect on the degree of inhibition caused by CORM-3 on respiration (Figure 5.11D). This allows us to conclude that the inhibition of respiration by CORM-3 is prevented by thiol-containing compounds via a mechanism that does not involve the quenching of reactive oxygen species. It seems clear that while ROS may be generated by high concentrations of some CO-RMs, this cannot account for all of the deleterious effects of these molecules. In particular, this hypothesis cannot explain why respiration is inhibited by CORM-3.

#### **5.3.4 The effects of NAC on the uptake of CORM-2 and CORM-3 by bacterial cells**

Finally, the results presented in this chapter show that NAC has a striking ability to reduce the entry of both CORM-2 and CORM-3 into growing *E. coli* cells. The substantial reduction in CORM-2 and CORM-3 entry into bacterial cells in the presence of NAC could explain why both these CO-RM compounds are much less toxic in the presence of NAC.

In the presence of NAC, ruthenium from CORM-3 accumulates inside the cell to approximately the same concentration that is present outside the cell. Little is known about how CO-RMs are transported into bacterial cells; for example, it is not known whether CO-RMs enter cells by active transport, or by free diffusion. It is possible that NAC modifies ruthenium-containing CO-RMs (and perhaps other CO-RMs) in some way rendering it unable to use a specific transporter.

However, this reduced uptake cannot explain all of the effects seen with thiol compounds on CO-RM activity, as in this work it has been shown that thiol compounds also prevent respiratory inhibition in bacterial membrane particles, in which presumably, CORM-3 access is not a constraint.

### 5.3.5 Conclusions

It is now clear that there is likely to be more than one mechanism by which thiol compounds prevent the deleterious effects of CO-RMs. The work presented in this chapter has contributed to the understanding of how thiol compounds prevent the effects of CO-RMs, by eliminating hypotheses suggested in the literature and by the significant finding that these compounds drastically reduce the uptake of CO-RMs; however, more work is needed in order to fully understand the mechanisms by which these compounds exert their effects. One difficulty encountered when trying to understand how thiol compounds affect CO-RM activity, is that each research group that has investigated this phenomenon has used different CO-RMs, at different concentrations, with different experimental designs, which makes it difficult to make generalisations and to determine the effects of thiol compounds on different types of CO-RM. In this regard, the recently published study by Desmard *et al.* (2012) was particularly rigorous and helpful as it compared the effects of NAC on two ruthenium based CO-RMs with fast CO release rates, with those of a manganese based CO-RM and a boranocarbonate CO-RM, both of which had slow CO - release rates. NAC was found to completely prevent the effects of CORM-2 and CORM-3 on growth, but only partially alleviate growth inhibition caused by low concentrations of CORM-371 and had no effect on growth inhibition caused by CORM-A1 (Desmard *et al.*, 2012). It seems therefore, that NAC only interferes with the effects of metal-containing CO-RMs, particularly those containing ruthenium. In light of this information, it would be helpful to know if non-ruthenium CO-RMs are able to produce significant amounts of ROS, particularly hydroxyl radicals. That the uptake of ruthenium based CO-RMs is significantly reduced by the presence of NAC provides a clear explanation for why this compound reduces the efficacy of these CO-RMs; however, it will be important to ascertain whether NAC also reduces the uptake of non-ruthenium CO-RMs including CO-RMs for which the activity is not affected by thiol compounds such as CORM-A1 (Desmard *et al.*, 2012). It would also be interesting to see if other thiol compounds are also able to reduce CO-RM uptake by bacteria.

The results of the current work, when viewed alongside the literature, suggest that the low concentrations of CORM-3 that are effective in decreasing oxygen consumption, growth and viability in bacterial systems, do not produce significant amounts of ROS, and therefore the ability of thiol compounds to abrogate these effects is likely to be



distinct from the antioxidant properties of these compounds. However, the literature has shown that high concentrations of CORM-2 do produce hydroxyl radicals (Tavares *et al.*, 2011), a property that may explain why CORM-2 is a more potent bactericidal agent than CORM-3, despite having similar CO-release profiles.

## Chapter 6

### The generation and characterisation of CORM-2 resistant mutants

#### 6.1 Introduction

In order to understand more about the bacterial targets of CO-RMs and their mechanisms of toxicity in *E. coli*, work was done to generate and characterise mutants of *E. coli* that exhibited a CO-RM-resistant phenotype.

The EZ-Tn5 <R6K<sub>Yori</sub>/KAN-2>Tnp Transposome™ Kit (Epicentre Technologies) was used to generate random transposon mutants of the parent strain *I<sup>q</sup> Express E. coli* (New England Biolabs). This method utilizes a hyperactive Tn5 transposon system (Goryshin and Reznikoff, 1998), which randomly inserts into the genomic DNA of the host. A kanamycin marker allows transposon mutants to be selected. The insertion site of the transposon in mutants of interest can then be identified by sequencing outwards from the transposon into the chromosomal DNA. No host proteins are required for transposition, allowing this system to be used in a wide variety of organisms (Goryshin and Reznikoff, 1998); for example, a derivative of EZ-Tn5 <R6K<sub>gori</sub>/KAN-2> has been used successfully to generate a large pool of mutants of *Salmonella enterica* serovar Typhi, which enabled candidate essential genes in this organism to be identified (Langridge *et al.*, 2009).

Tn5 causes transposition by a ‘cut and paste’ mechanism as opposed to replicative transposition (Berg, 1977; Goryshin and Reznikoff, 1998). It naturally has a low level of transposition, which can be beneficial, allowing long-term, stable associations with the host genome; however the introduction of 3 mutations modified this transposon causing it to have a much higher frequency of transposition (1000-fold higher), making it ideal for use as a genetic tool (Goryshin and Reznikoff, 1998). Another beneficial feature of this system is that this transposon inserts into the genome randomly (Kirby, 2007).

Tn5 comprises 3 antibiotic genes, including one conferring kanamycin resistance, the transposase (Tnp), and the negative regulator *Inh*, the synthesis of which is blocked in this system. There are also 19-bp inverted repeats at either end of the transposon that are recognised by transposase (Goryshin and Reznikoff, 1998). Once the transposome has been introduced into the host cell by transformation, interaction of the transposase with  $Mg^{2+}$  activates this enzyme (reviewed by Kirby, 2007). The transposase enzyme binds to sequences at either end of the transposable element and then catalyses the cleavage of the phosphodiester bonds at either end of the transposable element. This multifaceted enzyme then inserts the transposon into random sites in the target DNA by strand exchange, before being released.

This chapter describes the generation of random transposon mutants using the EZ-Tn5 <R6K $\gamma$ ori/KAN-2>Tnp Transposome<sup>TM</sup> described above, followed by screening of the resulting mutants for resistance to CORM-2. Various assays were performed in order to verify the CORM-2 resistance of transposon mutants of interest and then nucleotide sequencing was used to identify the disrupted gene.

## **6.2 Results**

### **6.2.1 The use of random transposon mutagenesis to generate *E. coli* mutants followed by screening for CORM -2 resistance.**

Critical in this work was the design of a screen to select for CO-RM resistance. CORM-2 was used in this screen as, unlike CORM-3, it is commercially available and therefore more financially viable for use in large screens. *I<sup>f</sup>* Express *E. coli* (a BL21 derivative, purchased from New England Biolabs) was used as the recipient strain for the transposon, as it is a chemically competent strain with a high efficiency for transformation. Initial trials to determine the minimum concentration of CORM-2 that is toxic to *I<sup>f</sup>* Express *E. coli* revealed that exposure of cultures to 40  $\mu$ M CORM-2 for 30 min resulted in complete loss of viability (Figure 6.1). Therefore, this concentration was used in the mutant screen.

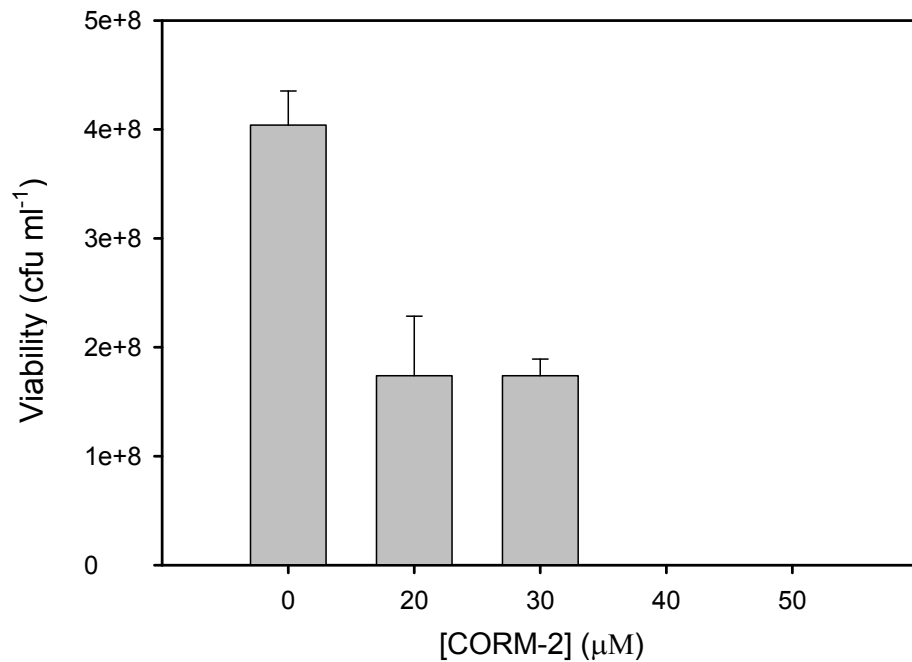


**Figure 6.1** The survival of *I<sup>q</sup> Express E. coli* in the presence of various concentrations of CORM-2. *E. coli* was grown aerobically to an OD<sub>600</sub> of 50 Klett units, various concentrations of CORM-2 (0 – 50 μM) were added, and the cultures incubated at 37 °C with shaking at 200 rpm. After 30 min, samples (50 μl) were taken and serially diluted to allow viability counts to be performed. Data shows the mean and standard deviation of 5 technical replicates, and are representative of 2 biological replicates.

Transposon mutagenesis was performed using the EZ-Tn5™ <R6K $\gamma$ ori/KAN-2>Tnp Transposome™ Kit from Epicentre Biotechnologies, according to the manufacturer's instructions. Briefly, the transposome complex (1  $\mu$ l) was used to transform *I<sup>g</sup>* Express chemically competent *E. coli* (50  $\mu$ l) using the high efficiency transformation protocol (heat shock) as described in section 2.4.3. Transformants were selected by plating the cell suspension on to nutrient agar, supplemented with kanamycin (30  $\mu$ g ml<sup>-1</sup>).

Mutagenised cultures of *I<sup>g</sup>* Express were grown to early exponential phase (50 Klett units) in 30 ml defined minimal medium by incubation at 37 °C with shaking at 250 rpm, then exposed to a bactericidal concentration of CORM-2 (40  $\mu$ M) for 30 min and then spread onto nutrient agar plates containing kanamycin and incubated at 37 °C overnight. It was expected that only a small number of mutants would be 'CORM-2 resistant' and therefore survive this screen; however nearly 300 were obtained. It is likely that many of these survivors are siblings generated during the outgrowth stage following mutagenesis. A control, in which the mutagenized cultures were treated with the vehicle DMSO, yielded too many colonies to count, confirming that treatment with CORM-2 had successfully killed a large portion of the kanamycin resistant colonies.

A second selection process of the putative CORM-2 resistant colonies was performed. A trial was done in a 96-well plate in order to establish the concentration of CORM-2 that would substantially reduce the growth of the parent strain *I<sup>g</sup>* Express. The parental strain was incubated at 37 °C, until the cultures reached an OD<sub>600</sub> of 0.2. A range of CORM-2 concentrations (0 - 60  $\mu$ M) were added to the wells: 10  $\mu$ M CORM-2 caused 3.9% less growth than the control in which no compound was added, 20  $\mu$ M CORM-2 caused 14.6% less growth than the control and concentrations above 30  $\mu$ M caused between 64 and 69% growth inhibition. This led to 40  $\mu$ M CORM-2 being used as a stringent selection for CORM-2-resistant mutants.

Each mutant was inoculated into 200  $\mu$ l defined minimal medium in individual wells of a 96-well plate and incubated at 37 °C for 8 h until a typical OD<sub>600</sub> of between 0.1 and 0.3 was reached. CORM-2 (40  $\mu$ M) was then added to each well and incubated at 37 °C with shaking for 16 h and the OD<sub>600</sub> measured using a multilabel reader (Victor™ X3, Perkin Elmer). The change in OD<sub>600</sub> was calculated and an increase of more than 0.2

was considered to indicate substantial growth in the presence of CORM-2. This identified 4 mutants as CORM-2 resistant, designated 1B2 ( $A_{600}$  increase of 0.404), 1B11 ( $\Delta A_{600} = 0.413$ ), 3A33 ( $\Delta A_{600} = 0.200$ ) and 3B8 ( $\Delta A_{600} = 0.216$ ), according to their position in the 96-well plates. The  $OD_{600}$  of each of these mutants before and after the addition of CORM-2 and the subsequent change in absorbance are given in Table 6.1. The mutant 1B11 is of particular interest as it appeared to have low growth initially, but then grew well in the presence of CORM-2. 1B2 is also of interest because it had a large increase in growth following the addition of CORM-2.

### **6.2.2 Characterisation of mutants of interest.**

The 4 mutants of interest were then further characterised by conducting growth studies in larger volumes of medium in the presence of 25  $\mu\text{M}$  CORM-2 (Figure 6.2). The addition of 25  $\mu\text{M}$  CORM-2 to the parent strain *I<sup>q</sup> Express*, reduced the growth rate of this strain and caused a delay in the onset of exponential phase of approximately 2 h, whereas the growth profiles of the transposon mutants were not affected.

The relative CORM-2 resistance of each mutant of interest was further investigated by performing CORM-2 susceptibility assays. At the point of inoculation, various concentrations of CORM-2 (0 – 2  $\mu\text{M}$ ) were added to cultures of the parent strain *I<sup>q</sup> Express* and the 4 transposon mutants of interest. This assay uses extremely low concentrations of CORM-2, because the stressor is added at the point of inoculation, at which higher concentrations would completely prevent growth. Cultures were incubated at 37 °C with shaking at 250 rpm for 17 h, before the  $OD_{600}$  was measured using a spectrophotometer (Jenway). Figure 6.3 shows the growth for each strain subjected to various concentrations of CORM-2 as a percentage of growth for that strain in the absence of CORM-2. All four mutants exhibited stronger growth in the presence of CORM-2 than the parental strain. In particular, the mutants 3B8, 1B2 and 1B11 exhibited much greater resistance to growth inhibition by CORM-2 than the parental strain, while the mutant 3A33 showed a more moderate ‘CORM-2-resistant’ phenotype.

Strain	OD <sub>600</sub> before CORM-2	OD <sub>600</sub> after CORM-2	ΔOD <sub>600</sub>
I <sup>q</sup>	0.162	0.168	0.006
1B2	0.145	0.549	0.404
1B11	0.063	0.476	0.413
3A33	0.198	0.398	0.200
3B8	0.171	0.387	0.216

**Table 6.1 OD<sub>600</sub> of the mutants of interest obtained from the second stage of the CORM-2 screen.** The OD<sub>600</sub> of each of the parental strain and the mutants of interest grown in defined minimal medium was measured using a multilabel reader (Victor™ X3, Perkin Elmer), before and after the addition of 40 μM CORM-2. The OD<sub>600</sub> and the subsequent change in absorbance are given for each mutant of interest.

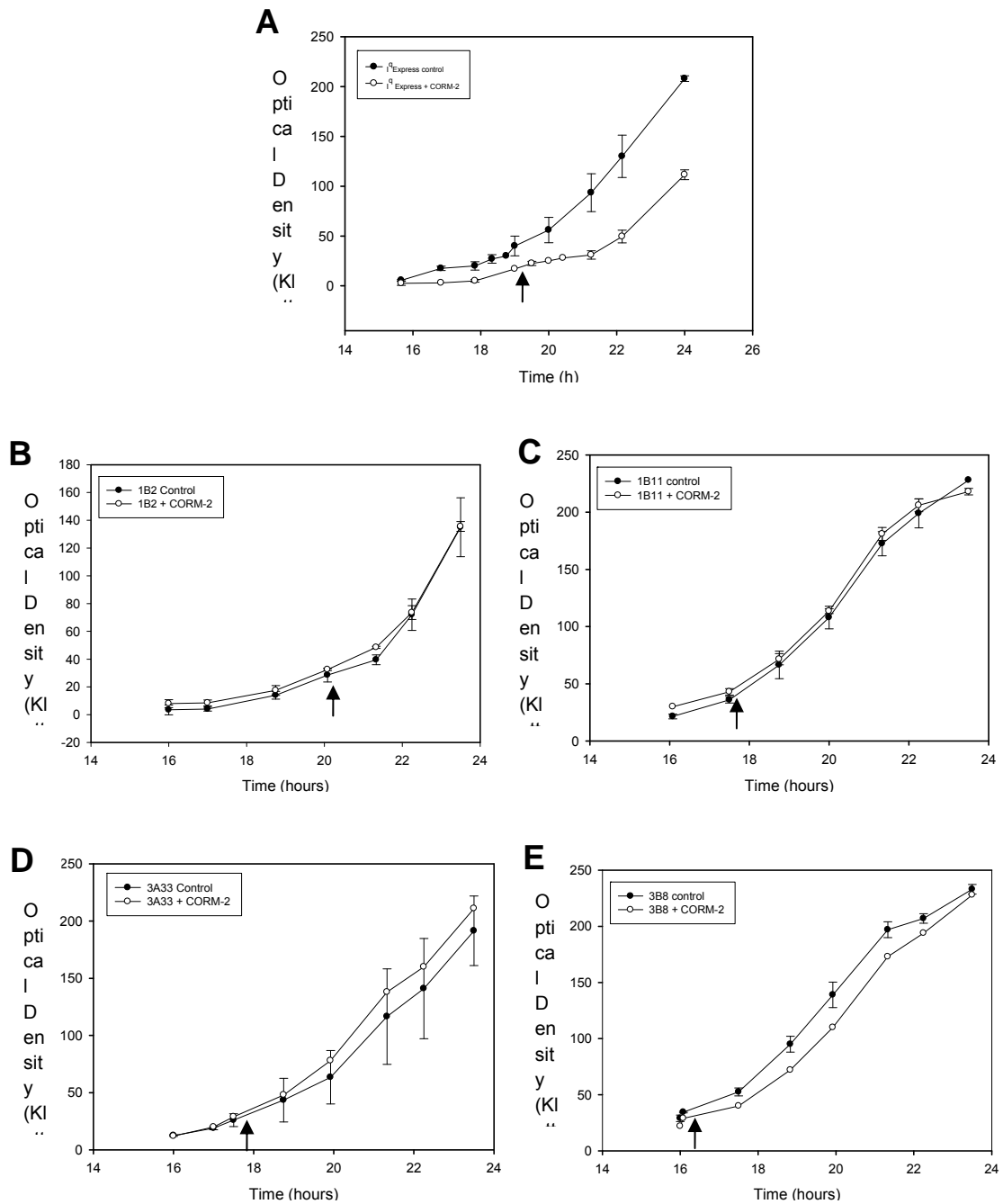


**Figure 6.2** The growth of selected transposon mutants in the presence and absence of CORM-2. Growth of the parent strain *I<sup>q</sup> Express* (A) and the transposon mutants; 1B2 (B), 1B11 (C), 3A33 (D) and 3B8 (E) was measured spectrophotometrically using a Klett meter in the presence of 25  $\mu$ M CORM-2 (open circles) or the equivalent volume of the vehicle DMSO (closed circles). CORM-2 or DMSO was added when cultures reached an OD<sub>600</sub> of approximately 30 Klett units (as indicated by the arrows). Cultures were inoculated at time = 0. Data are the means and standard deviations of two biological replicates.



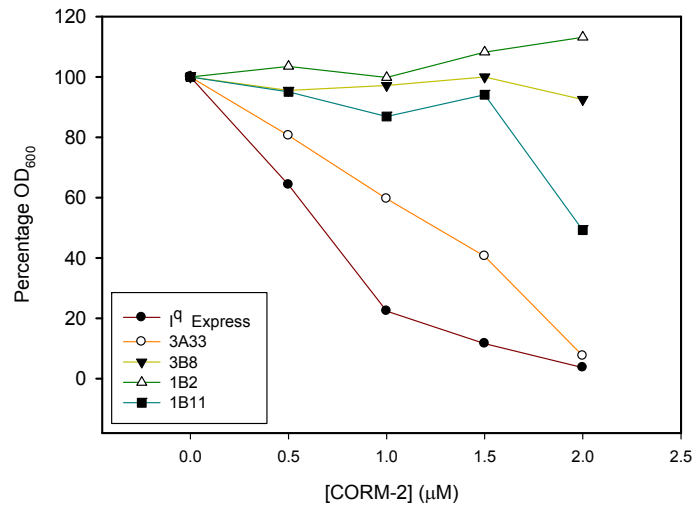


**Figure 6.3 CORM-2 susceptibility assay.** At the point of inoculation, various concentrations of CORM-2 (0 – 1.5 µM) were added to cultures of the parent strain *I<sup>q</sup> Express* (closed circles, burgundy line), and the 4 transposon mutants of interest: 3A33 (open circles, orange line), 3B8 (closed triangles, yellow line), 1B2 (open triangles, green line) and 1B11 (closed squared, blue line). The OD<sub>600</sub> was measured 17 h after inoculation using a spectrophotometer and the growth in the presence of CORM-2 compared to that in the absence of CORM-2 for each strain to generate a percentage. These data are representative of 3 biological replicates.

Each transposon mutant was then grown on nutrient agar plates containing increasing concentrations of CORM-2 (30  $\mu\text{M}$  – 40  $\mu\text{M}$ ; Table 6.2). Overnight cultures of each mutant of interest and the parental strain were grown and 50  $\mu\text{l}$  was added to 2.95 ml of molten defined minimal medium (cooled to 50  $^{\circ}\text{C}$ ) with 0.7% agar, before the addition of various concentrations of CORM-2 (20 - 40  $\mu\text{M}$ ). This mixture was poured onto a base layer of defined minimal medium with 1.5% agar and incubated overnight. The ability of each strain to grow on the plates containing CORM-2 was assessed by eye and characterised according to their ability to grow. The results obtained suggest that all four transposon mutants are more resistant to CORM-2 than cultures of *I<sup>q</sup> Express*, which had poor growth on plates containing 35  $\mu\text{M}$  CORM-2 and was unable to grow on plates containing 40  $\mu\text{M}$  CORM-2, whereas each transposon mutant tested was able to grow on plates containing up to 40  $\mu\text{M}$  CORM-2. The transposon mutant 3B8 had the most growth on CORM-2 plates at all concentrations.

Finally, in order to further assess the relative ability of the transposon mutants of interest to grow in the presence of this compound, CORM-2 gradient plates were made (Gerhardt, 1994). Gradient plates involve two layers of agar, the first of which was constructed from defined minimal medium containing 1.5 % agar, which was set with the petri dish at an angle (achieved by balancing the plate on the edge of a plate lid). The second layer consisted of defined minimal medium containing 0.7% agar, to which (after cooling to approximately 50  $^{\circ}\text{C}$ ) 60  $\mu\text{M}$  CORM-2 was added. This agar containing CORM-2 is poured on to the first layer, resulting in a level agar plate that has a maximal quantity of CORM-2 at one apex of the plate, which decreases gradually across the plate (for a diagrammatic representation of the construction of this plate, see Figure 6.4A and B). Cultures of each transposon mutant of interest, and the parent strain, were grown overnight in LB (10 ml) at 37  $^{\circ}\text{C}$  with shaking at 250 rpm, these cultures were then harvested as described above, washed by resuspending in defined minimal medium, harvested once more and finally resuspended in 200  $\mu\text{l}$  defined minimal medium. 50  $\mu\text{l}$  of this suspension was streaked onto the CORM-2 gradient plates using a Gilson pipette to release the cell suspension along the concentration gradient, starting at the apex that had the least CORM-2. Care was taken to apply the suspension evenly and consistently between strains. More resistant strains are expected to grow further along the plate towards the higher concentration of CORM-2. In each

	Growth on plates containing CORM-2?		
	30 $\mu$ M	35 $\mu$ M	40 $\mu$ M
<i>I<sup>q</sup></i> Express	**	*	-
1B2	**	**	**
1B11	**	**	**
3B8	***	***	***
3A33	**	**	**

**Table 6.2 The growth of transposon mutants of interest on plates containing CORM-2.** The information in this table indicates the ability of each transposon mutant of interest, and the parent strain *I<sup>q</sup>* Express, to grow on nutrient agar plates containing a range of CORM-2 concentration (30 – 40  $\mu$ M). \*\*\* strong growth, \*\* intermediate growth, \* little growth, - indicates no growth. These results are representative of two biological replicates.

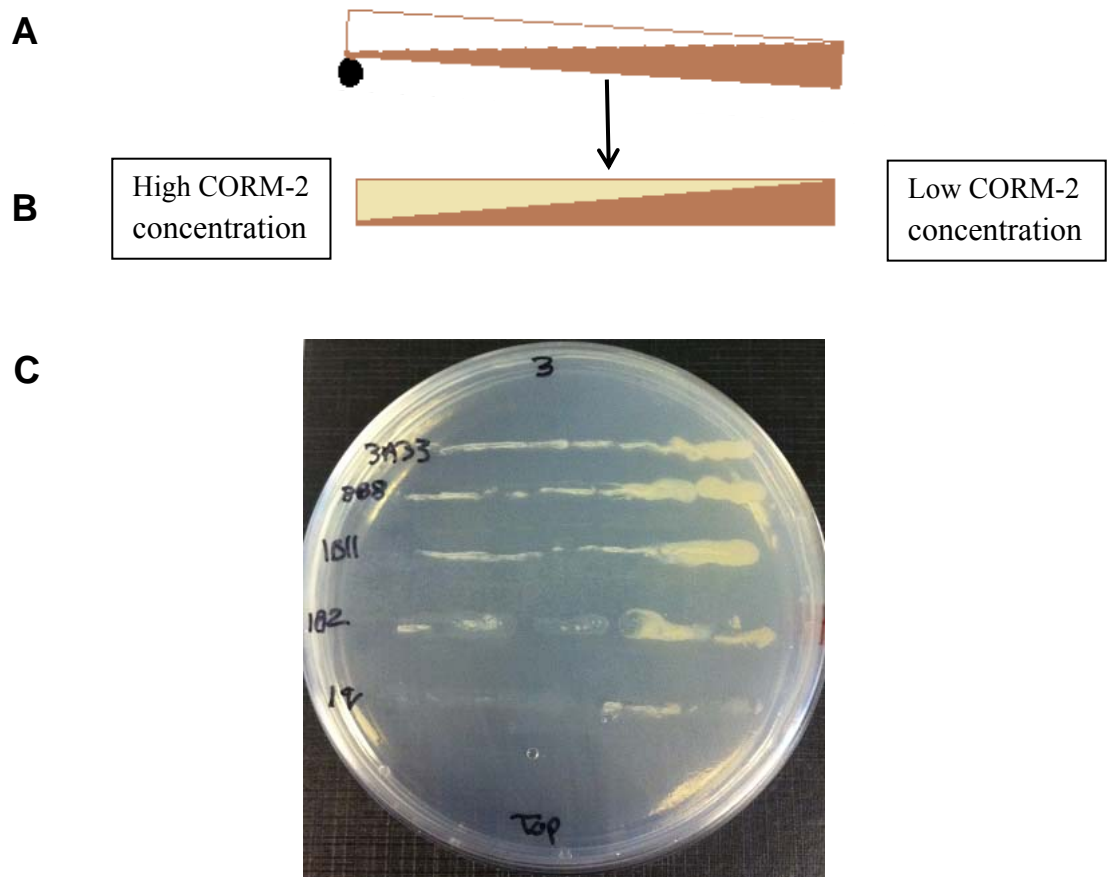


**Figure 6.4 CORM-2 gradient plates.** (A) and (B) represent the stages involved in making a gradient plate. In (A) the petri dish is tilted by resting one edge on the lid of a petri dish. 12.5 ml defined minimal medium with 1.5% agar was then poured into the plate and allowed to solidify on an angle. The plate is then returned to a flat surface and defined minimal medium containing 0.7% agar and 60  $\mu$ M CORM-2 was poured on to make a level plate with a CORM-2 gradient (B). A concentrated suspension (50  $\mu$ l) of each mutant was then applied to a plate in a line parallel with the concentration gradient. (C) shows a photograph of a gradient plate obtained from one biological replicate and is representative of the results obtained on each.

biological replicate, all 4 mutants exhibited stronger growth, and grew further along the CORM-2 concentration gradient than the parental strain *I<sup>g</sup>* express (Figure 6.4C). This provides further evidence of the CORM-2 resistant phenotype of these mutants.

### 6.2.3 Sequencing the CORM-2 resistant mutants

In order to determine where the transposon had been inserted into the *E. coli* genome, genomic DNA was extracted from each transposon mutant and digested by the restriction enzyme *RsaI*. This restriction enzyme recognises the sequence 5'GTAC3' and cuts between the T and the A to generate blunt ends. *RsaI* cuts once inside the kanamycin resistance gene, although it cuts several times within the R6K origin of replication and many times within the genomic DNA of *E. coli*. The sequence of the EZ Tn5 transposon is given in Figure 6.5 and the *RsaI* cut sites are marked. The digested chromosomal DNA was then ligated using T4 DNA ligase to form small, circular fragments of DNA, which were then amplified using the KAN-2 FP1 Forward Primer from the EZ-Tn5 <R6Kγori/KAN-2>Tnp Transposome™ Kit, in conjunction with a primer designed to be internal to the *RsaI* site using the polymerase chain reaction (PCR). The sequence of both primers is given in Table 2.2, while Figure 6.6 shows a diagrammatic representation of the rescue cloning process. The PCR product generated from these primers with DNA from each transposon mutant of interest was sent for nucleotide sequencing (Beckman Coulter genomics) using the KAN-2 FP1 Forward Primer. An NCBI nucleotide blast search was then done to identify the sequence, and positive matches were found for three of the four sequences, a summary of the results is shown in Table 6.3.

The transposon mutant strain 3B8 was found to have 97% sequence identity with the gene *frvB*, also known as *yiiJ*. This gene is 1452 bp in length and encodes the enzyme IIB and IIC domains of a predicted PEP-dependent sugar-transporting phosphotransferase system. It is an inner membrane protein and a predicted transporter. Sequence similarity of *frvB* to characterized fructose-specific enzymes IIBC suggests this transporter may be specific for fructose (Reizer *et al.*, 1994)

The transposon mutant strain 1B11 was found to have 98% sequence identity with the gene *sgaU*, also known as *ulaE*. This gene is 855 bp in length and encodes the enzyme

**CTGTCTTATACACATCT**CAACCATCATCGATGAATTGCTTCGTTAATACAGATGTAGGTGTTCCACAG  
 GGTAGCCAGCAGCATCCTGCGATGCAGATCCGGATGCCATTTCAATTACCTCTTTCTCCGCACCCGACAT  
 AGATCCGAAGATCAGCAGTTCAACCTGTTGATAGTACGTACTAAGCTCTCATGTTTCACGTACTAAGCT  
 CTCATGTTTAAACGTACTAAGCTCTCATGTTTAAACGAACTAAACCCTCATGGCTAACGTACTAAGCTCTCA  
 TGGCTAACGTACTAAGCTCTCATGTTTCACGTACTAAGCTCTCATGTTTGAACAATAAAATTAATATAA  
 ATCAGCAACTTAAATAGCCTCTAAGGTTTAAAGTTTTATAAGAAAAAAAAAGAATATATAAGGCTTTTTAA  
 AGCTTTTAAAGGTTTAAACGGTTGTGGACAACAAGCCAGGGATCTGCCATTTCAATTACCTCTTTCTCCGCAC  
 CCGACATAGATCCGGAACATAATGGTGCAGGGCGCTGACTTCCGCGTTTCCAGACTTTACGAAACACGG  
 AAACCGAAGACCATTATGTTGTTGCTCAGGTCGCAGACGTTTTGCAGCAGCAGTCGCTTACGTTTCGC  
 TCGCGTATCGGTGATTCAATTCTGCTAACCCAGTAAGGCAACCCCGCCAGCCTAGCCGGGTCTCAACGAC  
 AGGAGCACGATCATGCGCACCCGTTGGCCAGGACCAACGCTGCCCGAGATGCGCCGCGTGC GGCTGCT  
 GGAGATGGCGGACGCGATGGATATGTTCTGCCAAGGTTGGTTTGCGCATTCACAGGGTGTCTCAAAAT  
 CTCTGATGTTACATTGCACAAGATAAAAATATATCATCATGAACAATAAACTGTCTGCTTACATAAAC  
 AGTAATACAAGGGTGTATGAGCCATATTCAACGGGAAACGTCTTGCTCGAGGCCGCGATTAAATTC  
 AACATGGATGCTGATTTATATGGGTATAAATGGGCTCGCGATAATGTCGGGCAATCAGGTGCGACAATC  
 TATCGATTGTATGGGAAGCCCGATGCGCCAGAGTTGTTTCTGAAACATGGCAAAGGTAGCGTTGCCAAT  
 GATGTTACAGATGAGATGGTCAGACTAAACTGGCTGACGGAATTTATGCCTCTTCCGACCATCAAGCAT  
 TTTATCCGTACTCTGATGATGCATGGTTACTCACCCTGCGATCCCCGAAAAACAGCATTCCAGGTA  
 TTAGAAGAATATCCTGATTCAGGTGAAAATATTGTTGATGCGCTGGCAGTGTTCCTGCGCCGGTTGCAT  
 TCGATTCCTGTTTGTAAATTGCTCTTTTAAACAGCGATCGCGTATTTCTGCTCAGGCGCAATCACGAA  
 TGAATAACGGTTTGGTTGATGCGAGTGATTTTATGACGAGCGTAATGGCTGGCCTGTTGAACAAGTCT  
 GGAAAGAAATGCATAAACTTTTGCCATTCTCACCGGATTACGTCGTCACACTCATGGTGATTTTCTACTTGA  
 TAACCTTATTTTACGAGGGGAAATTAATAGGTTGTATTGATGTTGGACGAGTCGGAATCGCAGACCG  
 ATACCAGGATCTTGCCATCCTATGGAAGTGCCTCGGTGAGTTTTCTCCTTATTACAGAAACGGCTTTTT  
 CAAAAATATGGTATTGATAATCCTGATATGAATAAATTGCAGTTTCATTTGATGCTCGATGAGTTTTTCT  
 AATCAGAATTGGTTAATTGGTTGTAACACTGGCAGAGCATTACGCTGACTTGACGGGACGGCGGCTTTG  
 TTGAATAAATCGAACTTTTGTGAGTTGAAGGATCAGATCACGCATCTTCCCACAACGCAGACCGTTC  
 CGTGGCAAAGCAAAGTTCAAATCACC AACTGGTCCACCTACAACAAGCTCTCATCAACC GTGGCG  
 GGGATCCTCTAGAGTCGACCTGCAGGCATGCAAGCTTCAGGGTTG**AGATGTGTATAAGAGACAG**

**Figure 6.5 The sequence of the EZ Tn5 transposon.** The Tn5 Mosaic Ends are highlighted in yellow, the *RsaI* cut sites in grey. The R6k origin of replication is given in a blue font, while the Tn903 Kanamycin resistance gene is in orange. In order to identify the insertion site of the transposon in mutants of interest, the forwards primer from the EZ-Tn5 <R6K $\gamma$ ori/KAN-2>Tnp Transposome<sup>TM</sup> Kit was used, the sequence complementary to this primer (Kan2FP-1) is highlighted in turquoise, while the primer internal to Kanamycin *RsaI* site (highlighted in green) was designed by Iain Kean for the purpose of allowing sequencing of the genetic material adjacent to the transposon.

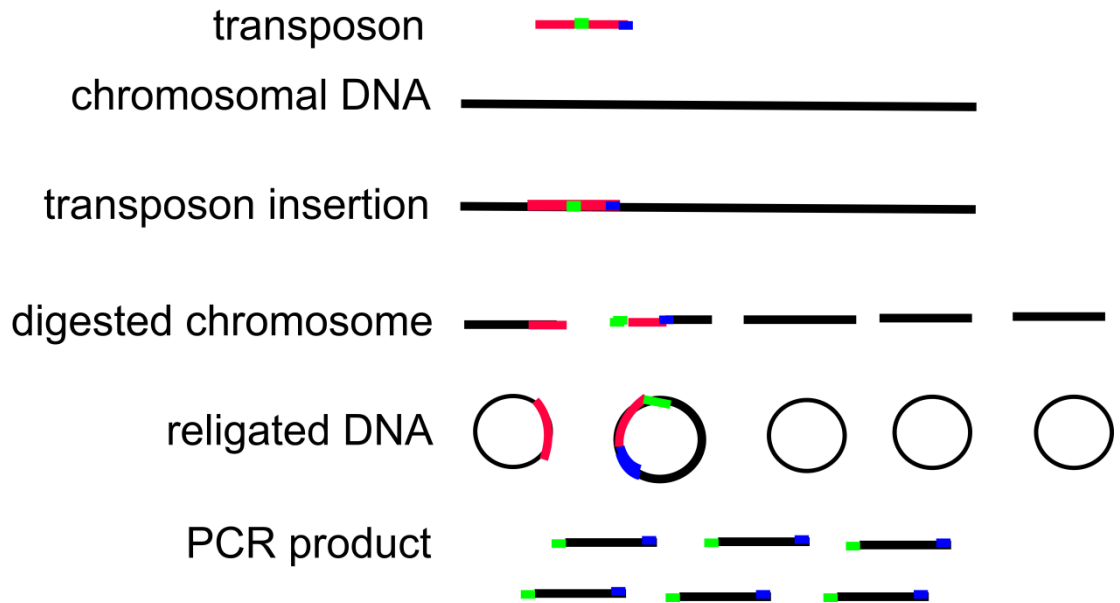


**Figure 6.6 Identifying the transposon insertion site.** Following insertion of the transposon (shown in pink) into the chromosomal DNA (shown in black) of the host, genomic DNA was extracted from the mutants of interest and digested with the restriction enzyme *RsaI*. This cuts once within the transposon and at many sites within the genomic DNA. The DNA fragments were ligated using T4 DNA ligase, and then the DNA adjacent to the transposon was amplified by PCR using a primer complementary to the sequence immediately following the *RsaI* cut site internal to the transposon (shown in green), in conjunction with a primer matching the DNA sequence at the 3' end of the transposon (shown in blue).

<b>Transposon Mutant</b>	<b>Disrupted gene (all commonly used names)</b>	<b>Sequence identity (%)</b>	<b>Gene size (bp)</b>	<b>Gene function</b>
3B8	<i>frvB</i> <i>yiiJ</i>	97	1452	Putative fructose-like PTS system enzyme IIB
1B11	<i>sgaU</i> <i>ulaE</i>	98	855	L-xylulose 5-phosphate 3-epimerase
3A33	<i>manX</i>	91	972	PTS system mannose - specific transporter subunit IIC
1B2	No successful sequence match obtained			

**Table 6.3 The genes disrupted in the transposon mutant strains that have been identified as CORM-2 resistant.**



L-xylulose 5-phosphate 3-epimerase, an isomerase that catalyses the conversion of L-xylulose 5-phosphate to L-ribulose 5-phosphate, a step in the catabolism of L-ascorbate in *E. coli* (Yew and Gerlt, 2002). Interestingly, the *sga* operon encodes three components of a PTS system that imports L-ascorbate into the cell.

The transposon mutant strain 3A33 was found to have 91% sequence identity to a short section (21 bp) of the gene *manX*. This gene is 972 bp in length and encodes subunit IIC of a mannose - specific transporter in the inner membrane, which like FrvB and SgaU, is a component of the sugar PTS system. This transporter is required for bacteriophage lambda DNA penetration (Esquinas-Rychen and Erni, 2001).

After several attempts, the PCR product from IB11 failed to give a sequence that matched any known gene in the *E. coli* gene database. Therefore, due to time constraints, work with this mutant was terminated.

It seemed significant that all three of the genes identified in this work encode components of a PTS transport system, which may indicate that CORM-2 enters cells via these, or related transporters. This suggests that a key mechanism of bacterial resistance to CO-RMs could be the disruption of transport of these compounds into the cell.

#### **6.2.4 The characterisation of independent mutants**

In order to verify that mutations in the 3 genes mentioned above are sufficient to cause resistance to CORM-2, and that this phenotype was not caused by downstream effects of the transposon insertion, independent mutants were sought. Mutants in *manX*, *frvB* and *sgaU* from the Keio collection were obtained from Simon Andrews, The University of Reading. These mutations were then transferred by P1 *vir* phage transduction into an MG1655 background, and the transductants selected on kanamycin plates.

Primers were designed using Primer 3 software, version 0.4.0 to allow amplification of these three genes. These primers were then used to amplify the relevant section of DNA in each of the mutants and in the wild type MG1655 strain, and the PCR products were then run on an agarose gel. As expected, each primer pair generated a sole product of

the correct size from the wild type DNA, but produced a differently sized product in each of the transductants, indicating the absence of the gene (and replacement with a kanamycin marker) in each case (Figure 6.7), confirming that the appropriate mutations had been transferred to an MG1655 background.

The sensitivity of these independently generated mutants to CORM-2 was then compared to the wild type MG1655 strain. Cultures of each strain were grown in defined minimal medium (30 ml) with glycerol (0.5%) as a carbon source to 30 Klett units as described previously (section 2.1.6). CORM-2 (4  $\mu\text{M}$ ) was added and the growth was monitored over time and compared to that of the MG1655 wild type strain (Figure 6.8). Under these conditions, the growth of the *sgaU* and *frvB* mutants (Figure 6.8B and C respectively) was actually increased by this low concentration of CORM-2. The growth of the *manX* mutant was not enhanced by this concentration of CORM-2; however, in this assay, the growth of this mutant was less inhibited by CORM-2 than that of the wild type strain (Figure 6.8A). This provides evidence that mutations in these genes cause a CORM-2 resistant phenotype, and may, in some cases, result in enhanced growth in the presence of this compound.

The growth of these three mutants in the presence of CORM-2 was assessed further by performing CORM-2 susceptibility assays in which low concentrations of CORM-2 (0 – 1  $\mu\text{M}$ ) were added to cultures of MG1655 wild type and the 3 mutants of interest. The *sgaU* mutant was significantly more resistant than the wild type strain at 0.25  $\mu\text{M}$  CORM-2 ( $P < 0.05$ ) and at 0.5  $\mu\text{M}$  CORM-2 ( $P < 0.1$ ) (Figure 6.9A, yellow bars). The *manX* mutant was significantly more sensitive to CORM-2 (0.25 and 0.5  $\mu\text{M}$ ) than the wild type ( $P < 0.1$ ) (Figure 6.9A, green bars). However, while the *frvB* mutant appeared to be more resistant to CORM-2 than the wild type strain (Figure 6.9A, orange bars); this was not statistically significant. Importantly, the growth of all of the strains was not affected by up to 3  $\mu\text{M}$   $\text{RuCl}_2(\text{DMSO})_4$  (Figure 6.9B). It should be noted however that the statistical analysis was performed on percentage data which compared the growth of each strain with CORM-2 to that without CORM-2. This was done in order to account for differences in the growth of each strain in the absence of CORM-2. It is acknowledged that it is not ideal to perform statistical tests on percentage data, and so care must be taken when interpreting these results.

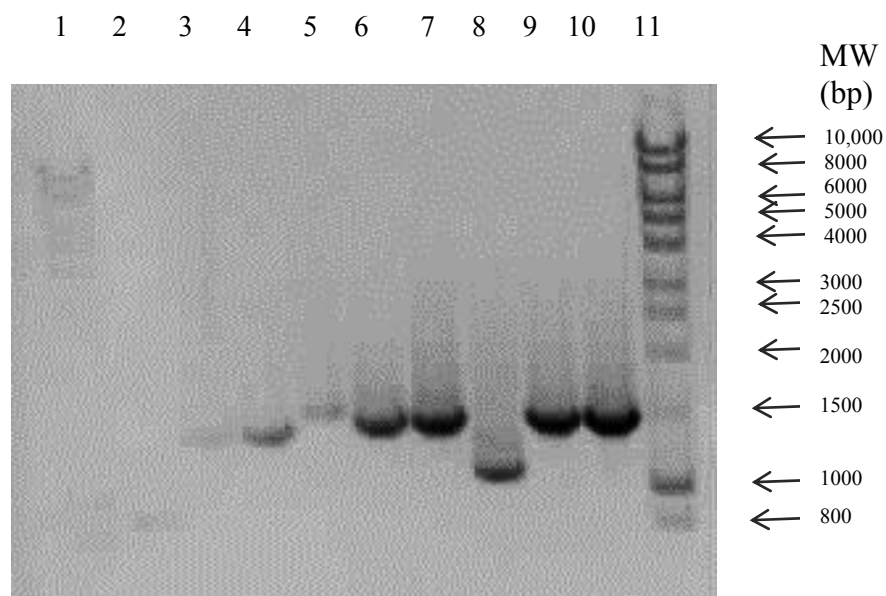


**Figure 6.7 Confirmation of the absence of the mutated gene in the MG1655 transductants.** Genomic DNA was extracted from a kanamycin resistant colony from each transduction event (*sgaU*, *frvB*, *manX*). A PCR reaction was performed on each DNA sample using primers designed to amplify the mutated gene in each case. (Lanes 2 - 4 contain the PCR product of the *SgaU* primers from wild type DNA (lane 2, positive control, 800 bp) and the *sgaU* DNA (lanes 3 and 4, replicates, 1350 bp), lanes 5 - 7 contain the PCR product of the *FrvB* primers from wild type DNA (lane 5, positive control, 1450 bp) and the *frvB* DNA (lanes 6 and 7, replicates, 1400 bp), finally, lanes 8 - 10 contain the PCR product of the *ManX* primers from wild type DNA (lane 8, positive control, 1100 bp) and the *manX* DNA (lanes 9 and 10, replicates, 1400 bp), Lanes 1 and 11 show the molecular weight marker (Hyperladder 1, Bionline), the sizes of which are indicated on the right hand side.

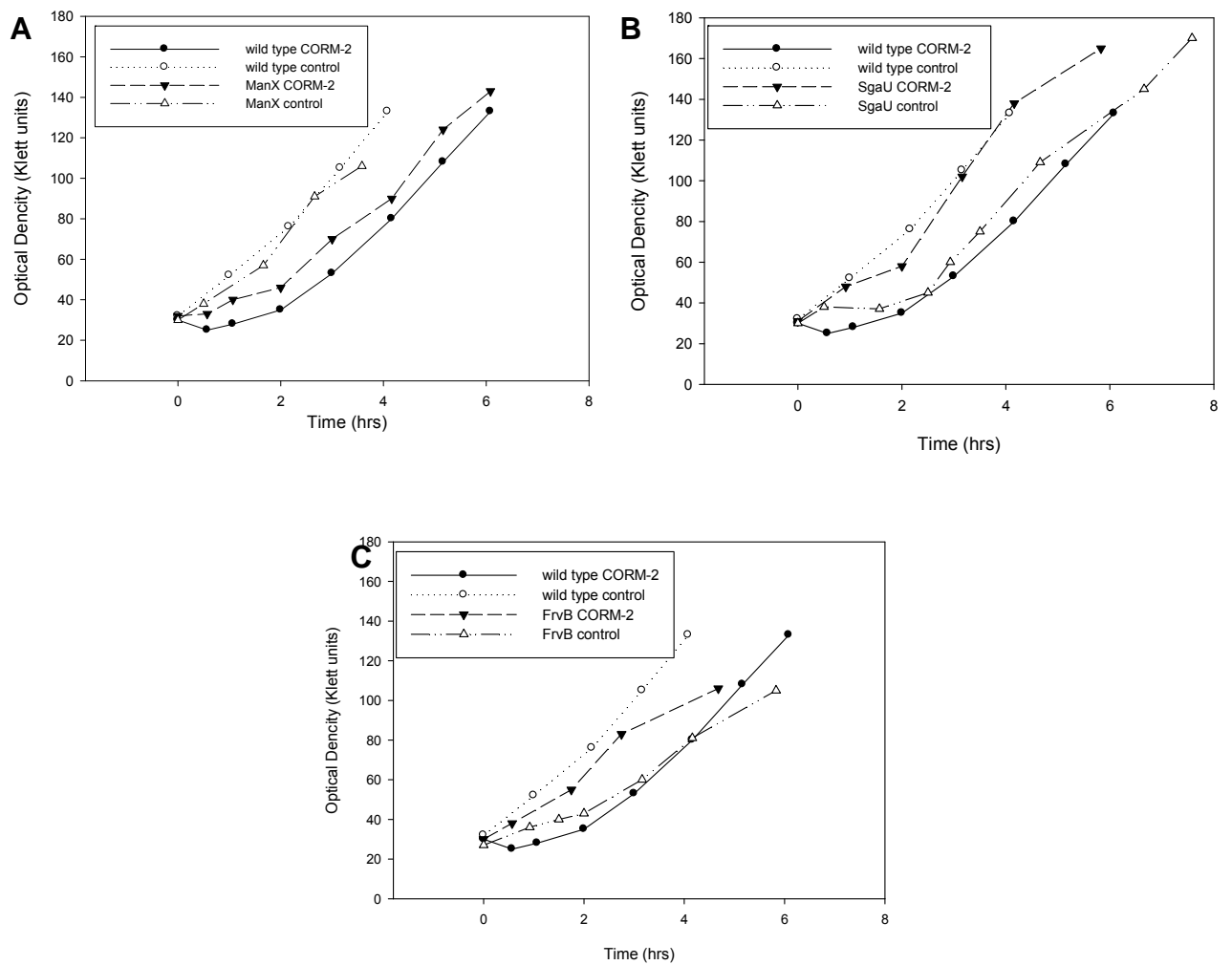


**Figure 6.8 CORM-2 growth assays with the putative CORM-2 resistant mutants in an MG1655 background.** CORM-2 (4  $\mu$ M) was added at early exponential phase to cultures of *E. coli*: **(A)** *manX*, **(B)** *sgaU* and **(C)** *manX*. Nothing was added to the controls. The growth of the wild type MG1655 strain with and without CORM-2 is shown in each case for comparison.

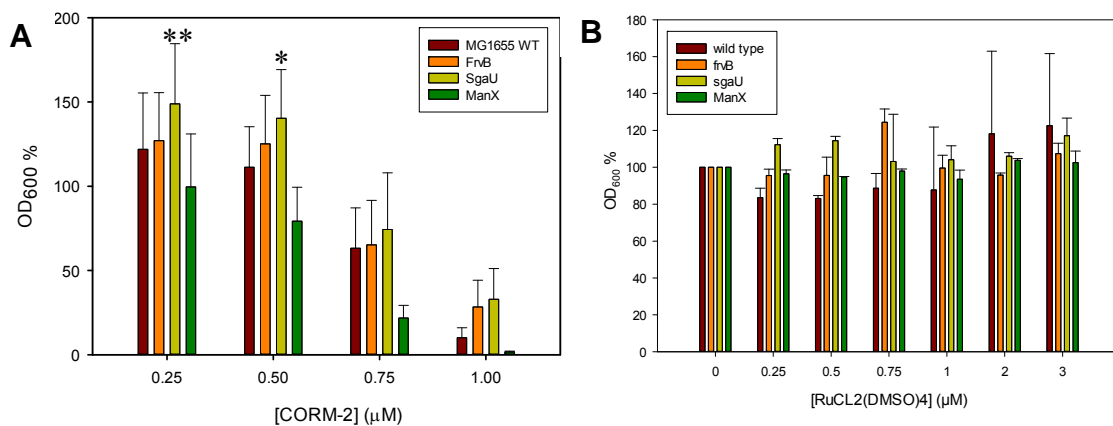


**Figure 6.9 CORM-2 susceptibility assay with the putative CORM-2 resistant mutants in an MG1655 background.** At the point of inoculation, various concentrations of (A) CORM-2 (0.25 - 1 μM) or (B) RuCl<sub>2</sub>(DMSO)<sub>4</sub> (0 - 3 μM) were added to cultures of the wild type MG1655 (brown) and the 3 mutants of interest: *frvB* (orange), *sgaU* (yellow) and *manX* (green). OD<sub>600</sub> was measured spectrophotometrically and the percentage growth for each strain in the presence of each concentration of compound, compared to the growth in the absence of compound was calculated. Data for CORM-2 are averages and standard errors of 6 biological replicates, and for RuCl<sub>2</sub>(DMSO)<sub>4</sub> are the averages and standard deviations of 2 biological replicates. Asterisks indicate significantly higher percentage growth of the mutant strain compared to wild type in the presence of CORM-2 as measured using Student's *t* test (\*, *P* < 0.1; \*\*, *P* < 0.05). It is however acknowledged that it is not ideal to perform statistical analysis on percentage data.

### **6.2.5 The effects of sub-inhibitory concentrations of CO-RM on bacterial growth**

Interestingly, very low concentrations of CORM-2 caused an increase in growth in the wild type MG1655 strain, as well as the mutant strains (Figure 6.9). It was ruled out that this was caused by the addition of the vehicle DMSO, as addition of a volume of DMSO equivalent to the largest volume of CORM-2 added in the previous experiment did not result in any change in optical density compared to growth of the strains with no additions (data not shown). Consequently, the effects of very low concentrations of both CORM-3 (a ruthenium containing CO-RM) and CORM-401 (a manganese-based CO-RM) was then investigated with two aims: 1) to assess whether the mutant strains exhibited resistance to CO-RMs other than CORM-2, and 2) to investigate whether sub-inhibitory concentrations of these CO-RMs also caused a stimulation of growth as seen with CORM-2.

None of the mutant strains exhibited resistance to CORM-3 (Figure 6.10A) or CORM-401 (Figure 6.10B), which suggests that any resistance these strains have to CORM-2 is specific to this compound, and not to wider features of CO-RMs in general or to CO. It is notable however that all strains, including wild type, also exhibited increased growth in the presence of low concentrations of CORM-3 and CORM-401. Wild type cultures grew approximately 80% more than untreated cultures when treated with 0.5  $\mu\text{M}$  CORM-3, and approximately 50% more when treated with 1  $\mu\text{M}$  CORM-3, and yet treatment with 2  $\mu\text{M}$  CORM-3 almost completely prevented growth of this strain (Figure 6.10A, brown bars). Similarly, sub-inhibitory concentrations of CORM-401 (< 50  $\mu\text{M}$ ) had a stimulatory effect on the growth of wild type cultures, with maximal stimulation (40% more than untreated cultures) occurring at 15  $\mu\text{M}$  CORM-401. The stimulation of growth by sub-inhibitory concentrations of both ruthenium- (CORM-2 and CORM-3) and manganese- (CORM-401) containing CO-RMs is an unexpected and interesting finding that requires further investigation.

### **6.2.6 Uptake of CORM-2 by *sgaU* and *frvB* mutants**

It was hypothesised that the *sgaU* and *frvB* mutants may be partially resistant to CORM-2 because of reduced uptake of this compound into the bacterial cell caused by a defect in the PTS system, encoded by the *sga* and *frv* operons, which usually import L-ascorbate and fructose, respectively. Therefore ruthenium uptake in *sgaU* and *frvB*

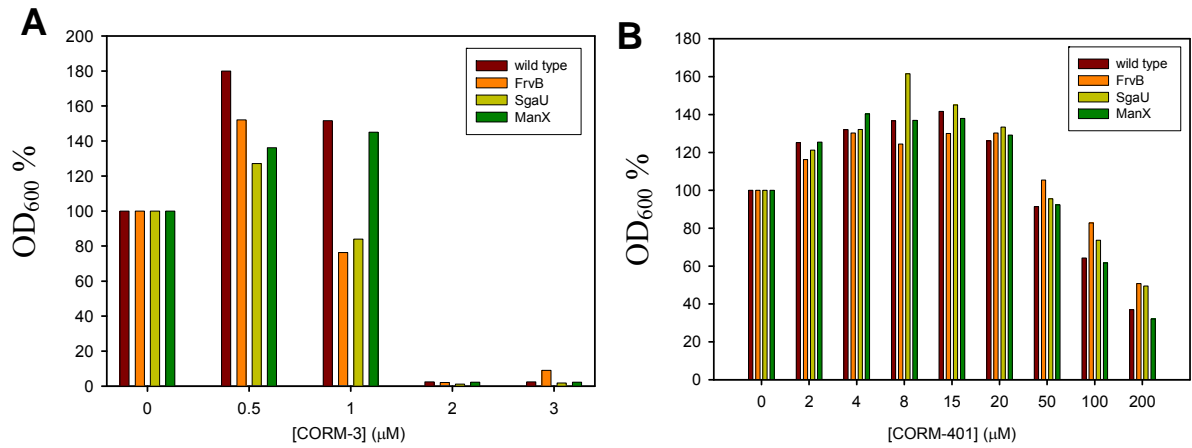


**Figure 6.10 CORM-3 and CORM-401 susceptibility assay with the putative CORM-2 resistant mutants in an MG1655 background.** At the point of inoculation, various concentrations of (A) CORM-3 (0 - 3  $\mu\text{M}$ ) or (B) CORM-401 (0 - 200  $\mu\text{M}$ ) were added to cultures of the wild type strain MG1655 and the 3 mutants of interest: *frvB* (orange), *sgaU* (yellow) and *manX* (green).  $\text{OD}_{600}$  was measured spectrophotometrically and the percentage growth for each strain in the presence of each concentration of CO-RM, compared to the growth in the absence of the CO-RM was calculated.

mutant cells treated with CORM-2 was measured over a time-course using ICP-MS analysis, as described previously (section 5.2.10), and compared to that in wild type MG1655 cells. The results of this investigation indicate that CORM-2 enters both *sgaU* cells (Figure 6.11A) and *frvB* cells (Figure 6.11B) at a similar initial rate as in wild type cells, but that ruthenium reaches a slightly lower equilibrium level within the mutant cells. This difference is significant in *frvB* cells at the 40 min time point ( $p = 0.055$ ) and in *sgaU* cells at the 40 min time point ( $p = 0.01$ ) and the 80 min time point ( $p = 0.06$ ).

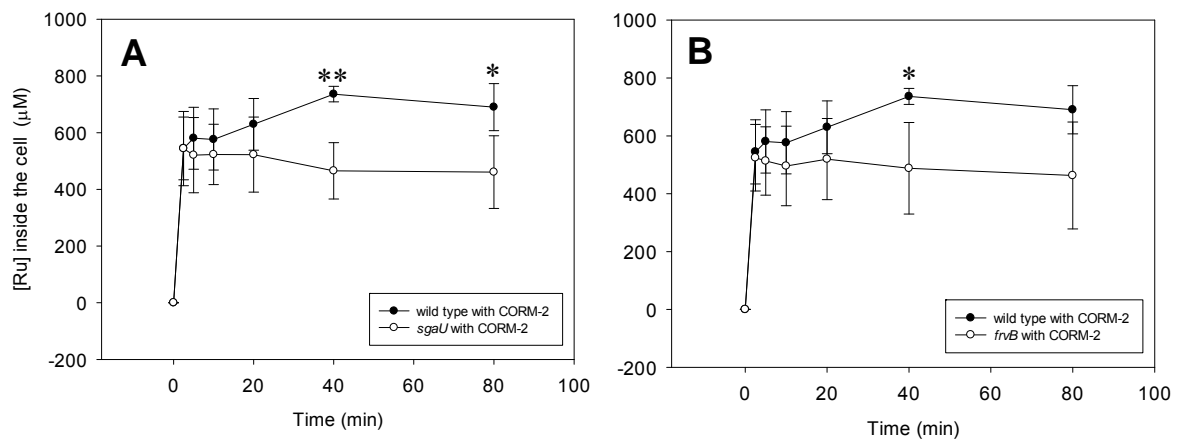
### 6.3 Discussion

There are still many unanswered questions surrounding the interaction of CO-RMs with bacteria and the nature of their bactericidal effects. It was therefore considered useful to generate and characterise CO-RM resistant strains of *E. coli* in the hope that this would reveal previously unappreciated targets of CO-RMs and facilitate a better understanding of the bacterial response to these compounds.

The approach taken was the generation of a large pool of random transposon mutants, followed by selecting for CORM-2 resistant mutants by the application of a concentration of CORM-2 that is toxic to the parental strain (40  $\mu$ M, Figure 6.1). Surviving mutants were screened further to confirm their CORM-2 resistant phenotype (Figure 6.2, 6.3, 6.4 and Table 6.2) and then the insertion sites of the transposon in the resistant mutants were identified by rescue cloning.

It is very interesting that all three of the CORM-2 resistant mutants identified in this work had mutations in genes encoding components of sugar-transporting PTS enzymes. This could indicate that CORM-2 enters *E. coli* cells via PTS transporters, as this would explain why mutations in genes that encode components of these transporters might be resistant to CORM-2. Currently, almost nothing is known about the transport of CO-RMs into bacterial cells, and therefore the comments made in this discussion are largely speculative. It is possible that CO-RMs enter bacterial cells by free diffusion through the membrane, perhaps down a concentration gradient, which provides the driving force; however, it seems plausible that CO-RMs enter bacterial cells using a transporter system, either by a passive or active mechanism. Some PTS transporters are able to



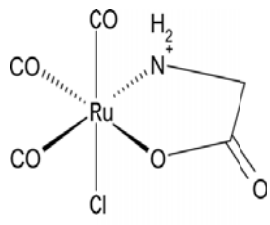
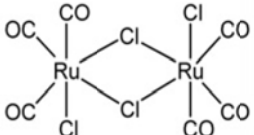
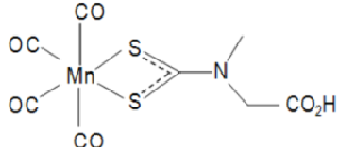


**Figure 6.11 The uptake of CORM-2 by wild type MG1655 *E. coli* and the *sgaU* and *frvB* mutants.** Cultures of MG1655 wild type and the *sgaU* mutant of *E. coli* in an MG1655 background (**A**, open circles) and *frvB* mutant (**B**, open circles) both in an MG1655 background were grown to mid-log phase ( $OD_{600} \sim 0.5$ ) prior to the removal of a 20 ml sample from each, both before and at regular intervals after the addition of CORM-2 (20  $\mu\text{M}$ ). Cell pellets were assayed for ruthenium content by inductively coupled plasma - mass spectrometry. Data are the means and standard deviations of 3 biological replicates. Asterisks indicate statistically significant differences in the ruthenium content of cultures of the mutant strains compared to wild type as measured using Student's *t* test (\*,  $P \leq 0.06$ ; \*\*,  $P = 0.01$ ).

transport only one specific sugar; for example, *N*-acetylglucosamine is the only sugar that can be transported by EII<sup>Nag</sup> from *E. coli*, which is encoded by *nagE*. Interestingly though, this transporter has been shown to transport the antibiotic streptozotocin into the cell (Lengeler, 1980). In contrast, the mannose PTS transporter, encoded by the *manXYZ* operon has a diverse substrate specificity, and is able to transport a variety of hexose sugars, including mannose, glucose, fructose and the amino sugars, glucosamine and *N*-acetylglucosamine. It is therefore feasible that CO-RMs could use sugar transporters to enter bacterial cells. CORM-2 has a molecular weight of 512, whereas that of CORM-3 is 310, both of which are larger than the molecular weights of ascorbate, mannose and fructose, which are 176 for the former and 180 for each of the latter. There are however some broad similarities in the structures of ascorbate and CORM-3, such as the pentose ring containing an oxygen atom and a double bond to oxygen from the adjacent carbon atom in the ring. Table 6.4 shows the chemical structures of CORM-2, CORM-3 and CORM-401, and the sugars ascorbate (transported by the product of the *sga* operon), fructose (transported by the product of the *frv* operon), and mannose (transported by the product of the *man* operon).

The ruthenium uptake measurements are consistent with the the *sgaU* and *frvB* mutants importing lower levels of CORM-2 into the cell. However, the observation that a large portion of the ruthenium applied as CORM-2 is still able to enter these mutants suggests that there are other mechanisms of entry of CORM-2 into the cell, perhaps by free diffusion, or by other transport proteins. This is consistent with these mutants only being partially resistant to growth inhibition by CORM-2. Moreover, preliminary data were collected, which suggested that the entry of CORM-3 into both of these mutant strains did not differ from that of wild type cells (data not shown), which combined with a lack of resistance of these mutants to CORM-3, suggests that this CO-RM enters the cell via different transporters.

Subsequent measurements of the growth of independently generated mutants of *sgaU*, *frvB* and *manX* in an MG1655 background, in the presence of CORM-2, revealed that only the *sgaU* mutant was statistically significantly resistant to this compound (Figure 6.9, yellow bars). The gene *sgaU* encodes the enzyme L-xylulose 5-phosphate 3-

CO-RM	Molecular weight	Sugar	Molecular weight
<p>CORM-3</p>  <p>[Ru(CO)<sub>3</sub>Cl(glycinate)]</p>	310.0	Ascorbate	176.12
<p>CORM-2</p> 	512.02	Mannose	180.16
<p>CORM-401</p> 	331.4	Fructose	180.16

**Table 6.4** The chemical structures and molecular weights of CORM-2 and CORM-3 and the sugars ascorbate, mannose and fructose, the PTS transporters of which, when mutated in *E. coli*, may result in resistance to CORM-2.

epimerase, which catalyses the isomerisation of L-xylulose 5-phosphate to L-ribulose 5-phosphate; a subsequent epimerase conversion, catalysed by another member of the operon, converts this to D-xylulose-5-phosphate, an intermediate of the pentose phosphate pathway (Yew and Gerlt, 2002). Members of the operon upstream of *sgaU* encode proteins responsible for the uptake and phosphorylation of L-ascorbate, via a phosphotransferase uptake system (Zhang *et al.*, 2003). Mutants with deletions in the *sga* operon are unable to ferment L-ascorbate (Yew and Gerlt, 2002). Structural similarities of the active site of SgaU to the active sites of other epimerases suggest a metal-dependent epimerization mechanism for this enzyme (Shi *et al.*, 2008).

The original transposon mutants exhibited a stronger CORM-2 resistance phenotype than the independently generated mutants. This is likely to be due to the different genetic backgrounds of the strains. The transposon mutants were BL21 derivatives with a series of genetic modifications, which rendered the strain highly competent and ideal for the overexpression of proteins. The genotype of this strain is given in Table 2.1. The *I<sup>q</sup>* express parent strain appears to be more sensitive to CORM-2 than MG1655 (data not shown). This is not ideal, and with hindsight, it seems that further attempts should have been made to generate MG1655 that were sufficiently competent to allow the transposon mutagenesis to be performed directly in this strain.

It is possible that the CORM-2 resistant phenotype of the original transposon mutants were caused partly, or completely, by downstream effects of the transposon insertion, this may be particularly true in the case of the transposon mutant designated 3A33 (later identified as *manX*) as the independently generated *manX* mutant did not appear to be resistant to CORM-2, and in fact, was significantly more sensitive to CORM-2 than the wild type strain. The *manX* gene is up-regulated 13.2-fold by organic solvents (Okochi *et al.*, 2007), which may explain the sensitivity of this strain to CORM-2 as this compound is delivered in the organic solvent DMSO. Alternatively, it is possible that the transposon insertion site in this mutant was incorrectly identified, as it only matched the *manX* gene by 91% over a 21 base pair sequence, although there were no better matches for the transposon insertion site in this mutant. Furthermore, the transposon mutant 3A33 exhibited the weakest CORM-2 resistant phenotype in the initial resistance screen with a change in OD<sub>600</sub> of 0.2 (assigned as the minimum change to

indicate significant growth) following the addition of CORM-2, and in the initial characterisation assays (Figure 6.3, orange line).

Although the characterisation of independently generated strains with mutations in the genes identified by transposon mutagenesis as conferring resistance to CORM-2 was an important control, if time had allowed, these strains would have ideally been complemented with the appropriate functional gene in order to confirm that this restored the wild type phenotype. This would provide unequivocal evidence that mutations in these genes were the cause of the CORM-2 resistance.

Analysis of the transcriptome of *E. coli* following exposure to sub-lethal concentrations of CO-RMs is an alternative approach to identify previously unappreciated effects of CO-RMs and to further our understanding of the global effects of these compounds on bacterial cells. Such studies have been carried out by this laboratory using CORM-3 (Davidge *et al.*, 2009b; McLean *et al.*, 2013) as mentioned previously (section 1.3.4) and the manganese based CO-RM, CORM-401 (Lauren Wareham, unpublished). Searches of these transcriptomic databases for the genes identified in the current work revealed that *sgaU* is down-regulated 1.62-fold in the presence of 40  $\mu$ M CORM-3 30 min after addition of the compound, and that this down-regulation is maintained at 80 min after addition (Samantha McLean, unpublished). This trend is seen with many genes in the *sga* operon, with the most significant change being the 2-fold down-regulation of *sgaB*. This supports the hypothesis that some CO-RMs may enter *E. coli* cells via this transporter. Interestingly, despite the lack of CORM-2 resistance in the independent *manX* mutant in the MG1655 background, the *manXYZ* operon was down-regulated by 2.78 - 3.22-fold 40 min after the addition of CORM-3. This mutant was not found to exhibit resistance to CORM-3 (Figure 6.10A, green bars). The expression of *frvB* was slightly up-regulated across the time-course by CORM-3.

In contrast, CO gas (bubbled at a rate of 50 ml min<sup>-1</sup>) caused a very slight up-regulation of the *sga* and *man* operons across the time-course. There was, however, an overall down-regulation of the *frv* operon, with *frvB* being down-regulated by approximately 2-fold at all time-points after 5 min following exposure to CO. The different effects of CO gas and CO-RMs on the transcriptome emphasise the very different effects of these

compounds on the bacterial cell. Their different effects on the genes of interest here suggest that it is not CO, but the CO-RM compound itself that causes the down-regulation of the *sga* and *manXYZ* operons, consistent with the free diffusion of CO through lipid bilayers, and so the absence of the need for a transporter for CO gas.

Treatment with the manganese based CO-RM, CORM-401 (66.7  $\mu$ M), caused a 2.5-fold up-regulation of *manX* after 40 min and a 3-fold up-regulation at 80 min. In contrast, *frvB* was down-regulated by 3-fold at 5 min and 2.7-fold at 10 min following the addition of this CO-RM; however, expression of *frvB* returned to basal levels by the 80 min time-point. The *sgaU* gene was slightly up-regulated, by approximately 1.8-fold at 2.5, 40 and 80 min, following CORM-401 addition (Lauren Wareham, unpublished). Again, the mutants of interest did not exhibit resistance to this CO-RM (Figure 6.10B), which was not unexpected, as these CO-RMs, particularly CORM-401, differ greatly in their size, structure and chemical properties; therefore it is likely that they enter the cell via different pathways.

While conclusions cannot be drawn from this data as it describes the transcriptomic responses of *E. coli* to CORM-3 and CORM-401, but not CORM-2, it is interesting to note that both the *sgaU* operon and the *manX* operon are slightly down-regulated in response to CORM-3. This could reflect a bacterial defence against the import of ruthenium based CO-RMs.

An alternative approach to this work would have been the screening of an established library of transposon mutants of *E. coli* (or indeed a pathogenic bacterial species) with CO-RMs. This would have the advantage of allowing mutants in every non-essential gene in an organism to be screened for CO-RM resistance, or indeed sensitivity, allowing a much more thorough and systematic investigation of the response of mutants to CO-RMs.

An interesting and unexpected finding of this work was that very low concentrations of CORM-2 (Figure 6.9), CORM-3 (Figure 6.10A) and CORM-401 (Figure 6.10B) added at the point of inoculation cause increased growth of wild type MG1655 *E. coli* and the mutant strains. The growth of these strains with low levels of the CO-RMs was not

followed over time and so conclusions about the effect of these compounds on the rate of growth cannot be made, but it is clear that the final culture density is significantly greater in the presence of sub-inhibitory concentrations of CO-RM (wild type cultures grew approximately 80% more than untreated cultures when treated with 0.5  $\mu\text{M}$  CORM-3 and 40% more when treated with 15  $\mu\text{M}$  CORM-401). This could suggest that a factor, such as exhaustion of the carbon source glycerol, is preventing growth in the absence of CORM, but is not limiting in the presence of CO-RM. Initially, it was considered that DMSO could be acting as a substrate for *E. coli* treated with CORM-2 (for which DMSO is the vehicle), however this was considered unlikely due to the very small amount of DMSO added, and indeed a control in which an equivalent volume of DMSO was added to the *E. coli* cultures was not found to stimulate or inhibit growth (data not shown). If time had allowed, an important control would be to investigate the effects of very low amounts of CO gas on bacterial growth. An interesting hypothesis for why some bacteria may grow better in the presence of CO or CO-RMs is that the up-regulation of HO by CO activates a variety of cytoprotective pathways within the cell (Motterlini and Otterbein, 2010). However, this is not the cause of the increase in growth in this case as *E. coli* K12 does not contain a HO enzyme.

There is currently no literature on the effects of very low levels of CO or CO-RMs on bacterial growth; however, there is much on the effects of these compounds on mammalian cells as outlined in the introduction to this thesis (sections 1.1.3.5 and 1.2.8). For example, CO has been shown to prevent excessive production of ROS in mitochondria by uncoupling electron transport from ATP production (Lo Iacono *et al.*, 2011), while brief exposure of astrocytes to CO has been shown to improve respiration (Almeida *et al.*, 2012). Furthermore, the concentration of CO has been shown to be critical in determining the response. Low concentrations of CORM-3 (0.5 and 1  $\mu\text{M}$ ) caused an increase in the respiratory control ratio and mitochondrial transmembrane potential in isolated heart mitochondria, while higher concentrations (5 and 10  $\mu\text{M}$ ) caused a decrease in these values (Lancel *et al.*, 2009).

Treatment of intact *E. coli* with CORM-3 has been shown to result in a transient stimulation of respiration prior to respiratory inhibition (Wilson *et al.*, 2013). It was concluded that this stimulation was the result of transport of  $\text{K}^+$  and  $\text{Na}^+$  ions across the

bacterial membrane. It is possible that an increased rate of respiration in the presence of low concentrations of CO-RMs causes the improved growth observed in the current work.

An alternative possibility is that exposure to low levels of CO-RMs (and perhaps other non-specific stressors) activates cellular machinery that is able to counteract stress rendering the cell better equipped to deal with stress, and indeed better able to grow, in the absence of stress. This hypothesis emphasises the multifaceted effects of CO-RMs. It is likely that some cellular processes are benefited by interaction with CO and the CO-RM molecules, while others are inhibited; however at high concentrations of CO-RM, the beneficial effects are masked by the inhibitory effects.



## Chapter 7

### General Discussion

#### 7.1 Summary

The work presented in this thesis has developed knowledge of the antibacterial properties of a range of CO-RM compounds, but in particular the ruthenium-containing compounds CORM-2 and CORM-3, in comparison with CO gas. Several similarities between these CO-RMs and CO gas were demonstrated; for example, cytochrome *bd-I* was found to be the most resistant oxidase of *E. coli* to CORM-3, as is true for CO gas. It is hypothesised that in both cases, this resistance is caused by the fast dissociation rate of CO from this oxidase (Borisov, 2008). Furthermore, inhibition of *E. coli* respiration by CORM-3, as with CO gas, is shown here to be photosensitive, suggesting that CO from CORM-3 binds to ferrous haems in a classical, light-sensitive manner. However, CORM-3 does not merely act as a CO donor. Unlike CO gas, CORM-3 was not preferentially inhibitory to bacterial respiration when added at low oxygen tensions, a difference hypothesised to be caused by an accumulation of CO in the micro-domains of the target sites inside bacterial cells. This intracellular accumulation of CORM-2 and CORM-3 is demonstrated here using ICP-MS (Chapters 5 and 6) and is thought to explain in part the increased potency of these compounds as antimicrobial agents in comparison with CO gas.

One of the most significant findings of this work was the demonstration that the thiol compound NAC dramatically reduces the uptake of both CORM-2 and CORM-3 into *E. coli* cells. This is important due to the many previously unexplained reports in the literature that thiol compounds are able to abrogate many of the effects of CO-RMs, particularly those containing ruthenium (Desmard *et al.*, 2012), in both prokaryotic (Desmard *et al.*, 2009; Murray *et al.*, 2012) and eukaryotic systems (Sawle *et al.*, 2005; Taille *et al.*, 2005). Other researchers in the field have proposed that thiol compounds protect against the deleterious effects of CO-RMs by virtue of their antioxidant properties (Tavares *et al.*, 2011); however, data are presented herein that suggest that

CORM-3, at the concentrations routinely used in biological experiments, does not produce significant amounts of ROS, in agreement with the work of others (Desmard *et al.*, 2009; Desmard *et al.*, 2012), and that other antioxidants, which do not contain thiol groups, are unable to confer the same protection (Figure 5.11). It should now be explored whether thiol-containing compounds also reduce the uptake of CO-RMs in eukaryotic systems as this could have implications for the therapeutic applications of CO-RMs.

### **7.1.1 The effects of CO-RMs on bacterial respiration**

The work described here provides the first evidence that CO from CORM-3 binds to all three terminal oxidases of *E. coli*. The data confirm that application of CORM-3 to suspensions of *E. coli* membrane particles leads to immediate inhibition of respiration. It was shown, for the first time, that membranes containing cytochrome *bd-I* as the only terminal oxidase are more resistant to this inhibition than membranes containing the other oxidase types, and that this oxidase can confer resistance to growth inhibition by CORM-3, as discussed in Chapter 3. This thesis also contains the first report of inhibition of a non-haem containing oxidase by CO-RMs, as discussed below.

This thesis aimed to further the understanding of the extent to which inhibition of respiration is the cause of the bactericidal nature of the CO-RMs. It is clear that CO from CORM-2 and CORM-3 (Figures 3.1 and 3.6) binds to and inhibits terminal oxidases and that at high concentrations, this inhibition could be sufficient to kill the bacteria. It is shown here (Figure 3.10) that the viability of *E. coli* treated with 30  $\mu$ M CORM-3 was reduced by 95% within 1 h, but that killing was reduced to 70% when a bright light was shone on to the culture vessel, causing the photolysis of haem-CO bonds. This provides the first conclusive evidence that the binding of CO from CORM-3 to haem proteins contributes to killing by these compounds. However, these data do not allow a distinction between the relief of CO inhibition of respiration and the lysis of haem-CO bonds in other haemoproteins within the bacterial cell. Therefore it is not possible to determine based on these results whether the reduction in killing in the light was caused by alleviation of the inhibition of respiration, or the lysis of haem-CO bonds in other haemoproteins. Furthermore, the substantial killing effect (70%) in the presence

of CORM-3 and light could imply that there are other causes of killing by CORM-3, as discussed below.

A difficulty associated with the use of *E. coli* as a model organism in these studies is that it has flexible respiratory pathways, and so is able to rapidly adapt to a range of environmental conditions. Indeed, transcriptomic analyses by this laboratory have shown altered expression of the individual terminal oxidases of this organism in response to CORM-3 (Davidge *et al.*, 2009b; McLean *et al.*, 2013) and CORM-401 (Lauren Wareham, unpublished). This gives rise to the possibility that following treatment with CO-RM, particularly at lower concentrations that do not kill all bacteria within a short time, *E. coli* may either synthesise more terminal oxidases, or switch to an alternative form of energy generation, such as fermentation, and therefore continue to grow after a lag phase. It would therefore be interesting to study the effects of CO-RMs on *E. coli* grown on a non-fermentable substrate such as succinate to investigate whether this prevented such recovery. Preliminary data suggests that this is the case (Samantha McLean, unpublished). This transient inhibition was not observed in the current work with CORM-2 and CORM-3, which appear to be two of the most potent antibacterial CO-RMs, possibly due to their ruthenium centre, as will be discussed further below. However, CORM-401 (Lauren Wareham, unpublished) and the photoCO-RM  $\text{Mn}(\text{CO})_3(\text{tpa-}\kappa^3\text{N})\text{Br}$  (Christoph Nagel and Samantha McLean, unpublished) are much less detrimental to the growth of *E. coli* than ruthenium-based CO-RMs, which suggests that inhibition of respiration limits growth only transiently until the bacteria can switch to an alternative method of energy production. If inhibition of respiration by CO-RMs were the main cause of killing by these compounds, then it would be expected that all CO-RMs would have similar levels of toxicity, or rather that CO-RMs that release more CO per molecule, or had faster rates of CO-release, would be more toxic. However, this does not seem to be the case; CORM-401 is much less toxic to *E. coli* than CO-RMs 2 and 3, despite releasing approximately three times more CO per mole than these compounds. The notion that inhibition of aerobic respiration is not wholly responsible for killing by CO-RMs is also consistent with reports of the growth inhibition of anaerobically grown *E. coli* by both CORM-2 (Nobre *et al.*, 2007) and CORM-3 (Davidge *et al.*, 2009b).

It seems therefore that ruthenium containing CO-RMs cause killing by other mechanisms, in addition to the inhibition of respiration. In order for these mechanisms to be elucidated, a thorough understanding of the chemistry of the intact CO-RM and of the breakdown products following CO release is required. Initially, the potential effects of these CO-RM backbones were not fully appreciated, because control experiments using 'inactive' compounds devoid of CO did not elicit the same effects as the active CO-RMs in a range of growth, viability and respiratory experiments. The need for robust control compounds is discussed further below.

The recent paper by Desmard *et al.* (2012) provides the most thorough comparative report to date of the bactericidal effects of a range of CO-RMs. They show that CO-RMs with different chemical properties differentially influence bacterial growth and O<sub>2</sub> consumption and that the kinetics of CO release from CO-RMs does not determine their antibacterial effects. They conclude that the inhibition of oxygen consumption by CO released from CO-RMs is not the only factor influencing their bactericidal effect, and that the nature of the transition metal is important in determining the antibacterial activity exerted by CO-RMs.

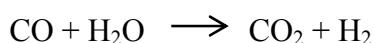
### **7.1.2 The redox properties of CO-RMs**

Following the realisation that the inhibition of respiration is not the sole cause of the bactericidal effects of CO-RMs, the hypothesis that the production of reactive oxygen species by these compounds leads to their toxic effects, as proposed by Tavares *et al.* (2011), was explored.

This work demonstrates that while CORM-2 does produce small amounts of ROS, probably hydroxyl radicals as reported by Tavares *et al.* (2011) (Figure 5.14), low concentrations of CORM-3 that are effective in decreasing oxygen consumption, growth and viability in bacterial systems, do not produce significant amounts of ROS *in vitro* (Figure 5.10 and 5.15) or *in vivo*, as demonstrated by an assay for hydrogen peroxide production (data not shown). The production of ROS by CORM-2 may explain why this compound is a more potent bactericidal agent than CORM-3 despite having similar CO-release profiles. In this work, the ability of thiol compounds to abrogate the effects of CO-RMs was shown to be unrelated to the antioxidant properties of these compounds,

but rather is likely to be caused by a dramatic reduction in CO-RM uptake into the bacterial cell in the presence of certain thiol compounds such as NAC (Figure 5.16).

This work raises questions about the redox properties of CO-RMs. This is an area that is currently not well understood. Some transition metal carbonyls e.g. Na[Mo(CO)<sub>3</sub>(histidinate)] and Na<sub>3</sub>[Mo(CO)<sub>3</sub>(citrate)] can cause hydroxyl radical formation (Seixas, 2010). In addition, the CO-RM ALF062 is also hypothesised to produce hydroxyl radicals by reaction of the electron-dense molybdenum with H<sub>2</sub>O and O<sub>2</sub> (Tavares *et al.*, 2011) and CORM-2 is hypothesised to produce these radicals via the water gas shift reaction (see below) involving the reduction of oxygen by ruthenium species.



CORM-3 is thought to take part in the first stage of the water gas shift reaction. Under acidic conditions (CORM-3 has a pH of around 3 in solution), CORM-3 becomes [Ru(CO)<sub>2</sub>(CO<sub>2</sub>H)Cl(glycinate)], which could then lose a proton to form [Ru(CO)<sub>2</sub>(CO<sub>2</sub>)Cl(glycinate)]<sup>2-</sup> between pH 6 and 7. The two electrons could then be used to reduce a substrate leading to the release of CO<sub>2</sub> (Brian Mann, personal communication). The ability of CORM-2 and CORM-3 to reduce a variety of tetrazolium dyes has been demonstrated recently in this laboratory (Salar Ali, unpublished). However in contrast, the Hb spectra shown in the current work (Figure 5.5) appear to show oxidation of this haemoprotein upon addition of CORM-3. This emphasises the complex redox properties of these compounds, which are likely to vary under different environmental conditions. It will be important for the future use of CO-RMs as research tools and potential pharmacological agents that the redox properties of these compounds are understood. Cyclic voltammetry could provide a possible means by which to investigate these properties.

### 7.1.3 Other potential mechanisms of killing by CO-RMs

The results described above suggest that neither inhibition of respiration by CO released from CORM-3, nor reactive oxygen species, are fully responsible for the bactericidal properties of this compound. As indicated previously (in this discussion and by

Desmard *et al.* (2012)), it seems that the chemistry of the ruthenium center must be considered as a possible contributing factor of killing by CORM-2 and CORM-3.

Non-carbonylated ruthenium(II) compounds have been reported to possess potent antibacterial properties against the pathogens *P. aeruginosa*, *E. coli*, *Proteus vulgaris* and *Proteus mirabilis* (Anthonysamy *et al.*, 2008). Ruthenium compounds at micromolar concentrations have also been shown to inhibit ATPase activity in *E. coli* (Scott *et al.*, 1980). In contrast, Desmard *et al.* (2009) demonstrated that bacterial growth was not affected by ruthenium chloride (1 - 10  $\mu$ M), however, it has not been demonstrated that this compound is able to enter bacterial cells.

The transcriptomic response of *E. coli* to CORM-3 indicates that there is a global cellular response to CORM-3, and probabilistic modelling of these data implicates several transcription factors in this response, although the mechanism by which CORM-3 affects these transcription factors, with the exception of ArcA / FNR (as described in section 1.3.4) is not understood (Davidge *et al.*, 2009b).

The transcriptomic data suggest that the metabolism and transport of several metals including iron is greatly disrupted by CORM-3 (Davidge *et al.*, 2009b, McLean *et al.*, 2013) and this is supported by measurements of the intracellular concentration of these metals. Genes involved in sulfur metabolism, such as *tauABC*, *ssuAD*, *cysWA* and *sbp*, and in methionine metabolism, including *metNI* and *metBLF* are up-regulated by CORM-2 (Nobre, 2009) and CORM-3 (McLean *et al.*, 2013) and so this reveals another route by which CO-RMs disrupt normal cellular homeostasis.

An investigation into the effects of CORM-3 on a *hemA* mutant of *E. coli* that is unable to synthesise haem (Wilson, 2012) revealed that this mutant was more sensitive than wild type to the bactericidal effects of CORM-3, which emphasises the importance of non-haem targets in killing by this compound. It may also suggest that haem groups in wild type *E. coli* may act as CO sinks, protecting other cellular components from damage by CO. The work revealed that CORM-3 differentially alters the transcription of genes involved in iron homeostasis and in Fe-S cluster assembly and repair in the *hemA* mutant compared to wild type, which implicates these as targets of CORM-3.

The finding presented in the current work that the non-haem oxidase AOX from *V. fischeri* is hypersensitive to inhibition by CO-RMs also provides further evidence that either CO or the CO-RM centre, are able to interact with and inhibit non-haem targets. The insensitivity of this oxidase to CO gas suggests that it is some other feature of these compounds that are interacting with and inhibiting the activity of this oxidase. A report by Santos-Silva *et al.* (2011) used X-ray crystallography to demonstrate that CORM-3 is able to bind to hen egg white lysozyme by interacting with histidine and aspartate. There is also a report of CORM-2, but not CO gas or iCORM-2, activating ATP-gated, human P2X4 receptors by acting as an antagonist (Wilkinson and Kemp, 2011). These results emphasise the importance of considering non-haem targets for CO-RMs and the potential effects of interactions between the backbone of CO-RMs with proteins.

#### **7.1.4 The entry of CO-RMs into bacterial cells**

Several papers have reported the uptake of the metal center of CO-RMs into cells (Desmard *et al.*, 2009; Jesse *et al.*, 2013; McLean *et al.*, 2013; Meister *et al.*, 2010; Nobre *et al.*, 2007), and there is spectroscopic evidence that CO from these compounds also enters bacterial cells (Lauren Wareham, unpublished), but currently, little is known about the mechanisms by which CO-RMs enter bacterial (or indeed mammalian) cells.

It is possible that CO-RMs enter bacterial cells by passive diffusion, but it seems more likely given their size, that transporters are involved in their uptake. The present work has identified sugar transporting phosphotransferase systems as a possible means of CO-RM entry into the bacterial cell because of a partial CORM-2-resistant phenotype of *E. coli* with deletions in the *frvB* gene (encoding a component of the PTS fructose transporter) and *sgaU* (a component of a xylulose PTS transporter, see Chapter 6). This hypothesis is strengthened by data showing reduced entry of CORM-2 into each of these mutant strains (Figure 6.11). It now needs to be considered whether it is structurally and chemically possible for these transporters to enable CORM-2 entry into the bacterial cell, and other means of CO-RM entry should also be sought.

The work presented in this thesis also adds to the current understanding of the bacterial uptake of CORM-2 and CORM-3 by demonstrating that the thiol compound NAC dramatically reduces the uptake of these compounds. It is hypothesised that this is due

to the thiol compound altering the structure of the CO-RM, thereby rendering it unsuitable for transport by the usual mechanisms.

In the future, it will be important to investigate the interactions of CO-RMs with transporters that accumulate CO-RMs against a concentration gradient. It would also be interesting to investigate whether CO-RMs enter bacterial cells by active or passive transport. This could be done by measuring the rate of transport (assayed as intracellular ruthenium by ICP-MS) in the presence of different concentrations of CO-RM. Furthermore, ATPase mutants and uncouplers could be used in order to investigate the involvement of the proton motive force in CO-RM transport. The involvement of the multidrug efflux pump, implicated by transcriptomics (Davidge *et al.*, 2009b; McLean *et al.*, 2013), could be studied by investigating the rate of entry and exit of CO-RMs and the sensitivity of an *mdt* mutant to these compounds. The Mdt protein could be purified and CO-RM binding to this protein assayed by fluorimetry, CD, NMR, scintillation-proximity or other methods. It is known that some CO-RMs are more toxic to bacterial cells than to eukaryotic cells (Desmard *et al.*, 2009) and it would be interesting to investigate whether this is because bacteria can import CO-RMs more effectively than eukaryotic cells.

## **7.2 Future directions and outstanding questions**

CO-RMs have shown great promise since their advent in the early 2000s as potential drugs in a wide range of human diseases and as antimicrobial agents, and this has led to the development of a wide range of new CO-RMs. With regards to understanding the antimicrobial properties of CO-RMs, it is important that each of these compounds is characterised and systematically assessed for its antimicrobial properties under standard conditions. Such data should allow clear patterns to emerge, which should further the current understanding of why CO-RMs are bactericidal. For example, it will be important to know which CO-RMs produce ROS and whether this contributes to the biological effects of these compounds.

Throughout this work, it has become increasingly apparent that the compounds used currently as controls are far from ideal and, in many cases, do not accurately mimic the chemical properties of the intracellular breakdown products of CO-RMs. This is a major



limitation in the study of CO-RMs and in many cases prevents clear conclusions being drawn as to whether the effects seen are caused by CO from the CO-RM, or are caused by undesired, and in many cases, poorly understood, side reactions involving the CO-RM metal centre devoid of CO. These limitations are not confined to the present work, and in many published works no control compounds are used, or the appropriate solvent is added in place of a control (Desmard *et al.*, 2007; Desmard *et al.*, 2009; Nobre *et al.*, 2007).

Within the current work, three different control compounds have been used.  $\text{RuCl}_2(\text{DMSO})_4$  is used as a control for CORM-2 as both compounds contain chloride ligated to a central ruthenium and the compounds are broadly structurally similar, but with the carbonyl groups of the CO-RM replaced with DMSO in the control; however, the chemistry of the two compounds in solution is not identical. This compound has been used in published work as a control for CORM-3 (Davidge *et al.*, 2009b).

Another control compound used in this work and in published work (Clark *et al.*, 2003; Santos-Silva *et al.*, 2011) is iCORM-3. iCO-RM is a term used to indicate an inactive form of the compound, produced by prolonged incubation of the CO-RM in solvent or buffer to allow all labile CO to be released. However, our recent increased understanding of the mechanisms and triggers of CO release from ruthenium based CO-RMs (ie. the need for a compound, such as dithionite, to be present (McLean *et al.*, 2013)), suggests that many iCO-RMs, particularly iCORM-3 may not have lost CO, but rather have formed a stable tricarbonyl structure (McLean *et al.*, 2013) in which components of the buffer prevent CO loss from the compound, even when it is later exposed to dithionite in the myoglobin assay. A recent paper has provided the most detailed analysis to date of the global effects of iCORM-3 on the transcriptome of *E. coli*, and showed that, while this control compound caused a much smaller impact on gene expression than CORM-3, it still had some effects distinct from those of the active compound (McLean *et al.*, 2013). For example, the transcription factor ArcA, which represses respiratory metabolism, was much less affected by iCORM-3 than CORM-3, whereas IscR, which is involved in the regulation of iron-sulfur cluster assembly, was affected similarly by CORM-3 and iCORM-3, suggesting that damage to iron-sulfur clusters could be a consequence of exposure to the ruthenium centre of CORM-3. This

work also revealed that ruthenium from iCORM-3 accumulates in cells approximately 10-fold less than from CORM-3, which may explain why this compound has a smaller impact on bacterial cells (and perhaps mammalian cells, although this has not been demonstrated). An alternative explanation for the effects observed in cultures treated with iCORM-3 is that the causative agent is a small amount of CO that is released from this compound (iCORM-3 preparations typically release up to 5% of the CO compared to CORM-3). Despite the progress made in understanding the effects of this control compound, it is clear that our comprehension of its chemistry is far from complete, and so its use as a control poses more questions than it answers.

The third control compound used in this work is termed miCORM-3 (myoglobin-inactivated CORM-3 (Wilson *et al.*, 2013)). In many ways this is the best control compound as it has been exposed to biological molecules (myoglobin); however, although precautions were taken to use the minimum quantity of dithionite require to reduce the myoglobin used in the preparation of this control compound, it is possible that some remains in the final preparation, which is obviously not ideal. A possible solution to this would be to bubble the miCORM-3 solution with air prior to use in order to oxidise any residual dithionite, although this would still leave some residual species from the breakdown of dithionite in the solution.

Attempts to use myoglobin to inactivate other CO-RM compounds, such as CORM-401, have been unsuccessful and, the best control available for this compound has been the suspected breakdown products of this CO-RM ( $\text{MnSO}_4$  and dithiocarbamate), however work is currently underway to use haemoglobin to biologically remove the CO from this CO-RM (Lauren Wareham, unpublished).

Those working on the rational design of new CO-RMs are beginning to show awareness of the importance of the availability of well-characterised control compounds; for example new photoCO-RMs are in development that carry additional ligands for each labile CO. These are then able to replace CO group(s) following their release (Nagel and Schatzschneider, unpublished). This results in stable and well characterised breakdown products following intracellular CO release and such compounds can be synthesised separately and used as accurate control compounds.

As mentioned several times throughout this thesis, the discovery in 2012 that dithionite promotes CO release from CORM-2 and CORM-3 necessitates that several pieces of CO-RM dogma be reconsidered (McLean *et al.*, 2013). A systematic assessment of the kinetics of CO entry into cells in the absence of dithionite has begun using the truncated globin Ctb from *C. jejuni* as a reporter when overexpressed in *E. coli* (Mariana Tinajero Trejo and Lauren Wareham, unpublished). This will provide important information as to the rate and amount of CO that is able to enter cells under native biological conditions from a range of CO-RMs.

Furthering our understanding of CO-release kinetics and of the interactions of CO-RMs with bacterial cells could provide important information about the effects of these compounds on mammalian cells where they are hoped to have great potential as therapeutic agents. For example, the finding that the thiol compound NAC prevents the entry of ruthenium-containing CO-RMs into bacterial cells may have implications for mammalian CO-RM research, where the abrogation of the effects of CO-RMs by thiol compounds is also seen (Sawle *et al.*, 2005; Taille *et al.*, 2005).

It will be important for the future use of CO-RMs as a treatment for bacterial infections to consider the effects of CO-RMs on bacteria within a host. Preliminary studies have already been done to investigate the effects of CORM-3 on the uptake and killing of *Neisseria meningitidis* in macrophages (Wilson, 2012). These studies found that CORM-3 had no significant effect on the ability of macrophages to phagocytose *N. meningitidis*, or to kill bacteria that had already been internalised. In contrast, the ability of macrophages to phagocytose *P. aeruginosa* is improved by CORM-3 (Desmard *et al.*, 2009), and the CO-RM ALF-186 is able to promote clearance of *S. typhimurium* in mice by promoting the bactericidal activities of macrophages (Onyiah *et al.*, 2013). These results are interesting, because, as an anti-inflammatory agent, it could be expected that CO-RMs would suppress the immune response to infection (Chin and Otterbein, 2009).

### **7.3 Conclusions**

This thesis reports an investigation into the mechanisms by which CO-RMs affect the respiration and growth of bacteria. While several key findings have advanced our

understanding of these processes, there is still much work to be done in order for the mechanisms of the antibacterial activity of CO-RMs to be fully understood.

When the antibacterial properties of CO-RMs first became apparent, they were considered to have great promise in the treatment of antibiotic-resistant infections, which pose a looming global crisis. However, it is becoming apparent that CO-RMs differ in their bactericidal properties; CORM-2 and CORM-3 have potent antimicrobial effects, while other CO-RMs may only transiently inhibit growth.

One potential use of CO-RMs in the fight against antimicrobial infections is as an adjunctive or adjuvant treatment (Pena *et al.*, 2012). Research is underway to investigate whether CO-RMs could be used in combination with established antibiotics in order to reduce the dose of antibiotic needed, or perhaps even potentiate the effects of antibiotics (Salar Ali and Robert Poole, unpublished).

It seems unlikely that CORM-2 and CORM-3 would ever be suitable therapeutic agents to treat bacterial infections, due to the limitations of using a non-biological metal in such treatments. It will therefore be important to develop new CO-RMs which are potent antibacterial agents, and yet are not toxic to mammalian cells. This may be achieved through the use of biologically innocuous metals in place of ruthenium, or by modifications that allow the more precise targeting of these CO-RMs to prokaryotic cells. A thorough understanding of the mechanisms of action of each new CO-RM will be required in order to allow the rational design of therapeutically viable CO-RMs.

## References

- Akamatsu, Y., Haga, M., Tyagi, S., Yamashita, K., Graca-Souza, A. V., Ollinger, R., Czismadia, E., May, G. A., Ifedigbo, E., Otterbein, L. E., Bach, F. H. and Soares, M. P. (2004). Heme oxygenase-1-derived carbon monoxide protects hearts from transplant associated ischemia reperfusion injury. *FASEB J.* **18**, 771-2.
- Akhter, S., McDade, H. C., Gorlach, J. M., Heinrich, G., Cox, G. M. and Perfect, J. R. (2003). Role of alternative oxidase gene in pathogenesis of *Cryptococcus neoformans*. *Infect. Immun.* **71**, 5794-802.
- Alberto, R. and Motterlini, R. (2007). Chemistry and biological activities of CO-releasing molecules (CO-RMs) and transition metal complexes. *Dalton Trans.*, 1651-60.
- Almeida, A. S., Queiroga, C. S. F., Sousa, M. F. Q., Alves, P. M. and Vieira, H. L. A. (2012). Carbon monoxide modulates apoptosis by reinforcing oxidative metabolism in astrocytes. Role of Bcl-2. *J. Biol. Chem.* **287**, 10761-10770.
- Alonso, J. R., Cardellach, F., Lopez, S., Casademont, J. and Miro, O. (2003). Carbon monoxide specifically inhibits cytochrome *c* oxidase of human mitochondrial respiratory chain. *Pharmacol. Toxicol.* **93**, 142-146.
- Andersson, M. E. and Nordlund, P. (1999). A revised model of the active site of alternative oxidase. *FEBS Lett.* **449**, 17-22.
- Anthonyamy, A., Balasubramanian, S., Shanmugaiah, V. and Mathivanan, N. (2008). Synthesis, characterization and electrochemistry of 4'-functionalized 2,2':6',2''-terpyridine ruthenium(II) complexes and their biological activity. *Dalton Trans.*, 2136-43.
- Antonini, E. and Brunori, M. (1971). "Hemoglobin and myoglobin in their reactions with ligands". North-Holland Publishing, Amsterdam.
- Aono, S. (2003). Biochemical and biophysical properties of the CO-sensing transcriptional activator CooA. *Acc. Chem. Res.* **11**, 825-831.
- Aono, S., Nakajima, H., Saito, K. and Okada, M. (1996). A novel heme protein that acts as a carbon monoxide-dependent transcriptional activator in *Rhodospirillum rubrum*. *Biochem. Biophys. Res. Commun.* **228**, 752-756.
- Aono, S., Ohkubo, K., Matsuo, T. and Nakajima, H. (1998). Redox-controlled ligand exchange of the heme in the CO-sensing transcriptional activator CooA. *J. Biol. Chem.* **273**, 25757-25764.
- Armstrong, F. A. (2004). Hydrogenases: active site puzzles and progress. *Curr. Opin. Chem. Biol.* **8**, 133-140.
- Arregui, B., Lopez, B., Garcia Salom, M., Valero, F., Navarro, C. and Fenoy, F. J. (2004). Acute renal hemodynamic effects of dimanganese decacarbonyl and cobalt protoporphyrin. *Kidney Int.* **65**, 564-74.
- Artinian, L. R., Ding, J. M. and Gillette, M. U. (2001). Carbon monoxide and nitric oxide: interacting messengers in muscarinic signaling to the brain's circadian clock. *Exp. Neurol.* **171**, 293-300.
- Aslund, F., Berndt, K. D. and Holmgren, A. (1997). Redox potentials of glutaredoxins and other thiol-disulfide oxidoreductases of the thioredoxin superfamily determined by direct protein-protein redox equilibria. *J. Biol. Chem.* **272**, 30780-6.

- Assembly of Life Sciences (U.S.). Committee on Medical and Biologic Effects of Environmental Pollutants. (1977). "Ozone and other photochemical oxidants". National Academy of Sciences, Washington D.C.
- Atkin, A. J., Lynam, J. M., Moulton, B. E., Sawle, P., Motterlini, R., Boyle, N. M., Pryce, M. T. and Fairlamb, I. J. S. (2011). Modification of the deoxy-myoglobin/carbonmonoxy-myoglobin UV-vis assay for reliable determination of CO-release rates from organometallic carbonyl complexes. *Dalton Trans.* **40**, 5755-5761.
- Atlung, T. and Brondsted, L. (1994). Role of the transcriptional activator AppY in regulation of the *cyx appA* operon of *Escherichia coli* by anaerobiosis, phosphate starvation, and growth phase. *J. Bacteriol.* **176**, 5414-5422.
- Avetisyan, A. V., Dibrov, P. A., Semeykina, A. L., Skulachev, V. P. and Sokolov, M. V. (1991). Adaptation of *Bacillus FTU* and *Escherichia coli* to alkaline conditions - The Na<sup>+</sup>-motive respiration. *Biochim. Biophys. Acta* **1098**, 95-104.
- Babcock, G. T. and Wikstrom, M. (1992). Oxygen activation and the conservation of energy in cell respiration. *Nature* **356**, 301-309.
- Babior, B. M., Lambeth, J. D. and Nauseef, W. (2002). The neutrophil NADPH oxidase. *Arch. Biochem. Biophys.* **397**, 342-4.
- Bani-Hani, M. G., Greenstein, D., Mann, B. E., Green, C. J. and Motterlini, R. (2006). Modulation of thrombin-induced neuroinflammation in BV-2 microglia by carbon monoxide-releasing molecule 3. *J. Pharmacol. Exp. Ther.* **318**, 1315-1322.
- Bekker, M., de Vries, S., Ter Beek, A., Hellingwerf, K. J. and de Mattos, M. J. (2009). Respiration of *Escherichia coli* can be fully uncoupled via the nonelectrogenic terminal cytochrome *bd-II* oxidase. *J. Bacteriol.* **191**, 5510-7.
- Belcher, J. D., Mahaseth, H., Welch, T. E., Otterbein, L. E., Hebbel, R. P. and Vercellotti, G. M. (2006). Heme oxygenase-1 is a modulator of inflammation and vaso-occlusion in transgenic sickle mice. *J. Clin. Invest.* **116**, 808-816.
- Berg, D. E. (1977). "Insertion and excision of the transposable kanamycin resistance determinant Tn5. In *DNA Insertion Elements, Plasmids, and Episomes*". Cold Spring Harbor Press, Cold Spring Harbor, New York.
- Berthold, D. A., Andersson, M. E. and Nordlund, P. (2000). New insight into the structure and function of the alternative oxidase. *Biochimica et Biophysica Acta Bioenergetics* **1460**, 241-254.
- Berthold, D. A. and Stenmark, P. (2003). Membrane-bound diiron carboxylate proteins. *Annu Rev Plant Biol* **54**, 497-517.
- Berthold, D. A., Voevodskaya, N., Stenmark, P., Graslund, A. and Nordlund, P. (2002). EPR studies of the mitochondrial alternative oxidase - Evidence for a diiron carboxylate center. *Journal of Biological Chemistry* **277**, 43608-43614.
- Bjorklof, K., Zickermann, V. and Finel, M. (2000). Purification of the 45 kDa, membrane bound NADH dehydrogenase of *Escherichia coli* (NDH-2) and analysis of its interaction with ubiquinone analogues. *FEBS Lett.* **467**, 105-110.
- Blattner, F. R., Plunkett, G., Bloch, C. A., Perna, N. T., Burland, V., Riley, M., ColladoVides, J., Glasner, J. D., Rode, C. K., Mayhew, G. F., Gregor, J., Davis, N. W., Kirkpatrick, H. A., Goeden, M. A., Rose, D. J., Mau, B. and Shao, Y. (1997). The complete genome sequence of *Escherichia coli* K-12. *Science* **277**, 1453-1462.
- Bloch, K. D., Ichinose, F., Roberts, J. D., Jr. and Zapol, W. M. (2007). Inhaled NO as a therapeutic agent. *Cardiovasc. Res.* **75**, 339-48.

- Blumer, C. and Haas, D. (2000). Mechanism, regulation, and ecological role of bacterial cyanide biosynthesis. *Arch. Microbiol.* **173**, 170-177.
- Boczkowski, J., Poderoso, J. J. and Motterlini, R. (2006). CO-metal interaction: vital signaling from a lethal gas. *Trends Biochem. Sci.* **31**, 614-621.
- Boettcher, K. J. and Ruby, E. G. (1990). Depressed light emission by symbiotic *Vibrio fischeri* of the sepiolid squid *Euprymna scolopes*. *J. Bacteriol.* **172**, 3701-6.
- Bonam, D., Lehman, L., Roberts, G. P. and Ludden, P. W. (1989). Regulation of carbon monoxide dehydrogenase and hydrogenase in *Rhodospirillum rubrum* - Effects of CO and oxygen on synthesis and activity. *J. Bacteriol.* **171**, 3102-3107.
- Bonnett, R. and McDonagh, A. F. (1973). The meso-reactivity of porphyrins and related compounds. VI. Oxidative cleavage of the haem system. The four isomeric biliverdins of the IX series. *J Chem Soc Perkin I* **9**, 881-8.
- Borisov, V. B. (1996). Cytochrome *bd*: Structure and properties. A review. *Biochemistry - Moscow* **61**, 565-574.
- Borisov, V. B. (2008). Interaction of *bd*-type quinol oxidase from *Escherichia coli* and carbon monoxide: Heme *d* binds CO with high affinity. *Biochemistry-Moscow* **73**, 14-22.
- Borisov, V. B., Forte, E., Sarti, P., Brunori, M., Konstantinov, A. A. and Giuffre, A. (2007). Redox control of fast ligand dissociation from *Escherichia coli* cytochrome *bd*. *Biochem. Biophys. Res. Commun.* **355**, 97-102.
- Borisov, V. B., Gennis, R. B., Hemp, J. and Verkhovskiy, M. I. (2011a). The cytochrome *bd* respiratory oxygen reductases. *Biochim. Biophys. Acta Bioen.* **1807**, 1398-1413.
- Borisov, V. B., Murali, R., Verkhovskaya, M. L., Bloch, D. A., Han, H. Z., Gennis, R. B. and Verkhovskiy, M. I. (2011b). Aerobic respiratory chain of *Escherichia coli* is not allowed to work in fully uncoupled mode. *Proc. Natl. Acad. Sci. U. S. A.* **108**, 17320-17324.
- Borisov, V. B., Sedelnikova, S. E., Poole, R. K. and Konstantinov, A. A. (2001). Interaction of cytochrome *bd* with carbon monoxide at low and room temperatures. Evidence that only a small fraction of heme *b*<sub>595</sub> reacts with CO. *J. Biol. Chem.* **276**, 22095-22099.
- Brouard, S., Berberat, P. O., Tobiasch, E., Seldon, M. P., Bach, F. H. and Soares, M. P. (2002). Heme oxygenase-1-derived carbon monoxide requires the activation of transcription factor NF-kappa B to protect endothelial cells from tumor necrosis factor-alpha-mediated apoptosis. *J. Biol. Chem.* **277**, 17950-61.
- Brown, S. B., Brown, E. A. and Walker, I. (2004). The present and future role of photodynamic therapy in cancer treatment. *Lancet Oncology* **5**, 497-508.
- Bruckmann, N. E., Wahl, M., Reiss, G. J., Kohns, M., Watjen, W. and Kunz, P. C. (2011). Polymer Conjugates of Photoinducible CO-Releasing Molecules. *Eur. J. Inorg. Chem.*, 4571-4577.
- Bruggemann, H., Bauer, R., Raffestin, S. and Gottschalk, G. (2004). Characterization of a heme oxygenase of *Clostridium tetani* and its possible role in oxygen tolerance. *Arch. Microbiol.* **182**, 259-263.
- Calhoun, M. W. and Gennis, R. B. (1993). Demonstration of separate genetic loci encoding distinct membrane-bound respiratory NADH dehydrogenases in *Escherichia coli*. *J. Bacteriol.* **175**, 3013-3019.
- Calhoun, M. W., Oden, K. L., Gennis, R. B., Demattos, M. J. T. and Neijssel, O. M. (1993). Energetic efficiency of *Escherichia coli* - Effects of mutations in components of the aerobic respiratory chain. *J. Bacteriol.* **175**, 3020-3025.

- Carraway, M. S., Ghio, A. J., Suliman, H. B., Carter, J. D., Whorton, A. R. and Piantadosi, C. A. (2002). Carbon monoxide promotes hypoxic pulmonary vascular remodeling. *American journal of physiology. Lung cellular and molecular physiology* **282**, L693-702.
- Carre, J. E., Affourtit, C. and Moore, A. L. (2011). Interaction of purified alternative oxidase from thermogenic *Arum maculatum* with pyruvate. *FEBS Lett.* **585**, 397-401.
- Castor, L. N. and Chance, B. (1955). Photochemical action spectra of carbon monoxide-inhibited respiration. *J. Biol. Chem.* **217**, 453-465.
- Castor, L. N. and Chance, B. (1959). Photochemical determinations of the oxidases of bacteria. *J. Biol. Chem.* **234**, 1587-1592.
- Cepinskas, G., Katada, K., Bihari, A. and Potter, R. F. (2008). Carbon monoxide liberated from carbon monoxide-releasing molecule CORM-2 attenuates inflammation in the liver of septic mice. *Am. J. Physiol.-Gastr. L.* **294**, G184-G191.
- Chance, B., Erecinska, M. and Wagner, M. (1970). Mitochondrial responses to carbon monoxide toxicity. *Ann. N. Y. Acad. Sci.* **174**, 193-204.
- Chance, B., Smith, L. and Castor, L. (1953). New methods for the study of the carbon monoxide compounds of respiratory enzymes. *Biochim. Biophys. Acta* **12**, 289-298.
- Cheesman, M. R., Watmough, N. J., Pires, C. A., Turner, R., Brittain, T., Gennis, R. B., Greenwood, C. and Thomson, A. J. (1993). Cytochrome *bo* from *Escherichia coli* - Identification of haem ligands and reaction of the reduced enzyme with carbon monoxide. *Biochem. J.* **289**, 709-718.
- Chin, B. Y. and Otterbein, L. E. (2009). Carbon monoxide is a poison... to microbes! CO as a bactericidal molecule. *Curr Opin Pharmacol* **9**, 490-500.
- Chlopicki, S., Olszanecki, R., Marcinkiewicz, E., Lomnicka, M. and Motterlini, R. (2006). Carbon monoxide released by CORM-3 inhibits human platelets by a mechanism independent of soluble guanylate cyclase. *Cardiovasc. Res.* **71**, 393-401.
- Chung, S. W., Hall, S. R. and Perrella, M. A. (2009). Role of haem oxygenase-1 in microbial host defence. *Cell. Microbiol.* **11**, 199-207.
- Chung, S. W., Liu, X., Macias, A. A., Baron, R. M. and Perrella, M. A. (2008). Heme oxygenase-1-derived carbon monoxide enhances the host defense response to microbial sepsis in mice. *J. Clin. Invest.* **118**, 239-247.
- Clark, D. S., Lentz, C. P. and Roth, L. A. (1976). Use of carbon-monoxide for extending shelf-life of prepackaged fresh beef. *Canadian Institute of Food Science and Technology Journal-Journal De L Institut Canadien De Science Et Technologie Alimentaires* **9**, 114-117.
- Clark, J. E., Naughton, P., Shurey, S., Green, C. J., Johnson, T. R., Mann, B. E., Foresti, R. and Motterlini, R. (2003). Cardioprotective actions by a water-soluble carbon monoxide-releasing molecule. *Circ. Res.* **93**, e2-8.
- Clark, R. W., Youn, H., Lee, A. J., Roberts, G. P. and Burstyn, J. N. (2007). DNA binding by an imidazole-sensing CooA variant is dependent on the heme redox state. *J. Biol. Inorg. Chem.* **12**, 139-146.
- Coburn, R. F. (1979). Mechanisms of carbon-monoxide toxicity. *Prev. Med.* **8**, 310-322.
- Coburn, R. F., Forster, R. E. and Blakemore, W. S. (1963). Endogenous Carbon Monoxide Production in Man. *J. Clin. Invest.* **42**, 1172-1178.



- Collman, J. P., Hallber, T. R. and Suslick, K. S. (1980). "Metal Ion Activation of Dioxygen". Wiley, New York.
- Cooper, C. E. and Brown, G. C. (2008). The inhibition of mitochondrial cytochrome oxidase by the gases carbon monoxide, nitric oxide, hydrogen cyanide and hydrogen sulfide: chemical mechanism and physiological significance. *J. Bioenerg. Biomembr.* **40**, 533-539.
- Cooper, C. E., Torres, J., Sharpe, M. A. and Wilson, M. T. (1997). Nitric oxide ejects electrons from the binuclear centre of cytochrome *c* oxidase by reacting with oxidised copper: a general mechanism for the interaction of copper proteins with nitric oxide? *FEBS Lett.* **414**, 281-284.
- Cooper, M., Tavankar, G.R. and Williams, H.D. (2003). Regulation of expression of the cyanide-insensitive terminal oxidase in *Pseudomonas aeruginosa*. *Microbiology* **149**, 1275-1284.
- Cotton, F. A. and Wilkinson, G. (1980). "Advances in Organic Chemistry". Wiley, New York.
- Crook, S. H., Mann, B. E., Meijer, A., Adams, H., Sawle, P., Scapens, D. and Motterlini, R. (2011). Mn(CO)<sub>4</sub>[S<sub>2</sub>CNMe(CH<sub>2</sub>CO<sub>2</sub>H)], a new water-soluble CO-releasing molecule. *Dalton Trans.* **40**, 4230-4235.
- Cunningham, L., Pitt, M. and Williams, H. D. (1997). The *cioAB* genes from *Pseudomonas aeruginosa* code for a novel cyanide-insensitive terminal oxidase related to the cytochrome *bd* quinol oxidases. *Mol. Microbiol.* **24**, 579-591.
- Cunningham, L. and Williams, H. D. (1995). Isolation and characterization of mutants defective in the cyanide-insensitive respiratory pathway of *Pseudomonas aeruginosa*. *J. Bacteriol.* **177**, 432-438.
- D'Amico, G., Lam, F., Hagen, T. and Moncada, S. (2006). Inhibition of cellular respiration by endogenously produced carbon monoxide. *J. Cell Sci.* **119**, 2291-2298.
- D'mello, R., Hill, S. and Poole, R. K. (1995). The oxygen affinity of cytochrome *bo'* in *Escherichia coli* determined by the deoxygenation of oxyleghemoglobin and oxymyoglobin: *K<sub>m</sub>* values for oxygen are in the submicromolar range. *J. Bacteriol.* **177**, 867 - 870.
- D'mello, R., Hill, S. and Poole, R. K. (1996). The cytochrome *bd* quinol oxidase in *Escherichia coli* has an extremely high oxygen affinity and two oxygen-binding haems: implications for regulation of activity *in vivo* by oxygen inhibition. *Microbiology* **142**, 755-763.
- Das, A. K., Helps, N. R., Cohen, P. T. and Barford, D. (1996). Crystal structure of the protein serine/threonine phosphatase 2C at 2.0 Å resolution. *EMBO J.* **15**, 6798-809.
- Dassa, J., Fsihi, H., Marck, C., Dion, M., Kieffer-Bontemps, M. and Boquet, P. L. (1991). A new oxygen-regulated operon in *Escherichia coli* comprises the gene for a putative third cytochrome oxidase and for pH 2.5 acid phosphatase (*appA*). *Mol. Gen. Genet.* **229**, 341-352.
- Davidge, K. S., Motterlini, R., Mann, B. E., Wilson, J. L. and Poole, R. K. (2009a). Carbon monoxide in biology and microbiology: surprising roles for the "Detroit perfume". *Adv. Microb. Physiol.* **56**, 85-167.
- Davidge, K. S., Sanguinetti, G., Yee, C. H., Cox, A. G., McLeod, C. W., Monk, C. E., Mann, B. E., Motterlini, R. and Poole, R. K. (2009b). Carbon monoxide-releasing antibacterial molecules target respiration and global transcriptional regulators. *J. Biol. Chem.* **284**, 4516-4524.

- Day, D. A., Millar, A. H., Wiskich, J. T. and Whelan, J. (1994). Regulation of alternative oxidase activity by pyruvate in soybean mitochondria. *Plant Physiol.* **106**, 1421-1427.
- Delgado-Nixon, V. M., Gonzalez, G. and Gilles-Gonzalez, M. A. (2000). Dos, a heme-binding PAS protein from *Escherichia coli*, is a direct oxygen sensor. *Biochemistry* **39**, 2685-2691.
- Desmard, M., Boczkowski, J., Poderoso, J. and Motterlini, R. (2007). Mitochondrial and cellular heme-dependent proteins as targets for the bioactive function of the heme oxygenase/carbon monoxide system. *Antiox. Redox Signal.* **9**, 2139-2155.
- Desmard, M., Davidge, K. S., Bouvet, O., Morin, D., Roux, D., Foresti, R., Ricard, J. D., Denamur, E., Poole, R. K., Montravers, P., Motterlini, R. and Boczkowski, J. (2009). A carbon monoxide-releasing molecule (CORM-3) exerts bactericidal activity against *Pseudomonas aeruginosa* and improves survival in an animal model of bacteraemia. *FASEB J.* **23**, 1023-1031.
- Desmard, M., Foresti, R., Morin, D., Dagouassat, M., Berdeaux, A., Denamur, E., Crook, S. H., Mann, B. E., Scapens, D., Montravers, P., Boczkowski, J. and Motterlini, R. (2012). Differential antibacterial activity against *Pseudomonas aeruginosa* by carbon monoxide-releasing molecules. *Antioxid. Redox Signal.* **16**, 153-63.
- Dioum, E. M., Rutter, J., Tuckerman, J. R., Gonzalez, G., Gilles-Gonzalez, M. A. and McKnight, S. L. (2002). NPAS2: A gas-responsive transcription factor. *Science* **298**, 2385-2387.
- Dordelmann, G., Pfeiffer, H., Birkner, A. and Schatzschneider, U. (2011). Silicium dioxide nanoparticles as carriers for photoactivatable CO-releasing molecules (PhotoCORMs). *Inorg. Chem.* **50**, 4362-4367.
- Doudoroff, M. (1942). Studies on the Luminous Bacteria: II. Some Observations on the Anaerobic Metabolism of Facultatively Anaerobic Species. *J. Bacteriol.* **44**, 461-7.
- Dunn, A. K. (2012). In "*Vibrio fischeri* Metabolism: Symbiosis and Beyond In *Advances in Microbial Physiology*" (R. K. Poole, ed.), vol. 61, pp. 37-68. Academic Press.
- Dunn, A. K., Karr, E. A., Wang, Y. L., Batton, A. R., Ruby, E. G. and Stabb, E. V. (2010). The alternative oxidase (AOX) gene in *Vibrio fischeri* is controlled by NsrR and upregulated in response to nitric oxide. *Mol. Microbiol.* **77**, 44-55.
- Dunn, A. K. and Stabb, E. V. (2008). Genetic analysis of trimethylamine N-oxide reductases in the light organ symbiont *Vibrio fischeri* ES114. *J. Bacteriol.* **190**, 5814-23.
- Durante, W., Christodoulides, N., Cheng, K., Peyton, K. J., Sunahara, R. K. and Schafer, A. I. (1997). cAMP induces heme oxygenase-1 gene expression and carbon monoxide production in vascular smooth muscle. *Am. J. Physiol.* **273**, H317-23.
- El-Badawi, A., Samuels CE, Cain R and Anglemeir AF. (1964). Color and pigment stability of packaged refrigerated beef. *Food Technol* **18**, 159-163.
- Elbirt, K. K., Whitmarsh, A. J., Davis, R. J. and Bonkovsky, H. L. (1998). Mechanism of sodium arsenite-mediated induction of heme oxygenase-1 in hepatoma cells. Role of mitogen-activated protein kinases. *J. Biol. Chem.* **273**, 8922-31.
- Endley, S., McMurray, D. and Ficht, T.A. (2001). Interruption of the *cydB* locus in *Brucella abortus* attenuates intracellular survival and virulence in the mouse model of infection. *J. Bacteriol.* **183**, 2454-2462.

- Engel, R. R., Schwartz, S., Chapman, S. S. and Matsen, J. M. (1972). Carbon monoxide production from heme compounds by bacteria. *J. Bacteriol.* **112**, 1310-1315.
- Esquinas-Rychen, M. and Erni, B. (2001). Facilitation of bacteriophage lambda DNA injection by inner membrane proteins of the bacterial phosphoenol-pyruvate: carbohydrate phosphotransferase system (PTS). *J Mol Microbiol Biotechnol* **3**, 361-70.
- Evans, C. G. T., Herbert, D. and Tempest, D.W. (1970). "The continuous cultivation of microorganisms part 2 construction of a chemostat;". Elsevier Ltd., London and New York.
- Ewing, J. F. and Maines, M. D. (1992). *In situ* hybridization and immunohistochemical localization of heme oxygenase-2 mRNA and protein in normal rat brain: Differential distribution of isozyme 1 and 2. *Mol. Cell. Neurosci.* **3**, 559-70.
- Ewing, J. F. and Maines, M. D. (1995). Distribution of constitutive (HO-2) and heat-inducible (HO-1) heme oxygenase isozymes in rat testes: HO-2 displays stage-specific expression in germ cells. *Endocrinology* **136**, 2294-302.
- Farrer, N. J. and Sadler, P. J. (2008). Photochemotherapy: Targeted activation of metal anticancer complexes. *Aust. J. Chem.* **61**, 669-674.
- Ferrandiz, M. L., Maicas, N., Garcia-Amandis, I., Terencio, M. C., Motterlini, R., Devesa, I., Joosten, L. A. B., van den Berg, W. B. and Alcaraz, M. J. (2008). Treatment with a CO-releasing molecule (CORM-3) reduces joint inflammation and erosion in murine collagen-induced arthritis. *Ann. Rheum. Dis.* **67**, 1211-1217.
- Finkelstein, E., Rosen, G. M. and Rauckman, E. J. (1982). Production of hydroxyl radical by decomposition of superoxide spin-trapped adducts. *Mol. Pharmacol.* **21**, 262-5.
- Fisher, A. J., Thompson, T. B., Thoden, J. B., Baldwin, T. O. and Rayment, I. (1996). The 1.5-Å resolution crystal structure of bacterial luciferase in low salt conditions. *J. Biol. Chem.* **271**, 21956-68.
- Flatley, J., Barrett, J., Pullan, S. T., Hughes, M. N., Green, J. and Poole, R. K. (2005). Transcriptional responses of *Escherichia coli* to *S*-nitrosoglutathione under defined chemostat conditions reveal major changes in methionine biosynthesis. *J. Biol. Chem.* **280**, 10065-10072.
- Foresti, R., Hammad, J., Clark, J. E., Johnson, T. R., Mann, B. E., Friebe, A., Green, C. J. and Motterlini, R. (2004). Vasoactive properties of CORM-3, a novel water-soluble carbon monoxide-releasing molecule. *Br. J. Pharmacol.* **142**, 453-460.
- Fox, J. D., He, Y., Shelver, D., Roberts, G. P. and Ludden, P. W. (1996). Characterization of the region encoding the CO-induced hydrogenase of *Rhodospirillum rubrum*. *J. Bacteriol.* **178**, 6200-8.
- Freitas, A., Alves-Filho, J. C., Secco, D. D., Neto, A. F., Ferreira, S. H., Barja-Fidalgo, C. and Cunha, F. Q. (2006). Heme oxygenase/carbon monoxide-biliverdin pathway down regulates neutrophil rolling, adhesion and migration in acute inflammation. *Br. J. Pharmacol.* **149**, 345-354.
- Frejaville, C., Karoui, H., Tuccio, B., Le Moigne, F., Culcasi, M., Pietri, S., Lauricella, R. and Tordo, P. (1995). 5-(Diethoxyphosphoryl)-5-methyl-1-pyrroline N-oxide: a new efficient phosphorylated nitron for the *in vitro* and *in vivo* spin trapping of oxygen-centered radicals. *J. Med. Chem.* **38**, 258-65.
- Friebe, A., Mullershausen, F., Smolenski, A., Walter, U., Schultz, G. and Koesling, D. (1998). YC-1 potentiates nitric oxide- and carbon monoxide-induced cyclic GMP effects in human platelets. *Mol. Pharmacol.* **54**, 962-7.

- Furchgott, R. F. (1999). Endothelium-derived relaxing factor: Discovery, early studies, and identification as nitric oxide (Nobel lecture). *Angewandte Chemie International Edition* **38**, 1870-1880.
- Furchgott, R. F. and Jothianandan, D. (1991). Endothelium-dependent and endothelium-independent vasodilation involving cyclic GMP- Relaxation induced by nitric oxide, carbon monoxide and light. *Blood Vessels* **28**, 52-61.
- Furci, L. M., Lopes, P., Eakanunkul, S., Zhong, S. J., MacKerell, A. D. and Wilks, A. (2007). Inhibition of the bacterial heme oxygenases from *Pseudomonas aeruginosa* and *Neisseria meningitidis*: Novel antimicrobial targets. *J. Med. Chem.* **50**, 3804-3813.
- Gadalla, M. M. and Snyder, S. H. (2010). Hydrogen sulfide as a gasotransmitter. *J. Neurochem.* **113**, 14-26.
- Gallagher, L. A. and Manoil, C. (2001). *Pseudomonas aeruginosa* PA01 kills *Caenorhabditis elegans* by cyanide poisoning. *J. Bacteriol.* **183**, 6207-6214.
- Gerhardt, P., Murray, R. G. E., Wood, W. A., Krieg, N. R. (1994). "Methods For General and Molecular Bacteriology". The American Society of Microbiology, Washington D.C., USA.
- Gilberthorpe, N. J. and Poole, R. K. (2008). Nitric oxide homeostasis in *Salmonella typhimurium* - Roles of respiratory nitrate reductase and flavohemoglobin. *J. Biol. Chem.* **283**, 11146-11154.
- Gilles-Gonzalez, M. A., Ditta, G. S. and Helinski, D. R. (1991). A haemoprotein with kinase activity encoded by the oxygen sensor of *Rhizobium meliloti*. *Nature* **350**, 170-172.
- Goldbaum, L. R., Ramirez, R. G. and Absalon, K. B. (1975). What is the mechanism of carbon monoxide toxicity? *Aviat. Space Environ. Med.* **46**, 1289-91.
- Goldman, B. S., Gabbert, K. K. and Kranz, R. G. (1996). Use of heme reporters for studies of cytochrome biosynthesis and heme transport. *J. Bacteriol.* **178**, 6338-6347.
- Goryshin, I. Y. and Reznikoff, W. S. (1998). Tn5 *in vitro* transposition. *J. Biol. Chem.* **273**, 7367-74.
- Graham, A. I., Hunt, S., Stokes, S. L., Bramall, N., Bunch, J., Cox, A. G., McLeod, C. W. and Poole, R. K. (2009). Severe zinc depletion of *Escherichia coli*: roles for high affinity zinc binding by ZinT, zinc transport and zinc-independent proteins. *J. Biol. Chem.* **284**, 18377-89.
- Griffiths, M. J. and Evans, T. W. (2005). Inhaled nitric oxide therapy in adults. *New Engl. J. Med.* **353**, 2683-95.
- Grilli, A., De Lutiis, M. A., Patruno, A., Speranza, L., Gizzi, F., Taccardi, A. A., Di Napoli, P., De Caterina, R., Conti, P. and Felaco, M. (2003). Inducible nitric oxide synthase and heme oxygenase-1 in rat heart: direct effect of chronic exposure to hypoxia. *Ann. Clin. Lab. Sci.* **33**, 208-15.
- Gunsalus, R. P. (1992). Control of electron flow in *Escherichia coli* - Coordinated transcription of respiratory pathway genes. *J. Bacteriol.* **174**, 7069-7074.
- Gunsalus, R. P. and Park, S. J. (1994). Aerobic-anaerobic gene regulation in *Escherichia coli*: Control by the ArcAB and Fnr regulons. *Res. Microbiol.* **145**, 437-450.
- Gunther, L., Berberat, P. O., Haga, M., Brouard, S., Smith, R. N., Soares, M. P., Bach, F. H. and Tobiasch, E. (2002). Carbon monoxide protects pancreatic beta-cells from apoptosis and improves islet function/survival after transplantation. *Diabetes* **51**, 994-9.

- Guo, Y., Guo, G., Mao, X., Zhang, W., Xiao, J., Tong, W., Liu, T., Xiao, B., Liu, X., Feng, Y. and Zou, Q. (2008). Functional identification of HugZ, a heme oxygenase from *Helicobacter pylori*. *BMC Microbiol* **8**, 226.
- Gupta, K. J., Zabalza, A. and van Dongen, J. T. (2009). Regulation of respiration when the oxygen availability changes. *Physiol Plant* **137**, 383-91.
- Gutterman, D. D., Miura, H. and Liu, Y. (2005). Redox modulation of vascular tone: focus of potassium channel mechanisms of dilation. *Arterioscler. Thromb. Vasc. Biol.* **25**, 671-8.
- Haddock, B. A., Downie, J. A. and Garland, P. B. (1976). Kinetic characterization of the membrane-bound cytochromes of *Escherichia coli* grown under a variety of conditions by using a stopped-flow dual-wavelength spectrophotometer. *Biochem. J.* **154**, 285-294.
- Hanes, C. S. and Barker, J. (1931). The effects of cyanide on the respiration and sugar content of the potato at 15 C. *Proc. R. Soc. London Ser. B* **108**, 95-118.
- Hasegawa, U., van der Vlies, A. J., Simeoni, E., Wandrey, C. and Hubbell, J. A. (2010). Carbon monoxide-releasing micelles for immunotherapy. *J. Am. Chem. Soc.* **132**, 18273-80.
- Hendgen-Cotta, U. B., Merx, M. W., Shiva, S., Schmitz, J., Becher, S., Klare, J. P., Steinhoff, H. J., Goedecke, A., Schrader, J., Gladwin, M. T., Kelm, M. and Rassaf, T. (2008). Nitrite reductase activity of myoglobin regulates respiration and cellular viability in myocardial ischemia-reperfusion injury. *Proc. Natl. Acad. Sci. U. S. A.*
- Hewison, L., Crook, S. H., Johnson, T. R., Mann, B. E., Adams, H., Plant, S. E., Sawle, P. and Motterlini, R. (2010). Iron indenyl carbonyl compounds: CO-releasing molecules. *Dalton Trans.* **39**, 8967-75.
- Hill-Kapturczak, N., Chang, S. H. and Agarwal, A. (2002). Heme oxygenase and the kidney. *DNA Cell Biol.* **21**, 307-21.
- Hill, B. C., Hill, J.J. and Gennis, R.B. (1994). The room temperature reaction of carbon monoxide and oxygen with the cytochrome *bd* quinol oxidase from *Escherichia coli*. *Biochemistry* **33**, 15110 - 15115.
- Hill, B. C., Woon, T. C., Nicholls, P., Peterson, J., Greenwood, C. and Thomson, A. J. (1984). Interactions of sulfide and other ligands with cytochrome *c* oxidase - An electron paramagnetic resonance study. *Biochem. J.* **224**, 591-600.
- Hoefnagel, M. H., Millar, A. H., Wiskich, J. T. and Day, D. A. (1995). Cytochrome and alternative respiratory pathways compete for electrons in the presence of pyruvate in soybean mitochondria. *Arch. Biochem. Biophys.* **318**, 394-400.
- Hopkins, F. G. (1921). On an autoxidizable constituent of the cell. *Biochem. J.* **15**, 286-305.
- Hopkins, F. G. (1923). [A lecture on] An oxidative mechanism in the living cell. *Lancet*, 1251 - 1254.
- Hou, S., Xu, R., Heinemann, S. H. and Hoshi, T. (2008). The RCK1 high-affinity Ca<sup>2+</sup> sensor confers carbon monoxide sensitivity to Slo1 BK channels. *Proc. Natl. Acad. Sci. U. S. A.* **105**, 4039-43.
- Hou, S. B., Larsen, R. W., Boudko, D., Riley, C. W., Karatan, E., Zimmer, M., Ordal, G. W. and Alam, M. (2000). Myoglobin-like aerotaxis transducers in Archaea and Bacteria. *Nature* **403**, 540-544.
- Ignarro, L. J. (1999). Nitric oxide: A unique endogenous signaling molecule in vascular biology (Nobel lecture). *Angew. Chem. Int. Ed.* **38**, 1882-1892.

- Jacobitz, S. and Meyer, O. (1989). Removal of CO dehydrogenase from *Pseudomonas carboxydovorans* cytoplasmic membranes, rebinding of CO dehydrogenase to depleted membranes, and restoration of respiratory activities. *J. Bacteriol.* **171**, 6294-6299.
- Jasaitis, A., Borisov, V. B., Belevich, N. P., Morgan, J. E., Konstantinov, A. A. and Verkhovsky, M. I. (2000). Electrogenic reactions of cytochrome bd. *Biochemistry* **39**, 13800-13809.
- Jesse, H. E., Nye, T. L., McLean, S., Green, J., Mann, B. E. and Poole, R. K. (2013). Cytochrome *bd-I* in *Escherichia coli* is less sensitive than cytochromes *bd-II* or *bd'* to inhibition by the carbon monoxide-releasing molecule, CORM-3: N-acetylcysteine reduces CO-RM uptake and inhibition of respiration. *Biochim. Biophys. Acta* **1834**, 1693-1703.
- Johnson, G. L. and Lapadat, R. (2002). Mitogen-activated protein kinase pathways mediated by ERK, JNK, and p38 protein kinases. *Science* **298**, 1911-2.
- Johnson, T. R., Mann, B. E., Clark, J. E., Foresti, R., Green, C. J. and Motterlini, R. (2003). Metal carbonyls: A new class of pharmaceuticals. *Angewandte Chemie-International Edition* **42**, 3722-3729.
- Johnson, T. R., Mann, B. E., Teasdale, I. P., Adams, H., Foresti, R., Green, C. J. and Motterlini, R. (2007). Metal carbonyls as pharmaceuticals? [Ru(CO)<sub>3</sub>Cl(glycinate)], a CO-releasing molecule with an extensive aqueous solution chemistry. *Dalton Trans.*, 1500-1508.
- Jones, B. W. and Nishiguchi, M. K. (2004). Counterillumination in the Hawaiian bobtail squid, *Euprymna scolopes* Berry (Mollusca: Cephalopoda) *Marine Biol.* **144**, 1151-1155.
- Jones, C. W. and Poole, R. K. (1985). In "Methods in Microbiology" (G. Gottschalk, ed.), vol. 18, pp. 285 - 328. Academic Press.
- Jones, C. W. and Redfearn, E. R. (1966). Electron transport in *Azotobacter vinelandii*. *Biochim. Biophys. Acta* **113**, 467-481.
- Junemann, S. (1997). Cytochrome *bd* terminal oxidase. *Biochim. Biophys. Acta* **1321**, 107 - 127.
- Kajimura, M., Fukuda, R., Bateman, R. M., Yamamoto, T. and Suematsu, M. (2010). Interactions of multiple gas-transducing systems: Hallmarks and uncertainties of CO, NO, and H<sub>2</sub>S gas biology. *Antiox. Redox Signal.* **13**, 157-192.
- Kajimura, M., Nakanishi, T., Takenouchi, T., Morikawa, T., Hishiki, T., Yukutake, Y. and Suematsu, M. (2012). Gas biology: tiny molecules controlling metabolic systems. *Respir Physiol Neurobiol* **184**, 139-48.
- Kalnenieks, U., Galinina, N., Bringer-Meyer, S. and Poole, R. K. (1998). Membrane D-lactate oxidase in *Zymomonas mobilis*: evidence for a branched respiratory chain. *FEMS Microbiol. Lett.* **168**, 91-97.
- Kano, H. and Kageyama, M. (1977). Effects of cyanide on the respiration of musk melon. *Plant Cell Physiol.* **18**, 1149 - 1153.
- Karuzina, II, Zgoda, V. G., Kuznetsova, G. P., Samenkova, N. F. and Archakov, A. I. (1999). Heme and apoprotein modification of cytochrome P450 2B4 during its oxidative inactivation in monooxygenase reconstituted system. *Free Radic Biol Med* **26**, 620-32.
- Keilin, D. (1966). "The History of Cell Respiration and Cytochrome". Cambridge University Press, Cambridge.
- Kerby, R. L., Ludden, P. W. and Roberts, G. P. (1995). Carbon monoxide-dependent growth of *Rhodospirillum rubrum*. *J. Bacteriol.* **177**, 2241-2244.

- Kerby, R. L., Youn, H. and Roberts, G. P. (2008). RcoM: A new single-component transcriptional regulator of CO metabolism in bacteria. *J. Bacteriol.* **190**, 3336-3343.
- Kharitonov, S. A. and Barnes, P. J. (2002). Biomarkers of some pulmonary diseases in exhaled breath. *Biomarkers* **7**, 1-32.
- Kharitonov, V. G., Sharma, V. S., Pilz, R. B., Magde, D. and Koesling, D. (1995). Basis of guanylate cyclase activation by carbon monoxide. *Proc. Natl. Acad. Sci. U. S. A.* **92**, 2568-2571.
- King, G. M. and Weber, C. F. (2007). Distribution, diversity and ecology of aerobic CO-oxidizing bacteria. *Nat. Rev. Microbiol.* **5**, 107-118.
- Kinsella, J. P., Cutter, G. R., Walsh, W. F., Gerstmann, D. R., Bose, C. L., Hart, C., Sekar, K. C., Auten, R. L., Bhutani, V. K., Gerdes, J. S., George, T. N., Southgate, W. M., Carriedo, H., Couser, R. J., Mammel, M. C., Hall, D. C., Pappagallo, M., Sardesai, S., Strain, J. D., Baier, M. and Abman, S. H. (2006). Early inhaled nitric oxide therapy in premature newborns with respiratory failure. *New Engl. J. Med.* **355**, 354-64.
- Kirby, J. R. (2007). *In vivo* mutagenesis using EZ-Tn5. *Methods Enzymol.* **421**, 17-21.
- Korshunov, S. and Imlay, J. A. (2006). Detection and quantification of superoxide formed within the periplasm of *Escherichia coli*. *J. Bacteriol.* **188**, 6326-6334.
- Kostoglou-Athanassiou, I., Forsling, M. L., Navarra, P. and Grossman, A. B. (1996). Oxytocin release is inhibited by the generation of carbon monoxide from the rat hypothalamus-further evidence for carbon monoxide as a neuromodulator. *Brain Res. Mol. Brain Res.* **42**, 301-6.
- Kumar, A., Deshane, J. S., Crossman, D. K., Bolisetty, S., Yan, B. S., Kramnik, I., Agarwal, A. and Steyn, A. J. C. (2008). Heme oxygenase-1-derived carbon monoxide induces the *Mycobacterium tuberculosis* dormancy regulon. *J. Biol. Chem.* **283**, 18032-18039.
- Kumar, A., Toledo, J. C., Patel, R. P., Lancaster, J. R. and Steyn, A. J. C. (2007). *Mycobacterium tuberculosis* DosS is a redox sensor and DosT is a hypoxia sensor. *Proc. Natl. Acad. Sci. U. S. A.* **104**, 11568-11573.
- Laites, G. G. (1982). The cyanide-resistant, alternative path in higher plant respiration. *Ann. Rev. Plant. Physiol* **33**, 519-555.
- Lambers, H. (1982). Cyanide-resistant respiration: A non-phosphorylating electron transport pathway acting as an energy overflow. *Physiol. Plant.* **55**, 478-485.
- Lamrabet, O., Pieulle, L., Aubert, C., Mouhamar, F., Stocker, P., Dolla, A. and Bresseur, G. (2011). Oxygen reduction in the strict anaerobe *Desulfovibrio vulgaris* Hildenborough: characterization of two membrane-bound oxygen reductases. *Microbiology* **157**, 2720-2732.
- Lancel, S., Hassoun, S. M., Favory, R., Decoster, B., Motterlini, R. and Neviere, R. (2009). Carbon monoxide rescues mice from lethal sepsis by supporting mitochondrial energetic metabolism and activating mitochondrial biogenesis. *J. Pharmacol. Exp. Ther.* **329**, 641-648.
- Langridge, G. C., Phan, M. D., Turner, D. J., Perkins, T. T., Parts, L., Haase, J., Charles, I., Maskell, D. J., Peters, S. E., Dougan, G., Wain, J., Parkhill, J. and Turner, A. K. (2009). Simultaneous assay of every *Salmonella typhi* gene using one million transposon mutants. *Genome Res.* **19**, 2308-2316.
- Lee, Y. and Kim, J. (2007). Simultaneous electrochemical detection of nitric oxide and carbon monoxide generated from mouse kidney organ tissues. *Anal. Chem.* **79**, 7669-75.

- Lemberg, R. and Barrett, J. (1973). "Cytochromes". Academic Press, London.
- Lengeler, J. (1980). Characterisation of mutants of *Escherichia coli* K12, selected by resistance to streptozotocin. *Mol. Gen. Genet.* **179**, 49-54.
- Letoffe, S., Delepelaire, P. and Wandersman, C. (2006). The housekeeping dipeptide permease is the *Escherichia coli* heme transporter and functions with two optional peptide binding proteins. *Proc. Natl. Acad. Sci. U. S. A.* **103**, 12891-12896.
- Li, L., Hsu, A. and Moore, P. K. (2009). Actions and interactions of nitric oxide, carbon monoxide and hydrogen sulphide in the cardiovascular system and in inflammation - A tale of three gases! *Pharmacol. Ther.* **123**, 386-400.
- Liu, W. Q., Chai, C., Li, X. Y., Yuan, W. J., Wang, W. Z. and Lu, Y. (2011). The cardiovascular effects of central hydrogen sulfide are related to K(ATP) channels activation. *Physiol. Res.* **60**, 729-738.
- Lloyd, D., James, C. J. and Hastings, J. W. (1985). Oxygen affinities of the bioluminescence systems of various species of luminous bacteria. *J. Gen. Microbiol.* **131**, 2137 - 2140.
- Lo Iacono, L., Boczkowski, J., Zini, R., Salouage, I., Berdaux, A., Motterlini, R. and Morin, D. (2011). A carbon monoxide-releasing molecule (CORM-3) uncouples mitochondrial respiration and modulates the production of reactive oxygen species. *Free Rad. Biol. Med.* **50**, 1556-1564.
- Lou, P. H., Hansen, B. S., Olsen, P. H., Tullin, S., Murphy, M. P. and Brand, M. D. (2007). Mitochondrial uncouplers with an extraordinary dynamic range. *Biochem. J.* **407**, 129-140.
- Maines, M. D. and Panahian, N. (2001). The heme oxygenase system and cellular defense mechanisms. Do HO-1 and HO-2 have different functions? *Adv. Exp. Med. Biol.* **502**, 249-72.
- Maness, P. C., Huang, J., Smolinski, S., Tek, V. and Vanzin, G. (2005). Energy generation from the CO oxidation-hydrogen production pathway in *Rubrivivax gelatinosus*. *Appl. Environ. Microbiol.* **71**, 2870-4.
- Mann, B. E. (2012). CO-Releasing Molecules: A Personal View. *Organometallics* **31**, 5728-5735.
- Mann, B. E. and Motterlini, R. (2007). CO and NO in medicine. *Chemical communications (Cambridge, England)*, 4197-208.
- Mansfield, J. W. (1983). "Antimicrobial compounds". Wiley, London.
- Marks, G. S., Brien, J. F., Nakatsu, K. and McLaughlin, B. E. (1991). Does carbon monoxide have a physiological function? *Trends Pharmacol. Sci.* **12**, 185-8.
- Markwell, M. A. K., Haas, S. M., Bieber, L. L. and Tolbert, N. E. (1978). A modification of the Lowry procedure to simplify protein determination in membrane and lipoprotein samples. *Anal. Biochem.* **87**, 206-210.
- Masip, L., Veeravalli, K. and Georgiou, G. (2006). The many faces of glutathione in bacteria. *Antioxid. Redox Signal.* **8**, 753-62.
- Mason, M. G., Shepherd, M., Nicholls, P., Dobbin, P. S., Dodsworth, K. S., Poole, R. K. and Cooper, C. E. (2009). Cytochrome *bd* confers nitric oxide resistance to *Escherichia coli*. *Nat Chem Biol* **5**, 94-6.
- Matsushita, K., Yamada, M., Shinagawa, E., Adachi, O. and Ameyama, M. (1983). Membrane-bound respiratory chain of *Pseudomonas aeruginosa* grown aerobically. A KCN-insensitive alternate oxidase chain and its energetics. *J. Biochem., Tokyo* **93**, 1137 - 1144.



- McCoubrey, W. K., Jr., Huang, T. J. and Maines, M. D. (1997). Isolation and characterization of a cDNA from the rat brain that encodes hemoprotein heme oxygenase-3. *Eur. J. Biochem.* **247**, 725-32.
- McDonald, A. E. and Vanlerberghe, G. C. (2005). Alternative oxidase and plastoquinol terminal oxidase in marine prokaryotes of the Sargasso Sea. *Gene* **349**, 15-24.
- McFall-Ngai, M., Heath-Heckman, E. A., Gillette, A. A., Peyer, S. M. and Harvie, E. A. (2012). The secret languages of coevolved symbioses: insights from the *Euprymna scolopes-Vibrio fischeri* symbiosis. *Semin. Immunol.* **24**, 3-8.
- McFall-Ngai, M. J. and Ruby, E. G. (2000). Developmental biology in marine invertebrate symbioses. *Curr. Opin. Microbiol.* **3**, 603-7.
- McGrath, J. J. and Smith, D. L. (1984). Response of rat coronary circulation to carbon monoxide and nitrogen hypoxia. *Proc. Soc. Exp. Biol. Med.* **177**, 132-6.
- McLean, S., Begg, R., Jesse, H. E., Mann, B. E., Sanguinetti, G. and Poole, R. K. (2013). Analysis of the bacterial response to Ru(CO)<sub>3</sub>Cl(glycinate) (CORM-3) and the inactivated compound identifies the role played by the ruthenium compound and reveals sulfur-containing species as a major target of CORM-3 action. *Antioxid. Redox Signal.*
- McLean, S., Mann, B. E. and Poole, R. K. (2012). Sulfite species enhance carbon monoxide release from CO-releasing molecules: Implications for the deoxy-myoglobin assay of activity. *Anal. Biochem.* **427**, 36-40.
- Meeuse, B. (1975). Thermogenic respiration in aroids. *Annu. Rev. Plant Physiol. Plant Mol. Biol.* **26**, 117-126.
- Megias, J., Busserolles, J. and Alcaraz, M. J. (2007). The carbon monoxide-releasing molecule CORM-2 inhibits the inflammatory response induced by cytokines in Caco-2 cells. *Br. J. Pharmacol.*
- Meister, K., Niesel, J., Schatzschneider, U., Metzler-Nolte, N., Schmidt, D. A. and Havenith, M. (2010). Label-free imaging of metal-carbonyl complexes in live cells by Raman microspectroscopy. *Angew. Chem. Int. Ed. Engl.* **49**, 3310-2.
- Middendorff, R., Kumm, M., Davidoff, M. S., Holstein, A. F. and Muller, D. (2000). Generation of cyclic guanosine monophosphate by heme oxygenases in the human testis - a regulatory role for carbon monoxide in Sertoli cells? *Biol. Reprod.* **63**, 651-7.
- Millar, A. H., Wiskich, J. T., Whelan, J. and Day, D. A. (1993). Organic acid activation of the alternative oxidase of plant mitochondria. *FEBS Lett.* **329**, 259-62.
- Miller, J. H. (1972). "Experiments in Molecular Genetics". Cold Spring Harbor Laboratory, Cold Spring Harbor, New York 11724.
- Miller, M. J. and Gennis, R. B. (1986). Purification and reconstitution of the cytochrome *d* terminal oxidase complex from *Escherichia coli*. *Methods Enzymol.* **126**, 87-94.
- Minagawa, N., Sakajo, S., Komiyama, T. and Yoshimoto, A. (1990). Essential role of ferrous iron in cyanide-resistant respiration in *Hansenula anomala*. *FEBS Lett.* **267**, 114-116.
- Mishra, S., Fujita, T., Lama, V. N., Nam, D., Liao, H., Okada, M., Minamoto, K., Yoshikawa, Y., Harada, H. and Pinsky, D. J. (2006). Carbon monoxide rescues ischemic lungs by interrupting MAPK-driven expression of early growth response 1 gene and its downstream target genes. *Proc. Natl. Acad. Sci. U. S. A.* **103**, 5191-6.
- Mitchell, L. A., Channell, M. M., Royer, C. M., Ryter, S. W., Choi, A. M. and McDonald, J. D. (2010). Evaluation of inhaled carbon monoxide as an anti-

- inflammatory therapy in a nonhuman primate model of lung inflammation. *American journal of physiology. Lung cellular and molecular physiology* **299**, L891-7.
- Mitchell, R., Brown, S., Mitchell, P. and Rich, P. R. (1992). Rates of cyanide binding to the catalytic intermediates of mammalian cytochrome *c* oxidase, and the effects of cytochrome *c* and poly(L-lysine). *Biochim. Biophys. Acta* **1100**, 40-8.
- Mogi, T., Nakamura, H. and Anraku, Y. (1994). Molecular structure of a heme-copper redox center of the *Escherichia coli* ubiquinol oxidase: Evidence and model. *J. Biochem.* **116**, 471-477.
- Moore, A. L., Carre, J. E., Affourtit, C., Albury, M. S., Crichton, P. G., Kita, K. and Heathcote, P. (2008). Compelling EPR evidence that the alternative oxidase is a diiron carboxylate protein. *Biochim. Biophys. Acta Bioen.* **1777**, 327-330.
- Motterlini, R., Clark, J. E., Foresti, R., Sarathchandra, P., Mann, B. E. and Green, C. J. (2002). Carbon monoxide-releasing molecules: characterization of biochemical and vascular activities. *Circ. Res.* **90**, E17-24.
- Motterlini, R., Mann, B. E. and Foresti, R. (2005a). Therapeutic applications of carbon monoxide-releasing molecules. *Expert Opin Investig Drugs* **14**, 1305-18.
- Motterlini, R. and Otterbein, L. E. (2010). The therapeutic potential of carbon monoxide. *Nat. Rev. Drug Discov.* **9**, 728-743.
- Motterlini, R., Sawle, P., Hammad, J., Bains, S., Alberto, R., Foresti, R. and Green, C. J. (2005b). CORM-A1: a new pharmacologically active carbon monoxide-releasing molecule. *FASEB J.* **19**, 284-6.
- Muller, V. (2003). Energy conservation in acetogenic bacteria. *Appl. Environ. Microbiol.* **69**, 6345-53.
- Murad, F. (1999). Discovery of some of the biological effects of nitric oxide and its role in cell signaling. *Biosci. Rep.* **19**, 133-154.
- Murray, T. S., Okegbe, C., Gao, Y., Kazmierczak, B. I., Motterlini, R., Dietrich, L. E. P. and Bruscia, E. M. (2012). The carbon monoxide-releasing molecule CORM-2 attenuates *Pseudomonas aeruginosa* biofilm formation. *Plos One* **7**.
- Musameh, M. D., Green, C. J., Mann, B. E., Fuller, B. J. and Motterlini, R. (2007). Improved myocardial function after cold storage with preservation solution supplemented with a carbon monoxide-releasing molecule (CORM-3). *J. Heart Lung Transplant.* **26**, 1192-1198.
- Nakao, A., Choi, A. M. and Murase, N. (2006a). Protective effect of carbon monoxide in transplantation. *J Cell Mol Med* **10**, 650-71.
- Nakao, A., Faleo, G., Shimizu, H., Nakahira, K., Kohmoto, J., Sugimoto, R., Choi, A. M., McCurry, K. R., Takahashi, T. and Murase, N. (2008). *Ex vivo* carbon monoxide prevents cytochrome P450 degradation and ischemia/reperfusion injury of kidney grafts. *Kidney Int.* **74**, 1009-1016.
- Nakao, A., Kimizuka, K., Stolz, D. B., Neto, J. S., Kaizu, T., Choi, A. M., Uchiyama, T., Zuckerbraun, B. S., Nalesnik, M. A., Otterbein, L. E. and Murase, N. (2003). Carbon monoxide inhalation protects rat intestinal grafts from ischemia/reperfusion injury. *Am. J. Pathol.* **163**, 1587-98.
- Nakao, A., Toyokawa, H., Tsung, A., Nalesnik, M. A., Stolz, D. B., Kohmoto, J., Ikeda, A., Tomiyama, K., Harada, T., Takahashi, T., Yang, R., Fink, M. P., Morita, K., Choi, A. M. and Murase, N. (2006b). *Ex vivo* application of carbon monoxide in University of Wisconsin solution to prevent intestinal cold ischemia/reperfusion injury. *American journal of transplantation : official journal of the American*

- Society of Transplantation and the American Society of Transplant Surgeons* **6**, 2243-55.
- Nakayama, M., Takahashi, K., Kitamuro, T., Yasumoto, K., Katayose, D., Shirato, K., Fujii-Kuriyama, Y. and Shibahara, S. (2000). Repression of heme oxygenase-1 by hypoxia in vascular endothelial cells. *Biochem. Biophys. Res. Commun.* **271**, 665-71.
- Nath, K. A., Balla, G., Vercellotti, G. M., Balla, J., Jacob, H. S., Levitt, M. D. and Rosenberg, M. E. (1992). Induction of heme oxygenase is a rapid, protective response in rhabdomyolysis in the rat. *J. Clin. Invest.* **90**, 267-70.
- Niesel, J., Pinto, A., N'Dongo, H. W. P., Merz, K., Ott, I., Gust, R. and Schatzschneider, U. (2008). Photoinduced CO release, cellular uptake and cytotoxicity of a tris(pyrazolyl) methane (tpm) manganese tricarbonyl complex. *Chem. Commun.*, 1798-1800.
- Nobre, L. S., Al-Shahrour, F., Dopazo, J. and Saraiva, L. M. (2009). Exploring the antimicrobial action of a carbon monoxide-releasing compound through whole-genome transcription profiling of *Escherichia coli*. *Microbiology-Sgm* **155**, 813-824.
- Nobre, L. S., Seixas, J. D., Romao, C. C. and Saraiva, L. M. (2007). Antimicrobial action of carbon monoxide-releasing compounds. *Antimicrob. Agents Chemother.* **51**, 4303-4307.
- Obirai, J. C., Hamadi, S., Ithurbide, A., Wartelle, C., Nyokong, T., Zagal, J., Top, S. and Bedioui, F. (2006). UV-visible and electrochemical monitoring of carbon monoxide release by donor complexes to myoglobin solutions and to electrodes modified with films containing Hemin. *Electroanal* **18**, 1689-1695.
- Oelgeschlager, E. and Rother, M. (2008). Carbon monoxide-dependent energy metabolism in anaerobic bacteria and archaea. *Arch. Microbiol.* **190**, 257-269.
- Ohnishi, T., Sled, V. D., Rudnitzky, N. I., Jacobson, B. W., Fukumori, Y., Meinhardt, S. W., Calhoun, M. W., Gennis, R. B., Leif, H., Friedrich, T. and Weiss, H. (1994). Biophysical and biochemical studies of bacterial NADH:quinone oxidoreductase (Ndh-1). *Biochem. Soc. Trans.* **22**, S70.
- Ohta, K., Yachie, A., Fujimoto, K., Kaneda, H., Wada, T., Toma, T., Seno, A., Kasahara, Y., Yokoyama, H., Seki, H. and Koizumi, S. (2000). Tubular injury as a cardinal pathologic feature in human heme oxygenase-1 deficiency. *Am. J. Kidney Dis.* **35**, 863-70.
- Okochi, M., Kurimoto, M., Shimizu, K. and Honda, H. (2007). Increase of organic solvent tolerance by overexpression of *manXYZ* in *Escherichia coli*. *Appl. Microbiol. Biotechnol.* **73**, 1394-9.
- Onyiah, J. C., Sheikh, S. Z., Maharshak, N., Steinbach, E. C., Russo, S. M., Kobayashi, T., Mackey, L. C., Hansen, J. J., Moeser, A. J., Rawls, J. F., Borst, L. B., Otterbein, L. E. and Plevy, S. E. (2013). Carbon monoxide and heme oxygenase-1 prevent intestinal inflammation in mice by promoting bacterial clearance. *Gastroenterology* **144**, 789-98.
- Otterbein, L. E., Bach, F. H., Alam, J., Soares, M., Tao Lu, H., Wysk, M., Davis, R. J., Flavell, R. A. and Choi, A. M. (2000). Carbon monoxide has anti-inflammatory effects involving the mitogen-activated protein kinase pathway. *Nat. Med.* **6**, 422-8.
- Otterbein, L. E., Mantell, L. L. and Choi, A. M. (1999). Carbon monoxide provides protection against hyperoxic lung injury. *Am. J. Physiol.* **276**, L688-94.

- Otterbein, L. E., May, A. and Chin, B. Y. (2005). Carbon monoxide increases macrophage bacterial clearance through toll-like receptor (TLR)4 expression. *Cell. Mol. Biol.* **51**, 433-440.
- Parr, S. R., Wilson, M. T. and Greenwood, C. (1975). The reaction of *Pseudomonas aeruginosa* cytochrome *c* oxidase with carbon monoxide. *Biochem. J.* **151**, 51-9.
- Parshina, S. N., Sipma, J., Nakashimada, Y., Henstra, A. M., Smidt, H., Lysenko, A. M., Lens, P. N. L., Lettinga, G. and Stams, A. J. M. (2005). *Desulfotomaculum carboxydivorans* sp nov., a novel sulfate-reducing bacterium capable of growth at 100% CO. *Int. J. Syst. Evol. Microbiol.* **55**, 2159-2165.
- Patridge, E. V. and Ferry, J. G. (2006). WrbA from *Escherichia coli* and *Archaeoglobus fulgidus* is an NAD(P)H : Quinone oxidoreductase. *J. Bacteriol.* **188**, 3498-3506.
- Pena, A. C., Penacho, N., Mancio-Silva, L., Neres, R., Seixas, J. D., Fernandes, A. C., Romao, C. C., Mota, M. M., Bernardes, G. J. L. and Pamplona, A. (2012). A Novel Carbon Monoxide-Releasing Molecule Fully Protects Mice from Severe Malaria. *Antimicrob. Agents Chemother.* **56**, 1281-1290.
- Petersen, L. C. (1977). The effect of inhibitors on the oxygen kinetics of cytochrome *c* oxidase. *Biochim. Biophys. Acta* **460**, 299-307.
- Petrache, I., Otterbein, L. E., Alam, J., Wiegand, G. W. and Choi, A. M. (2000). Heme oxygenase-1 inhibits TNF-alpha-induced apoptosis in cultured fibroblasts. *American journal of physiology. Lung cellular and molecular physiology* **278**, L312-9.
- Petushkov, V. N. and Lee, J. (1997). Purification and characterization of flavoproteins and cytochromes from the yellow bioluminescence marine bacterium *Vibrio fischeri* strain Y1. *Eur. J. Biochem.* **245**, 790-6.
- Pfeiffer, H., Rojas, A., Niesel, J. and Schatzschneider, U. (2009). Sonogashira and "Click" reactions for the N-terminal and side-chain functionalization of peptides with [Mn(CO)<sub>3</sub>(tpm)](+)-based CO releasing molecules (tpm = tris(pyrazolyl)methane). *Dalton Trans.*, 4292-4298.
- Piantadosi, C. A. (2002). Biological chemistry of carbon monoxide. *Antiox. Redox Signal.* **4**, 259-270.
- Pirt, S. J. (1985). "Principles of Microbe and Cell Cultivation". Blackwell Scientific Publications, Oxford.
- Pitchumony, T. S., Spingler, B., Motterlini, R. and Alberto, R. (2010). Syntheses, structural characterization and CO releasing properties of boranocarbonate [H<sub>3</sub>BCO<sub>2</sub>H]- derivatives. *Org Biomol Chem* **8**, 4849-54.
- Pizarro, M. D., Rodriguez, J. V., Mamprin, M. E., Fuller, B. J. and Motterlini, R. (2009). Protective effects of a carbon monoxide-releasing molecule (CORM-3) during hepatic cold preservation. *Cryobiology* **58**, 248-255.
- Poderoso, J. J., Carreras, M. C., Schopfer, F., Lisdero, C. L., Riobo, N. A., Giulivi, C., Boveris, A. D., Boveris, A. and Cadenas, E. (1999). The reaction of nitric oxide with ubiquinol: Kinetic properties and biological significance. *Free Rad. Biol. Med.* **26**, 925-935.
- Poole, R. K. (1993). In "Biomembrane Protocols. 1. Isolation and Analysis" (J. M. Graham and J. A. Higgins, eds), vol. 19, pp. 109 - 122. Humana Press, Totowa, New Jersey.
- Poole, R. K. and Cook, G. M. (2000). In "Adv. Microb. Physiol." (R. K. Poole, ed.), vol. 43, pp. 165-224. Academic Press Ltd, London.

- Poole, R. K., Lloyd, D. and Kemp, R. B. (1973). Respiratory oscillations and heat evolution in synchronously dividing cultures of fission yeast *Schizosaccharomyces pombe* 972h. *J. Gen. Microbiol.* **77**, 209-220.
- Poole, R. K., Williams, H. D., Downie, J. A. and Gibson, F. (1989). Mutations affecting the cytochrome *d*-containing oxidase complex of *Escherichia coli* K12: Identification and mapping of a fourth locus, *cydD*. *J. Gen. Microbiol.* **135**, 1865-1874.
- Poss, K. D. and Tonegawa, S. (1997). Heme oxygenase 1 is required for mammalian iron reutilization. *Proc. Natl. Acad. Sci. U. S. A.* **94**, 10919-24.
- Preisig, O., Zufferey, R., Thonymeyer, L., Appleby, C. A. and Hennecke, H. (1996). A high-affinity *cbb<sub>3</sub>*-type cytochrome oxidase terminates the symbiosis-specific respiratory chain of *Bradyrhizobium japonicum*. *J. Bacteriol.* **178**, 1532-1538.
- Pudek, M. R. and Bragg, P. D. (1974). Inhibition by cyanide of the respiratory chain oxidases of *Escherichia coli*. *Arch. Biochem. Biophys.* **164**, 682-693.
- Pullan, S. T., Gidley, M. D., Jones, R. A., Barrett, J., Stevanin, T. A., Read, R. C., Green, J. and Poole, R. K. (2007). Nitric oxide in chemostat-cultured *Escherichia coli* is sensed by Fnr and other global regulators: Unaltered methionine biosynthesis indicates lack of S-nitrosation. *J. Bacteriol.* **189**, 1845-1855.
- Puri, S. and O'Brian, M. R. (2006). The *hmuQ* and *hmuD* genes from *Bradyrhizobium japonicum* encode heme-degrading enzymes. *J. Bacteriol.* **188**, 6476-6482.
- Puustinen, A., Finel, M., Haltia, T., Gennis, R. B. and Wikstrom, M. (1991). Properties of the two terminal oxidases of *Escherichia coli*. *Biochemistry* **30**, 3936-3942.
- Puustinen, A., Finel, M., Virkki, M. and Wikstrom, M. (1989). Cytochrome *o* (*bo*) is a proton pump in *Paracoccus denitrificans* and *Escherichia coli*. *FEBS Lett.* **249**, 163-167.
- Queiroga, C. S. F., Almeida, A. S., Alves, P. M., Brenner, C. and Vieira, H. L. A. (2011). Carbon monoxide prevents hepatic mitochondrial membrane permeabilization. *BMC Cell Biol.* **12**, 10.
- Ragsdale, S. W. (2004). Life with carbon monoxide. *Crit. Rev. Biochem. Mol. Biol.* **39**, 165-195.
- Ragsdale, S. W. and Kumar, M. (1996). Nickel-containing carbon monoxide dehydrogenase/acetyl-CoA synthase. *Chem. Rev.* **96**, 2515-2539.
- Rasmusson, A. G., Fernie, A. R. and van Dongen, J. T. (2009). Alternative oxidase: a defence against metabolic fluctuations? *Physiol Plant* **137**, 371-82.
- Ratliff, M., Zhu, W. M., Deshmukh, R., Wilks, A. and Stojiljkovic, I. (2001). Homologues of neisserial heme oxygenase in gram-negative bacteria: Degradation of heme by the product of the *pigA* gene of *Pseudomonas aeruginosa*. *J. Bacteriol.* **183**, 6394-6403.
- Reichelt, J. L. and Baumann, P. (1973). Taxonomy of marine, luminous bacteria. *Arch. Mikrobiol.* **94**, 283-330.
- Reizer, J., Michotey, V., Reizer, A. and Saier, M. H., Jr. (1994). Novel phosphotransferase system genes revealed by bacterial genome analysis: unique, putative fructose- and glucoside-specific systems. *Protein Sci.* **3**, 440-50.
- Reynolds, M. F., Parks, R. B., Burstyn, J. N., Shelver, D., Thorsteinsson, M. V., Kerby, R. L., Roberts, G. P., Vogel, K. M. and Spiro, T. G. (2000). Electronic absorption, EPR, and resonance raman spectroscopy of CooA, a CO-sensing transcription activator from *R. rubrum*, reveals a five-coordinate NO-heme. *Biochemistry* **39**, 388-396.

- Ribas-Carbo, M., Berry, J. A., Azcon-Bieto, J. and Siedow, J. N. (1994). The reaction of the plant mitochondrial cyanide-resistant alternative oxidase with oxygen. *Biochim. Biophys. Acta. Bioene* **1188**, 205-212.
- Rich, P. R., Meunier, B., Mitchell, R. and Moody, A. J. (1996). Coupling of charge and proton movement in cytochrome *c* oxidase. *Biochim. Biophys. Acta* **1275**.
- Richardson, A. R., Dunman, P. M. and Fang, F. C. (2006). The nitrosative stress response of *Staphylococcus aureus* is required for resistance to innate immunity. *Mol. Microbiol.* **61**, 927-939.
- Ridley, K. A., Rock, J. D., Li, Y. and Ketley, J. M. (2006). Heme utilization in *Campylobacter jejuni*. *J. Bacteriol.* **188**, 7862-7875.
- Rimmer, R. D., Richter, H. and Ford, P. C. (2010). A photochemical precursor for carbon monoxide release in aerated aqueous media. *Inorg Chem* **49**, 1180-5.
- Roberts, G. P., Thorsteinsson, M. V., Kerby, R. L., Lanzilotta, W. N. and Poulos, T. (2001). CooA: a heme-containing regulatory protein that serves as a specific sensor of both carbon monoxide and redox state. *Prog.Nucleic Acid Res.Mol.Biol.* **67**, 35-63.
- Rodgers, K. R. and Lukat-Rodgers, G. S. (2005). Insights into heme-based O<sub>2</sub> sensing from structure-function relationships in the FixL proteins. *J. Inorg. Biochem.* **99**, 963-977.
- Rodkey, F. L., O'Neal, J. D., Collison, H. A. and Uddin, D. E. (1974). Relative affinity of hemoglobin S and hemoglobin A for carbon monoxide and oxygen. *Clin. Chem.* **20**, 83-4.
- Romanski, S., Kraus, B., Schatzschneider, U., Neudorfl, J. M., Amslinger, S. and Schmalz, H. G. (2011). Acyloxybutadiene iron tricarbonyl complexes as enzyme-triggered CO-releasing molecules (ET-CORMs). *Angewandte Chemie-International Edition* **50**, 2392-2396.
- Romao, C. C., Blattler, W. A., Seixas, J. D. and Bernardes, G. J. L. (2012). Developing drug molecules for therapy with carbon monoxide. *Chem. Soc. Rev.* **41**, 3571-3583.
- Roughton, F. J. W. and Darling, R. C. (1944). The effect of carbon monoxide on the oxyhemoglobin dissociation curve. *Am. J. Physiol.* **141**, 0017-0031.
- Ruby, E. G. and McFall-Ngai, M. J. (1999). Oxygen-utilizing reactions and symbiotic colonization of the squid light organ by *Vibrio fischeri*. *Trends Microbiol.* **7**, 414-20.
- Ruby, E. G., Urbanowski, M., Campbell, J., Dunn, A., Faini, M., Gunsalus, R., Lostroh, P., Lupp, C., McCann, J., Millikan, D., Schaefer, A., Stabb, E., Stevens, A., Visick, K., Whistler, C. and Greenberg, E. P. (2005). Complete genome sequence of *Vibrio fischeri*: a symbiotic bacterium with pathogenic congeners. *Proc. Natl. Acad. Sci. U. S. A.* **102**, 3004-9.
- Rusch, D. B., Halpern, A. L., Sutton, G., Heidelberg, K. B., Williamson, S., Yooseph, S., Wu, D., Eisen, J. A., Hoffman, J. M., Remington, K., Beeson, K., Tran, B., Smith, H., Baden-Tillson, H., Stewart, C., Thorpe, J., Freeman, J., Andrews-Pfannkoch, C., Venter, J. E., Li, K., Kravitz, S., Heidelberg, J. F., Utterback, T., Rogers, Y. H., Falcon, L. I., Souza, V., Bonilla-Rosso, G., Eguiarte, L. E., Karl, D. M., Sathyendranath, S., Platt, T., Bermingham, E., Gallardo, V., Tamayo-Castillo, G., Ferrari, M. R., Strausberg, R. L., Neilson, K., Friedman, R., Frazier, M. and Venter, J. C. (2007). The Sorcerer II Global Ocean Sampling expedition: northwest Atlantic through eastern tropical Pacific. *PLoS Biol* **5**, e77.

- Ryter, S. W., Morse, D. and Choi, A. M. (2004). Carbon monoxide: to boldly go where NO has gone before. *Sci STKE* **2004**, RE6.
- Sambrook, J. and Russell, D. W. (2001). Molecular cloning: A laboratory manual. *Molecular cloning: A laboratory manual*.
- Sandouka, A., Balogun, E., Foresti, R., Mann, B. E., Johnson, T. R., Tayem, Y., Green, C. J., Fuller, B. and Motterlini, R. (2005). Carbon monoxide-releasing molecules (CO-RMs) modulate respiration in isolated mitochondria. *Cell. Mol. Biol.* **51**, 425-432.
- Sandouka, A., Fuller, B. J., Mann, B. E., Green, C. J., Foresti, R. and Motterlini, R. (2006). Treatment with carbon monoxide-releasing molecules (CO-RMs) during cold storage improves renal function at reperfusion. *Kidney Int.* **69**, 239-247.
- Santos-Silva, T., Mukhopadhyay, A., Seixas, J. D., Bernardes, G. J. L., Romao, C. C. and Romao, M. J. (2011). CORM-3 Reactivity toward Proteins: The Crystal Structure of a Ru(II) Dicarbonyl-Lysozyme Complex. *J. Am. Chem. Soc.* **133**, 1192-1195.
- Santos, M. F., Seixas, J. D., Coelho, A. C., Mukhopadhyay, A., Reis, P. M., Romao, M. J., Romao, C. C. and Santos-Silva, T. (2012). New insights into the chemistry of fac-[Ru(CO)<sub>3</sub>]<sub>2</sub><sup>+</sup> fragments in biologically relevant conditions: the CO releasing activity of [Ru(CO)<sub>3</sub>Cl<sub>2</sub>(1,3-thiazole)], and the X-ray crystal structure of its adduct with lysozyme. *J. Inorg. Biochem.* **117**, 285-91.
- Sarady-Andrews, J. K., Liu, F., Gallo, D., Nakao, A., Overhaus, M., Ollinger, R., Choi, A. M. and Otterbein, L. E. (2005). Biliverdin administration protects against endotoxin-induced acute lung injury in rats. *American journal of physiology. Lung cellular and molecular physiology* **289**, L1131-7.
- Sarady, J. K., Otterbein, S. L., Liu, F., Otterbein, L. E. and Choi, A. M. K. (2002). Carbon monoxide modulates endotoxin-induced production of granulocyte macrophage colony-stimulating factor in macrophages. *Am. J. Respir. Cell Mol. Biol.* **27**, 739-745.
- Sarady, J. K., Zuckerbraun, B. S., Bilban, M., Wagner, O., Usheva, A., Liu, F., Ifedigbo, E., Zamora, R., Choi, A. M. K. and Otterbein, L. E. (2004). Carbon monoxide protection against endotoxic shock involves reciprocal effects on iNOS in the lung and liver. *FASEB J.* **18**, 854-856.
- Sardana, M. K., Sassa, S. and Kappas, A. (1981). Differential responses to inducers of delta-aminolaevulinic synthase and haem oxygenase during pregnancy. *Biochem. J.* **198**, 403-8.
- Sasakura, Y., Hirata, S., Sugiyama, S., Suzuki, S., Taguchi, S., Watanabe, M., Matsui, T., Sagami, I. and Shimizu, T. (2002). Characterization of a direct oxygen sensor heme protein from *Escherichia coli* - Effects of the heme redox states and mutations at the heme-binding site on catalysis and structure. *J. Biol. Chem.* **277**, 23821-23827.
- Sawle, P., Foresti, R., Mann, B. E., Johnson, T. R., Green, C. J. and Motterlini, R. (2005). Carbon monoxide-releasing molecules (CO-RMs) attenuate the inflammatory response elicited by lipopolysaccharide in RAW264.7 murine macrophages. *Br. J. Pharmacol.* **145**, 800-810.
- Schatzschneider, U. (2010). Photoactivated biological activity of transition-metal complexes. *Eur. J. Inorg. Chem.*, 1451-1467.
- Schatzschneider, U. (2011). PhotoCORMs: Light-triggered release of carbon monoxide from the coordination sphere of transition metal complexes for biological applications. *Inorg. Chim. Acta* **374**, 19-23.

- Schmitt, M. P. (1997). Utilization of host iron sources by *Corynebacterium diphtheriae*: identification of a gene whose product is homologous to eukaryotic heme oxygenases and is required for acquisition of iron from heme and hemoglobin. *J. Bacteriol.* **179**, 838-845.
- Schuller, D. J., Zhu, W. M., Stojiljkovic, I., Wilks, A. and Poulos, T. L. (2001). Crystal structure of heme oxygenase from the Gram-negative pathogen *Neisseria meningitidis* and a comparison with mammalian heme oxygenase-1. *Biochemistry* **40**, 11552-11558.
- Scott, R. I., Gibson, J. F. and Poole, R. K. (1980). Adenosine triphosphatase activity and its sensitivity to ruthenium red oscillate during the cell-cycle of *Escherichia coli*-K12. *J. Gen. Microbiol.* **120**, 183-198.
- Scragg, J. L., Dallas, M. L., Wilkinson, J. A., Varadi, G. and Peers, C. (2008). Carbon monoxide inhibits L-type Ca<sup>2+</sup> channels via redox modulation of key cysteine residues by mitochondrial reactive oxygen species. *J. Biol. Chem.* **283**, 24412-24419.
- Seaver, L. C. and Imlay, J. A. (2001). Alkyl hydroperoxide reductase is the primary scavenger of endogenous hydrogen peroxide in *Escherichia coli*. *J. Bacteriol.* **183**, 7173-7181.
- Seixas, J. D. (2010). Development of CO-releasing molecules for the treatment of inflammatory diseases. *Doctoral Dissertaition, Instituto de Technoloia Quimica e Biologica da Universidade Nova de Lisboa.*
- Sharma, N., Bhattarai, J. P., Hwang, P. H. and Han, S. K. (2013). Nitric oxide suppresses L-type calcium currents in basilar artery smooth muscle cells in rabbits. *Neurol. Res.* **35**, 424-8.
- Shelver, D., Kerby, R. L., He, Y. P. and Roberts, G. P. (1995). Carbon monoxide-induced activation of gene expression in *Rhodospirillum rubrum* requires the product of *cooA*, a member of the cyclic AMP receptor protein family of transcriptional regulators. *J. Bacteriol.* **177**, 2157-2163.
- Shelver, D., Kerby, R. L., He, Y. P. and Roberts, G. P. (1997). *CooA*, a CO-sensing transcription factor from *Rhodospirillum rubrum*, is a CO-binding heme protein. *Proceeding Of The National Academy Of Sciences Of The United States Of America* **94**, 11216-11220.
- Shi, L. B., Sohaskey, C. D., Kana, B. D., Dawes, S., North, R. J., Mizrahi, V. and Gennaro, M. L. (2005). Changes in energy metabolism of *Mycobacterium tuberculosis* in mouse lung and under *in vitro* conditions affecting aerobic respiration. *Proc. Natl. Acad. Sci. U. S. A.* **102**, 15629-15634.
- Shi, R., Pineda, M., Ajamian, E., Cui, Q., Matte, A. and Cygler, M. (2008). Structure of L-xylulose-5-Phosphate 3-epimerase (UlaE) from the anaerobic L-ascorbate utilization pathway of *Escherichia coli*: identification of a novel phosphate binding motif within a TIM barrel fold. *J. Bacteriol.* **190**, 8137-44.
- Shiva, S., Huang, Z., Grubina, R., Sun, J., Ringwood, L. A., MacArthur, P. H., Xu, X., Murphy, E., Darley-Usmar, V. M. and Gladwin, M. T. (2007). Deoxymyoglobin is a nitrite reductase that generates nitric oxide and regulates mitochondrial respiration. *Circul. Res.* **100**, 654-61.
- Sipma, J., Henstra, A. M., Parshina, S. M., Lens, P. N., Lettinga, G. and Stams, A. J. (2006). Microbial CO conversions with applications in synthesis gas purification and bio-desulfurization. *Crit. Rev. Biotechnol.* **26**, 41-65.
- Sirs, J. A. (1974). The kinetics of the reaction of carbon monoxide with fully oxygenated haemoglobin in solution and erythrocytes. *J Physiol* **236**, 387-401.



- Sjostrand, T. (1949). Endogenous formation of carbon monoxide in man under normal and pathological conditions. *Nature* **164**, 580-581.
- Skaar, E. P., Gaspar, A. H. and Schneewind, O. (2004). IsdG and IsdI, heme-degrading enzymes in the cytoplasm of *Staphylococcus aureus*. *J. Biol. Chem.* **279**, 436-443.
- Skaar, E. P., Gaspar, A. H. and Schneewind, O. (2006). Bacillus anthracis IsdG, a heme-degrading monooxygenase. *J. Bacteriol.* **188**, 1071-1080.
- Slayman, C. (1977). "The function of an alternative terminal oxidase in *Neurospora*. In functions of alternative terminal oxidase". Pergamon, Oxford.
- Smith, H., Mann, B. E., Motterlini, R. and Poole, R. K. (2011). The carbon monoxide-releasing molecule, CORM-3 (Ru(CO)<sub>3</sub>Cl(Glycinate)), targets respiration and oxidases in *Campylobacter jejuni*, generating hydrogen peroxide. *IUBMB Life* **63**, 363-371.
- Snyder, S. H., Jaffrey, S. R. and Zakhary, R. (1998). Nitric oxide and carbon monoxide: parallel roles as neural messengers. *Brain Res. Brain Res. Rev.* **26**, 167-75.
- Srisook, K., Han, S. S., Choi, H. S., Li, M. H., Ueda, H., Kim, C. and Cha, Y. N. (2006). CO from enhanced HO activity or from CORM-2 inhibits both O<sub>2</sub><sup>-</sup> and NO production and downregulates HO-1 expression in LPS-stimulated macrophages. *Biochem. Pharmacol.* **71**, 307-318.
- Stabb, E. V., Reich, K. A. and Ruby, E. G. (2001). *Vibrio fischeri* genes *hvnA* and *hvnB* encode secreted NAD<sup>+</sup> glycohydrolases. *J. Bacteriol.* **183**, 309-17.
- Stenmark, P. and Nordlund, P. (2003). A prokaryotic alternative oxidase present in the bacterium *Novosphingobium aromaticivorans*. *FEBS Lett.* **552**, 189-92.
- Stewart, R. D. (1974). The effects of low concentration of carbon monoxide in man. *Scand. J. Respir. Dis. Suppl.* **91**, 56-62.
- Stocker, R., Yamamoto, Y., McDonagh, A. F., Glazer, A. N. and Ames, B. N. (1987). Bilirubin is an antioxidant of possible physiological importance. *Science* **235**, 1043-6.
- Stripp, S. T., Goldet, G., Brandmayr, C., Sanganas, O., Vincent, K. A., Haumann, M., Armstrong, F. A. and Happe, T. (2009). How oxygen attacks [FeFe] hydrogenases from photosynthetic organisms. *Proc. Natl. Acad. Sci. U. S. A.* **106**, 17331-17336.
- Sturr, M. G., Krulwich, T. A. and Hicks, D. B. (1996). Purification of a cytochrome *bd* terminal oxidase encoded by the *Escherichia coli* *app* locus from a delta *cyo* delta *cyd* strain complemented by genes from *Bacillus firmus* OF4. *J. Bacteriol.* **178**, 1742-1749.
- Suematsu, M., Kashiwagi, S., Sano, T., Goda, N., Shinoda, Y. and Ishimura, Y. (1994). Carbon monoxide as an endogenous modulator of hepatic vascular perfusion. *Biochem. Biophys. Res. Commun.* **205**, 1333-7.
- Suits, M. D. L., Pal, G. P., Nakatsu, K., Matte, A., Cygler, M. and Jia, Z. C. (2005). Identification of an *Escherichia coli* O157 : H7 heme oxygenase with tandem functional repeats. *Proc. Natl. Acad. Sci. U. S. A.* **102**, 16955-16960.
- Suliman, H. B., Carraway, M. S., Tatro, L. G. and Piantadosi, C. A. (2007). A new activating role for CO in cardiac mitochondrial biogenesis. *J. Cell Sci.* **120**, 299-308.
- Sulzenbacher, G., Roig-Zamboni, V., Pagot, F., Grisel, S., Salomoni, A., Valencia, C., Campanacci, V., Vincentelli, R., Tegoni, M., Eklund, H. and Cambillau, C. (2004). Structure of *Escherichia coli* YhdH, a putative quinone oxidoreductase. *Acta Crystallogr. D. Biol. Crystallogr.* **60**, 1855-62.

- Sun, J., Hoshino, H., Takaku, K., Nakajima, O., Muto, A., Suzuki, H., Tashiro, S., Takahashi, S., Shibahara, S., Alam, J., Taketo, M. M., Yamamoto, M. and Igarashi, K. (2002). Hemoprotein Bach1 regulates enhancer availability of heme oxygenase-1 gene. *EMBO J.* **21**, 5216-24.
- Svetlitchnyi, V., Peschel, C., Acker, G. and Meyer, O. (2001). Two membrane-associated NiFeS-carbon monoxide dehydrogenases from the anaerobic carbon-monoxide-utilizing eubacterium *Carboxydotherrnus hydrogenoformans*. *J. Bacteriol.* **183**, 5134-44.
- Svetlitchnyi, V., Sokolova, T. G., Gerhardt, M., Ringpfeil, M., Kostrikina, N. A. and Ga, Z. (1991). *Carboxydotherrnus hydrogenoformans* gen. nov., sp. nov., a CO-utilizing thermophilic anaerobic bacterium from hydrothermal environments of Kunashir Island. *Syst. Appl. Microbiol.* **14**, 254-260.
- Sylman, J. L., Lantvit, S. M., Vedepo, M. C., Reynolds, M. M. and Neeves, K. B. (2013). Transport limitations of nitric oxide inhibition of platelet aggregation under flow. *Ann. Biomed. Eng.*
- Sylvester, J. T. and McGowan, C. (1978). The effects of agents that bind to cytochrome P-450 on hypoxic pulmonary vasoconstriction. *Circul. Res.* **43**, 429-37.
- Szabo, C. (2010). Gaseotransmitters: New frontiers for translational science. *Sci. Transl. Med.* **2**.
- Taguchi, S., Matsui, T., Igarashi, J., Sasakura, Y., Araki, Y., Ito, O., Sugiyama, S., Sagami, I. and Shimizu, T. (2004). Binding of oxygen and carbon monoxide to a heme-regulated phosphodiesterase from *Escherichia coli* - Kinetics and infrared spectra of the full-length wild-type enzyme, isolated PAS domain, and Met-95 mutants. *J. Biol. Chem.* **279**, 3340-3347.
- Taille, C., El-Benna, J., Lanone, S., Boczkowski, J. and Motterlini, R. (2005). Mitochondrial respiratory chain and NAD(P)H oxidase are targets for the antiproliferative effect of carbon monoxide in human airway smooth muscle. *J. Biol. Chem.* **280**, 25350-60.
- Takahashi, K., Nakayama, M., Takeda, K., Fujia, H. and Shibahara, S. (1999). Suppression of heme oxygenase-1 mRNA expression by interferon-gamma in human glioblastoma cells. *J. Neurochem.* **72**, 2356-61.
- Tang, X. D., Xu, R., Reynolds, M. F., Garcia, M. L., Heinemann, S. H. and Hoshi, T. (2003). Haem can bind to and inhibit mammalian calcium-dependent Slo1 BK channels. *Nature* **425**, 531-535.
- Tavares, A. F., Teixeira, M., Romao, C. C., Seixas, J. D., Nobre, L. S. and Saraiva, L. M. (2011). Reactive oxygen species mediate bactericidal killing elicited by carbon monoxide-releasing molecules. *J. Biol. Chem.* **286**, 26708-26717.
- Tenhunen, R., Marver, H. S. and Schmid, R. (1969). The enzymatic conversion of hemoglobin to bilirubin. *Trans. Assoc. Am. Physicians* **82**, 363-71.
- Terry, C. M., Clikeman, J. A., Hoidal, J. R. and Callahan, K. S. (1999). TNF-alpha and IL-1alpha induce heme oxygenase-1 via protein kinase C, Ca<sup>2+</sup>, and phospholipase A2 in endothelial cells. *Am. J. Physiol.* **276**, H1493-501.
- Thijs, L., Vinck, E., Bolli, A., Trandafir, F., Wan, X. H., Hoogewijs, D., Coletta, M., Fago, A., Weber, R. E., Van Doorslaer, S., Ascenzi, P., Alam, M., Moens, L. and Dewilde, S. (2007). Characterization of a globin-coupled oxygen sensor with a gene-regulating function. *J. Biol. Chem.* **282**, 37325-37340.
- Thorn, J. M., Barton, J. D., Dixon, N. E., Ollis, D. L. and Edwards, K. J. (1995). Crystal structure of *Escherichia coli* QOR quinone oxidoreductase complexed with NADPH. *J. Mol. Biol.* **249**, 785-799.

- Tinajero Trejo, M., Jesse, H. E. and Poole, R. K. (2013). Gasotransmitters, Poisons and Antimicrobials: It's a gas, gas, gas! *F1000Prime Reports* **5** (28).
- Torres, J., Sharpe, M. A., Rosquist, A., Cooper, C. E. and Wilson, M. T. (2000). Cytochrome *c* oxidase rapidly metabolises nitric oxide to nitrite. *FEBS Lett.* **475**, 263-266.
- Trumpower, B. L. and Gennis, R. B. (1994). Energy transduction by cytochrome complexes in mitochondrial and bacterial respiration: The enzymology of coupling electron transfer reactions to transmembrane proton translocation. *Annu. Rev. Biochem.* **63**, 675-716.
- Tseng, C.-P., Albrecht, J.A. and Gunsalus, R.P. (1996). Effect of microaerophilic cell growth conditions on expression of the aerobic (*cyoABCDE* and *cydAB*) and anaerobic (*narGHJI*, *frdABCD*, and *dmsABC*) respiratory pathway genes in *Escherichia coli*. *J. Bacteriol.* **178**, 1094 - 1098.
- Umbach, A. L. and Siedow, J. N. (1993). Covalent and noncovalent dimers of the cyanide-resistant alternative oxidase protein in higher plant mitochondria and their relationship to enzyme activity. *Plant Physiol.* **103**, 845-854.
- Umbach, A. L., Wiskich, J. T. and Siedow, J. N. (1994). Regulation of alternative oxidase kinetics by pyruvate and intermolecular disulfide bond redox status in soybean seedling mitochondria. *FEBS Lett.* **348**, 181-4.
- Vadori, M., Seveso, M., Besenon, F., Bosio, E., Tognato, E., Fante, F., Boldrin, M., Gavasso, S., Ravarotto, L., Mann, B. E., Simioni, P., Ancona, E., Motterlini, R. and Cozzi, E. (2009). *In vitro* and *in vivo* effects of the carbon monoxide-releasing molecule, CORM-3, in the xenogeneic pig-to-primate context. *Xenotransplantation* **16**, 99-114.
- Vanlerberghe, G. C. and McIntosh, L. (1997). Alternative oxidase: From gene to function. *Annu Rev Plant Physiol Plant Mol Biol* **48**, 703-734.
- Vera, T., Henegar, J. R., Drummond, H. A., Rimoldi, J. M. and Stec, D. E. (2005). Protective effect of carbon monoxide-releasing compounds in ischemia-induced acute renal failure. *J. Am. Soc. Nephrol.* **16**, 950-958.
- Verma, A., Hirsch, D. J., Glatt, C. E., Ronnett, G. V. and Snyder, S. H. (1993). Carbon monoxide - A putative neural messenger. *Science* **259**, 381-384.
- Visick, K. L., Foster, J., Doino, J., McFall-Ngai, M. and Ruby, E. G. (2000). *Vibrio fischeri lux* genes play an important role in colonization and development of the host light organ. *J. Bacteriol.* **182**, 4578-86.
- Visick, K. L. and Ruby, E. G. (2006). *Vibrio fischeri* and its host: it takes two to tango. *Current Opinion in Microbiology* **9**, 632-638.
- Voggu, L., Schlag, S., Biswas, R., Rosenstein, R., Rausch, C. and Gotz, F. (2006). Microevolution of cytochrome *bd* oxidase in *Staphylococci* and its implication in resistance to respiratory toxins released by *Pseudomonas*. *J. Bacteriol.* **188**, 8079-8086.
- Wagner, A. M. and Moore, A. L. (1997). Structure and function of the plant alternative oxidase: its putative role in the oxygen defence mechanism. *Biosci. Rep.* **17**, 319-33.
- Wang, J., Karpus, J., Zhao, B. S., Luo, Z., Chen, P. R. and He, C. (2012). A selective fluorescent probe for carbon monoxide imaging in living cells. *Angew. Chem. Int. Ed. Engl.* **51**, 9652-6.
- Wang, R. (2003). The gasotransmitter role of hydrogen sulfide. *Antiox. Redox Signal.* **5**, 493-501.

- Wang, R. (2004). In "Signal Transduction and the Gasotransmitters. NO, CO and H<sub>2</sub>S in Biology and Medicine" (R. Wang, ed.), pp. 3-31. Humana Press, Totowa, New Jersey.
- Wang, R., Wu, L. and Wang, Z. (1997). The direct effect of carbon monoxide on KCa channels in vascular smooth muscle cells. *Pflugers Arch.* **434**, 285-91.
- Ward, J. S., Lynam, J. M., Moir, J. W. B., Sanin, D. E., Mountford, A. P. and Fairlamb, I. J. S. (2012). A therapeutically viable photo-activated manganese-based CO-releasing molecule (photo-CO-RM). *Dalton Trans.* **41**, 10514-10517.
- Way, S. S., Sallustio, S., Magliozzo, R. S. and Goldberg, M. B. (1999). Impact of either elevated or decreased levels of cytochrome *bd* expression on *Shigella flexneri* virulence. *J. Bacteriol.* **181**, 1229 - 1237.
- Wegele, R., Tasler, R., Zeng, Y. H., Rivera, M. and Frankenberg-Dinkel, N. (2004). The heme oxygenase(s)-phytochrome system of *Pseudomonas aeruginosa*. *J. Biol. Chem.* **279**, 45791-45802.
- Weigel, P. H. and Englund, P. T. (1975). Inhibition of DNA replication in *Escherichia coli* by cyanide and carbon monoxide. *J. Biol. Chem.* **250**, 8536-8542.
- White, K. A. and Marletta, M. A. (1992). Nitric oxide synthase is a cytochrome-P-450 type hemoprotein. *Biochemistry* **31**, 6627-6631.
- Wiesel, P., Patel, A. P., DiFonzo, N., Marria, P. B., Sim, C. U., Pellacani, A., Maemura, K., LeBlanc, B. W., Marino, K., Doerschuk, C. M., Yet, S. F., Lee, M. E. and Perrella, M. A. (2000). Endotoxin-induced mortality is related to increased oxidative stress and end-organ dysfunction, not refractory hypotension, in heme oxygenase-1-deficient mice. *Circulation* **102**, 3015-22.
- Wikstrom, M., Krab, K. and Saraste, M. (1981). "Cytochrome Oxidase. A Synthesis". Academic Press, London.
- Wilkinson, W. J. and Kemp, P. J. (2011). The carbon monoxide donor, CORM-2, is an antagonist of ATP-gated, human P2X<sub>4</sub> receptors. *Purinergic Signal.* **7**, 57-64.
- Wilson, J. L. (2012). In "The Anti-microbial Effects of Carbon Monoxide and Carbon Monoxide-Releasing Molecule-3 (CORM-3), Department of Molecular Biology and Biotechnology", vol. Ph.D. The University of Sheffield.
- Wilson, J. L., Jesse, H. E., Hughes, B., Lund, V., Naylor, K., Davidge, K. S., Cook, G. M., Mann, B. E. and Poole, R. K. (2013). Ru(CO)<sub>3</sub>Cl(Glycinate) (CORM-3): A carbon monoxide-releasing molecule with broad-spectrum antimicrobial and photosensitive activities against respiration and cation transport in *Escherichia coli*. *Antioxid. Redox Signal.*
- Winterbourn, C. C. (1982). Superoxide dismutase-inhibitable reduction of cytochrome-c by the alloxan radical - Implications for alloxan cytotoxicity. *Biochem. J.* **207**, 609-612.
- Wood, P. M. (1983). Why do *c*-type cytochromes exist? *FEBS Lett.* **164**, 223-226.
- Wood, P. M. (1984). Bacterial proteins with CO-binding *b*- or *c*-type haem. Functions and absorption spectroscopy. *Biochim. Biophys. Acta* **768**, 293-317.
- Wu, L. Y. and Wang, R. (2005). Carbon monoxide: Endogenous production, physiological functions, and pharmacological applications. *Pharmacol. Rev.* **57**, 585-630.
- Wu, R. Y., Skaar, E. P., Zhang, R. G., Joachimiak, G., Gornicki, P., Schneewind, O. and Joachimiak, A. (2005). *Staphylococcus aureus* IsdG and IsdI, heme-degrading enzymes with structural similarity to monooxygenases. *J. Biol. Chem.* **280**, 2840-2846.

- Xi, Q., Tcheranova, D., Parfenova, H., Horowitz, B., Leffler, C. W. and Jaggar, J. H. (2004). Carbon monoxide activates KCa channels in newborn arteriole smooth muscle cells by increasing apparent Ca<sup>2+</sup> sensitivity of alpha-subunits. *American journal of physiology. Heart and circulatory physiology* **286**, H610-8.
- Yachie, A., Niida, Y., Wada, T., Igarashi, N., Kaneda, H., Toma, T., Ohta, K., Kasahara, Y. and Koizumi, S. (1999). Oxidative stress causes enhanced endothelial cell injury in human heme oxygenase-1 deficiency. *J. Clin. Invest.* **103**, 129-135.
- Yang, C. M., Hsieh, H. L., Lin, C. C., Shih, R. H., Chi, P. L., Cheng, S. E. and Hsiao, L. D. (2013). Multiple factors from bradykinin-challenged astrocytes contribute to the neuronal apoptosis: involvement of astroglial ROS, MMP-9, and HO-1/CO system. *Mol. Neurobiol.* **47**, 1020-33.
- Yew, W. S. and Gerlt, J. A. (2002). Utilization of L-ascorbate by *Escherichia coli* K-12: assignments of functions to products of the *yjf-sga* and *yia-sgb* operons. *J. Bacteriol.* **184**, 302-6.
- Youn, H., Conrad, M., Chung, S. Y. and Roberts, G. P. (2006). Roles of the heme and heme ligands in the activation of CooA, the CO-sensing transcriptional activator. *Biochem. Biophys. Res. Commun.* **348**, 345-350.
- Zhang, Z., Aboulwafa, M., Smith, M. H. and Saier, M. H., Jr. (2003). The ascorbate transporter of *Escherichia coli*. *J. Bacteriol.* **185**, 2243-50.
- Zhao, H., Joseph, J., Zhang, H., Karoui, H. and Kalyanaraman, B. (2001). Synthesis and biochemical applications of a solid cyclic nitron spin trap: a relatively superior trap for detecting superoxide anions and glutathiyyl radicals. *Free Radic Biol Med* **31**, 599-606.
- Zhou, H., Lu, F., Latham, C., Zander, D. S. and Visner, G. A. (2004). Heme oxygenase-1 expression in human lungs with cystic fibrosis and cytoprotective effects against *Pseudomonas aeruginosa* *in vitro*. *Am. J. Respir. Crit. Care Med.* **170**, 633-40.
- Zhu, W. M., Hunt, D. J., Richardson, A. R. and Stojiljkovic, I. (2000a). Use of heme compounds as iron sources by pathogenic *Neisseriae* requires the product of the *hemO* gene. *J. Bacteriol.* **182**, 439-447.
- Zhu, W. M., Wilks, A. and Stojiljkovic, I. (2000b). Degradation of heme in gram-negative bacteria: the product of the *hemO* gene of *Neisseriae* is a heme oxygenase. *J. Bacteriol.* **182**, 6783-6790.
- Zlosnik, J. E. A., Tavankar, G. R., Bundy, J. G., Mossialos, D., O'Toole, R. and Williams, H. D. (2006). Investigation of the physiological relationship between the cyanide-sensitive oxidase and cyanide production in *Pseudomonas aeruginosa*. *Microbiology* **152**, 1407-1415.
- Zuckerbraun, B. S., Chin, B. Y., Bilban, M., d'Avila, J. D., Rao, J., Billiar, T. R. and Otterbein, L. E. (2007). Carbon monoxide signals via inhibition of cytochrome *c* oxidase and generation of mitochondrial reactive oxygen species. *FASEB J.* **21**, 1099-1106.